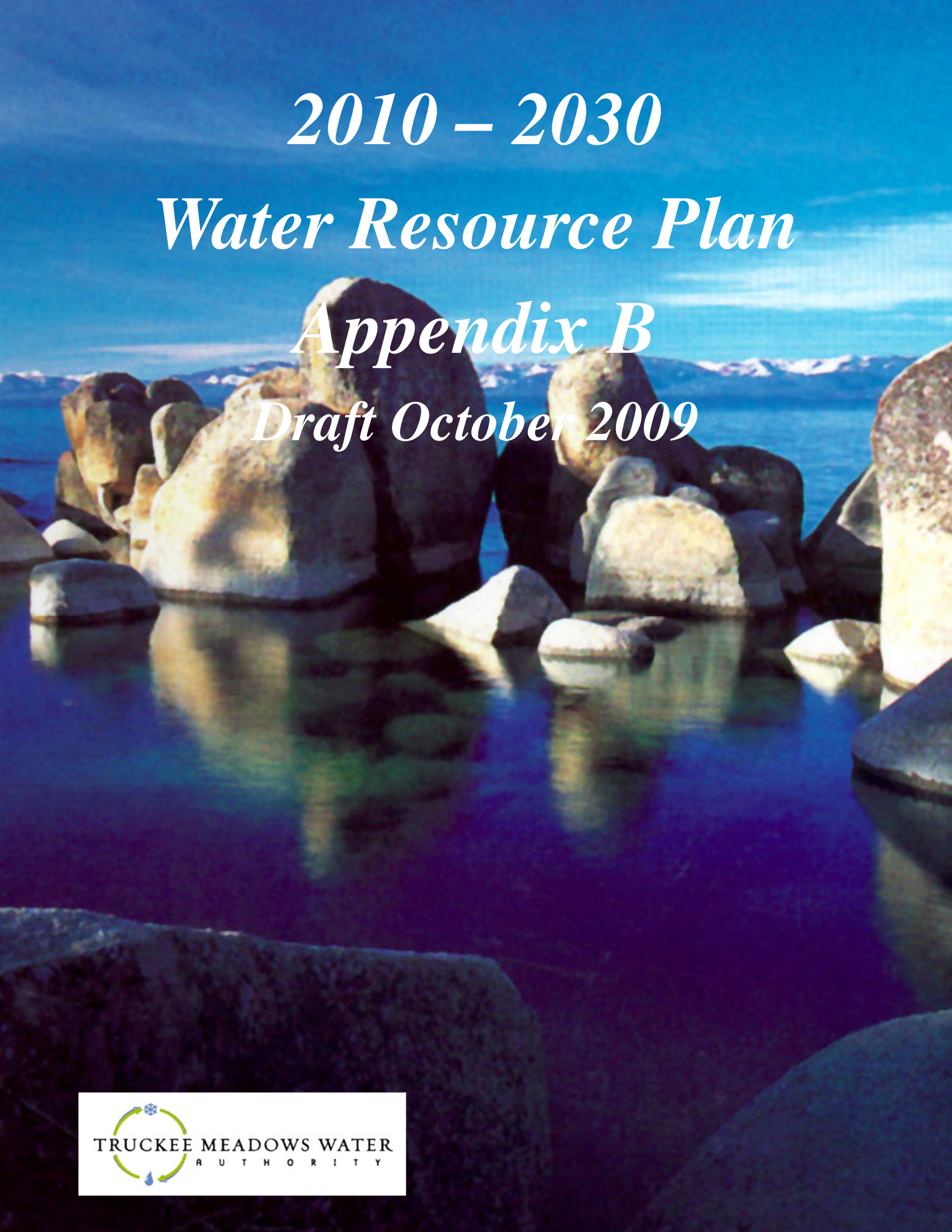

2010 – 2030
Water Resource Plan
Appendix B
Draft October 2009

TRUCKEE MEADOWS WATER AUTHORITY

Appendix B:
Climate Change Studies

Potential Climate Change and Impacts on Water Resources

prepared by

Mark Stone, Ph.D.
Division of Hydrologic Sciences
Desert Research Institute

Hilary Lopez, Ph.D.
Truckee Meadows Water Authority

prepared for

Truckee Meadows Water Authority
1355 Capital Boulevard
Reno, NV 89520

July 2006

Potential Climate Change and Impacts on Water Resources

Abstract

As a natural process of the climate system, the Earth's climate has been forever changing. Climate change in the last 100 years, however, is thought to have been influenced by human activities, in particular greenhouse gas (GHG) emissions. Early signs of this change, such as increased mean annual temperatures and thinner sea ice, have been observed in many regions of the world. According to global climate models, continued increases in greenhouse gas emissions could cause further changes in temperature, with the global mean temperature potentially rising by approximately 2.7 to 10.4º F by 2100. This potential change in climate could cause changes in atmospheric and oceanic circulation patterns, and in the hydrologic cycle, leading to altered patterns of precipitation and runoff. Warmer temperatures will potentially increase moisture availability and precipitation. However in mountainous regions, such as the Sierra Nevada, a larger fraction of the total precipitation could be in the form of rain, resulting in shorter snow accumulation periods, reduced annual snowpacks, earlier spring melting, and reduced summer flows. To plan effectively, it is important to understand how and why climate may change in the future and how that may affect water resources. The goal of this document is to summarize the current state-of-knowledge of climate change as it relates to water resources in the western United States.

Climate Change and Global Warming

As a natural process of the climate system, the Earth's climate has been forever changing. Most recently, within the past 100 years, scientists have witnessed a general warming trend in temperatures termed "global warming." Additionally, this "warming" seems to have accelerated during the past two decades. While natural processes contribute to global warming, it is also widely believed that human activities are attributing to the rapid temperature rise. A majority of scientists contend that human activities have "altered the chemical composition of the atmosphere through the buildup of greenhouse gases – primarily carbon dioxide, methane, and nitrous oxide" – and that this buildup has resulted in rising global temperatures (US EPA). However, it is important to point out that within the scientific community controversy continues regarding the extent and effects of human impacts on global climate change.

Atmospheric Greenhouse Gas and Aerosol Concentrations

The major greenhouse gasses, carbon dioxide, methane, nitrous oxide and water vapor, occur naturally in the atmosphere. These greenhouse gases trap and retain energy in the Earth's atmosphere and help keep temperatures hospitable. When there is an elevated buildup of these gases in the atmosphere, however, problems may arise. Human activities are releasing large quantities of these substances into the atmosphere. For example, according to the US Environmental Protection Agency (US EPA) since the beginning of the industrial revolution atmospheric concentrations of carbon dioxide have

increased nearly 30%, methane concentrations have more than doubled, and nitrous oxide concentrations have risen by about 15%.

While concentrations of carbon dioxide (CO_2) have increased, the exact source of the recent rise in atmospheric CO_2 has not been determined with certainty. It is likely caused by an interacting combination of natural and anthropogenic forces. This appears reasonable because the magnitudes of human release and atmospheric rise are comparable, and the atmospheric rise has occurred contemporaneously with the increase in production of CO_2 from human activities following the Industrial Revolution (Soon *et al.* 1999). However, the factors that influence CO_2 concentrations are not fully understood. The current increase in CO_2 follows a 300 year warming trend following a Little Ice Age (Keigwin 1996). Some have hypothesized that the recent changes in atmospheric CO_2 can be explained by the oceans emitting gases naturally as temperatures rise following the Little Ice Age (Segalstad 1998). However, the expected associated drop in ocean CO_2 concentrations has not been observed (Sabine *et al.* 2004).

Human activities have also increased concentrations of atmospheric aerosols (microscopic, airborne particles) since pre-industrial times. Aerosols are emitted by industrial processes (fossil-fuel combustion and biomass burning) and their increased concentration offsets simultaneous warming by reducing solar radiation to the ground. Unlike greenhouse gases, which are generally long-lived, aerosols fall out of the atmosphere fairly rapidly, either dry (through sedimentation) or within rain (as condensation nuclei), and therefore are not uniformly mixed across the globe.

Atmospheric composition will continue to change throughout the 21st century. The Intergovernmental Panel on Climate Change (IPCC) Special Report on Emission Scenarios (SRES)(IPCC 2000) summarizes the results of global climate models that were used to forecast atmospheric concentrations of greenhouse gases based upon a range of emission scenarios. According to the IPCC report, emissions of CO_2 due to fossil fuel burning will strongly influence trends in atmospheric CO_2 concentration during the 21st century. By 2100, atmospheric CO_2 concentrations are projected between 540 to 970 ppm (90 to 250% above the concentration of 280 ppm in the year 1750). These projections include land and ocean climate feedbacks.

Global Temperature Records

Records show a measurable warming trend in the Earth's surface temperature over the past 100 years, with a rapid acceleration in warming over the past two decades (Figure 1). Over the past century, the global average surface temperature has increased by approximately 1º F (0.5º C). Further, 9 of the 10 warmest years on record have occurred since 1995. According to recent data released by the National Climatic Data Center (www.ncdc.noaa.gov), 2005 was likely the warmest or second warmest year in the global instrumental temperature record.

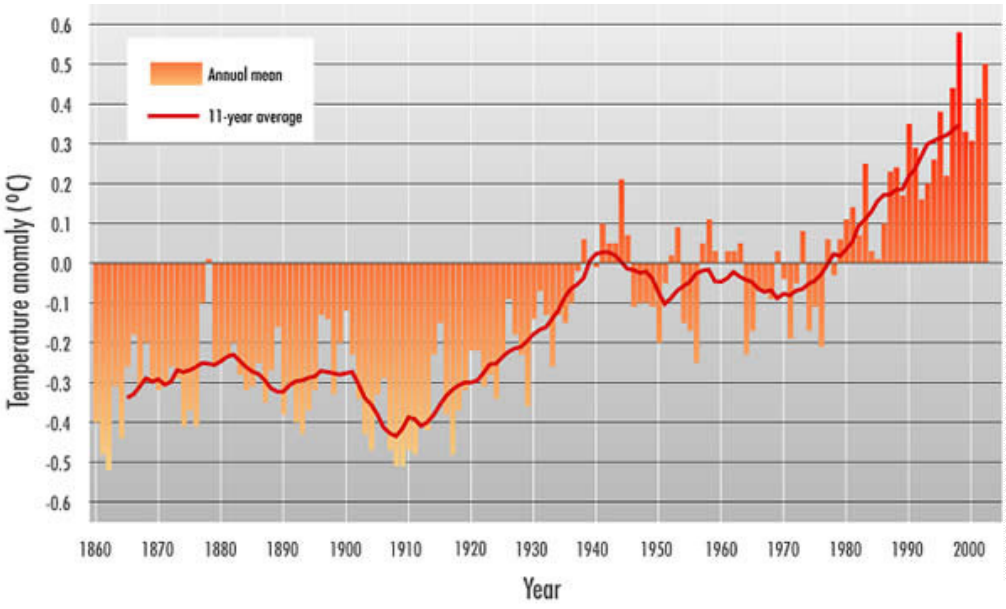

Figure1. Global mean land and sea-surface temperature anomalies for the duration of the instrumental record (Australian Bureau of Meteorology).

The Earth's surface temperature varies naturally over a wide range, but available temperature records are spatially and temporally limited. Records going back longer than 350 years are reconstructed from proxies. Reconstructed data produced from tree ring width, ice cores, and sedimentary deposits contain important limitations due to their required interpretation. For example, tree width and density have become less sensitive to changes in temperature over the last few decades (Briffa *et al.* 1998). The limited spatial extent of surface records results in only 18.4% of the Earth's surface being accurately described by direct measurement (Michaels *et al.* 2000). Further, the influence of land use change on temperature records is known to affect measurements through the urban heat island phenomenon. This systematic error has been extensively studied and debated. Peterson *et al.* (2003) found a bias in urban stations after 1990 at several stations. The researchers described the need to reassess designations of surface temperature stations as urban, suburban, or rural on a periodical basis.

Complex three-dimensional coupled ocean-atmosphere general circulation models (GCMs) can be used to predict future climate conditions under various greenhouse gas emission scenarios. Using an ensemble of GCMs and emission scenarios, the IPCC (IPCC WGI 2001) produced the range of predicted CO_2 and temperature changes shown in Figure 2. The globally averaged surface temperature is projected to increase by 2.7° to 10.4°F (1.4 to 5.8°C) over the period of 1990 to 2100. The projected rate of warming is much larger than the observed changes during the 20th century and very likely would be without precedent during at least the last 10,000 years. However, these models contain sources of uncertainty and there is a variety of debate with regards to these model predictions. An overview of the sources of uncertainty and debate is provided below.

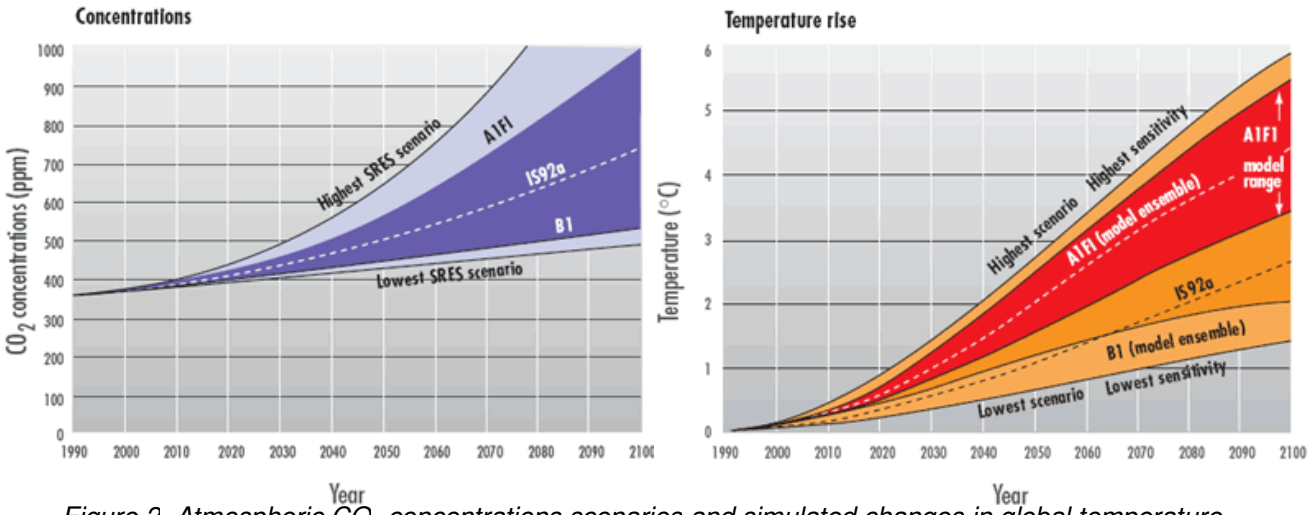

Figure 2. Atmospheric CO_2 concentrations scenarios and simulated changes in global temperature (Australian Bureau of Meteorology).

Sources of Uncertainty

As discussed above, the IPCC estimates that global average temperature will rise by between 2.7° to 10.4°F by the year 2100. Although climate models estimate that temperatures may warm, opponents of global warming theories point out that climate science cannot make definitive predictions yet because many of the physical processes modeled are only rudimentarily understood and are variously parameterized. Because the climate is a coupled, non-linear dynamic system, the climate models have many uncertainties. Without experimental validation of the models, the calculation of the climate response to increased anthropogenic atmospheric CO_2 will remain in doubt. For example, opponents of global warming theories that attribute temperature rise to human activities argue that the correlation between rising temperatures and CO_2 concentrations following the Industrial Revolution does not prove causation. The US EPA further reiterates the warning provided by all climate modelers to people considering the impacts of future climate change: *the projections of climate change in specific areas are not forecasts but are reasonable examples of how the climate might change* (US EPA).

The two primary sources of uncertainty are 1) forecasts of future greenhouse gas emissions; and 2) the nature of many feedback processes in the climate system. Future GHG emissions depend on the rate of growth of the world's economy and population, generation of energy technology, land use changes, and policies aimed at reducing emissions. Feedback processes may strongly influence global warming. For example, increased atmospheric water vapor may amplify warming, while changes in the extent of cloud cover and the characteristics of clouds may either enhance or diminish warming. Soon *et al.* (1999) discussed the following six important areas of uncertainty and error in climate modeling.

1) *Water vapor feedback* - The feedback process starts with increasing temperature that increases atmospheric water vapor concentration. Water vapor is itself a strong greenhouse agent, which in turn could amplify the warming caused by elevated CO_2. The model parameterization used to

describe this feedback mechanism is complex and has received criticism (e.g. Renno *et al.* 1994). Without adequate observations, it is difficult to determine the correct parameterization.

2) *Cloud forcing* – Climate models produce different projected temperature changes because they incorporate different estimates of the parameters that describe the behavior of cloud formation. Clouds are known to have an important influence on surface temperatures. However, current GCMs over-predict the coverage of high clouds by a factor as large as 2 to 5. The spatial distribution of clouds is also incorrect. Therefore, the parameterization of radiative, latent and convective effects of cloud forcing needs further improvements.

3) *Ocean-atmospheric interaction* – The dynamic nature of air-sea coupling is complex and requires intense *in situ* and satellite observations of heat, momentum, and freshwater fluxes. This is an active area of GCM research.

4) *Sea-ice-snow feedback* – Currently, GCM results under-predict the variance of sea-ice thickness in the Arctic on decadal to century time scales. This result emphasizes the importance of including realistic surface fluxes and modeling of convective overturning and vertical advection in both the Arctic and adjacent oceans.

5) *Biosphere-atmosphere-ocean feedbac*k – Biospheric feedback influences the global carbon budget because enhanced plant growth will sequester CO_2. Understanding this feedback holds the promise of an internally consistent description of the relationship of CO_2 to climate change.

6) *Flux errors* – Many models have substantial flux errors for which calibration adjustments are introduced into the calculations. One important consequence is the dampening of low-frequency variability in the simulation of climate state due to over stabilization.

The impacts of feedback mechanisms on predicted temperature are shown in Figure 3. Accounting for the range of uncertainty in these feedback processes results in a range of possible changes in global average temperatures for any given change in GHG concentrations. The range of temperature changes projected by the IPCC reflects the combined effects of all of these sources of uncertainty. Further, even greater uncertainty exists in regional predictions of climate change. Regional projections of impacts are most needed by decision-makers, and yet are not easily extracted from global climate model simulations. Results can sometimes even be contradictory at the regional scale, with either wetter or drier conditions predicted depending on the model used for the simulation.

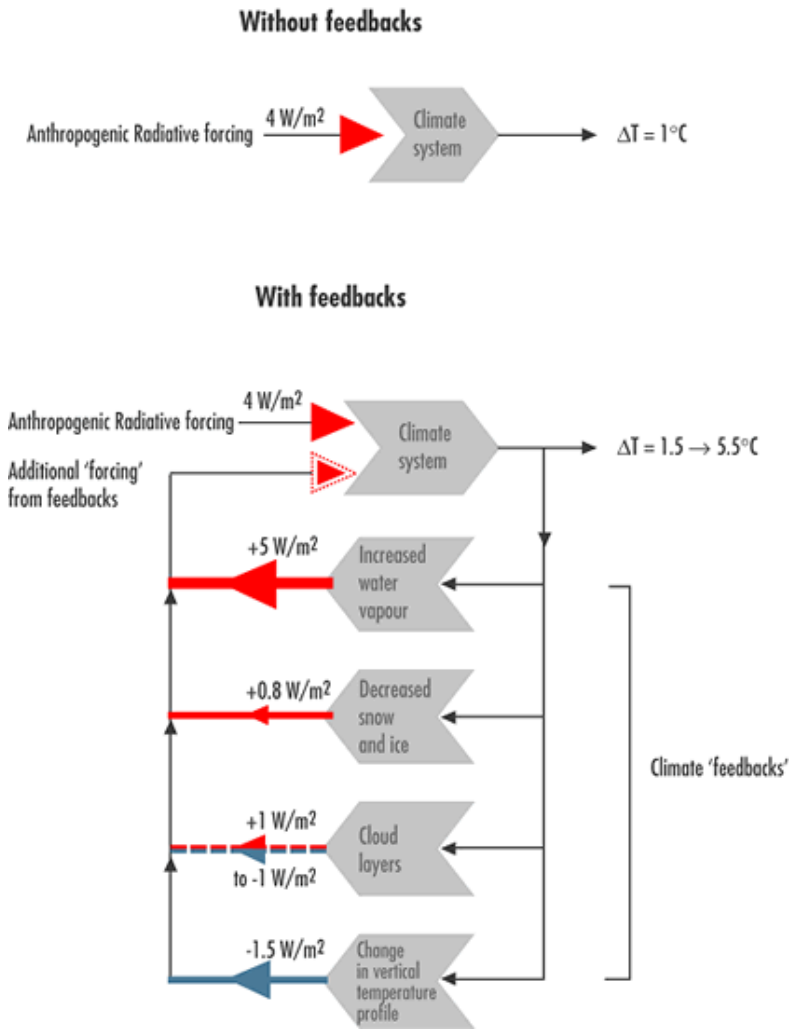

Figure 3. Schematic showing the influence of climate feedbacks on radiative forcing driving a climate model. The arrows are indicative of the magnitude and sign of individual feedbacks (Australian Bureau of Meteorology).

Potential Impacts of Climate Change on Water Resources

Although the science of climate change and predictions of future temperature and precipitation remain largely uncertain (particularly at the regional level), it is still appropriate to consider the potential impacts of such change on water resources. This information will enhance our ability to respond to change as the science advances and uncertainty is reduced. In this section, observed changes in hydrologic processes corresponding with recent warming trends in the western U.S. and potential impacts of future climate change on hydrologic processes are discussed.

Potential changes to the climate will likely alter the hydrologic cycle in ways that impact water resources. Regional climate-change projections are uncertain. However, the magnitude of projected warming combined with a strong regional reliance on mountain snowpack creates some consistency in the implication of climate change for the western U.S. The amount, intensity, and temporal distribution of precipitation could potentially change. Recent research suggests an intensification of the global

hydrological cycle, leading to more intense but possibly less frequent periods of precipitation (longer periods of drought alternating with spells of heavy rainfall) (Trenberth 2003). In the west, warmer temperatures could affect the proportion of winter precipitation falling as rain or snow, accumulation of snowpack, and snowmelt timing. Evapotranspiration could change with changes in soil moisture availability, and plant responses to elevated CO_2 concentrations. In addition, changes in the quantity of water percolating to groundwater storage could result in changes in aquifer levels, in base flows entering surface streams, and in seepage losses from surface water bodies to the groundwater system.

The overall scientific consensus is that globally the Earth will be warmer with higher globally averaged precipitation. However, current scientific understanding does not provide confident projections of the magnitude or precise nature of changed precipitation patterns. Unlike the projections of precipitation change, climate models are fairly consistent in predictions of regional surface temperature. Because temperature is central in determining the accumulation and melting of snow and ice, these scenarios are especially relevant to regions where snowpack dominates the hydrology. Even with wetter winters, a warmer climate will result in a greater portion of winter precipitation falling as rain rather than snow, an elevated winter snowline, and a decrease in the snow-covered areas and total winter snowpack (Figure 4). Some of the most sensitive areas are where winter temperatures are now only slightly below freezing. Temperature also determines the timing of melt-off, and a warmer climate will likely result in an earlier melt season. Many regions are likely to see an increase in winter or early spring stream flows and reduced summer flows.

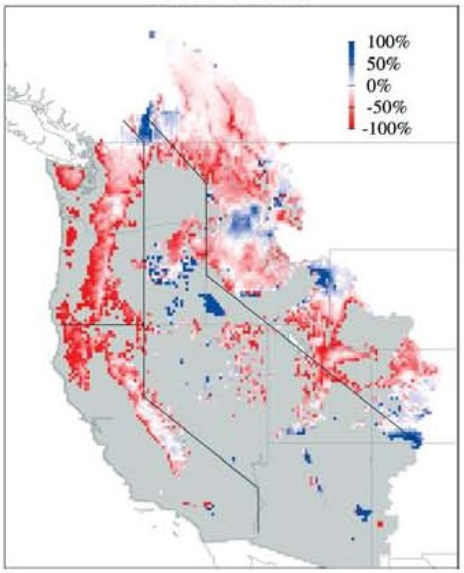

Figure 4. Linear trends in 1 Apr SWE for 1950–97 from a hydrologic simulation (Mote et al. 2003).

The results of warmer temperatures have been observed across the western U.S. Winter and spring temperatures have increased in western North America during the twentieth century (Folland *et al.* 2001), and there is a large body of evidence suggesting this widespread warming has produced changes in hydrology and plants. In the western U.S and southwestern Canada, spring snowpacks have been smaller and have been melting earlier in most mountain areas. Snow extent and depth have generally decreased in the west (Mote 2003). These declines have often occurred despite increases in total winter precipitation in those locations. The timing of spring snowmelt-driven streamflow has shifted earlier in the year (Cayan *et al.* 2001; Stewart *et al.* 2005), as is expected in a warming climate (Figure 5). There has also been a century-long downward trend in late spring and early summer flow as a proportion of total annual flow (Dettinger and Cayan 1995). Earlier spring melting and reduced spring snowpacks have been especially evident in the Cascade and northern Sierra Nevada Mountains, where winter temperatures are relatively mild. Some higher elevation mountain locations in the Southern Sierra Nevada and Rocky

Mountain ranges have shown an increasing trend in April 1 snowpacks, but even there the peak in spring runoff is generally occurring earlier (Stewart *et al.* 2004).

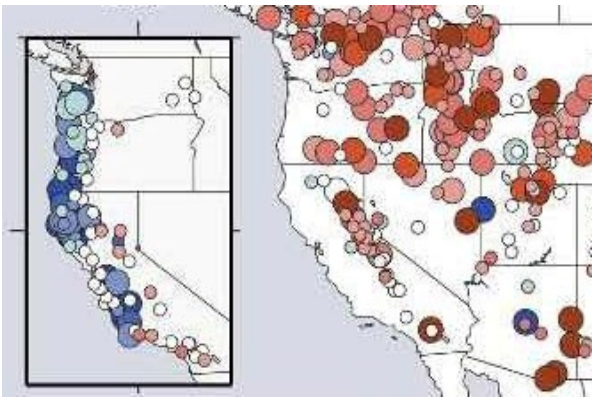

Figure 5. Trends in the date of center of mass of annual flow for snowmelt- and (inset) non-snowmelt-dominated gauges. Shading indicates magnitude of the trend expressed as the change (days) in timing over the 1948–2000 period (red negative and blue positive) (Stewart et al. 2005).

Dettinger *et al.* (2004) completed a simulation of hydrologic response to climate variation and change in three Sierra Nevada watersheds (including the Carson River watershed). The research used climate predictions from a GCM coupled with a hydrologic model to investigate future changes in streamflow. Although the climate model projections were near the lower edge of the available climate change simulations, in terms of warming and changes in precipitation, the results still showed significant and disruptive changes in the hydrology and ecosystems of the simulated basins. Predicted outcomes included large and clear trends towards earlier snowmelt runoff and reductions in summertime low flows and soil moisture. They found that snowmelt and streamflow could arrive about one month earlier by 2100 in response to an increased proportion of rain to snow and earlier snowmelt episodes.

Warming of the climate could increase total evaporation from open water, soil, shallow groundwater, and water stored on vegetation, along with transpiration through plants. The interplay between atmospheric energy, moisture, and turbulence, and plant water use efficiency under different water, energy, nutrient, and CO_2 levels is complex and not yet fully understood. In dry regions, water availability, surface temperature and wind are important determinants of actual evaporation. Increases in surface temperature and higher wind speeds promote potential evaporation, while the greatest change will likely result from an increase in the water-holding capacity of the atmosphere.

The loss of snowpack could have a greater impact on groundwater recharge than estimates based only on changes in the amount of precipitation would indicate. Because snowmelt yields more recharge per unit amount of precipitation than rain, even if total precipitation remains constant, a shift from snow to rain could cause significantly decreased recharge (Earman *et al.* 2006). While the lessened amount of snowfall would be one contributor to loss of recharge, the changed conditions could also reduce the recharge efficiency of snow compared to that observed today. Thinner snowpacks subjected to increased temperatures would melt more rapidly than at present, increasing the likelihood of the melt running off rather than infiltrating.

Future climate change could influence municipal and industrial water demands, as well as competing agricultural irrigation demands. Municipal demand depends on climate to a certain extent, especially for garden, lawn, and recreational field watering, but rates of use are highly dependent on utility

regulations. Shiklomanov (1999) notes different rates of use in different climate zones, although in making comparisons between cities it is difficult to account for variation in non-climatic factors. Studies in the UK (Herrington 1996) suggest that a rise in temperature of about 1.1°C by 2025 would lead to an increase in average per capita domestic demand of approximately 5 percent – in addition to non-climatic trends – but would result in a larger percentage increase in peak demands, since demands for landscape watering may be highly concentrated.

This section highlights some of the potential changes that could occur if regional climatic shifts occur as predicted from current climate models. While it is prudent to understand these potential impacts, further analyses are needed prior to concluding that global warming is impacting the Truckee Meadows region and implementing changes to water resource management.

Appendix

Long-term records of temperature and greenhouse gases

In order to provide context for recent changes in climate, it is helpful to investigate long-term climatic patterns. There is strong evidence that the Earth has experienced long periods during which average global temperatures were much colder and much warmer than today. Changes in the Earth's climate system throughout geologic time can be linked to changes in the components of the climate system, changes in the composition of the atmosphere, and the seasonal distribution and total amount of incoming solar energy.

The composition of the atmosphere has changed as a result of biological and geophysical processes, including storage of carbon in the ocean and its subsequent release, volcanic eruptions, and the occasional sudden release of methane from ocean floor sediments.

Three long-term cycles in the Earth's orbit combine to give a complicated pattern. Eccentricity is the change in the shape of the earth's orbit around the sun. Over a 95,000 year cycle, the earth's orbit around the sun changes from a thin ellipse to a circle and back again. When the orbit around the Sun is most elliptical, there is larger difference in the distance between the Earth and Sun at perihelion (period when the Earth is closet to the Sun) and aphelion (period when the Earth is farthest from the Sun). The Earth is currently in a period of low eccentricity (nearly circular). Obliquity describes the slight change in the Earth's tilt (22.1° and 24.5°) over a cycle that lasts about 42,000 years. When the tilt is larger, seasons are stronger and less snow melts in the polar regions because of the shorter days and reduced sunlight, allowing glaciers to form and spread. The Earth's tilt is currently 23.5°. The third type of orbital change is called precession, the cyclical wobble of Earth's axis in a circle. One complete cycle for Earth takes about 26,000 years. Precession does not directly cause temperature changes, but rather it changes the portion of the orbit at which a given season occurs. The current axis results in the Earth being closest to the Sun during the North American winter, resulting in milder seasonal fluctuations. This is important because glaciers require land on which to form. Most of the land surface on Earth is now in the northern hemisphere. Therefore, when the Earth's axis is oriented for northern winters to occur on the cooler part of the orbit, glaciers will tend to grow.

Changes in the seasonal distribution of incoming solar energy may have triggered the beginning and end of previous ice ages. However, the solar impacts were greatly amplified by positive feedbacks within the climate system, including changes in the reflection of sunlight back into space by ice-covered areas, changes in ocean circulation, and dramatic changes in atmospheric concentrations of greenhouse gases, especially CO_2 and CH_4.

Ice cores from glaciers and ice sheets around the world provide some of the best records of environmental conditions and climate change. In January 1998, the collaborative ice-drilling project between Russia, the United States, and France at the Vostok station in East Antarctica yielded the deepest ice core ever recovered, reaching a depth of 3,623 m (Petit *et al.* 1999). The Vostok ice-core record extends through four climate cycles, with ice slightly older than 420,000 years (Figure 6). The

Vostok data revealed a high correlation between GHG concentrations and temperature variations through four glacial cycles (Shackleton 2000). Atmospheric carbon dioxide concentrations varied from about *180 parts per million* (ppm) at the height of each glaciation to about *310 ppm* at the peak of each warming. Similarly, methane concentrations varied from approximately *350* to *800 parts per billion (ppb)*. The current atmospheric CO_2 concentration is approximately *375 ppm* and the methane concentration is approximately *1800 ppb* (Figure 3).

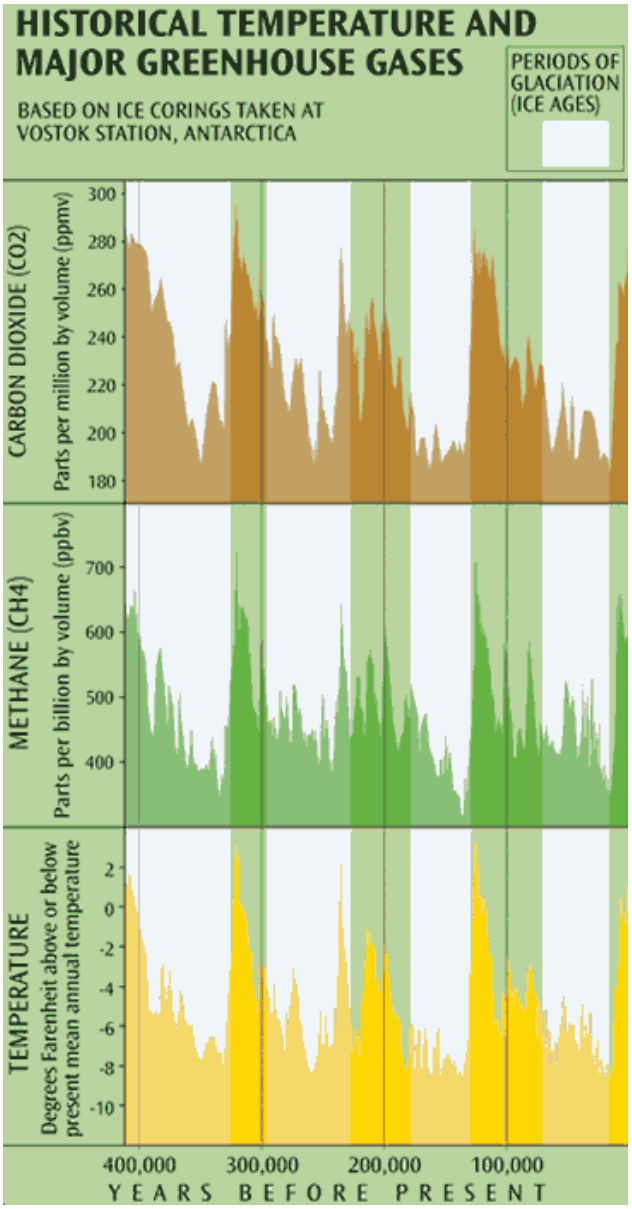

Figure 6. Temperature and GHG records from the Vostok Ice Corps (Petit et al. 1999).

Ocean Circulation Patterns

In addition to GHG concentrations, several natural processes influence the Earth's climate over various periods of time. Recent studies have shown the influence of coupled oceanic-atmospheric variability on climate of regions around the world. The most widely understood oceanic and atmospheric phenomenon is the El Niño-Southern Oscillation (ENSO). Other large-scale climate occurrences include the Pacific Decadal Oscillation (PDO), the Atlantic Multidecadal Oscillation (AMO), and the North Atlantic Oscillation (NAO).

ENSO is a major source of inter-annual climate variability in the western United States. ENSO variations are more commonly known as El Niño (the warm phase of ENSO) or La Niña (the cool phase of ENSO). An El Niño is characterized by stronger than average sea surface temperatures in the central and eastern equatorial Pacific Ocean, reduced strength of the easterly trade winds in the Tropical Pacific, and an eastward shift in the region of intense tropical rainfall (Figure 7). A La Niña is characterized by the opposite – cooler than average sea surface temperatures, stronger than normal easterly trade winds, and a westward shift in the region of intense tropical rainfall. Although ENSO is centered in the tropics, the changes associated with El Niño and La Niña events affect climate around the world. These events are typically on the order of 6 and 18 months in length (Tootle and Piechota 2004).

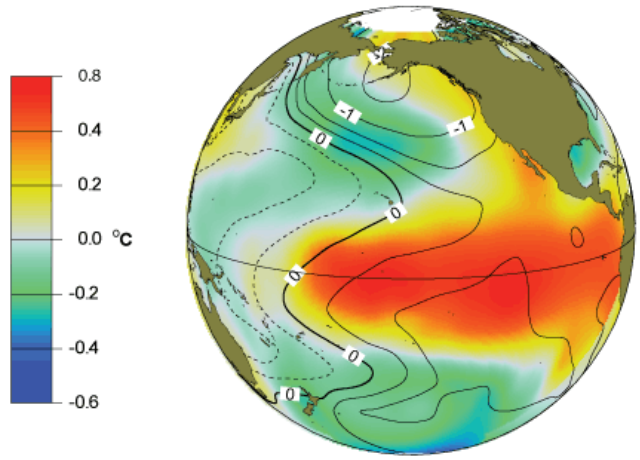

Figure 7. ENSO warm phase (http://www.cses.washington.edu/cig/).

The PDO is an oceanic-atmospheric phenomena associated with persistent, bimodal climate patterns in the northern Pacific Ocean that oscillate with a characteristic period on the order of 50 years (Mantua and Hare 2002). When the PDO is in its positive coastal warm phase, as it was for most of the period from 1977 through the mid-1990s, sea surface temperatures along the west coast of North America are unusually warm, the winter Aleutian low intensifies, and the Gulf of Alaska is unusually stormy. The slowly evolving state of the ocean, as measured by the PDO, interacts with the more rapid ENSO-related changes to influence storm tracks and, thus, the likelihood of unusually heavy or light seasonal precipitation. For example, a positive PDO appears to reinforce the effects of an El Niño, making wet winter conditions in the southwestern United States and dry conditions in the Pacific Northwest more likely than would be the case if the PDO were in the negative (coastal cool) phase.

The North Atlantic Oscillation (NAO) is associated with a meridional oscillation in atmospheric mass between Iceland and the Azores and has displayed quasi-biennial and quasi-decadal behavior since the late 1800s (Hurrell and Van Loon 1997) and its behavior is generally referred to as decadal. A positive NAO pattern drives strong, westerly winds over northern Europe, while southern Europe, the Mediterranean and Western Asia experience unusually cool and dry conditions. In the negative phase, winter conditions are unusually cold over northern Europe and milder than normal over Greenland, northeastern Canada, and the Northwest Atlantic. The Atlantic Multidecadal Oscillation (AMO) is observed through North Atlantic Ocean sea surface temperature variability with a periodicity of 65–80 years (Gray *et al.* 2004).

Thermohaline circulation in the World's oceans provides the connection between the movement of cold, salty water in the oceans' depths and the movement of warm, less saline water at the surface (Broecker 1997). Warm, low-salinity water from the tropical Pacific and Indian Oceans flows around the tip of South Africa and ultimately joins the Gulf Stream to transport heat from the Caribbean to Western Europe. As the water moves northward, evaporative heat loss cools the water and leaves it saltier and more dense. The cold, salty water sinks in the North Atlantic and flows back toward Antarctica, thus pushing the conveyor along. It is likely that increased high-latitude runoff and ice-melt caused by human-induced climate change will slow the thermohaline circulation. However, the impacts on projected temperature changes for Europe and the northern latitudes are not clear (IPCC WGI 2001).

References

Australian Bureau of Meteorology. 2006. http://www.bom.gov.au/publications.

Briffa, K. R., Jones, P. D., Schweingruber, F. H. and Osborn, T. J. 1998. Influence of volcanic eruptions on Northern Hemisphere summer temperature over the past 600 years. Nature, 6684: 450-454.

Broecker, W.S. 1997. Thermohaline Circulation, the Achilles Heel of Our Climate System: Will Man-Made CO2 Upset the Current Balance? Science, 278(5343): 1582 – 1588.

Cayan, D.R., Kammerdiener, S.A., Dettinger, M.D. and Caprio, J.M. 2001. Changes in the Onset of Spring in the Western United States. Bulletin of the American Meteorological Society, 82(3): 399-416.

Dettinger, M. D., Cayan, D. R., Meyer, M. K., and Jeton, A. E. 2004. Simulated Hydrologic Responses to Climate Variations and Change in the Merced, Carson, and American River Basins, Sierra Nevada, California, 1900-2099. Climatic Change, 62(1): 283-317.

Dettinger, M. D. and Cayan, D. R. 1995. Large-Scale Atmospheric Forcing of Recent Trends toward Early Snowmelt Runoff in California. Journal of Climate, 8(3): 606.

Earman, S., Campbell, A.R., Phillips, F.M. and Newman, B.D. 2006. Isotopic exchange between snow and atmospheric water vapor: Estimation of the snowmelt component of groundwater recharge in the southwestern U.S.A. Accepted for publication in Journal of Geophysical Research.

Folland, C. K., Rayner, N. A., Brown, S. J., Smith, T. M., Shen, S. S. P., Parker, D. E., Macadam, I., Jones, P. D., Jones, R. N. and Nicholls, N. 2001. Global temperature change and its uncertainties since 1861. Geophysical Research Letters, 28(13): 2621-2624.

Gray, S. T., Graumlich, L. J., Betancourt, J. L. and Pederson, G. T. 2004. A tree-ring based reconstruction of the Atlantic Multidecadal Oscillation since 1567 A.D. Geophysical Research Letters, 31(12): 12205.

Herrington, P. 1996. Climate change and the demand for water. Great Britain Dept. of the Environment, London. ISBN: 0117531383.

Hurrell, J.W. and Van Loon, H. 1997. Decadal Variations in Climate Associated with the North Atlantic Oscillation. 36(3): 301-326.

IPCC WGI. 2001. Third Assessment Report – Summary for Policymakers. http://www.ipcc.ch/pub/spm22-01.pdf.

IPCC. 2000. Special report on emissions scenarios : a special report of Working Group III of the Intergovernmental Panel on Climate Change. Cambridge University Press, UK. http://www.grida.no/climate/ipcc/emission.

Keigwin, L. D. 1996. The Little Ice Age and Medieval Warm Period in the Sargasso Sea. Science, 5292: 1504-1507.

Mantua, N. J. and Hare, S. R. 2002. The Pacific Decadal Oscillation. Journal of Oceanography, 58(1): 35.

Michaels, P.J., Knappenberger, P.C. and Davis. R.E. 2000. The way of warming. Regulation 33:10-16.

Mote, P.W. 2003. Trends in snow water equivalent in the Pacific Northwest and their climatic causes. Geophysical Research Letters, 30(12): 3-58.

Petit, J. R., Jouzel, J., Raynaud, D., Barkov, N. I., Barnola, J.-M., Basile, I., Bender, M., Chappellaz, J., Davis, M. and Delaygue, G. 1999. Climate and atmospheric history of the past 420,000 years from the Vostok Ice core, Antarctica. Nature, 6735: 429-436.

Peterson, T.C. 2003. Assessment of Urban Versus Rural In Situ Surface Temperatures in the Contiguous United States. Journal of Climate, 16(18): 2941-2959.

Renno, N. O., Stone, P. H. and Emanuel, K. A. 1994. Radiative-convective model with an explicit hydrologic cycle, 2, Sensitivity to large changes in solar forcing. Journal of Geophysical Research, 99(D/8): 17001.

Segalstad, T.V. 1998. Carbon cycle modelling and the residence time of natural and anthropogenic atmospheric CO2. Global Warming the Continuing Debate. Cambridge Press, Cambridge, UK.

Sabine, C. L., Feely, R. A., Gruber, N., Key, R. M., Lee, K., Bullister, J. L., Wanninkhof, R., Wong, C. S., Wallace, D. W. R. and Tilbrook, B. 2004. The Oceanic Sink for Anthropogenic CO2. Science, 305(5682): 367-370.

Shiklomanov, I.A. 1999. World Water Resources and their Use. Database on CD Rom. Paris, UNESCO.

Soon, W., Baliunas, S. L., Robinson, A. B. and Robinson, Z. W. 1999. Environmental effects of increased atmospheric carbon dioxide. Climate Research, 13(2): 149-164.

Stewart, I.T., Cayan, D.R. and Dettinger, M.D. 2004. Changes in Snowmelt Runoff Timing in Western North America under a `Business as Usual' Climate Change Scenario. Climatic Change, 62(3): 217-232.

Stewart, I.T., Cayan, D.R. and Dettinger, M.D. 2005. Changes toward Earlier Streamflow Timing across Western North America. Journal of Climate, 18: 1136.

Shackleton, N. J. 2000. The 100,000-Year Ice-Age Cycle Identified and Found to Lag Temperature, Carbon Dioxide, and Orbital Eccentricity. Science, 5486: 1897-1901.

Tootle, G.A. and Piechota, T.C. 2004. Evaluation of climate factors to forecast streamflow of the Upper Truckee River. Journal of the Nevada Water Resources Association, 1(1): 7-19.

Trenberth, K. E. 2003. The Changing Character of Precipitation. Bulletin of the American Meteorological Society, 84(9): 1205-1218.

U.S. EPA. 2006. Global Warming-Climate. http://yosemite.epa.gov/oar/globalwarming.

Hydrologic Trend Analyses for the Truckee Meadows Region

prepared by

Mark Stone, Ph.D.
Division of Hydrologic Sciences
Desert Research Institute

Hilary Lopez, Ph.D.
Truckee Meadows Water Authority

prepared for

Truckee Meadows Water Authority
1355 Capital Boulevard
Reno, NV 89520

July 2006

Hydrologic Trend Analyses for the Truckee Meadows Region

Executive Summary

Environmental change can result from a wide range of human induced activities and natural processes including land use change, resource management, and potential global climate change. These changes can influence all aspects of the hydrologic cycle including the magnitude, timing, and forms of precipitation, snowfall, streamflow, and lake volumes. The objective of this project was to investigate climate and hydrologic data in the Truckee Meadows region in order to reveal potential signs of environmental change that may be consistent and coincident with global warming. The analyses included investigations of temperature, precipitation, snow water equivalent, streamflow volume and timing, and reservoir volumes for the for the Lake Tahoe and Truckee River hydrographic basins.

Linear regression analyses were used to identify the following data trends:

- Temperature data revealed a slight trend towards increased minimum and maximum temperatures at most gages. However, a few stations showed trends towards decreased temperatures and year to year variability was quite high at all stations.
- Annual precipitation showed very high variability with an overall trend towards slightly reduced winter precipitation.
- Snow water equivalent (SWE) showed very high variability with some stations reporting a trend towards increased snowpack and others showing reduced snowpack trends.
- The SWE trends were highly correlated with instrument elevation, where high elevation stations observed increased SWE and the low elevation stations observed reduced SWE.
- Mean annual streamflow data varied widely between water years.
- Long-term streamflow volume and timing trends were investigated through linear regressions of the cumulative streamflow volumes. The records revealed no consistent trends in streamflow volume or timing for the period of record.
- Cumulative volume linear regression analyses were also used to investigate trends in reservoir volumes. The reservoir volumes displayed an obvious dependence on precipitation, as periods of drought strongly influenced reservoir volumes.

In order to investigate correlations between hydrologic variables and possible modifications in hydrologic processes, the following double-mass analyses were conducted:

- Relationships between streamflow and precipitation were studied at four paired stations. The results confirmed the expected high degree of correlation between these variables. The functions between precipitation and streamflow remained consistent throughout the records, indicating no observed modifications in large scale precipitation-runoff-streamflow processes at un-dammed gages.
- Double mass analysis of precipitation and reservoir volumes further demonstrated the high degree of correlation between these variables.
- Analyses of SWE and streamflow data revealed a slight deviation from historical trends over the past four water years.
- No consistent departures from long term patterns were observed between streamflow and reservoir volumes.
- Patterns between SWE and reservoir volumes remained consistent throughout the period of record.

To summarize, no significant changes were found in the climatic and hydrologic variables over the period of record. Temporal trends in temperature, winter precipitation, and SWE were observed at some stations. However, very high year-to-year variability was observed for all stations and parameters.

Methodology

Volume and timing analyses were performed on historic gage records throughout the region. A Geographic Information Systems (GIS) based inventory was produced containing regional weather stations, snowcourses, stream gages, and reservoir levels. Details of the database components are given below. The database was then used to investigate changes in precipitation, snowpack, streamflow volume and timing, and reservoir volumes over the period of record. This investigation was conducted using mass and double-mass analyses of the climate and hydrologic variables. The analyses are summarized in Table 1. The details of the analyses for specific variables are given within the discussion of results.

Table 1. Summary of mass and double-mass analyses

Mass Analyses	**Double-Mass Analyses**
- Temperature	- Precipitation vs. Snowpack
- Precipitation	- Precipitation vs. Streamflow
- Snowpack	- Precipitation vs. Reservoir Volumes
- Streamflow	- Streamflow vs. Snowpack
- Reservoir Volumes	- Streamflow vs. Reservoir Volumes
	- Reservoir Volumes vs. Snowpack

Database Development

Weather Stations

A GIS database was developed to store, retrieve, and analyze climate and hydrologic data. GIS shapefiles were obtained from Truckee Meadows Water Authority (TMWA), Environmental Protection Agency (EPA), and the United States Geologic Survey (USGS). Climate data were compiled from the National Weather Service (NWS) Cooperative Observer Program (COOP). Weather station records included precipitation and minimum and maximum temperature data. All COOP gages within 50 miles of the Truckee and Carson River basins were identified. The Carson River basin was included in this study to augment the limited number of qualified gages in the Truckee River basin, particularly for the double mass analyses. This process revealed approximately 35 gages. The study gages were filtered both geographically and according to available period of record. Filtering resulted in 11 gages being considered in the study (Figure 1). The station locations were added to the GIS database and the historical data was requested from the Western Regional Climate Center. The time series data were linked to the GIS database in a hyperlink format. Details of the gage records can be found in Appendix L.

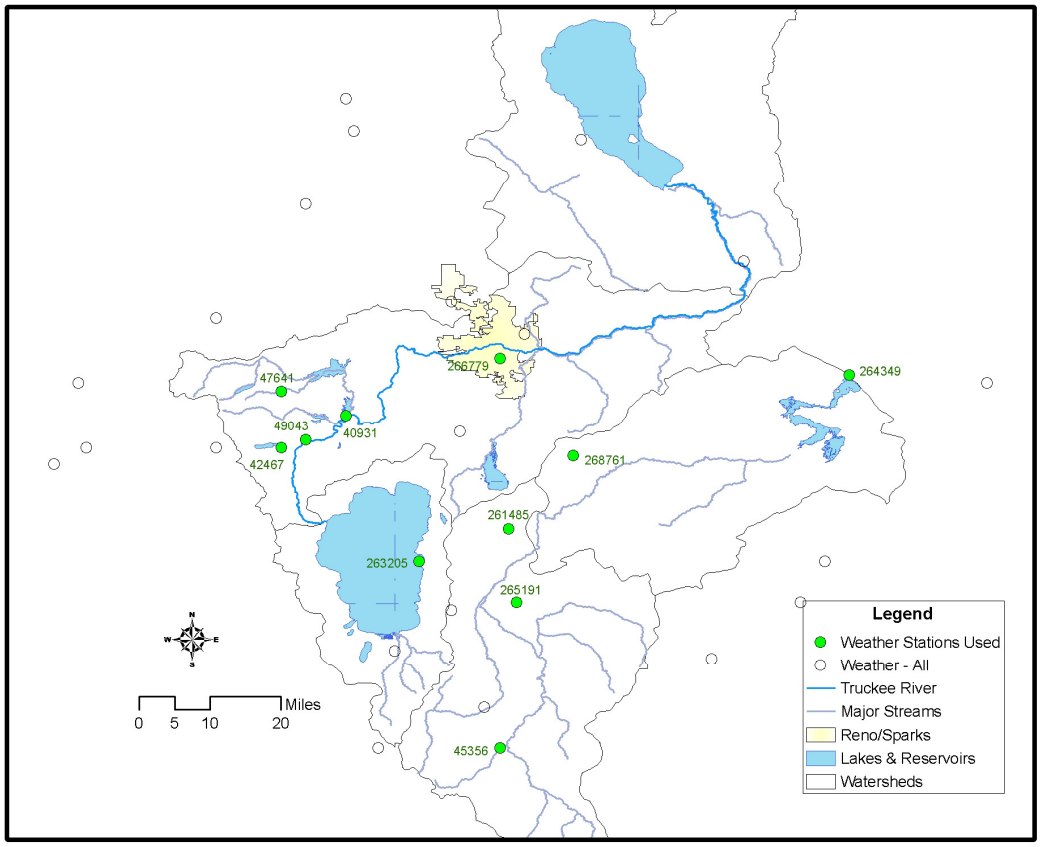

Figure 1. Truckee and Carson River basins and locations of study weather stations.

Reservoir Volume and Stream Discharge

Daily and monthly records of lake and reservoir storage volumes for all major water bodies were requested from the USGS and the data were linked to the GIS database. Daily historical streamflow records were downloaded from the USGS NWISWeb Water Data website. As with the climate data, data records and station coordinates were obtained for all stream gage stations in the region. The potential gages were then filtered to identify the gages with adequate periods of record. This resulted in 24 gages to be considered in the analysis (Figure 2). The time series data were linked to the GIS database in a hyperlink format. Details of the reservoir and stream gage records can be found in Appendix L.

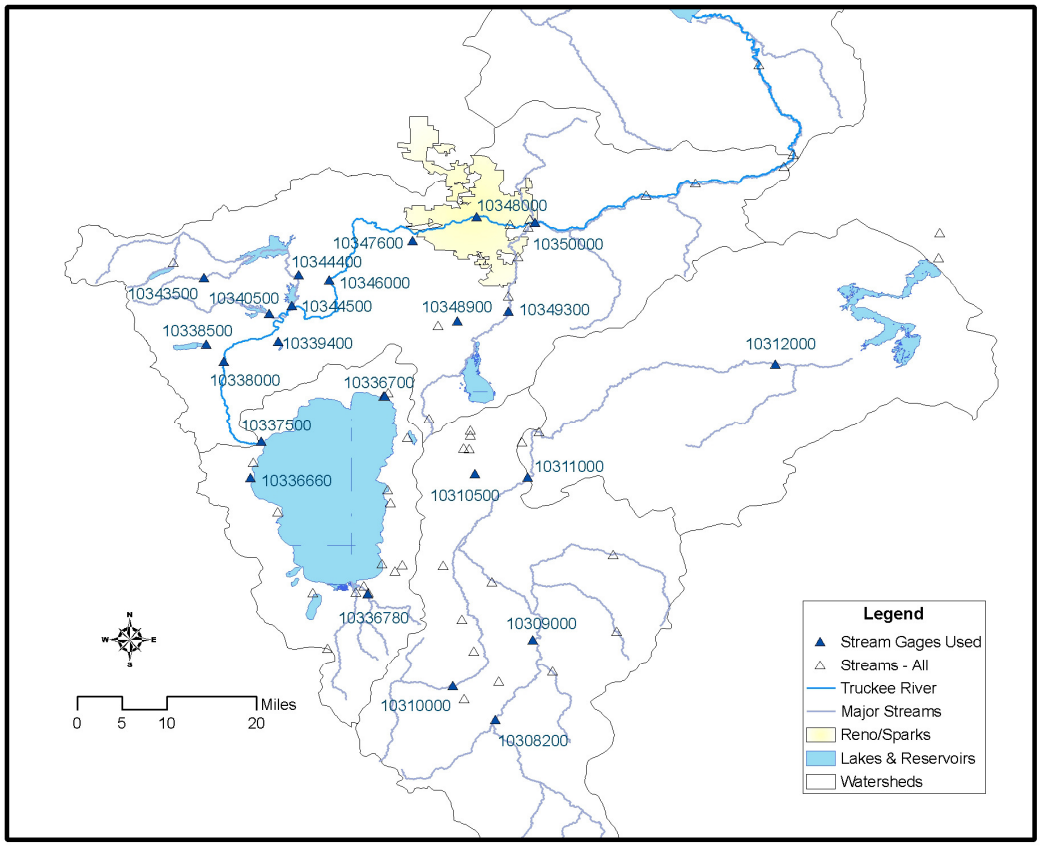

Figure 2. USGS streamgage stations for the Truckee and Carson River Basins.

SNOTEL and Snowcourse Data

Snow water equivalent data were first obtained for all regional NRCS SNOTEL stations. However, the SNOTEL data were only available from 1980 forward. To extend the period of analysis, historical snowcourse data were also obtained. Although the snowcourse data are only available at a limited temporal resolution, the periods of record extend back more than 50 years at many of the stations. The snowcourse stations used in the study are shown in Figure 3. The snowcourse data were linked to the GIS database in a hyperlink format. Details of the snowcourse records can be found in Appendix L.

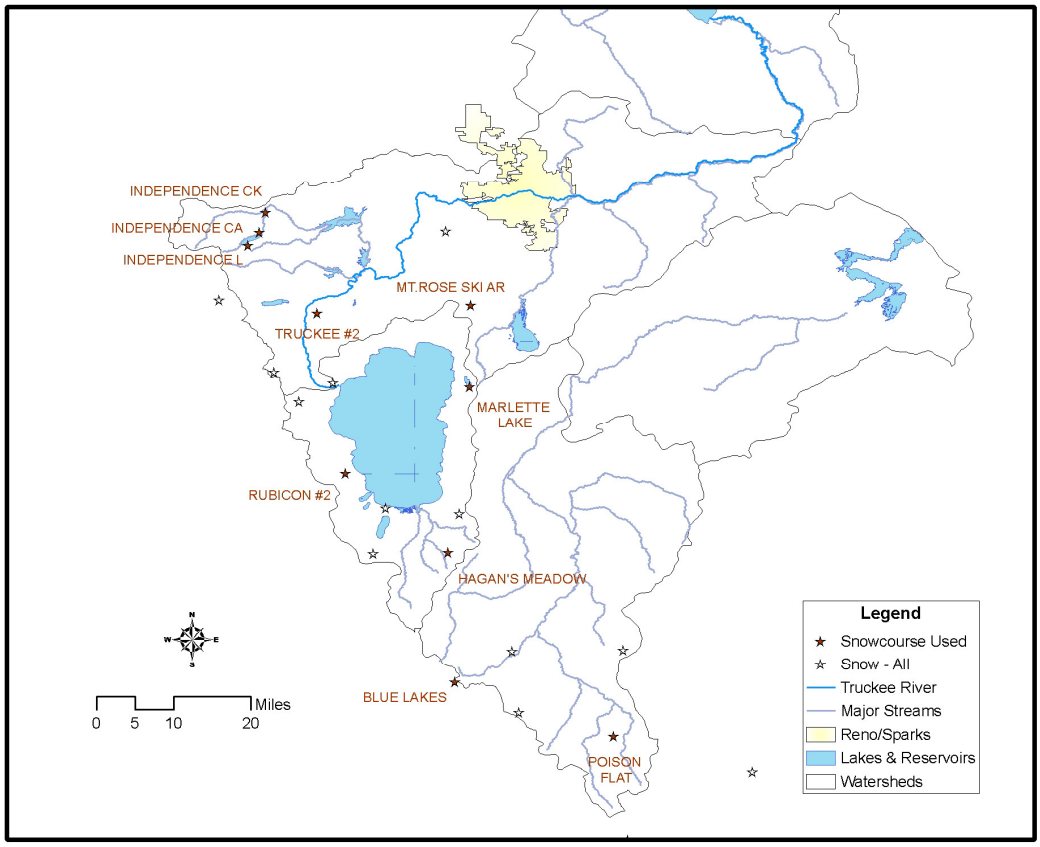

Figure 3. Snowcourse station locations in the Truckee and Carson River basins.

Results

Temperature Data

Linear regressions were used to evaluate trends in annual minimum and maximum temperature at eight weather stations. As an example of the regression results, Figure 4 shows temperature data for the Truckee Ranger Station. Results for the remaining stations can be found in Appendix A. The data revealed a slight trend towards increased minimum and maximum temperatures at five gages. However, three stations showed a trend towards decreased temperatures and year to year variability was quite high at all stations. The regional temperature trends were overall less than the observed global increase in surface temperature of approximately 1º F over the past century.

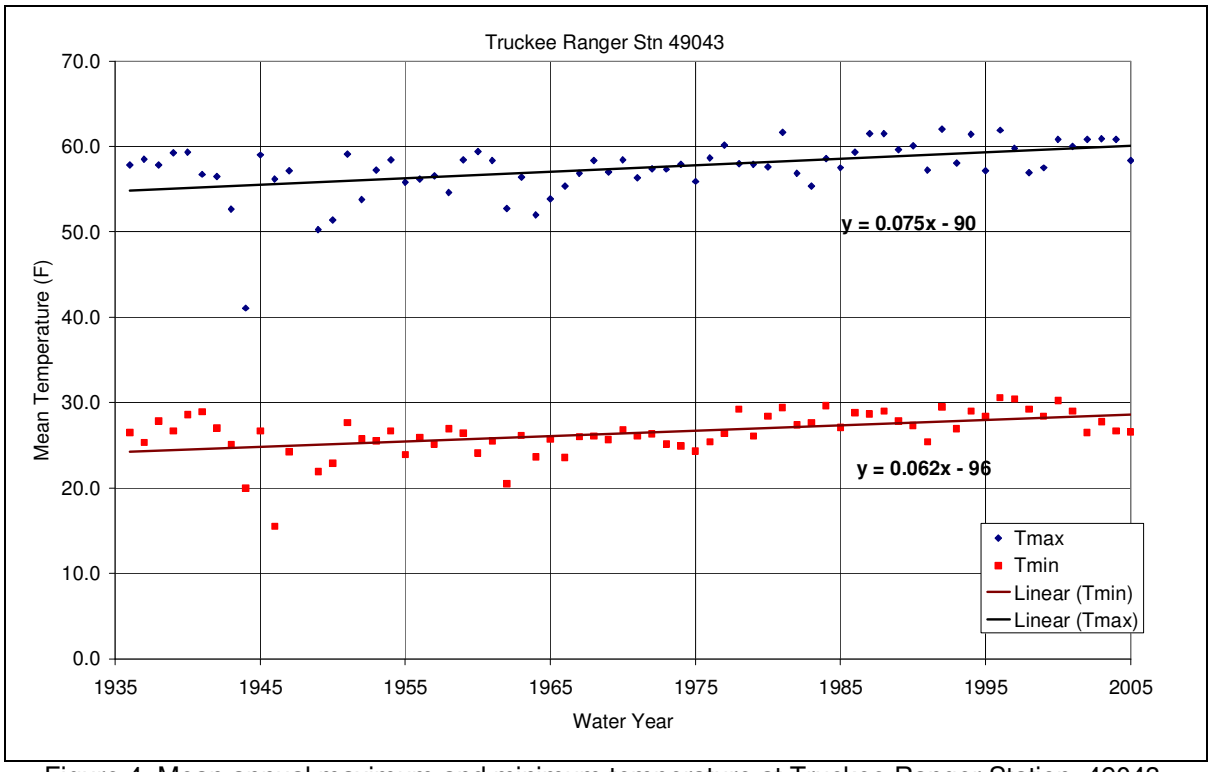

Figure 4. Mean annual maximum and minimum temperature at Truckee Ranger Station, 49043.

Precipitation

Precipitation data were examined over a range of temporal scales. Figures 5 and 6 contain seasonal precipitation trends for the Sagehen Creek and the Reno Airport, respectively. The seasons were defined as Winter (October through March) and Summer (April through September). The precipitation showed very high year-to-year variability at all stations. Winter precipitation displayed a slight decreasing trend for seven out of the nine stations. Little or no trend was observed in mean summer precipitation. Results for the remaining precipitation trends are shown in Appendix B.

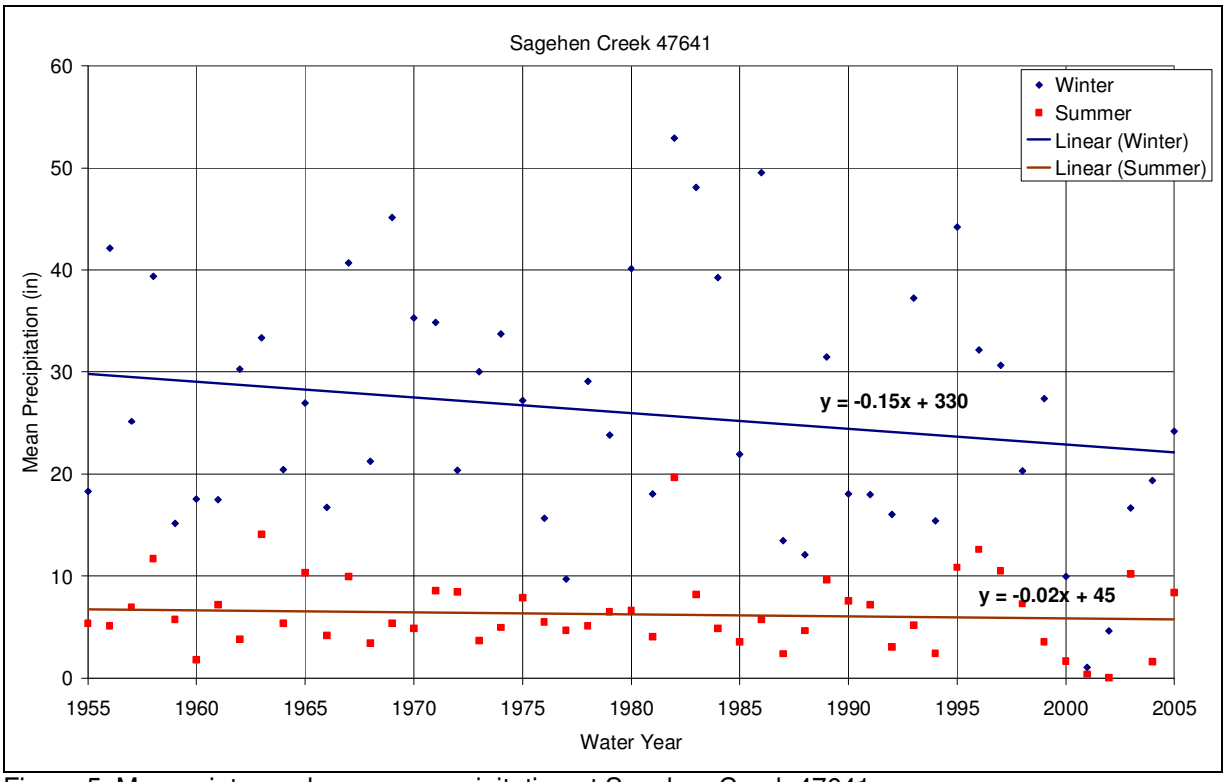

Figure 5. Mean winter and summer precipitation at Sagehen Creek 47641.

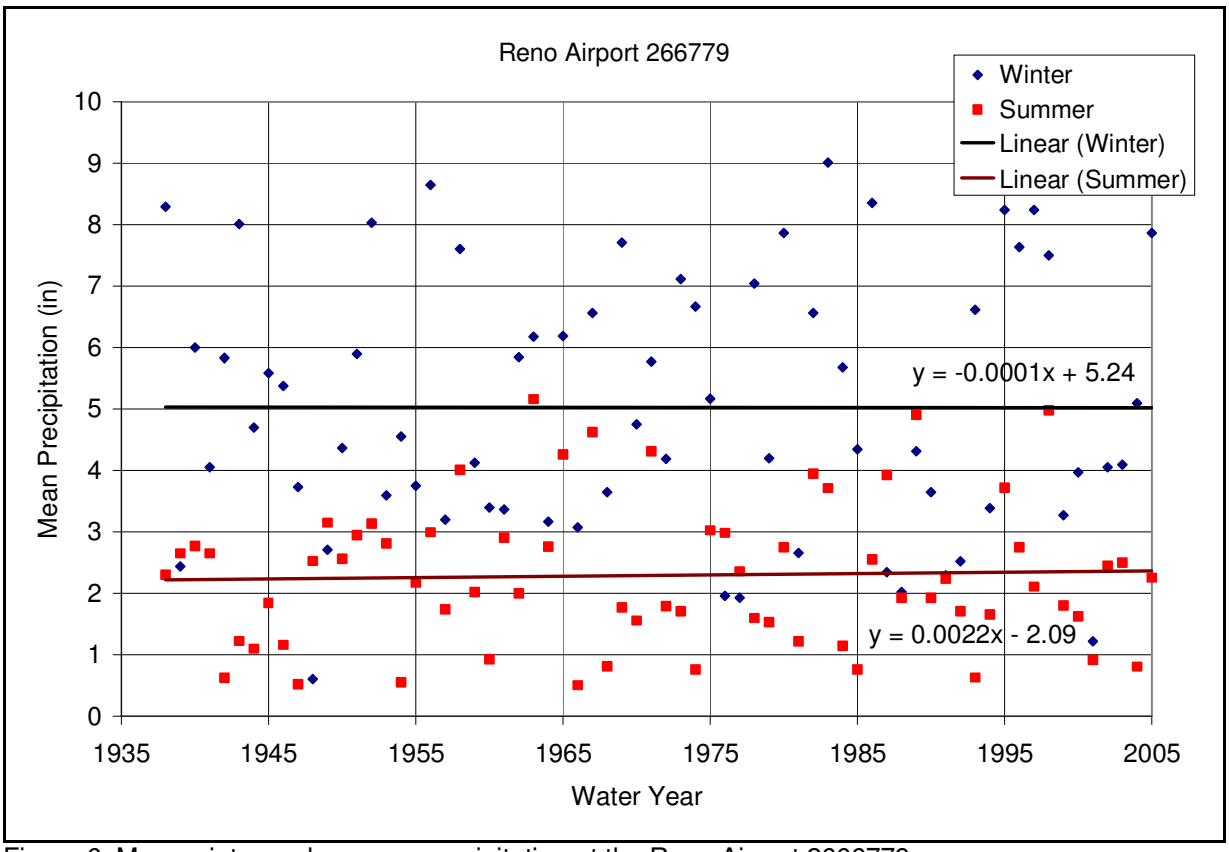

Figure 6. Mean winter and summer precipitation at the Reno Airport 2666779.

Snow Water Equivalent

Snow water equivalent (SWE) showed very high variability with some stations reporting a slight trend towards increased snowpack and others showing reduced snowpack trends. For example, SWE trends for Independence Creek and Mt. Rose Ski Area snowcourse stations are shown in Figures 7 and 8, respectively. Although SWE trends were very small, and variability was very high, the trends were highly correlated with instrument elevation. High elevation stations observed increased SWE and the low elevation stations observed reduced SWE (Figure 9). Although this observation is consistent with expectations for climate change, further investigations of precipitation and temperature trends in the Truckee Meadows (discussed above) did not corroborate this hypothesis. For example, high elevation weather stations did not observe increased precipitation and temperature changes were not correlated with elevation. The remaining SWE data can be found in Appendix C.

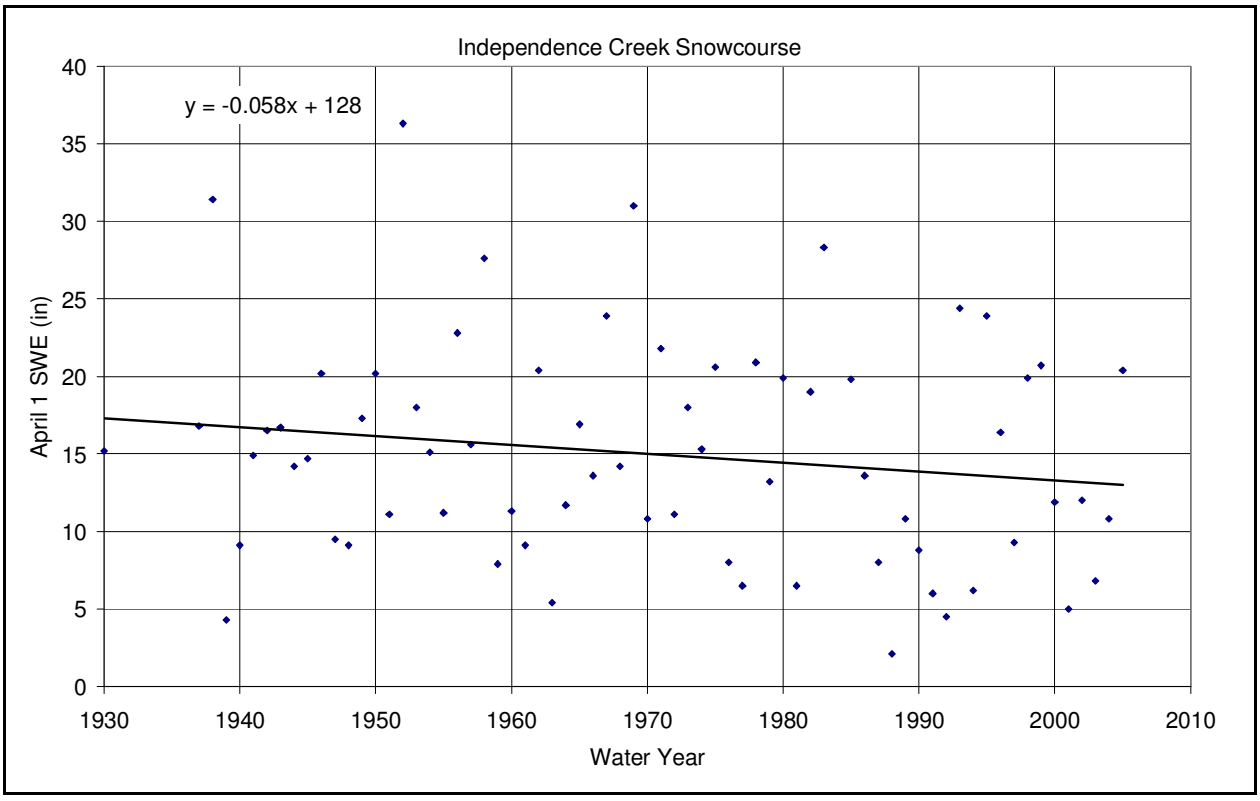

Figure 7. Annual April 1st SWE at the Independence Creek snowcourse station.

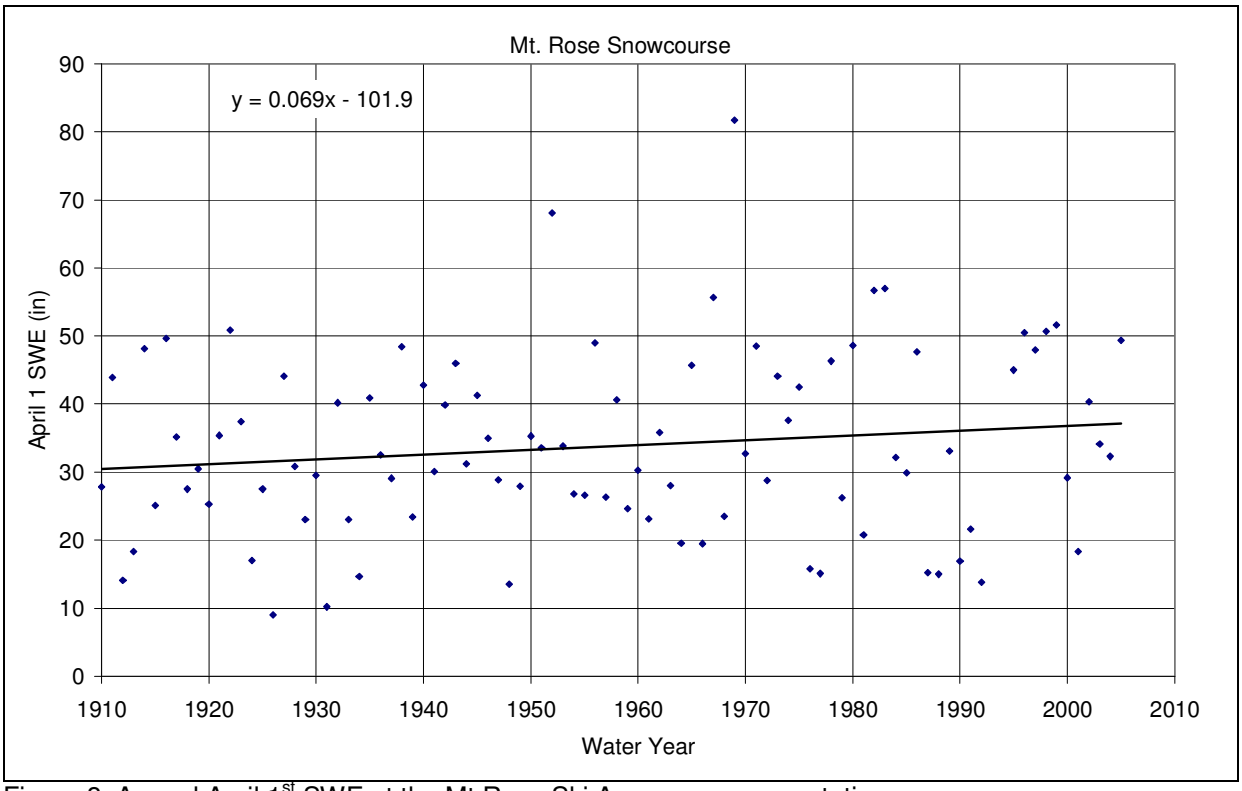

Figure 8. Annual April 1st SWE at the Mt Rose Ski Area snowcourse station.

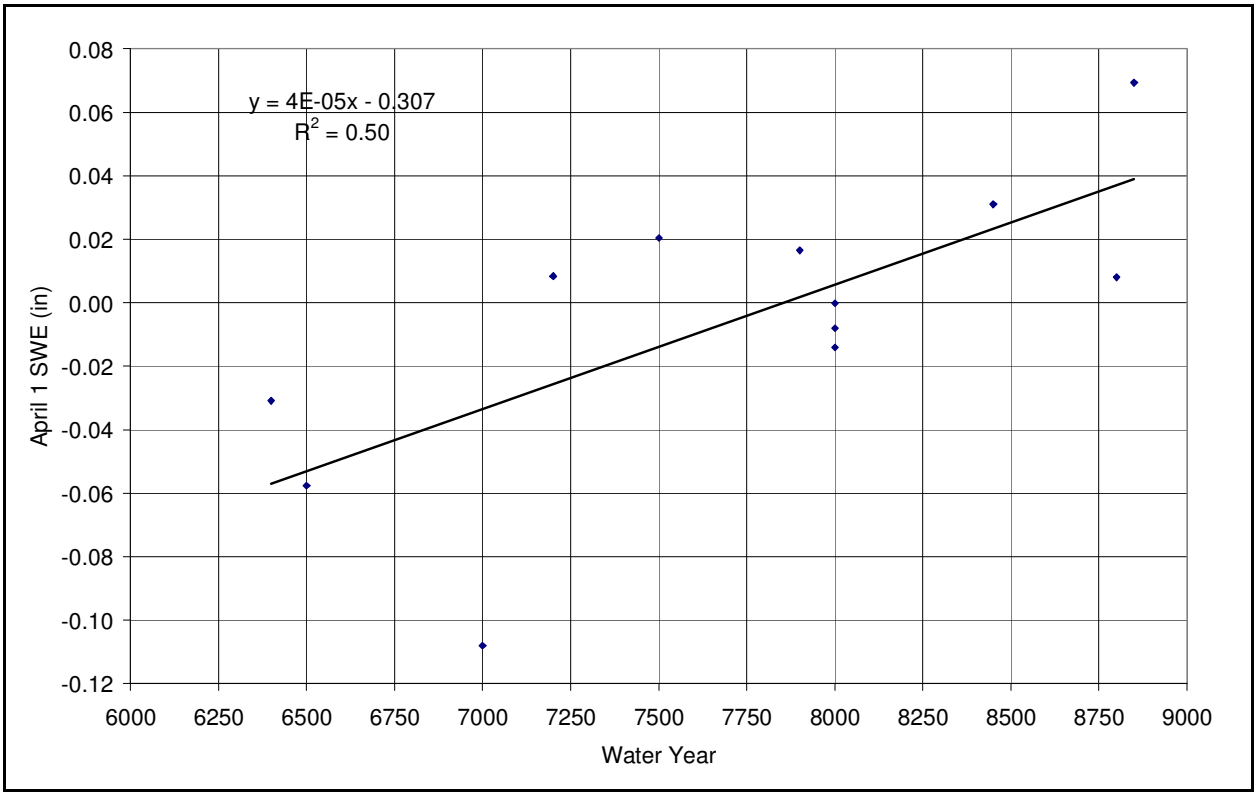

Figure 9. Trends in April 1 SWE snowcourse data as a function of station elevation.

Streamflow

Long term streamflow trends were investigated through a linear regression of the cumulative streamflow volumes. As expected, mean annual streamflow data varied widely between water years. The records revealed no observable trends over the period of record. Figure 10 contains an example of the streamflow data for the Truckee River at Reno. All other streamflow data can be found in Appendix D.

In addition to the streamflow volume analyses, streamflow timing was also studied. The timing was studied by investigating trends in the date at which the center of mass of the annual hydrograph occurred. As with the volume data, the center of mass data showed high year-to-year variability. A trend towards an earlier occurring date for the center of mass was observed for 14 out of the 21 stations. Figure 11 contains the center of mass data for the Little Truckee River above Boca Reservoir.

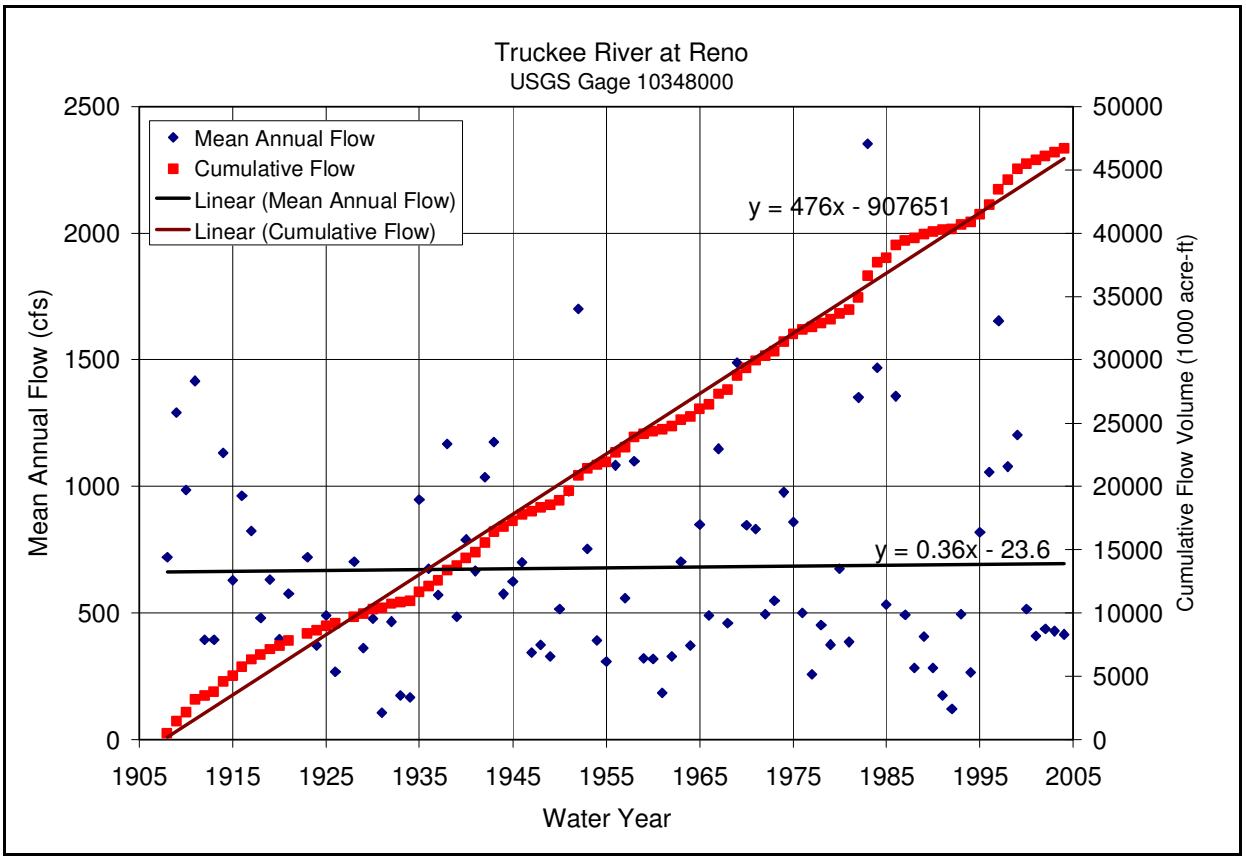

Figure 10. Mean annual streamflow and cumulative flow volumes for the Truckee River at Reno.

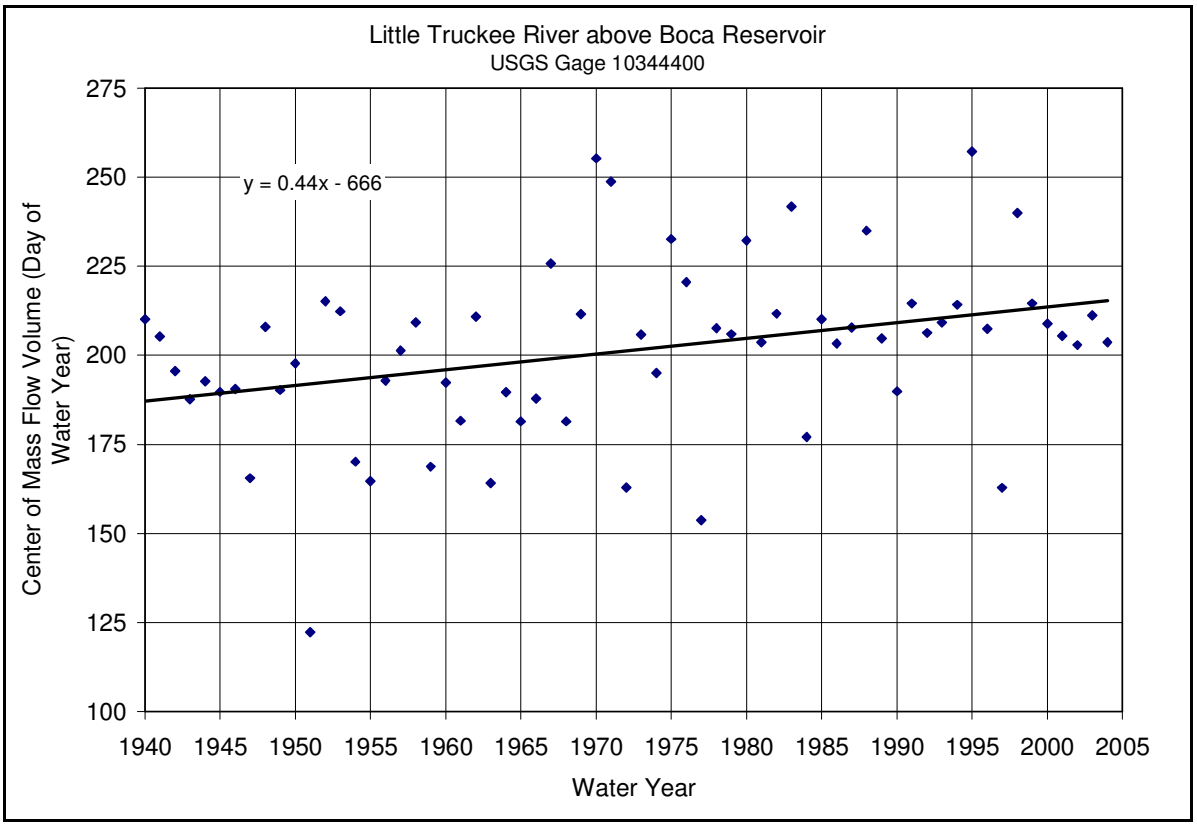

Figure 11. Little Truckee River above Boca Reservoir streamflow center of mass.

Reservoir Volumes

Mean annual reservoir storage volumes and cumulative mean annual storage were also investigated. The reservoir volumes displayed an obvious dependence on climate, as periods of drought clearly influenced reservoir volumes. This dependence is demonstrated by Figure 12, which contains data for Boca Reservoir. In periods of high precipitation and streamflow (e.g. 1972 to 1986), the reservoir volume was high and the cumulative volume climbed faster than the historical trend. However, during periods of drought (e.g. 1987 to 1995) the reservoir volumes dropped dramatically, and the cumulative storage volumes climbed slower than the historical trend. For Lake Tahoe, the storage volume became negative as the lake level fell below its natural rim. During this period, the cumulative storage volume trend was actually negative. Lake Tahoe trends, along with the other major regional reservoirs, are shown in Appendix E.

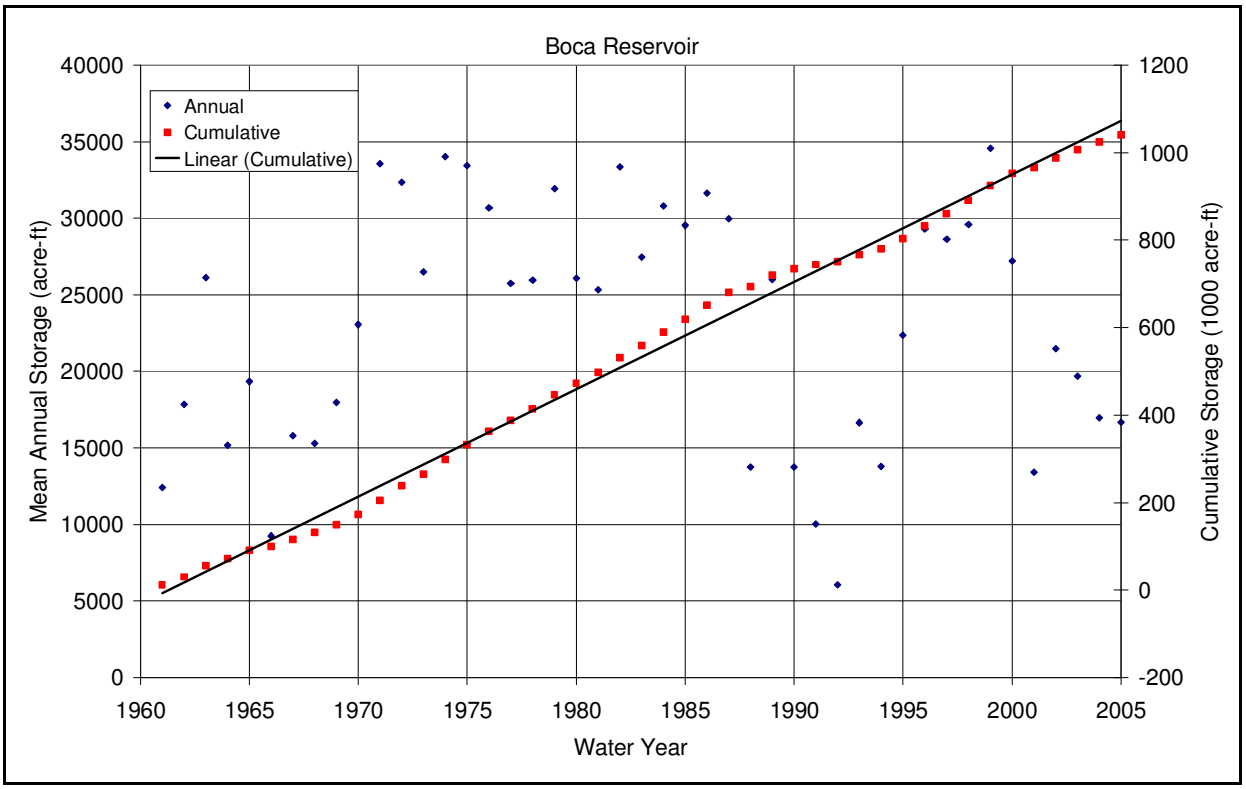

Figure 12. Mean annual storage and cumulative storage for Boca Reservoir.

Precipitation and Snowpack

Double mass analyses were conducted on precipitation and snowpack data at two sets of gages. Although snowfall and SWE is reported at the COOP stations, this data is considered less reliable than snowcourse stations. Thus, the analysis was restricted to COOP precipitation and snowcourse stations that were in close proximity. The results for the double mass analysis between annual precipitation at the Truckee Ranger Station and April 1st SWE at the Truckee #2 Snowcourse station are shown in Figure 13. The data reveals a very consistent trend between precipitation and SWE throughout the periods of record. This suggests that the form of precipitation and snowmelt patterns have not changed noticeably.

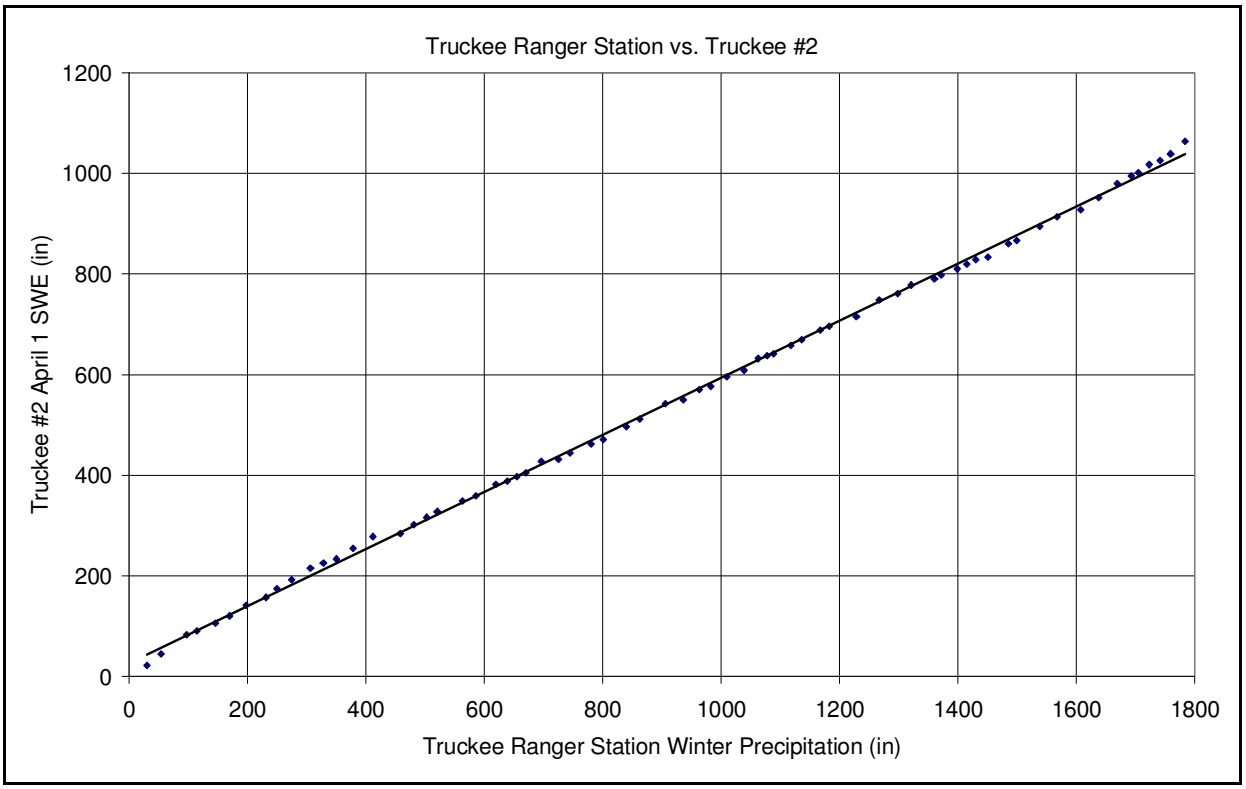

Figure 13. Double mass curve for Truckee #2 snowcourse station April 1 SWE and Truckee Ranger Station winter precipitation.

Precipitation and Streamflow

Relationships between streamflow and precipitation were studied at four paired stations. The stations were selected so that the gaged precipitation was 'representative' of the observed streamflow. Also, streamflow records that were influenced by reservoir construction and other local human activities were not considered. The results confirmed the expected high degree of correlation between precipitation and streamflow. The function between precipitation and streamflow remained consistent throughout the period of record, indicating no observed modifications in large scale precipitation-runoff-streamflow processes at un-dammed gages. Figure 14 contains the results of the double mass analysis for the Donner State Park weather station and the Donner Creek streamgage. The results of the remaining three analyses are shown in Appendix G.

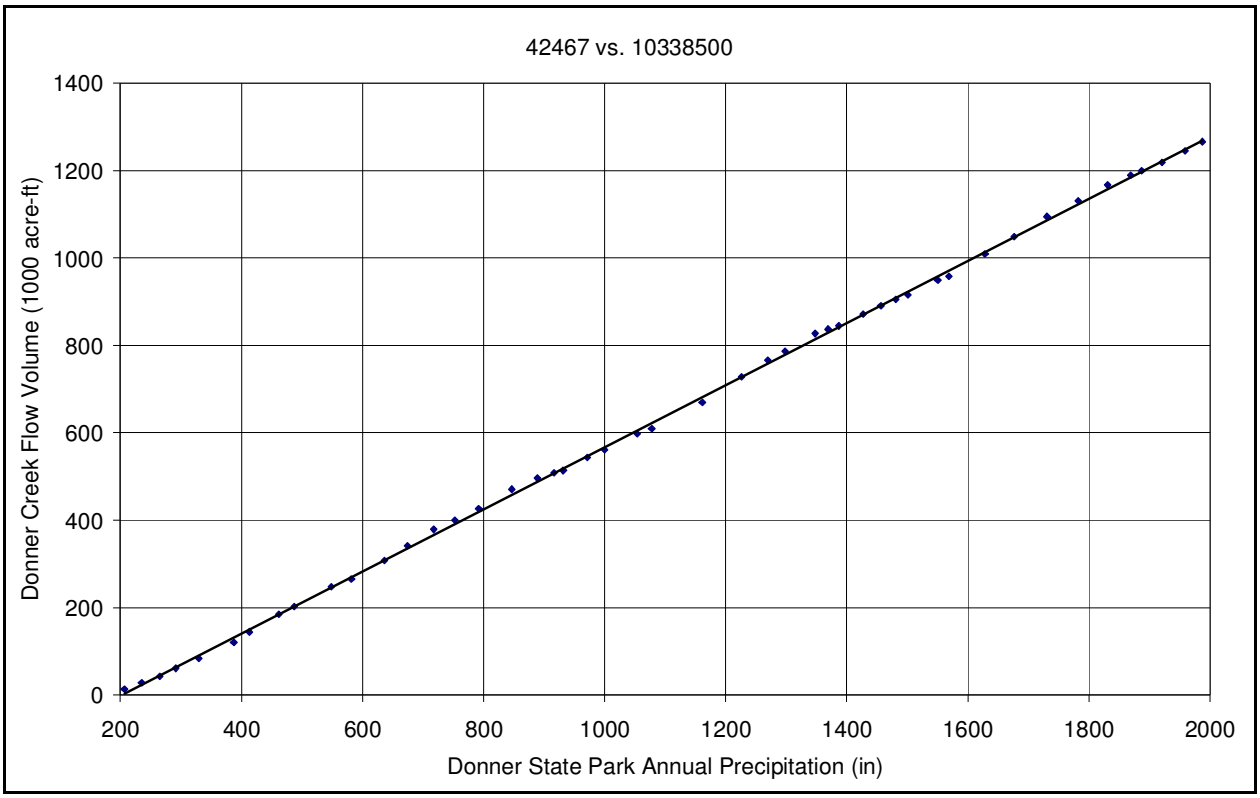

Figure 14. Double mass curve for streamflow volume for Donner Creek and annual precipitation at Donner State Park.

Precipitation and Reservoir Storage Volume

Double mass analysis of precipitation and reservoir storage volumes further demonstrated the high degree of correlation between these variables. The analyses were completed for five paired stations and the results can be found in Appendix H. An example of this data is shown in Figure 15, which contains the analyses between Boca Reservoir storage volumes and annual precipitation at the Boca weather station. The consistent linear long-term trend between these variables indicates that the underlying processes have not influenced by potential climate change.

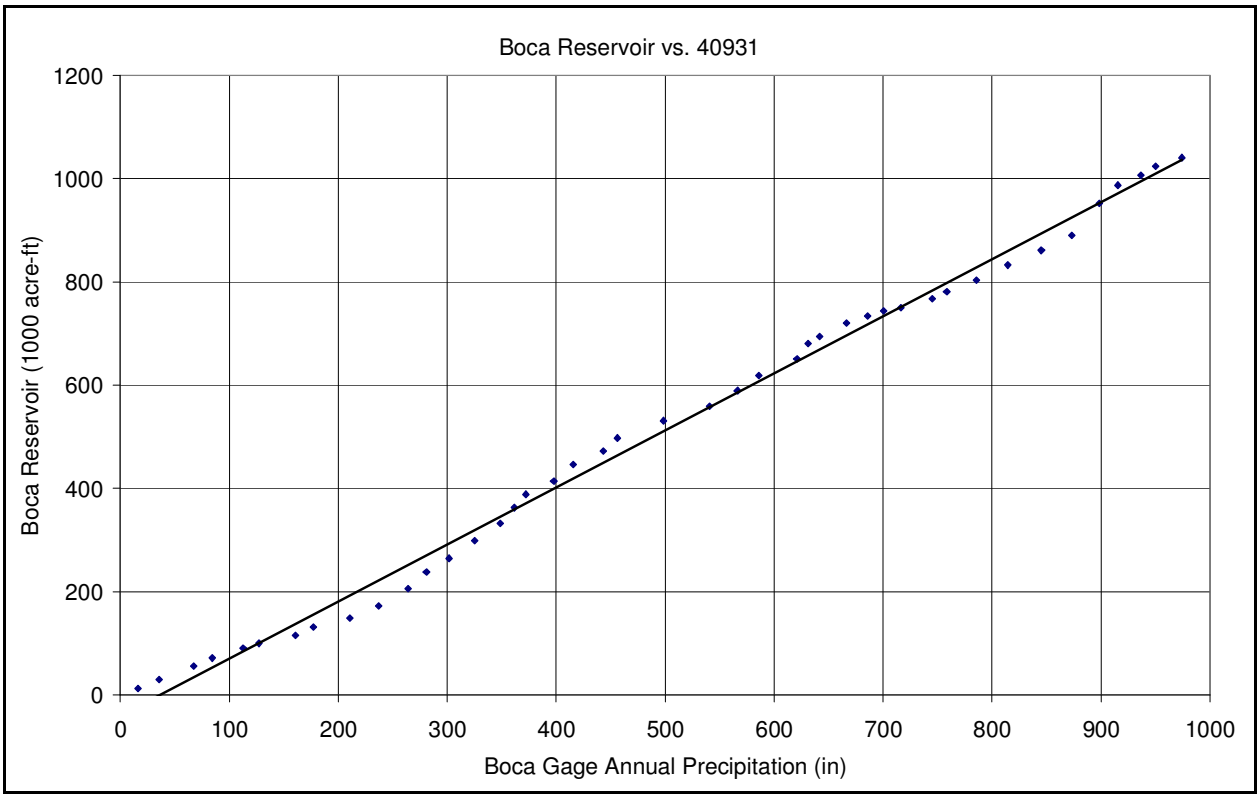

Figure 15. Double mass curve of Boca Reservoir storage and Boca annual precipitation.

Snow Water Equivalent and Streamflow

Relationships between streamflow and SWE were studied at six paired stations. The stations were selected so that the gaged SWE was representative of the observed streamflow. Figure 16 shows the results of the analysis between Independence Lake SWE and Sagehen Creek streamflow. The results for the remaining analyses can be found in Appendix I. The data showed a high degree of correlation between SWE and streamflow. Recent data showed no strong departure from long term trends. These results indicate that the processes of snowfall, snow accumulation, snowmelt, and runoff have remained relatively consistent throughout the period of record.

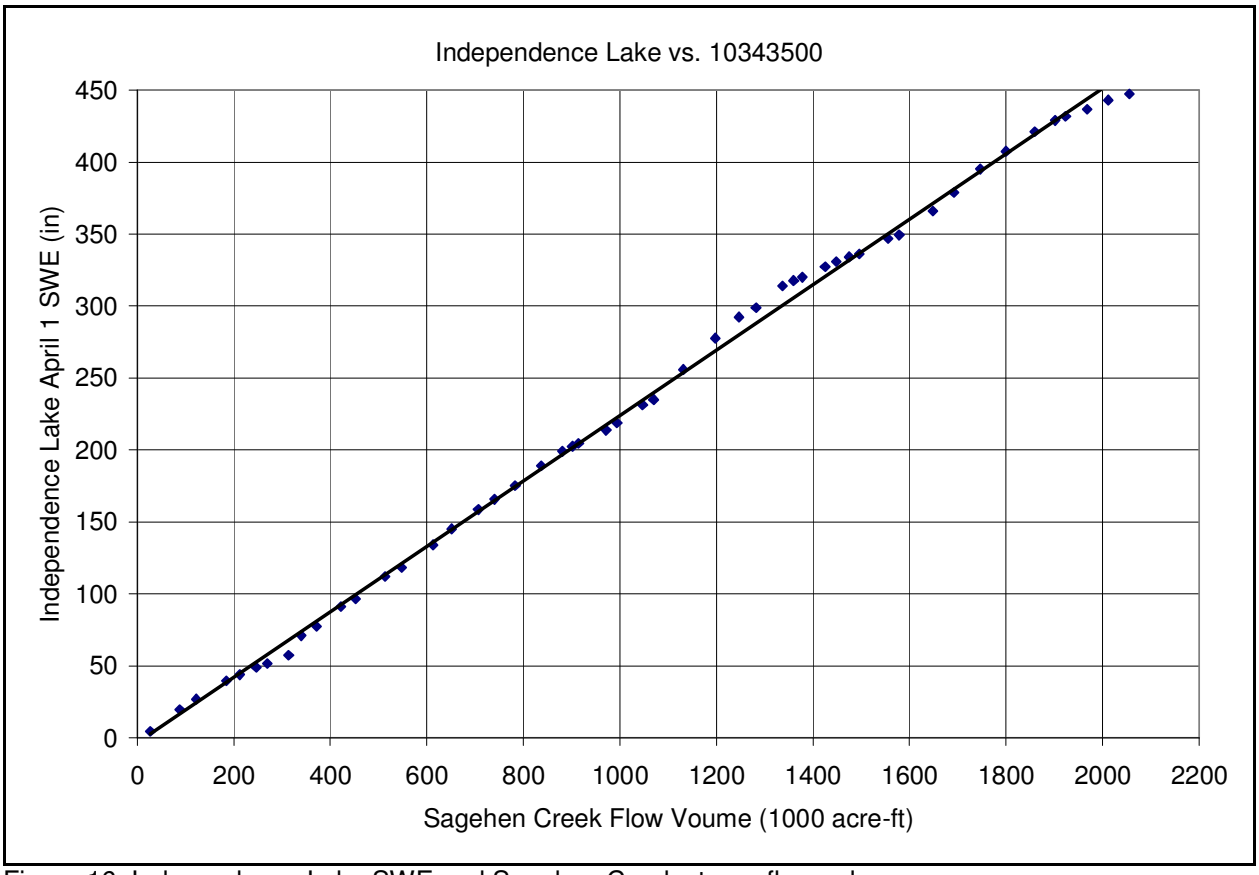

Figure 16. Independence Lake SWE and Sagehen Creek streamflow volumes.

Streamflow and Reservoir Volumes

Double mass analyses were conducted for Boca Reservoir, Donner Lake, Stampede Reservoir and Lake Tahoe. For Boca Reservoir and Lake Tahoe, inflow and outflow streams were both considered. Results of the Boca Reservoir Analysis are shown in Figure 17, and all other analyses can be found in Appendix J. No consistent departures from long term patterns were observed between streamflow and reservoir volumes. Further, consistent trends were observed between upstream and downstream streamflow records.

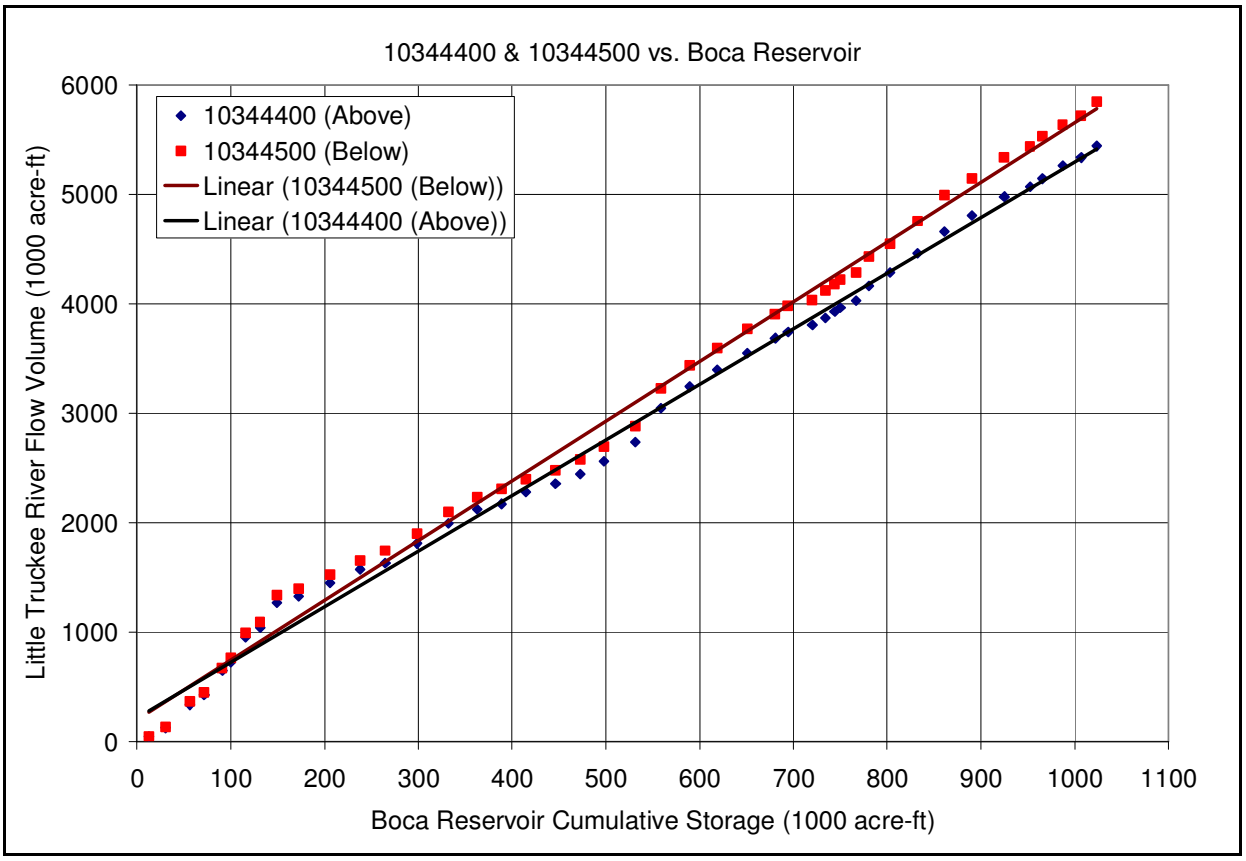

Figure 17. Little Truckee River streamflow volume and Boca Reservoir storage.

Snowpack and Reservoir Storage Volumes

Double mass analysis of April 1 SWE and reservoir storage volumes demonstrated the expected high degree of correlation between these variables. The analyses were completed for four paired stations and the results can be found in Appendix K. Figure 18 contains the double mass analysis of Lake Tahoe storage volume and Hagen's Meadow April 1 SWE. The data not only reveals the correlation between these datasets, but it also shows the impacts of major drought events that caused the Lake Tahoe volume to drop below its natural rim. After these events, SWE continues to accumulate while Lake Tahoe cumulative storage volumes actually decrease.

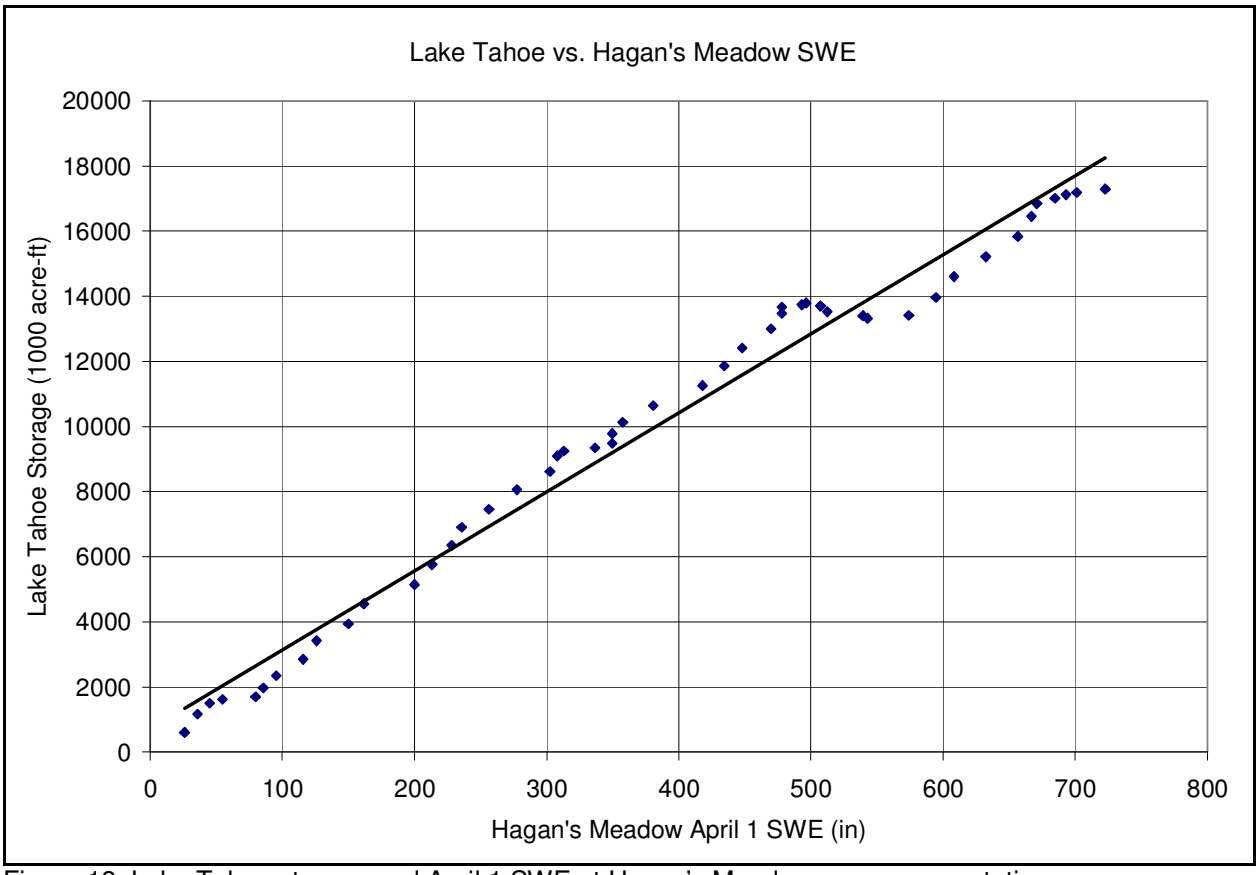

Figure 18. Lake Tahoe storage and April 1 SWE at Hagen's Meadow snowcourse station.

Summary

In order to reveal potential signs of environmental change in the Truckee Meadows region that may be consistent and coincident with global warming, historical climate and hydrologic data were evaluated. The data were compiled in a GIS database and linear regression and double mass analyses were performed. For all variables, year-to-year variability was very high; making it difficult to identify data trends. No consistent or prevalent changes in temperature, precipitation, SWE, hydrograph volume/ timing, or reservoir storage volumes were found. Further, relationships between variables appeared to remain consistent over time. No clear evidence of global warming or associated changes in volume or timing of hydrologic variables was found.

Appendix A

Temperature

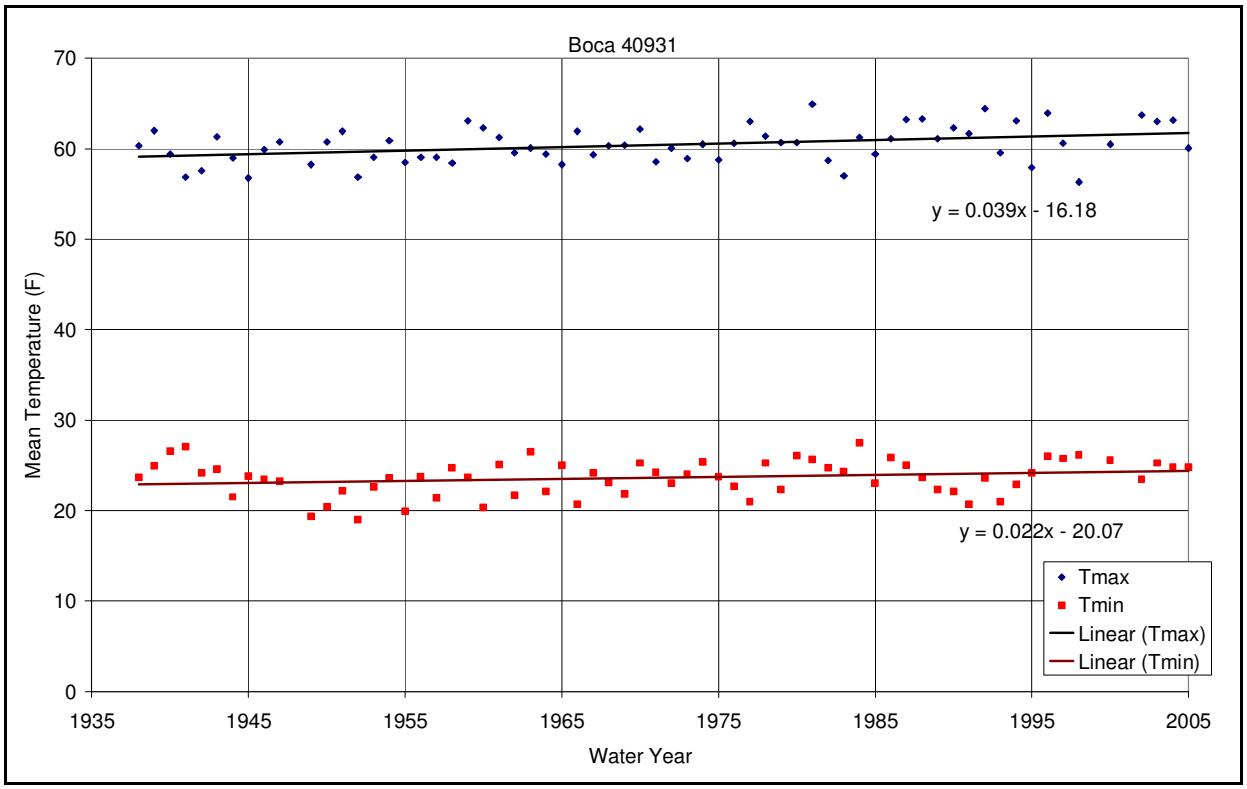

Figure A1. Mean annual maximum and minimum temperature at Boca Gage 40931.

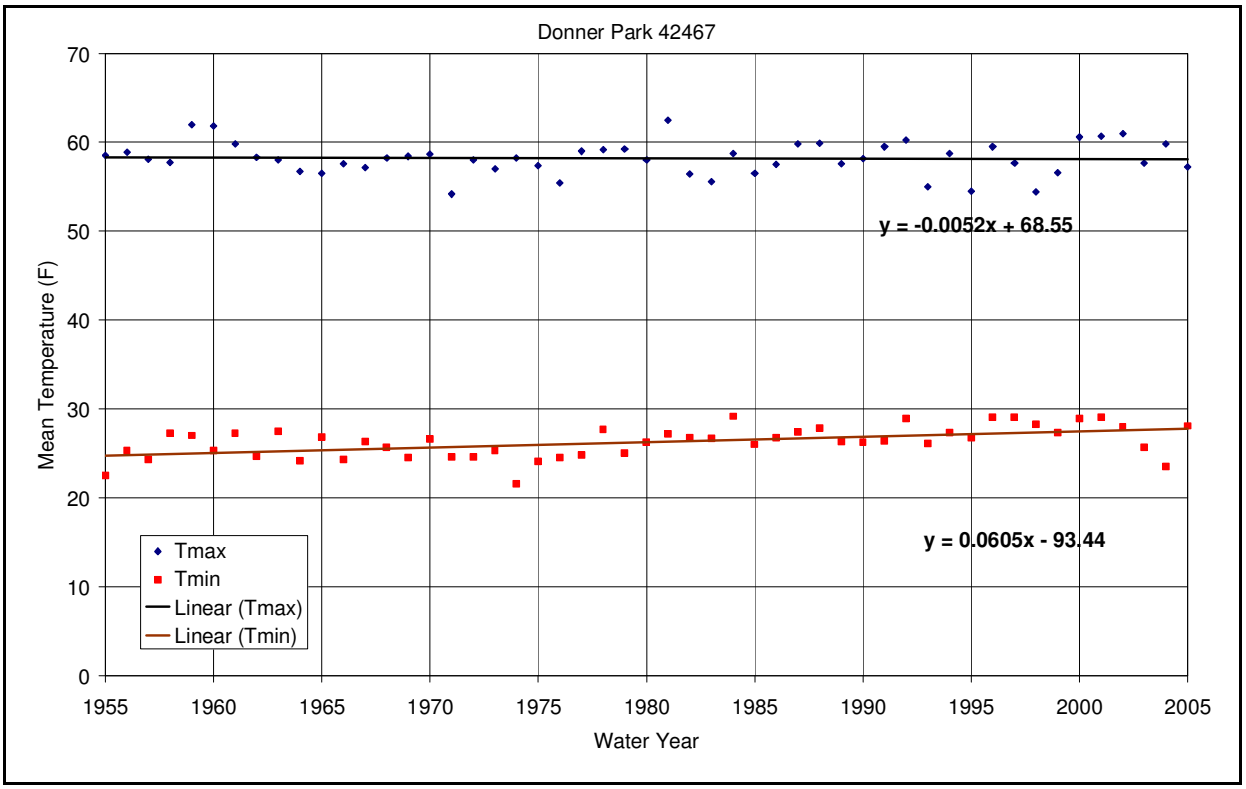

Figure A2. Mean annual maximum and minimum temperature at Donner Park 42467.

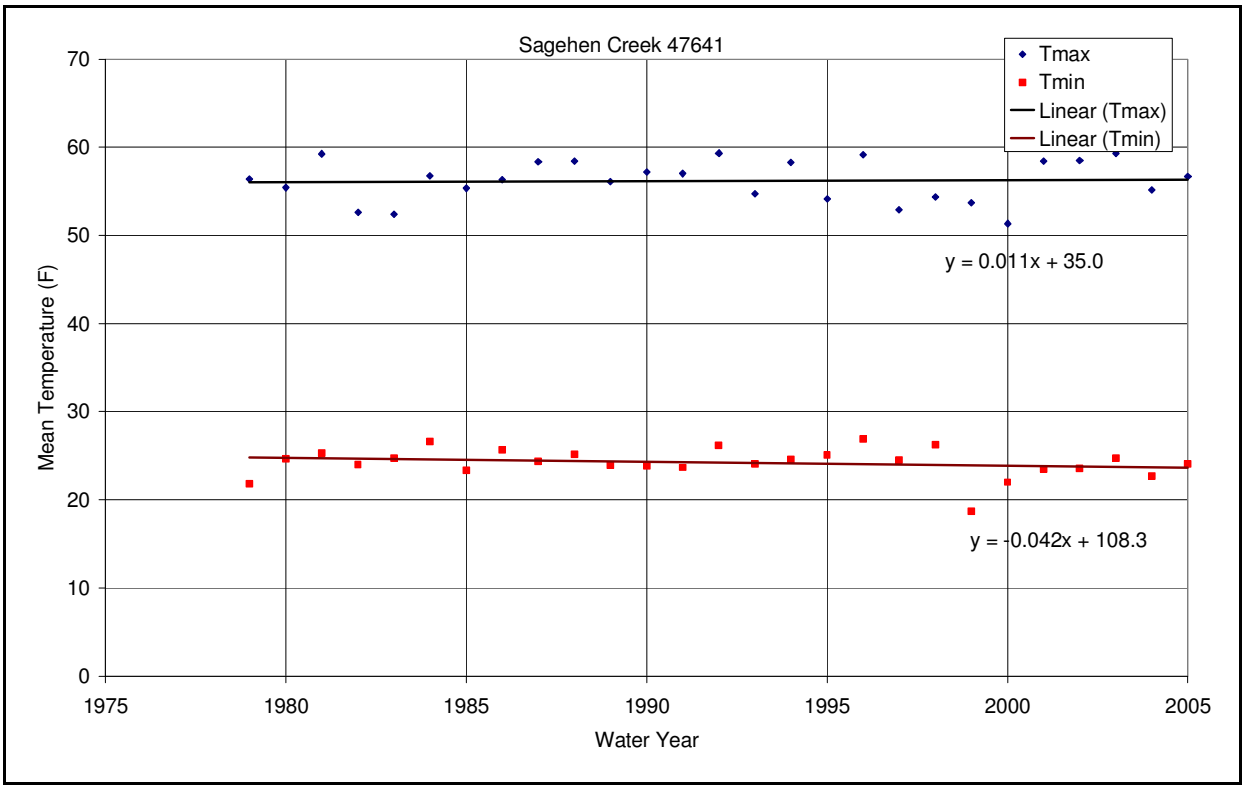

Figure A3. Mean annual maximum and minimum temperature at Sagehen Creek 47641.

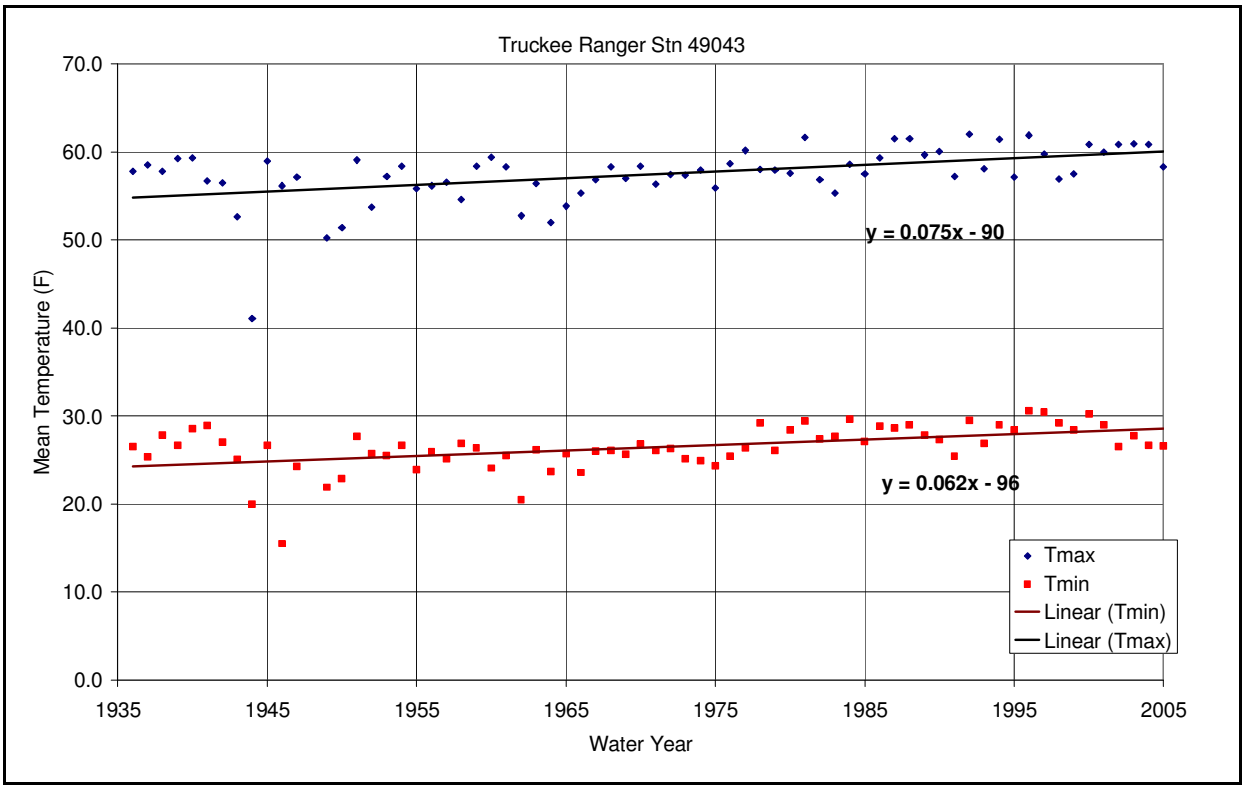

Figure A4. Mean annual maximum and minimum temperature at Truckee Ranger Station 49043.

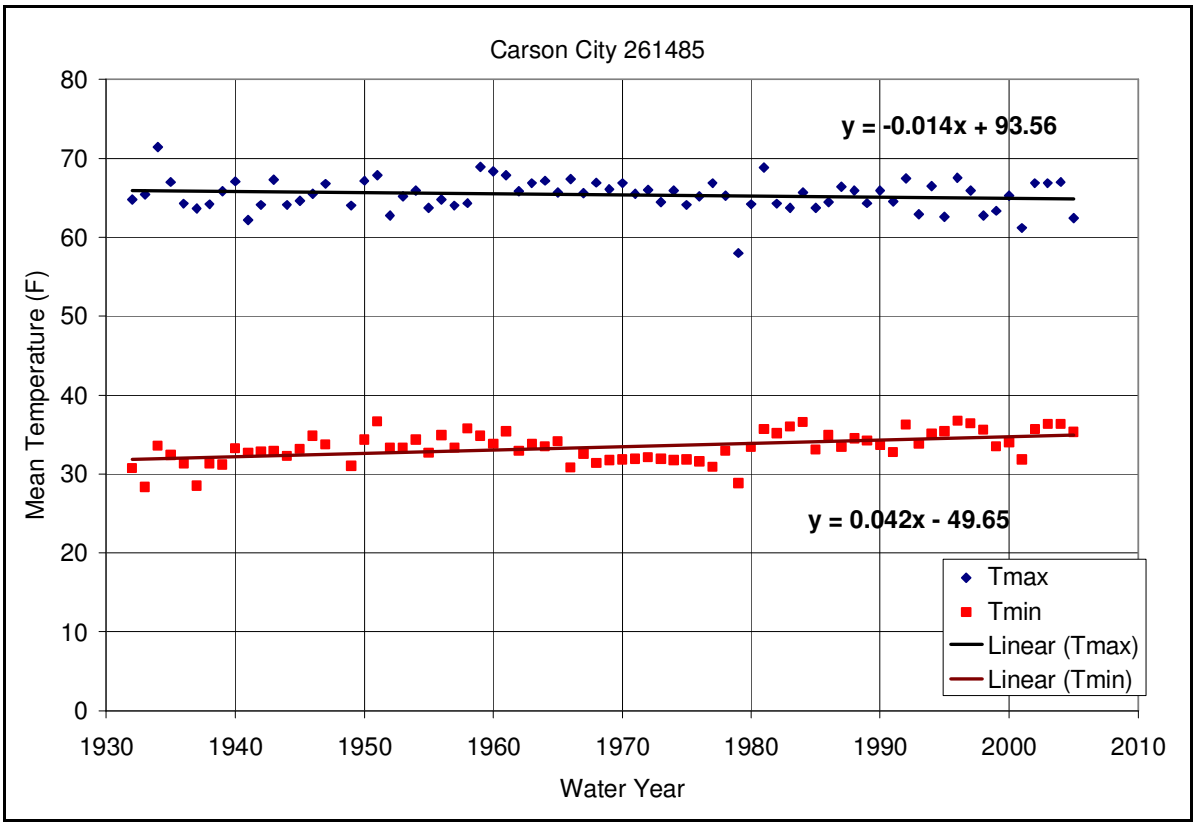

Figure A5. Mean annual maximum and minimum temperature at Carson City 261485.

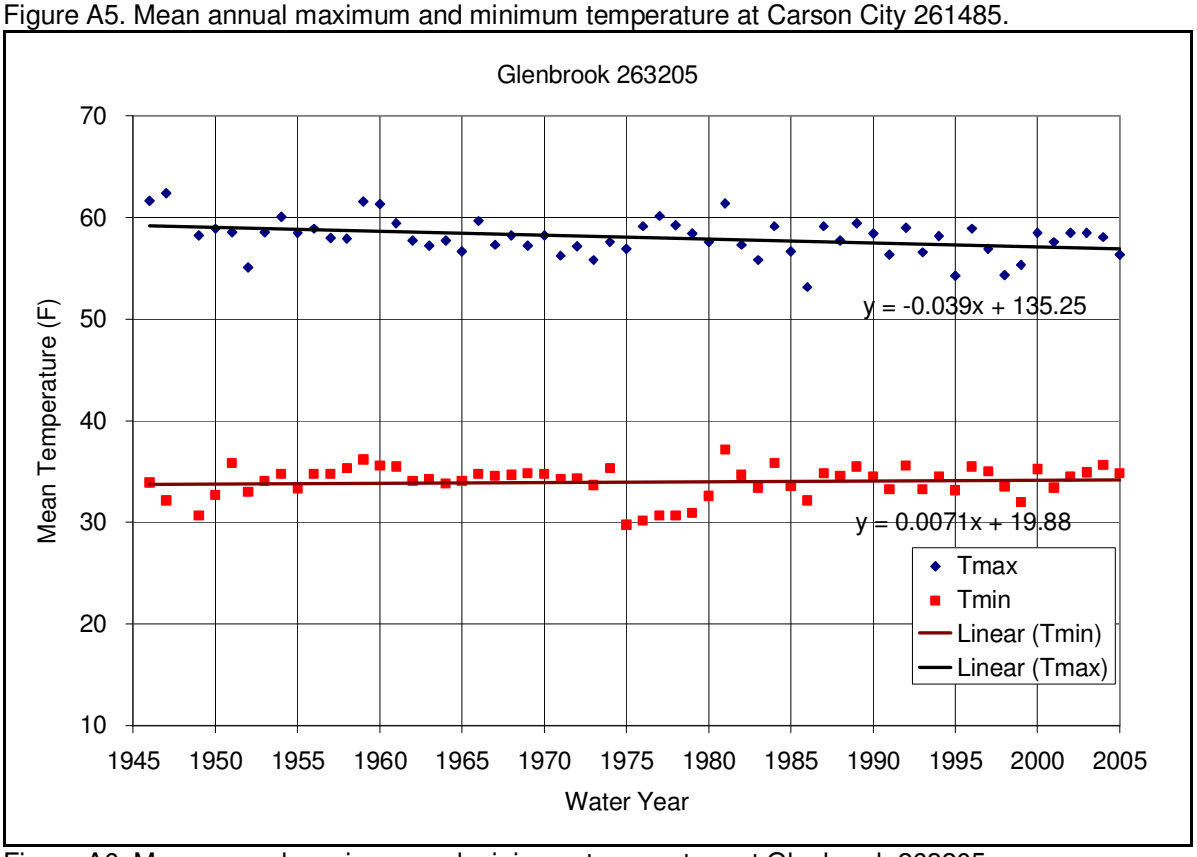

Figure A6. Mean annual maximum and minimum temperature at Glenbrook 263205.

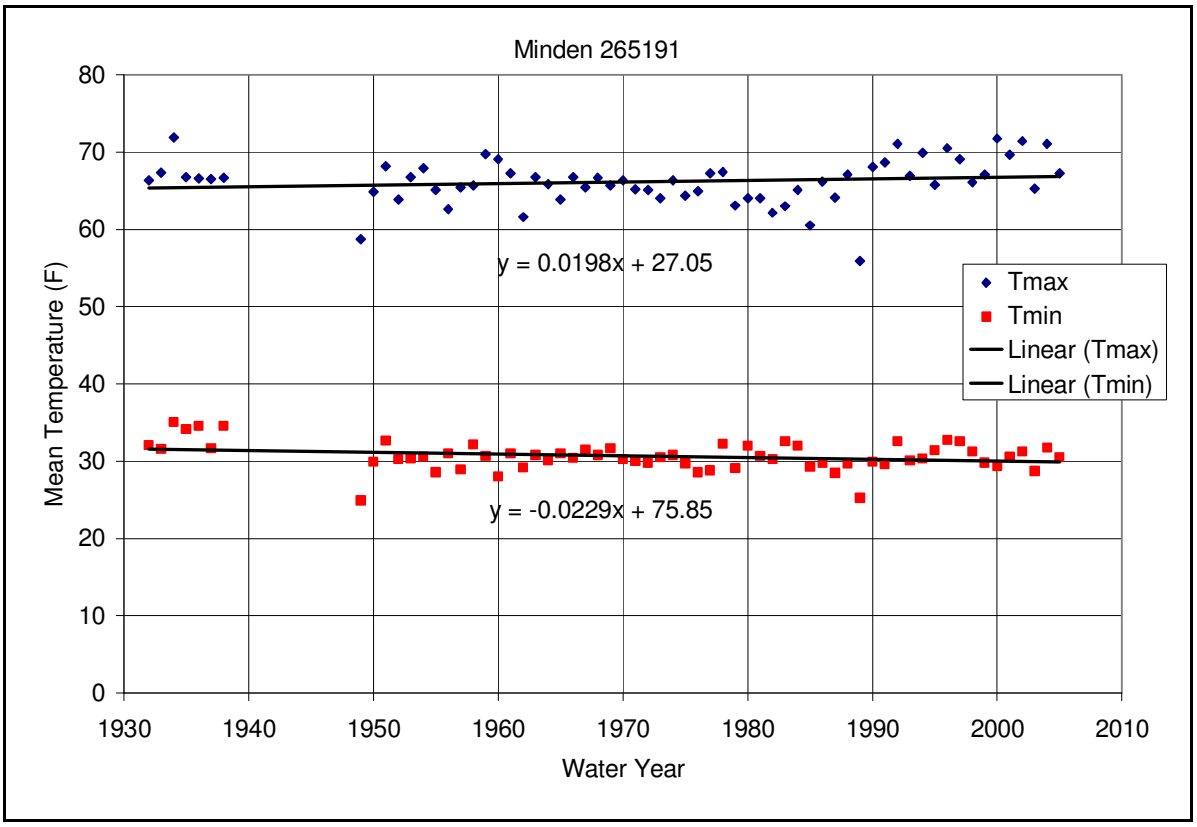

Figure A7. Mean annual maximum and minimum temperature at Minden 265191.

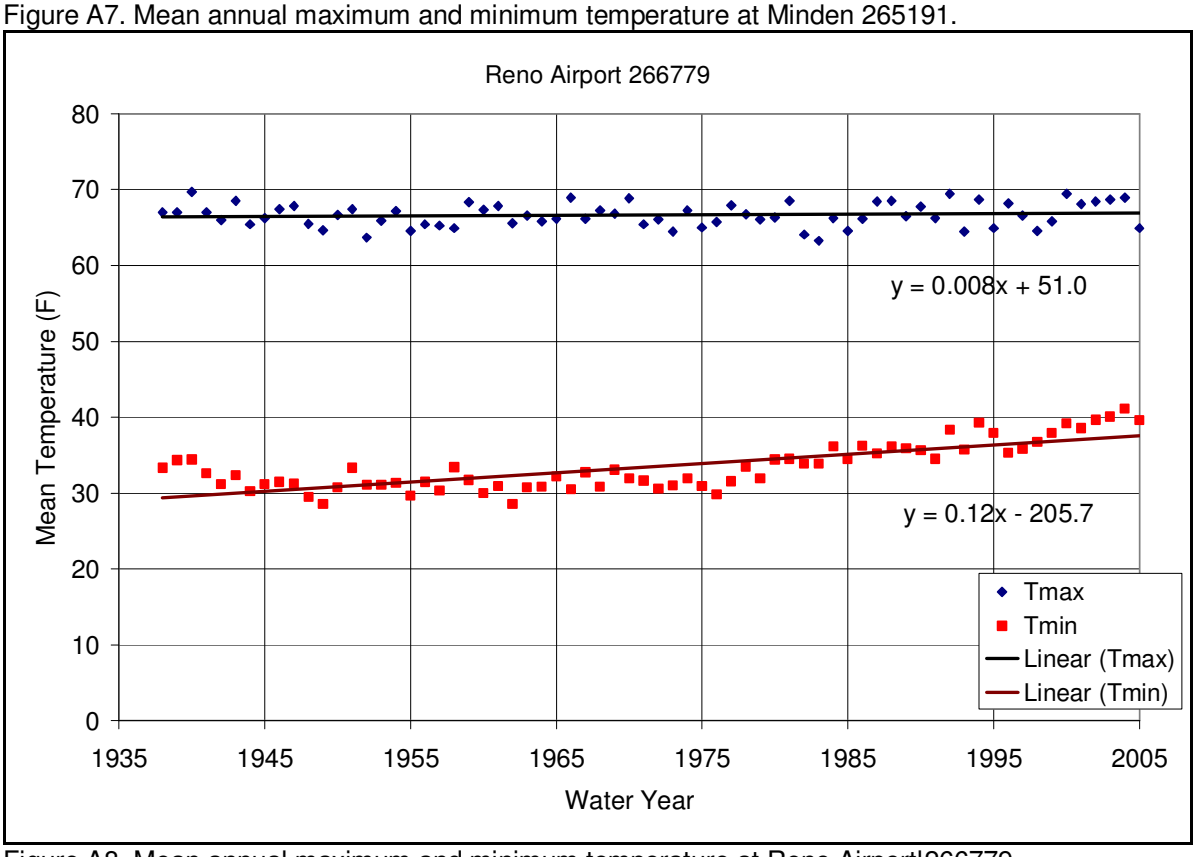

Figure A8. Mean annual maximum and minimum temperature at Reno Airport!266779.

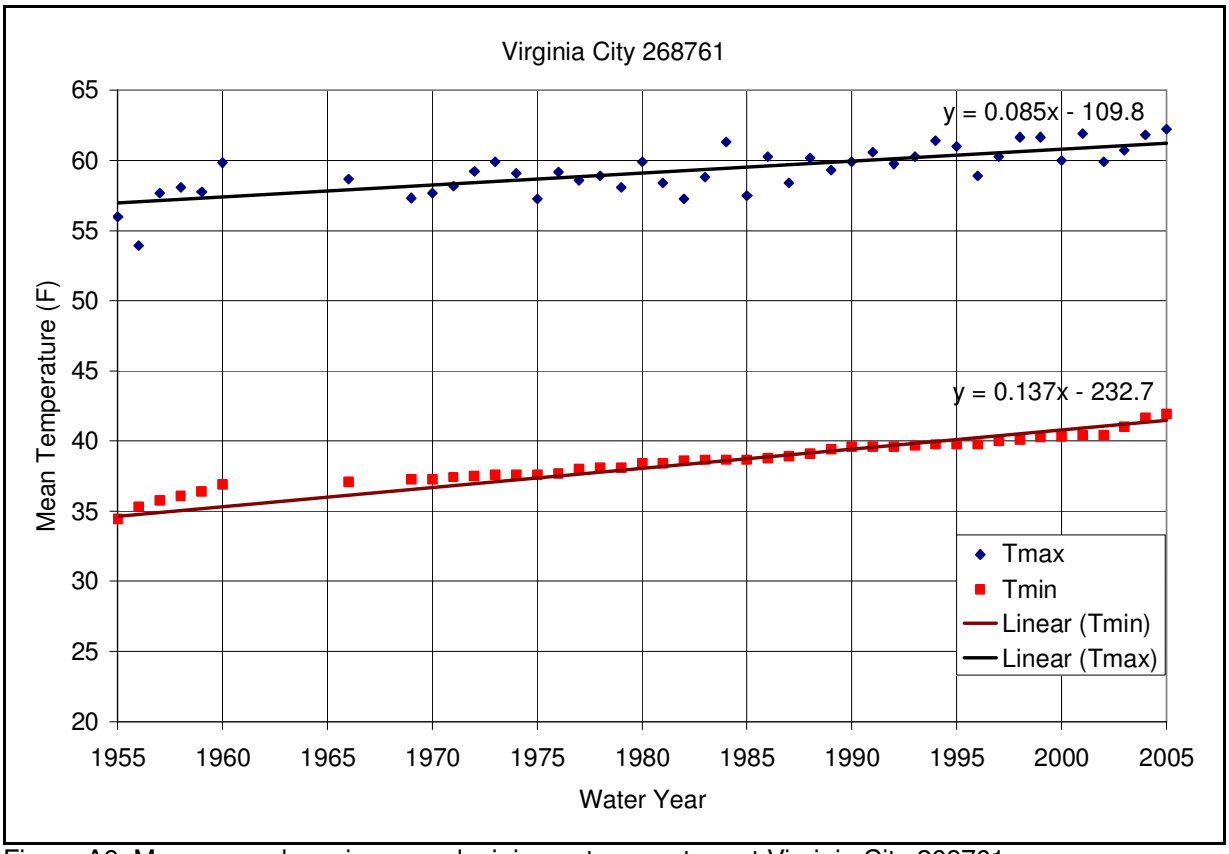

Figure A9. Mean annual maximum and minimum temperature at Virginia City 268761.

Appendix B

Precipitation

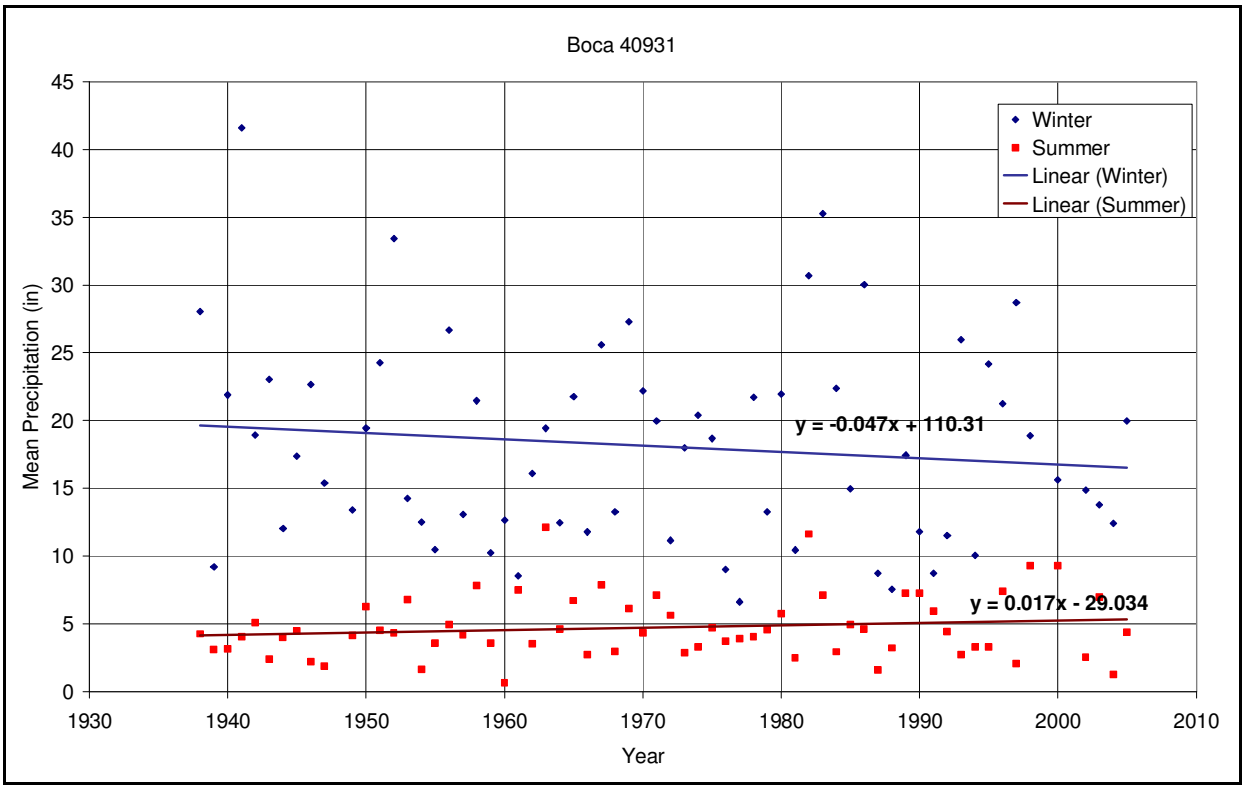

Figure B1. Mean winter (Oct-March) and summer (April-September) precipitation at Boca Gage 40931.

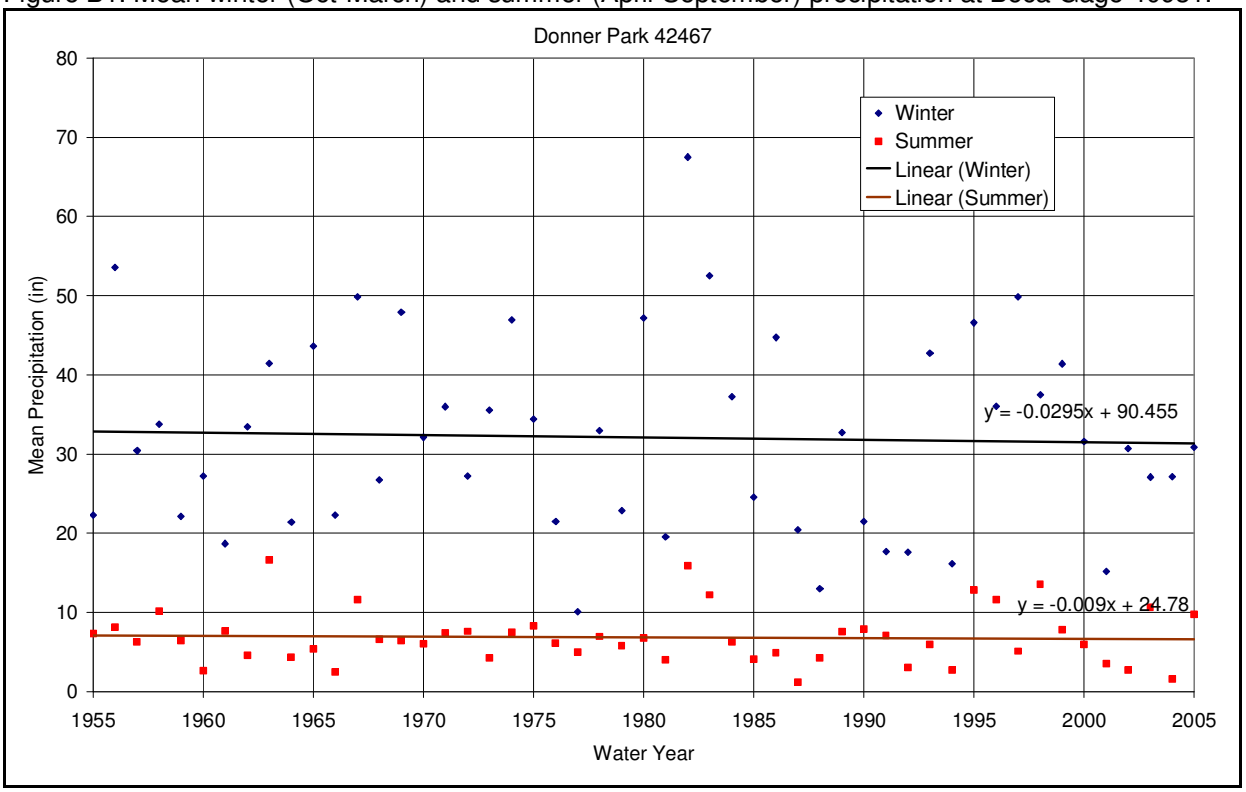

Figure B2. Mean winter and summer precipitation at Donner Park 42467.

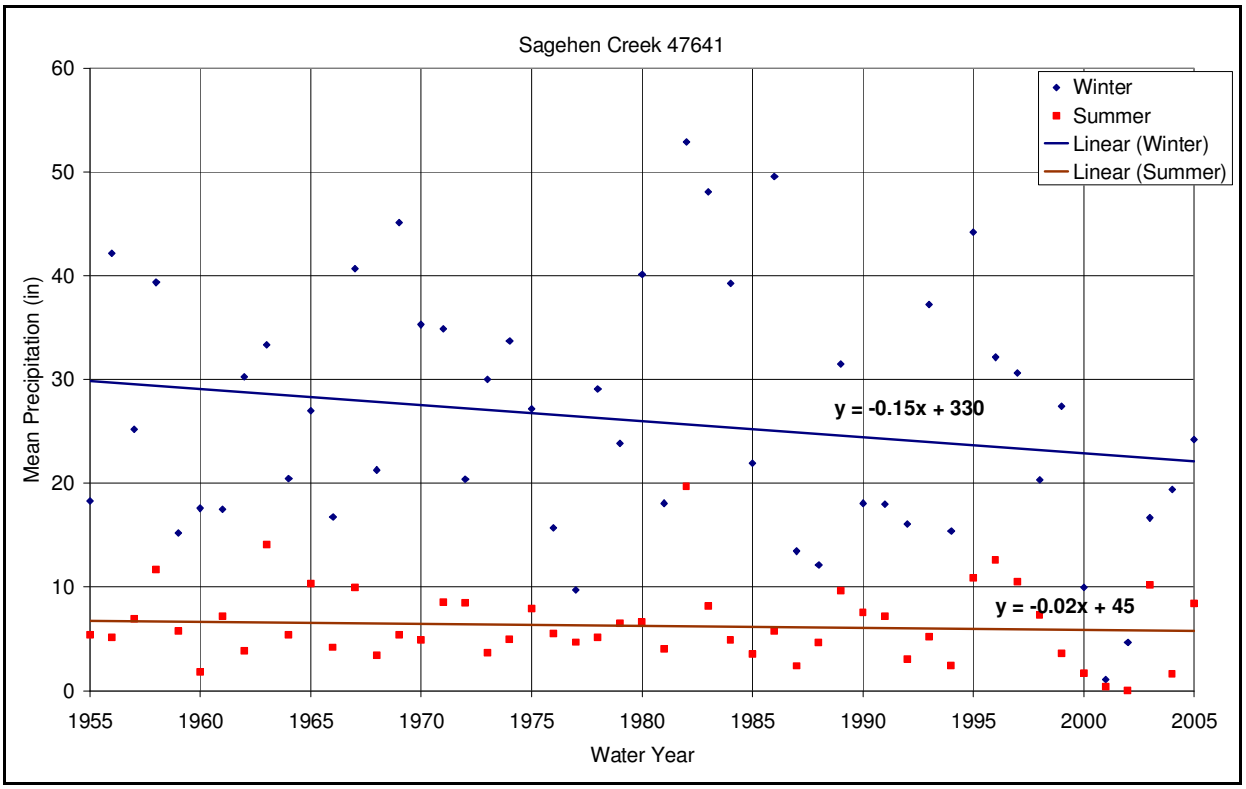

Figure B3. Mean winter and summer precipitation at Sagehen Creek 47641.

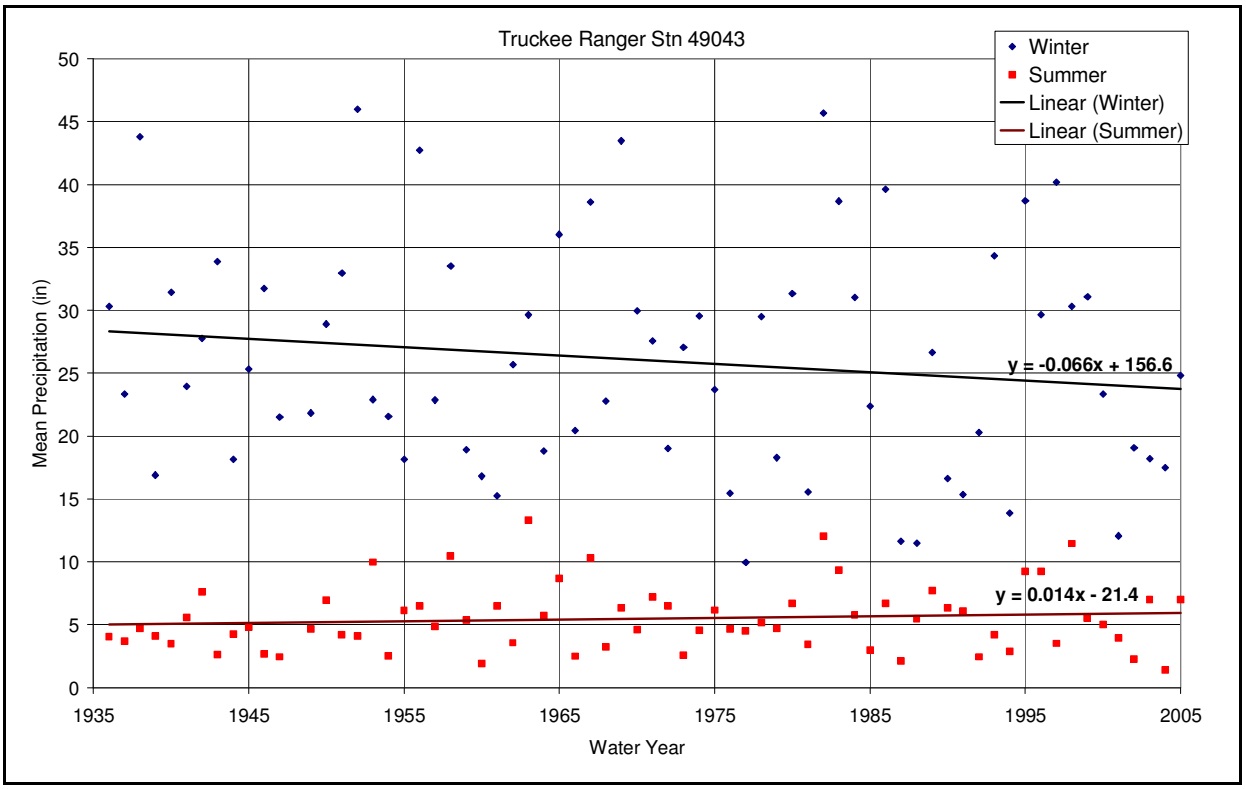

Figure B4. Mean winter and summer precipitation at Truckee Ranger Station 49043.

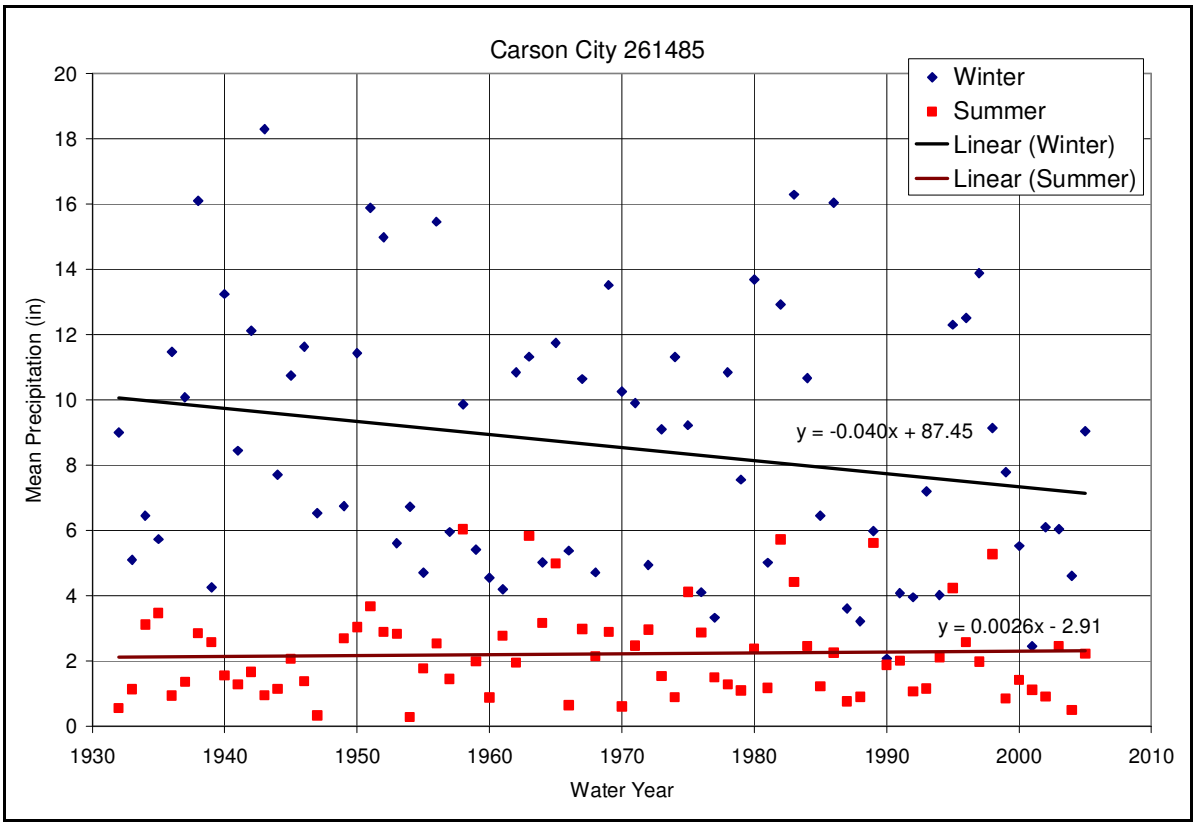

Figure B5. Mean winter and summer precipitation at Carson City 261485.

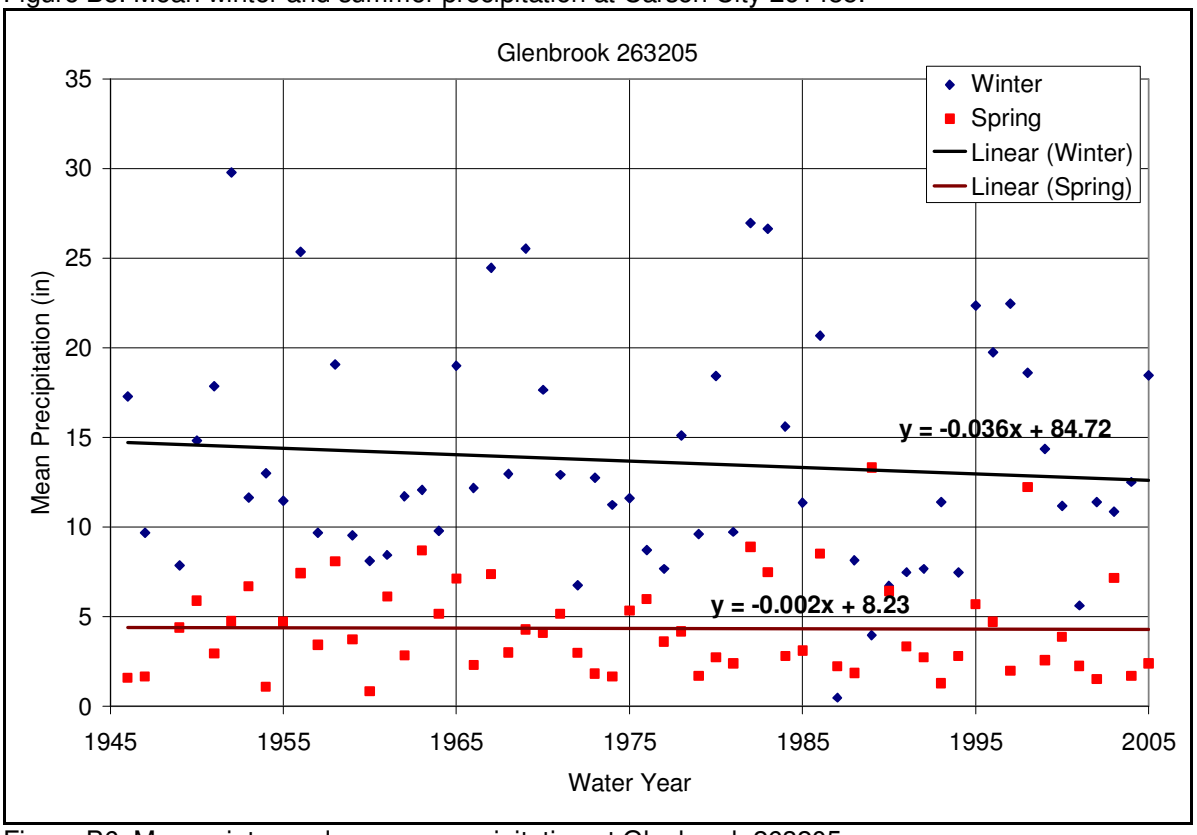

Figure B6. Mean winter and summer precipitation at Glenbrook 263205.

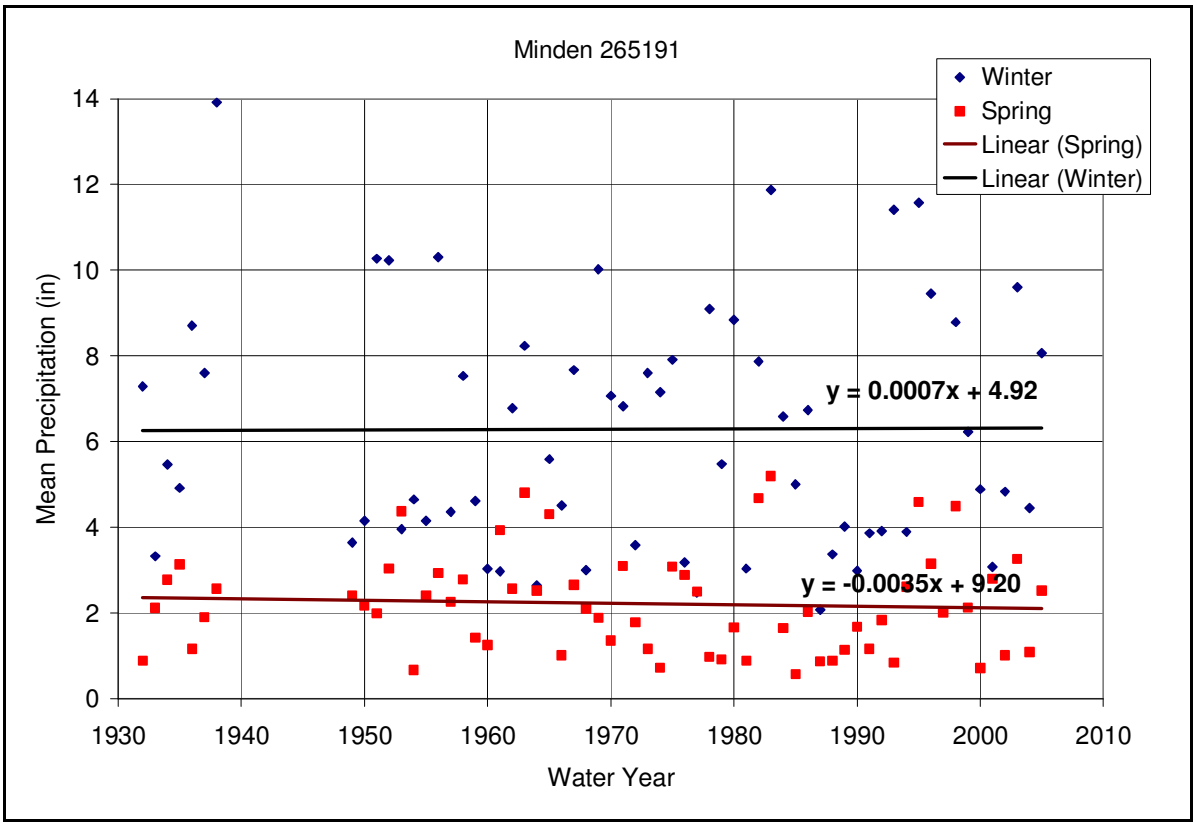

Figure B7. Mean winter and summer precipitation at Minden 265191.

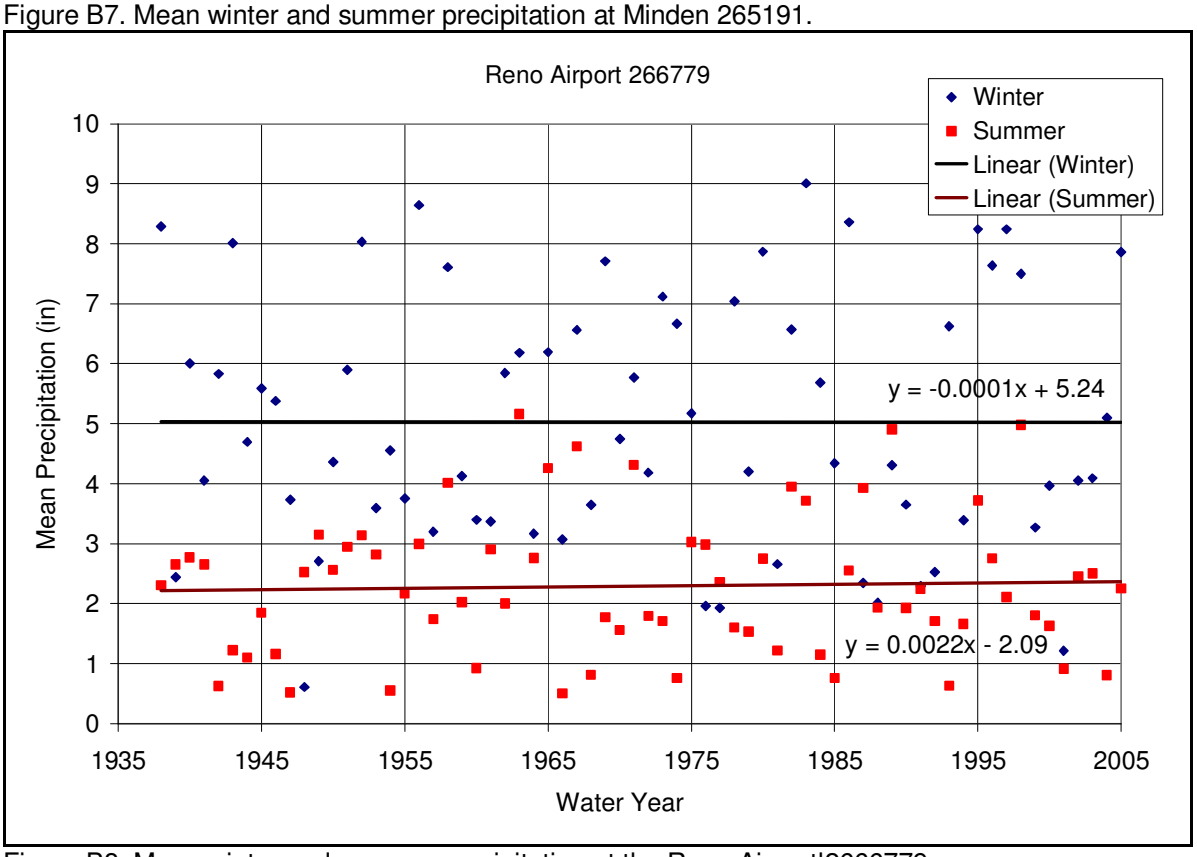

Figure B8. Mean winter and summer precipitation at the Reno Airport!2666779.

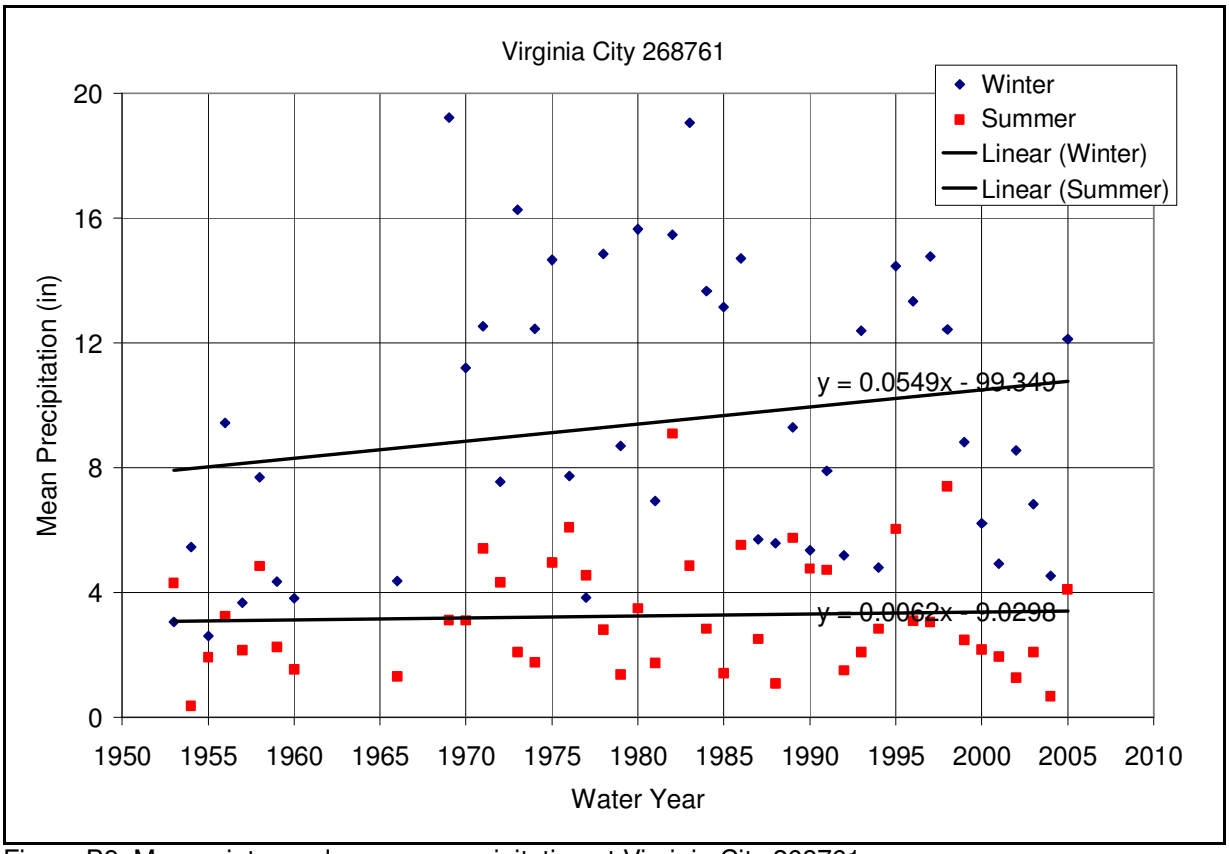

Figure B9. Mean winter and summer precipitation at Virginia City 268761.

Appendix C

Snowpack

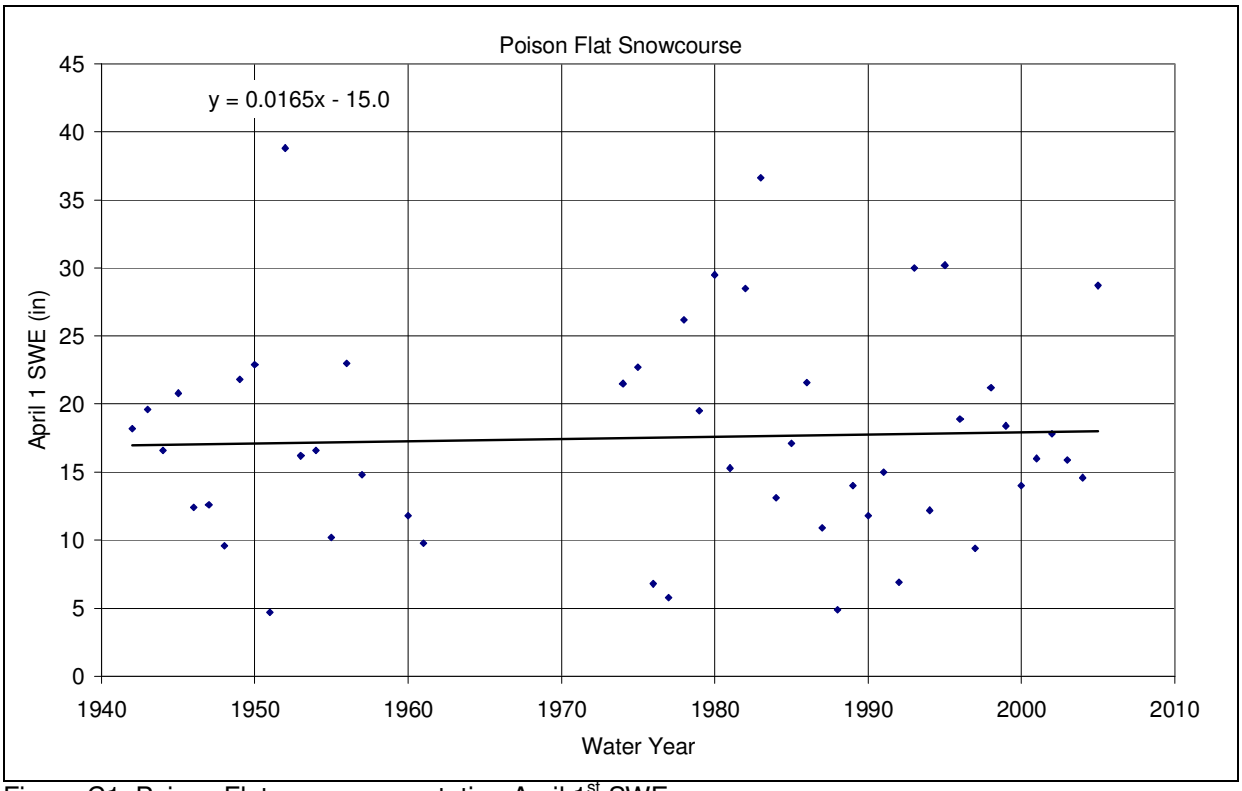

Figure C1. Poison Flat snowcourse station April 1st SWE.

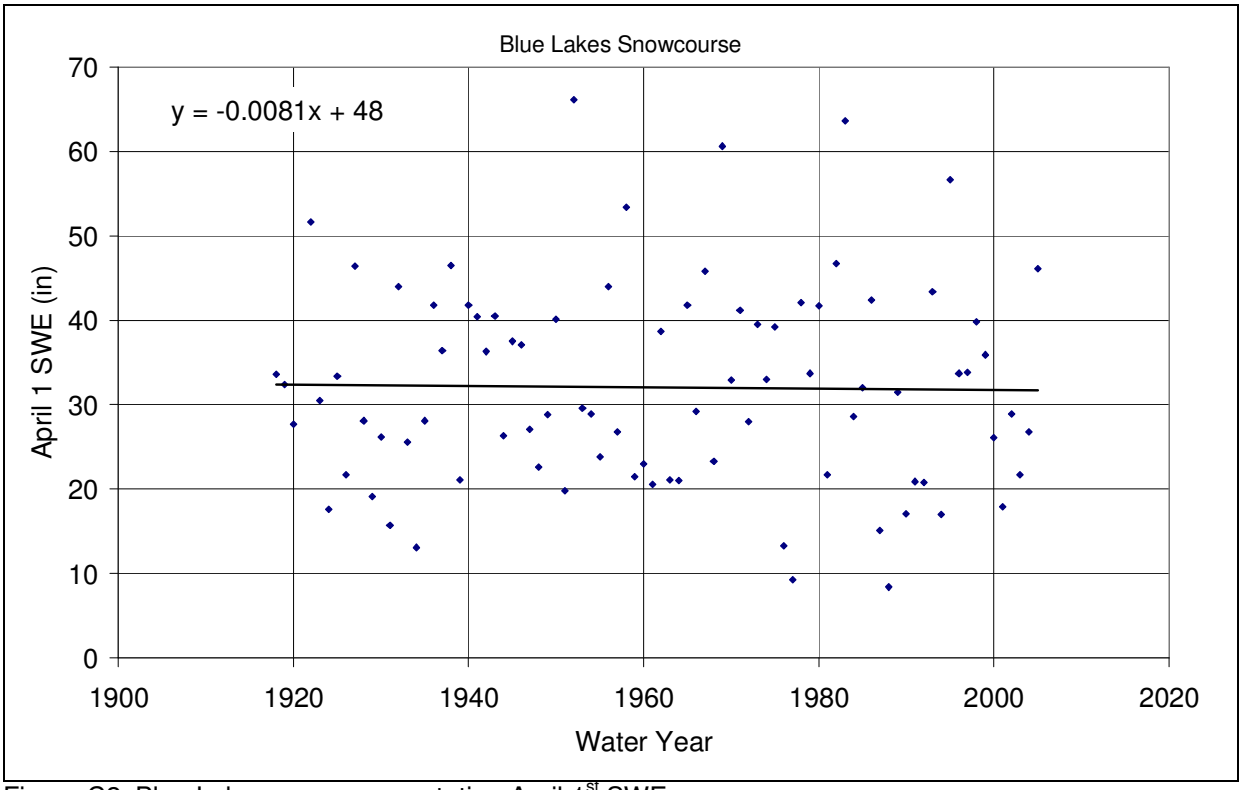

Figure C2. Blue Lakes snowcourse station April 1st SWE.

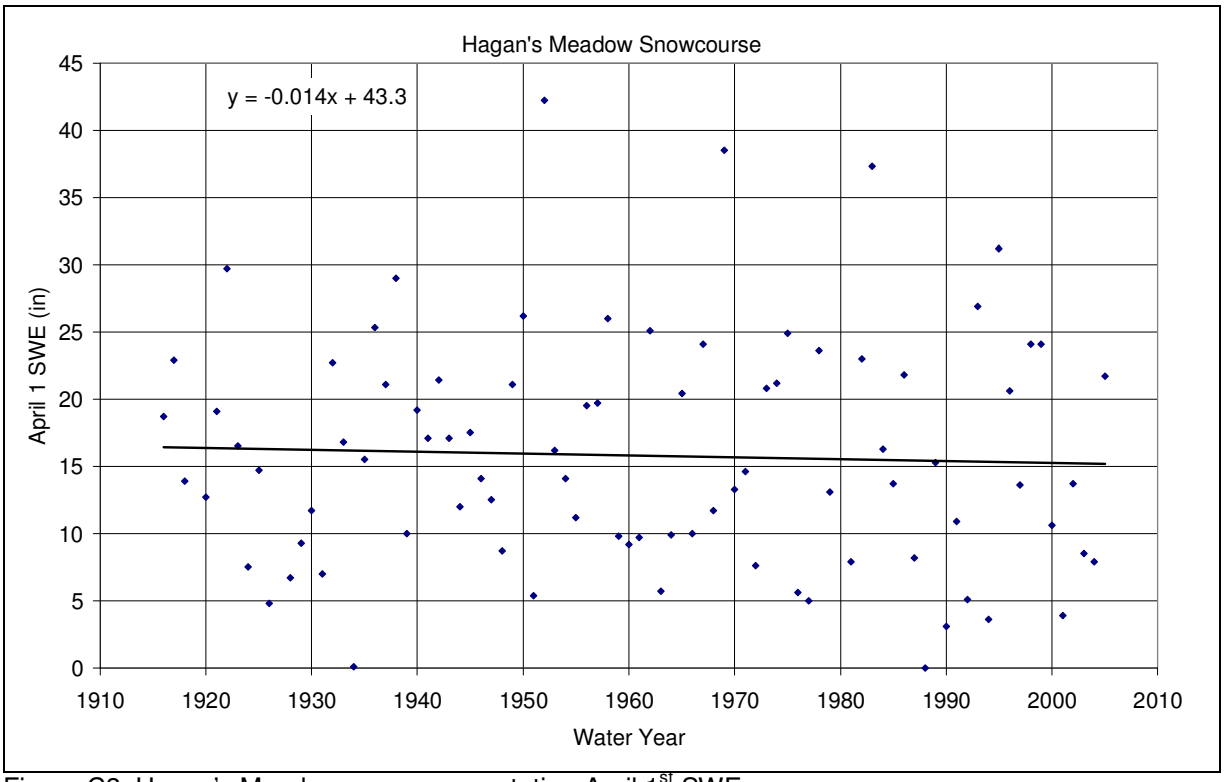

Figure C3. Hagan's Meadow snowcourse station April 1st SWE.

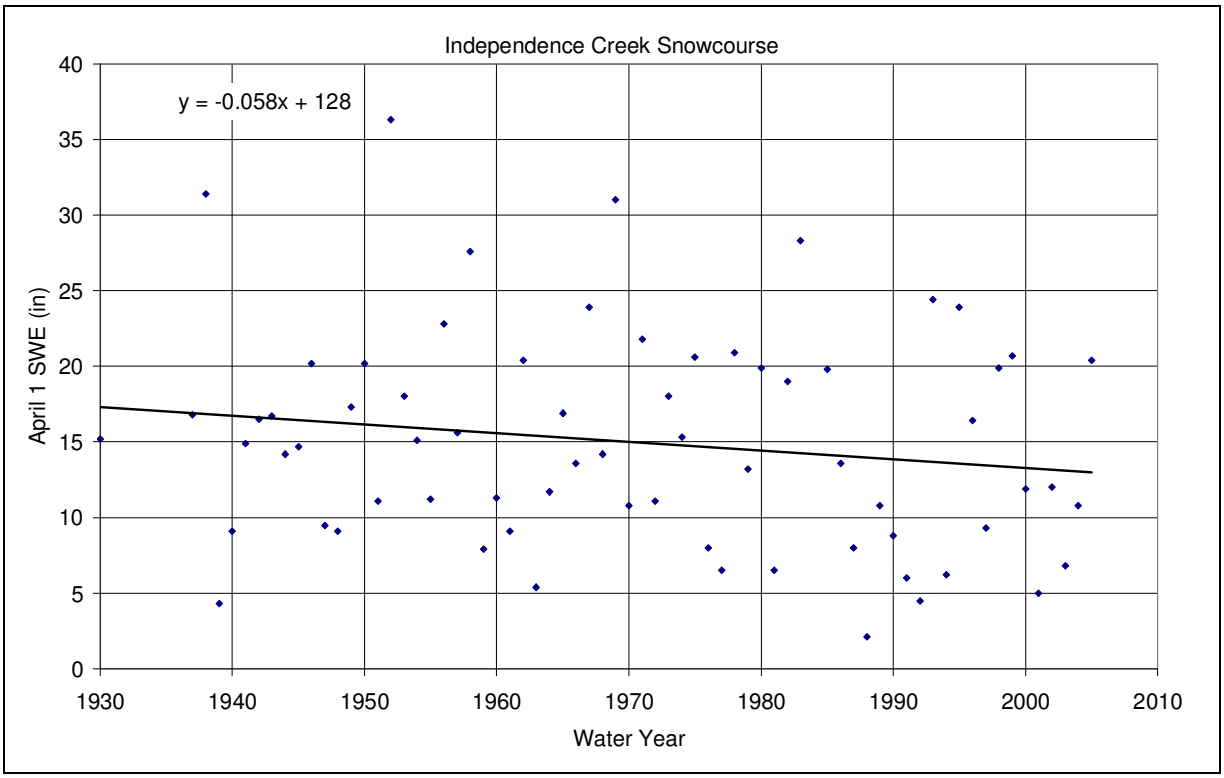

Figure C4. Independence Creek snowcourse station April 1st SWE.

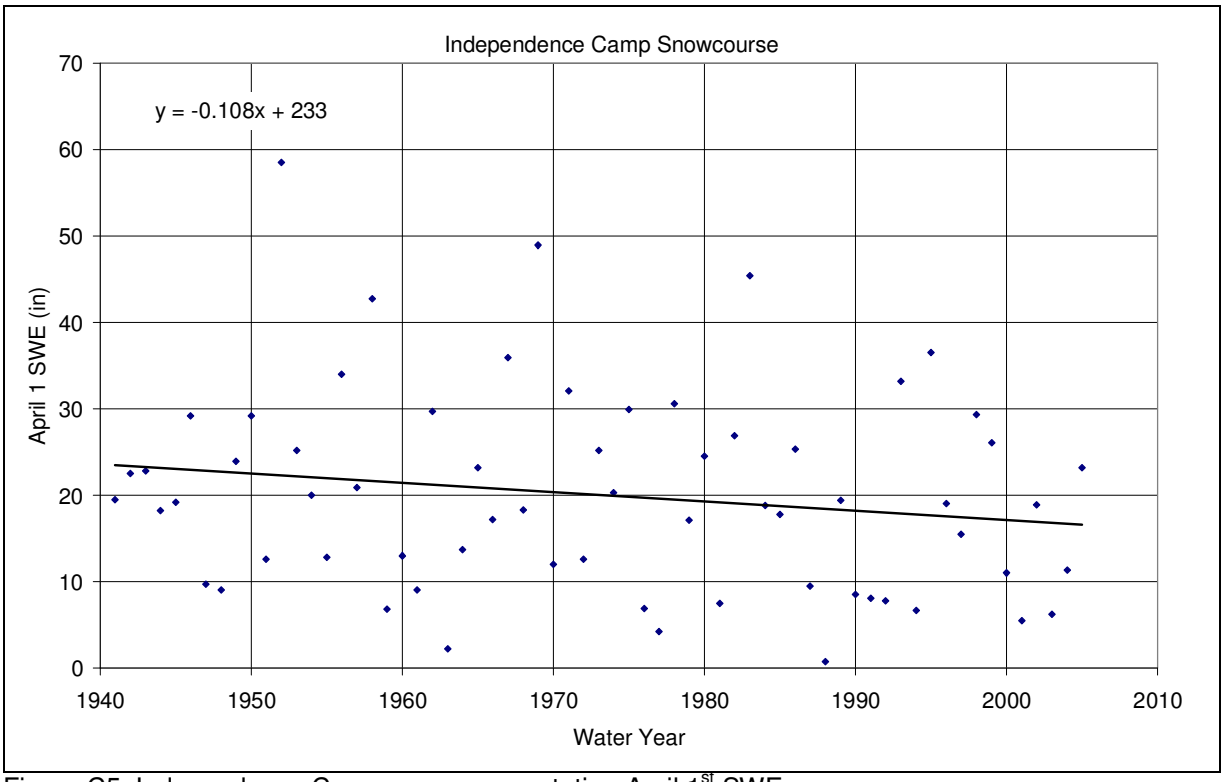

Figure C5. Independence Camp snowcourse station April 1st SWE.

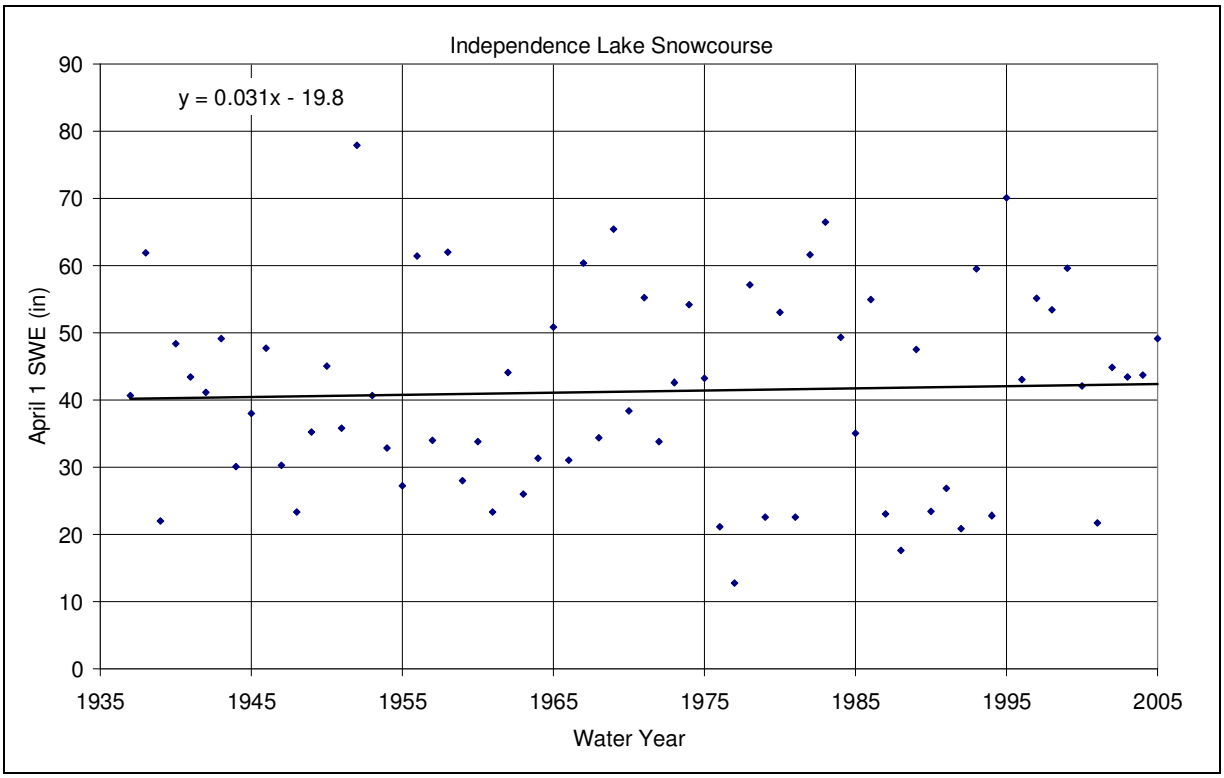

Figure C6. Independence Lake snowcourse station April 1st SWE.

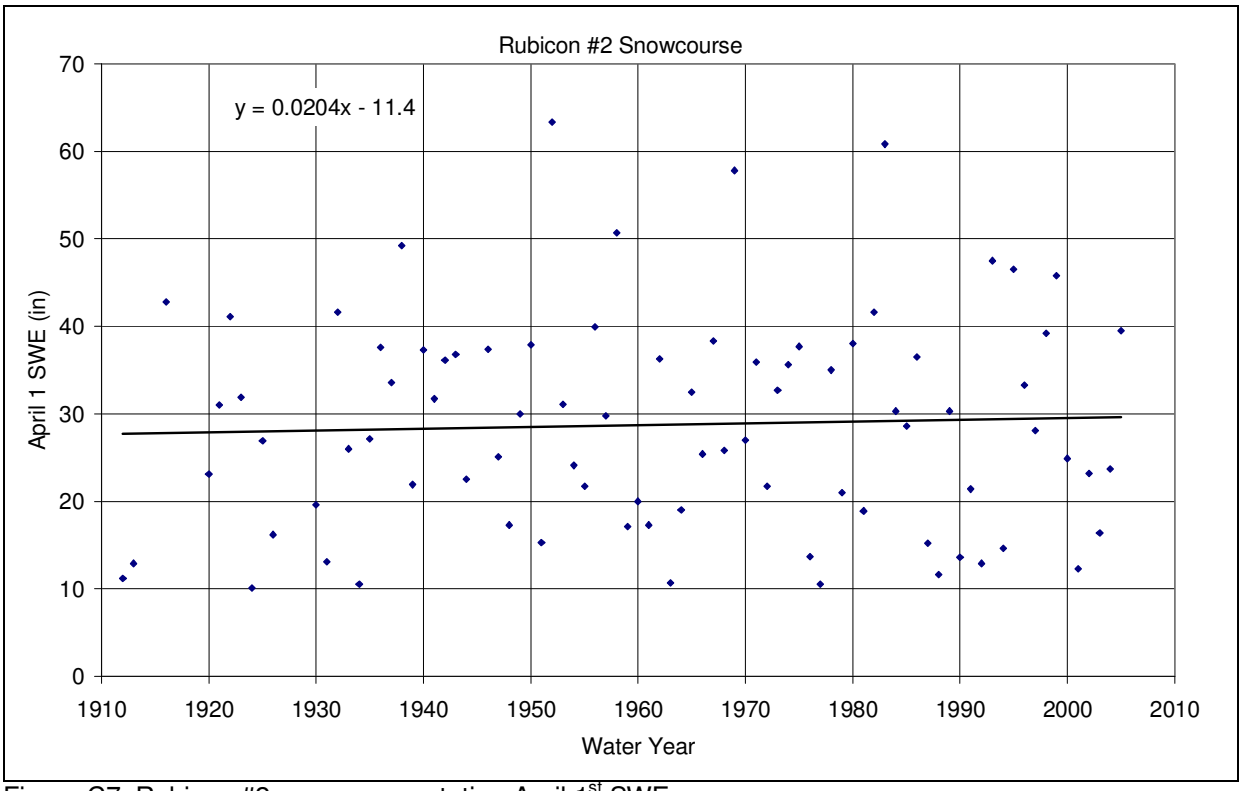

Figure C7. Rubicon #2 snowcourse station April 1st SWE.

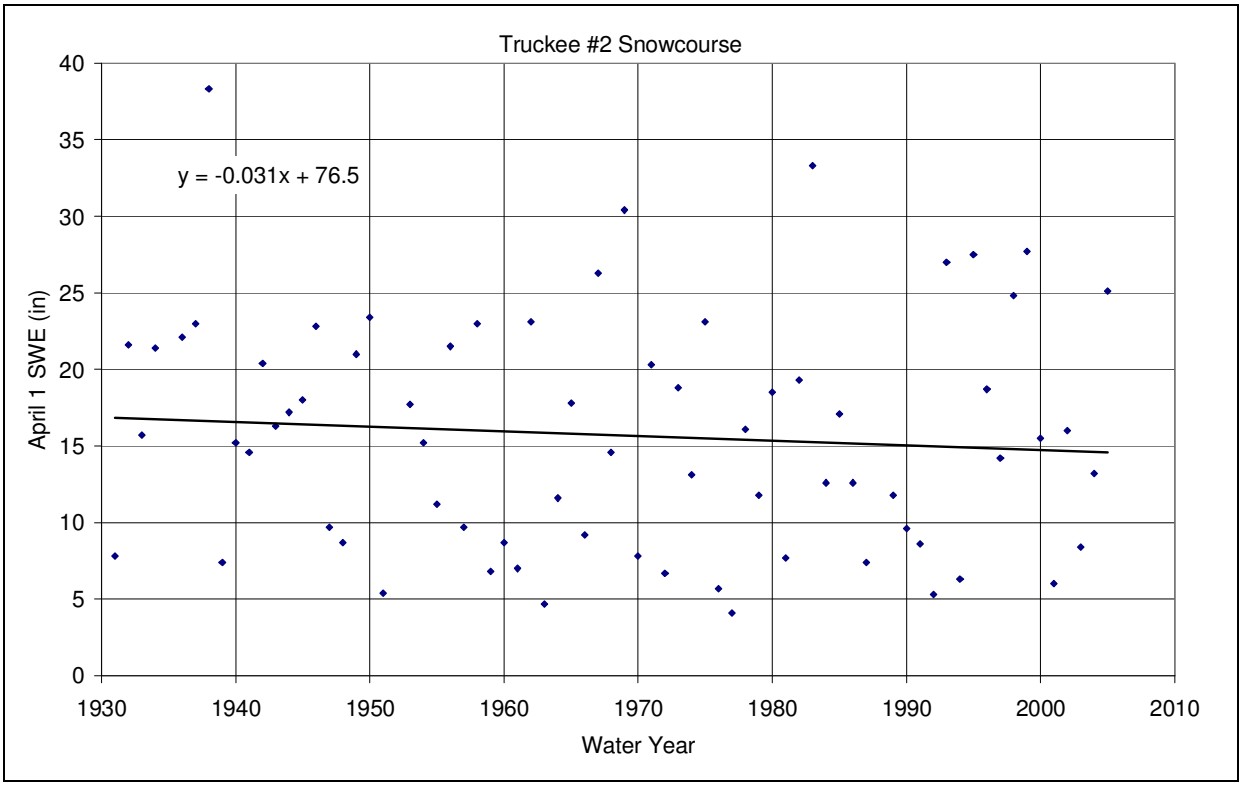

Figure C8. Truckee #2 snowcourse station April 1st SWE.

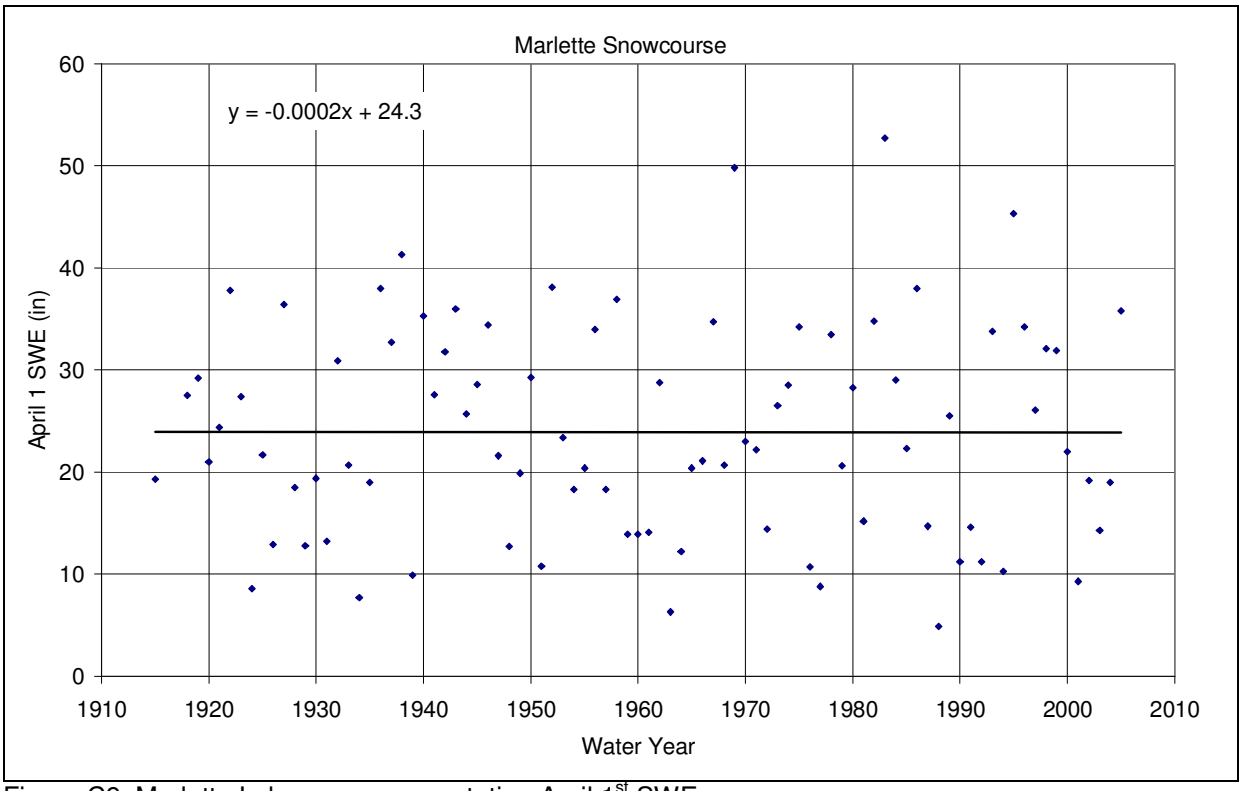

Figure C9. Marlette Lake snowcourse station April 1st SWE.

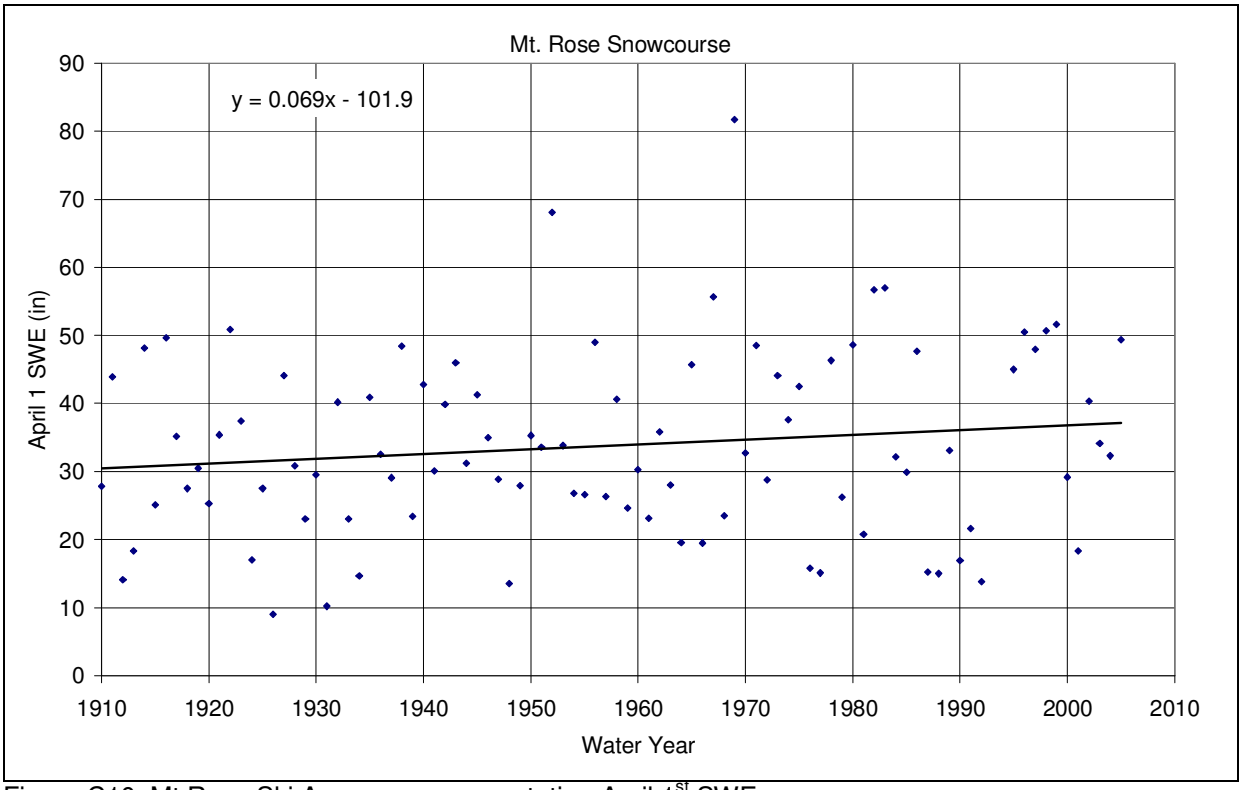

Figure C10. Mt Rose Ski Area snowcourse station April 1st SWE.

Appendix D

Streamflow

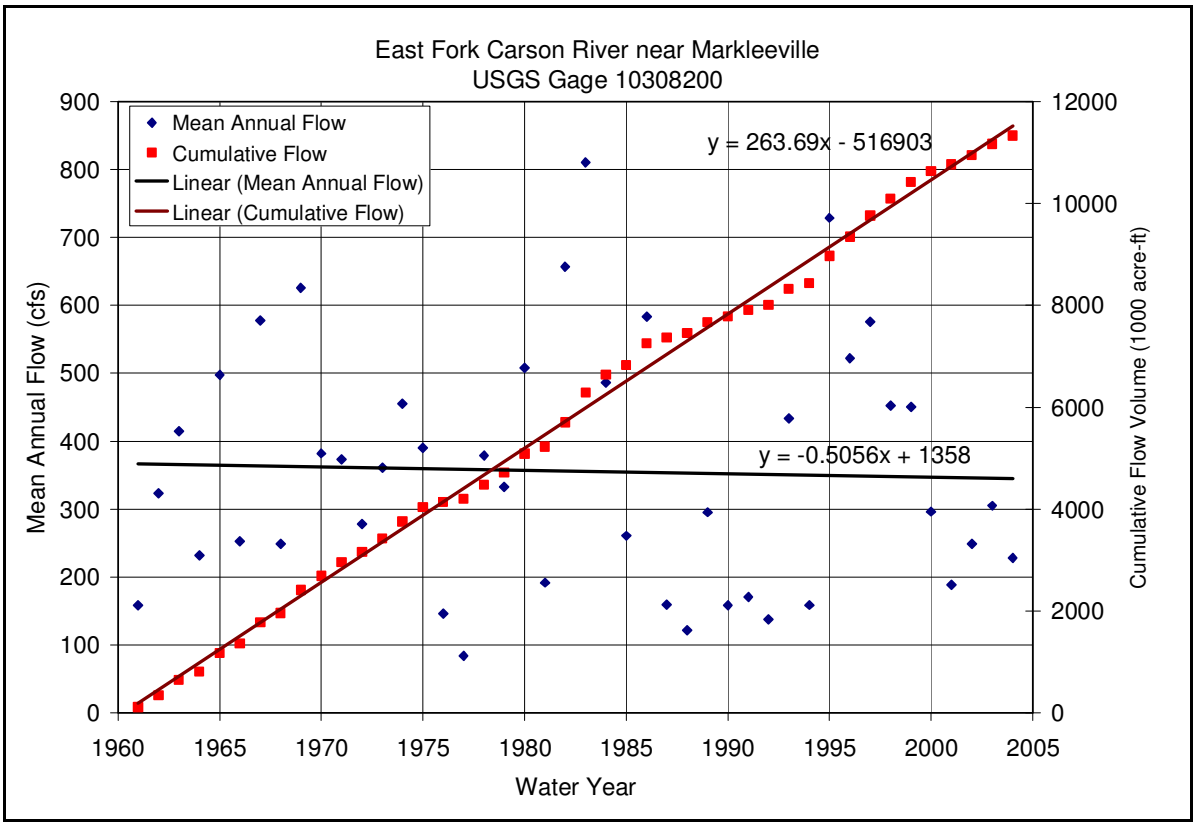

Figure D1. East Fork of the Carson River near Markleeville annual streamflow.

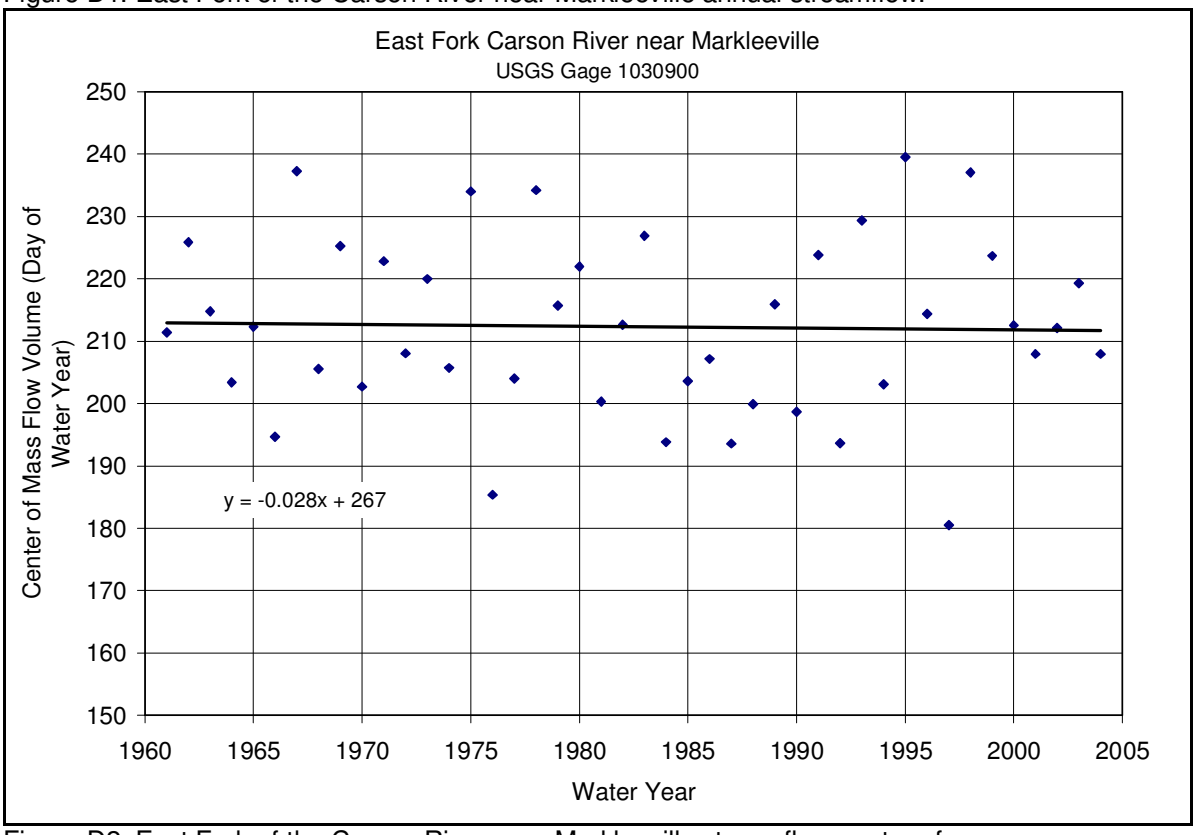

Figure D2. East Fork of the Carson River near Markleeville streamflow center of mass.

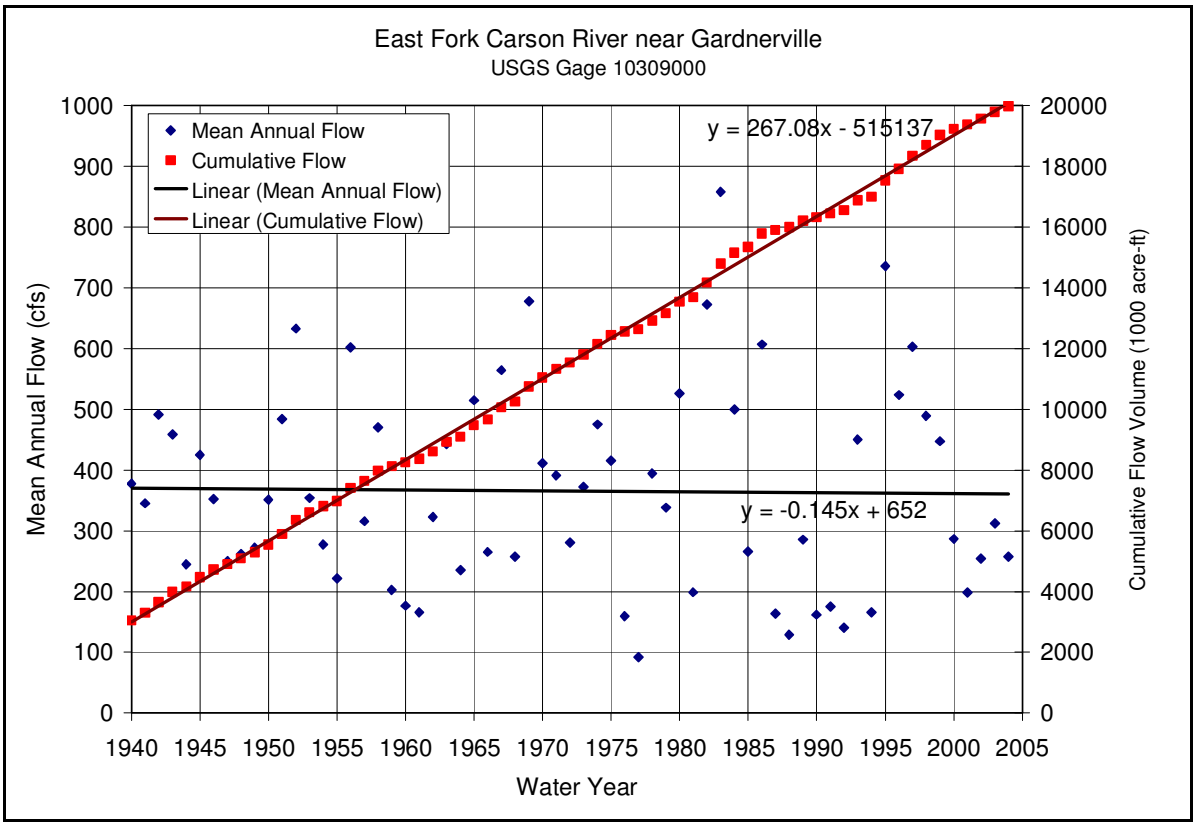

Figure D3. East Fork of the Carson River near Gardnerville annual streamflow.

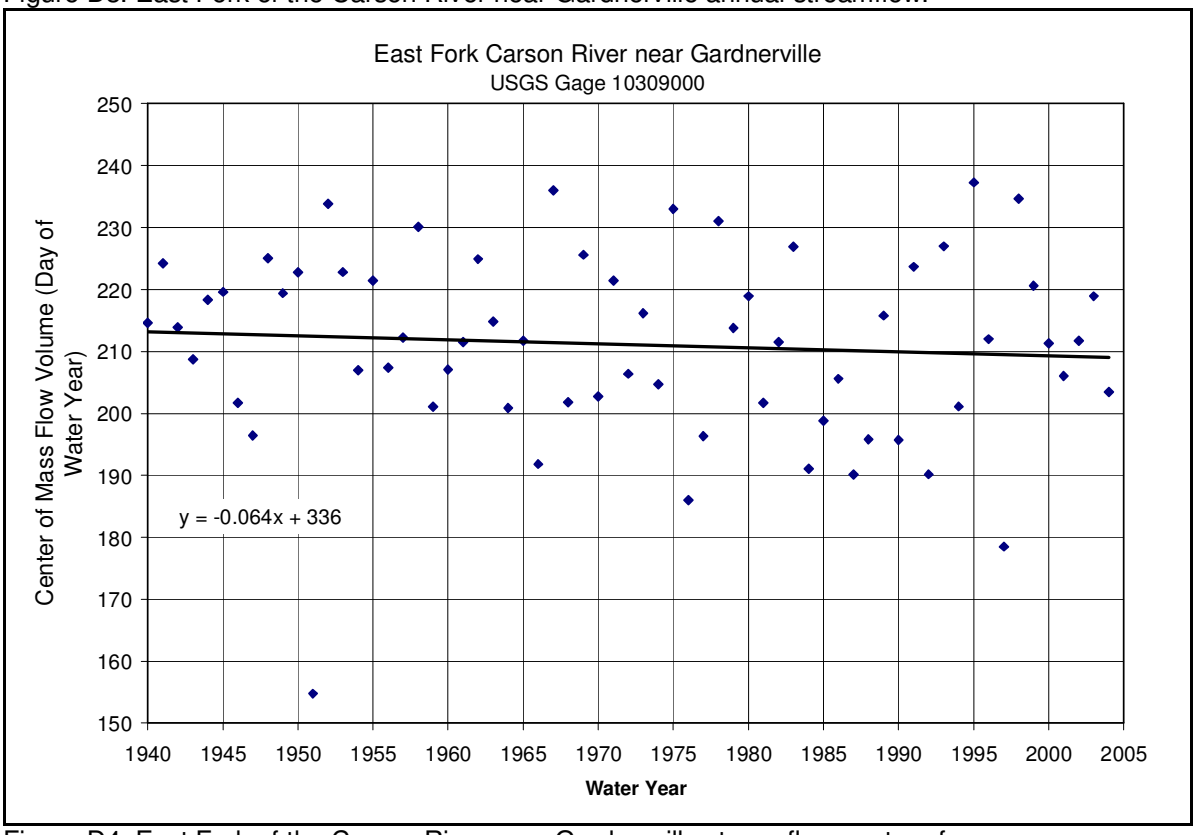

Figure D4. East Fork of the Carson River near Gardnerville streamflow center of mass.

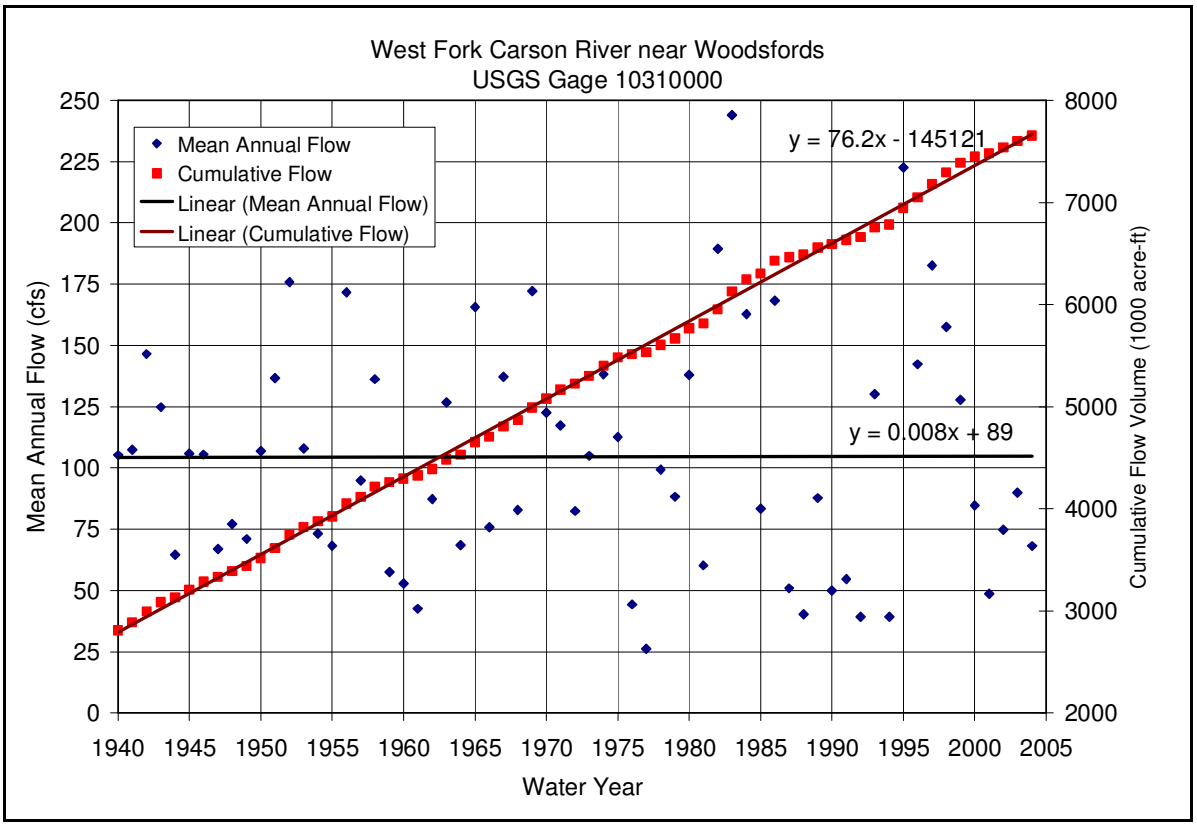

Figure D5. West Fork of the Carson River near Woodsford annual streamflow.

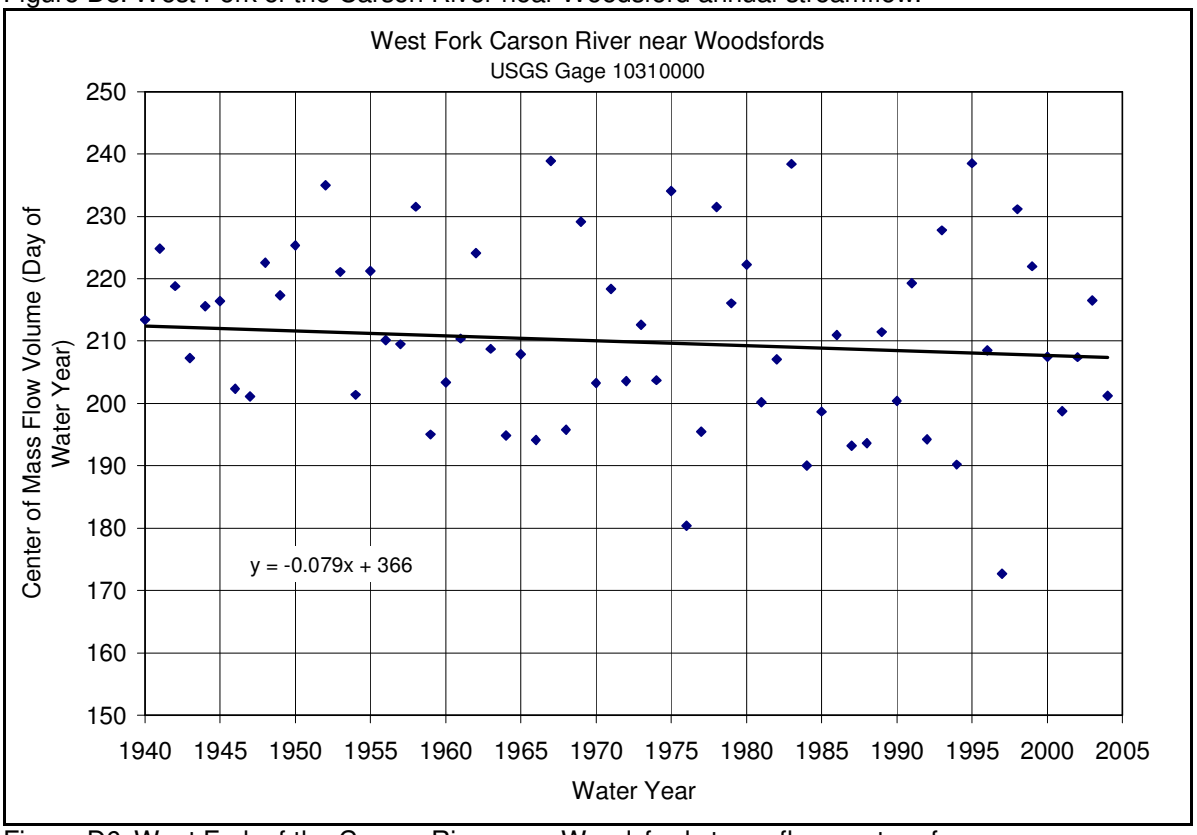

Figure D6. West Fork of the Carson River near Woodsford streamflow center of mass.

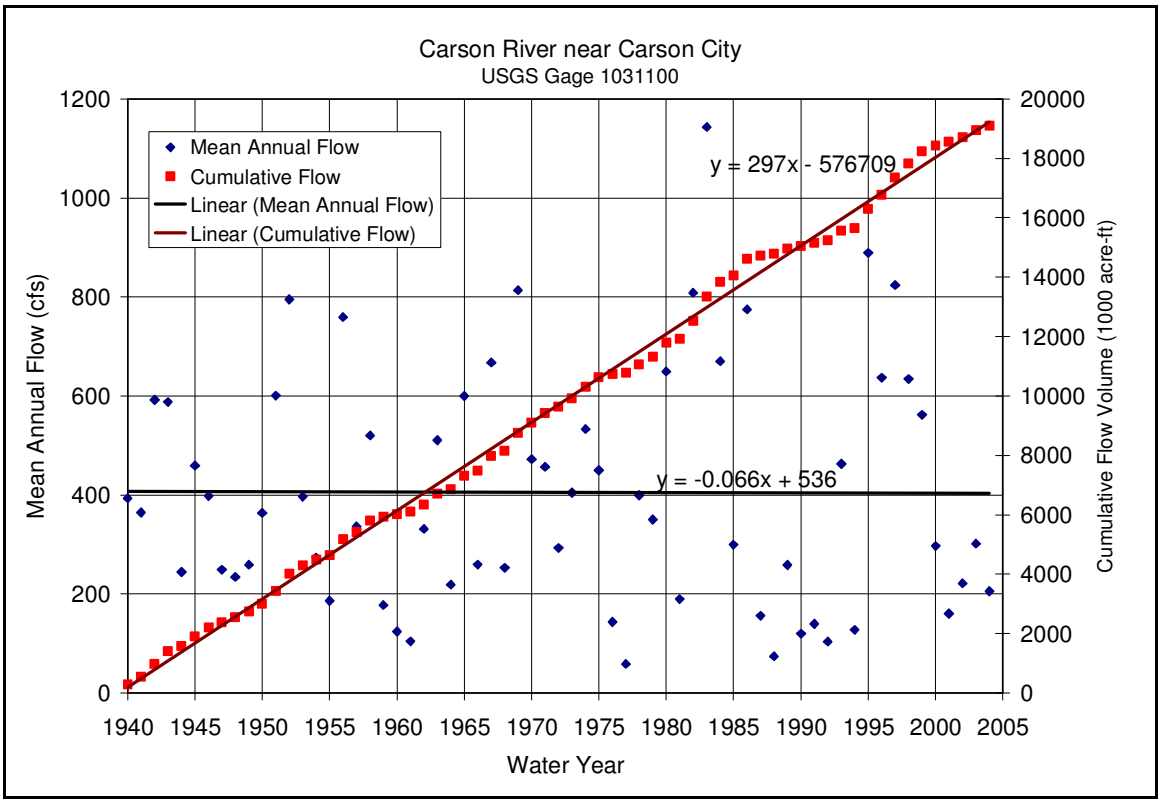

Figure D7. Carson River near Carson City annual streamflow.

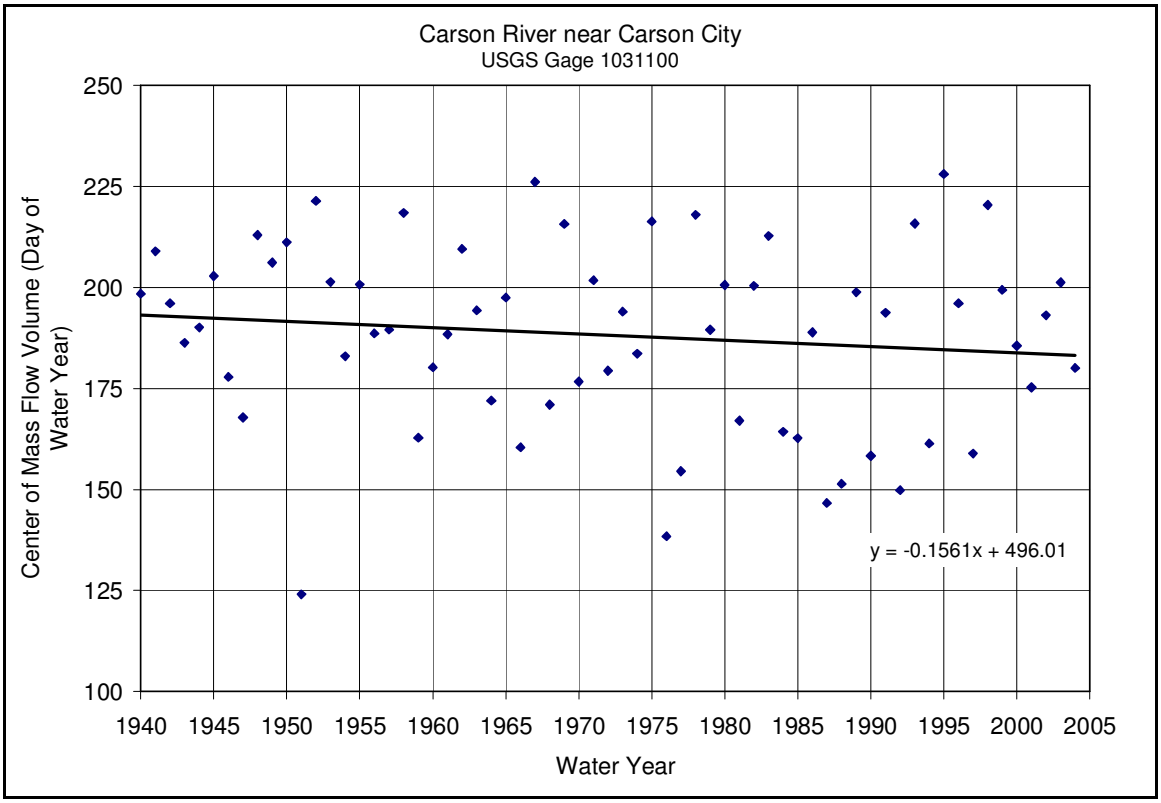

Figure D8. Carson River near Carson City streamflow center of mass.

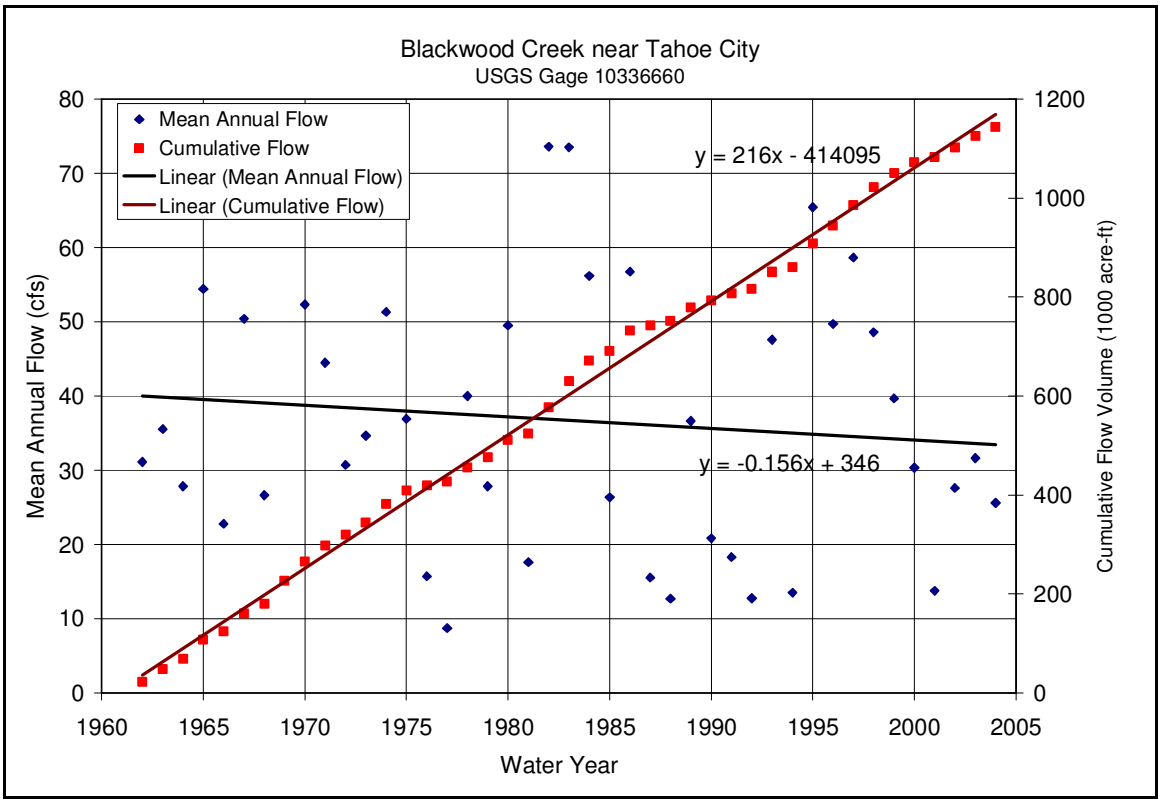

Figure D9. Blackwood Creek near Tahoe City annual streamflow.

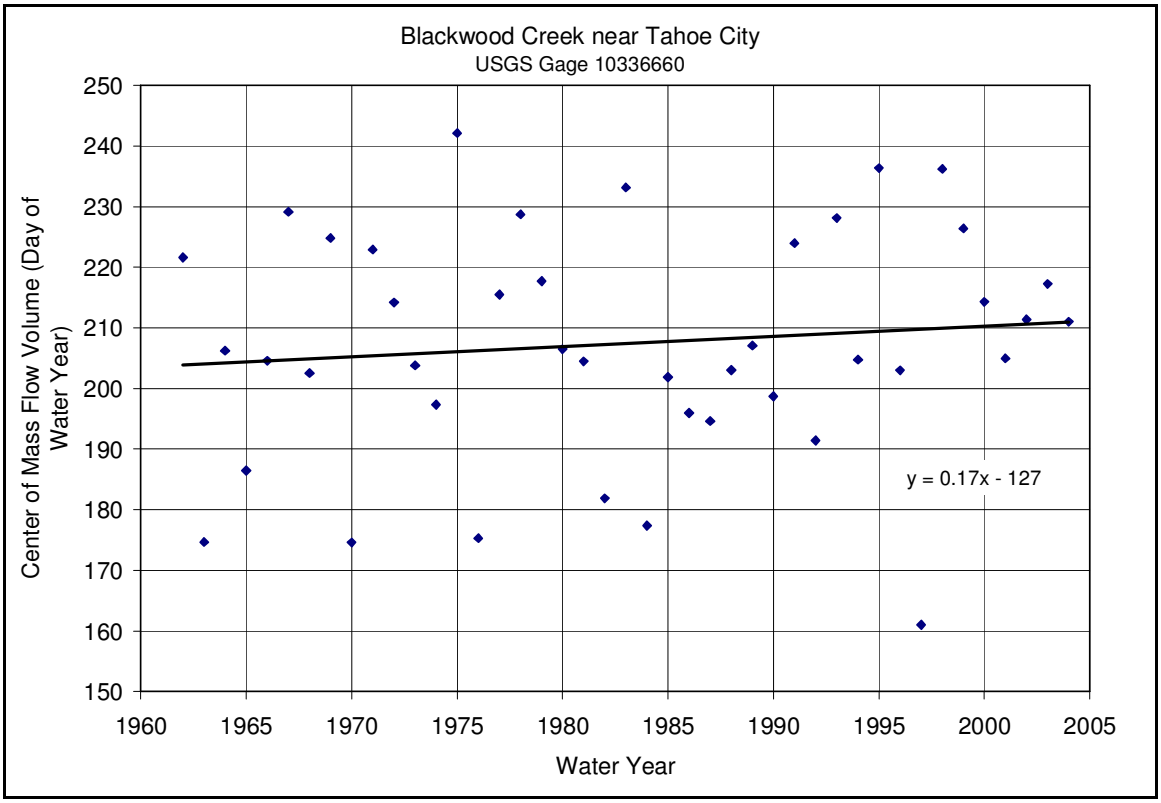

Figure D10. Blackwood Creek near Tahoe City streamflow center of mass.

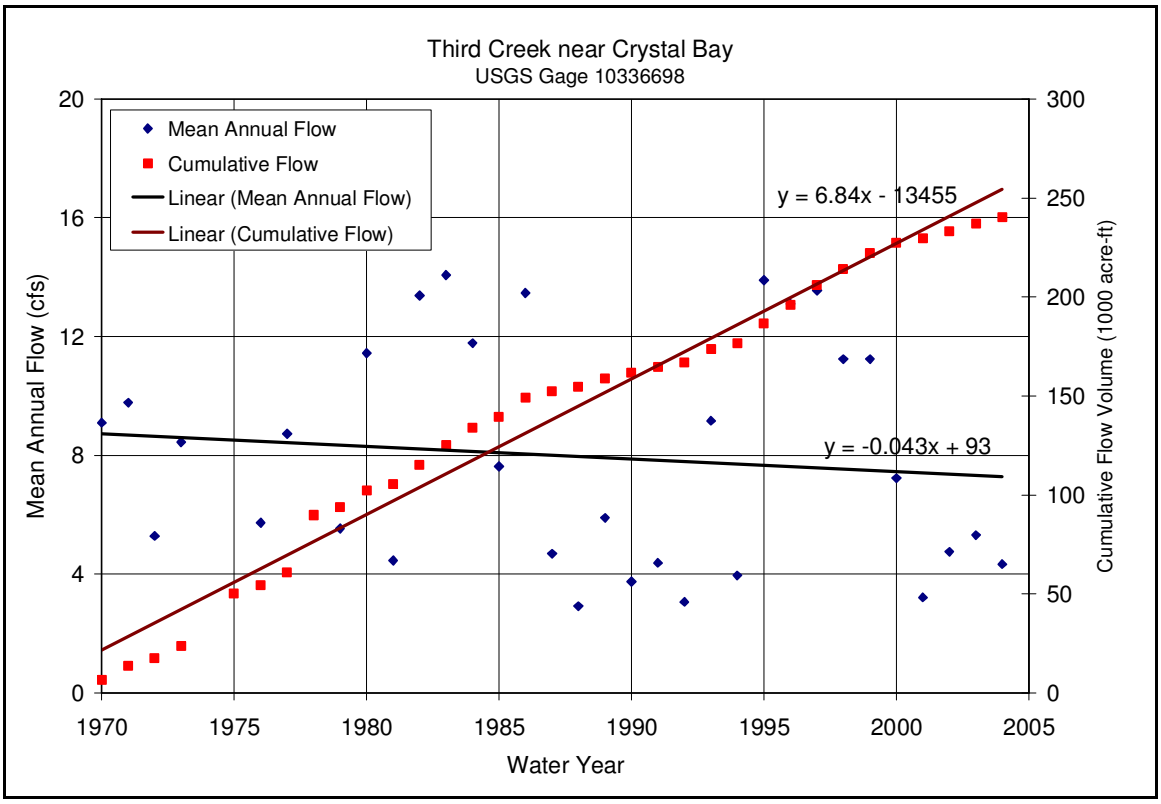

Figure D11. Third Creek near Crystal Bay annual streamflow.

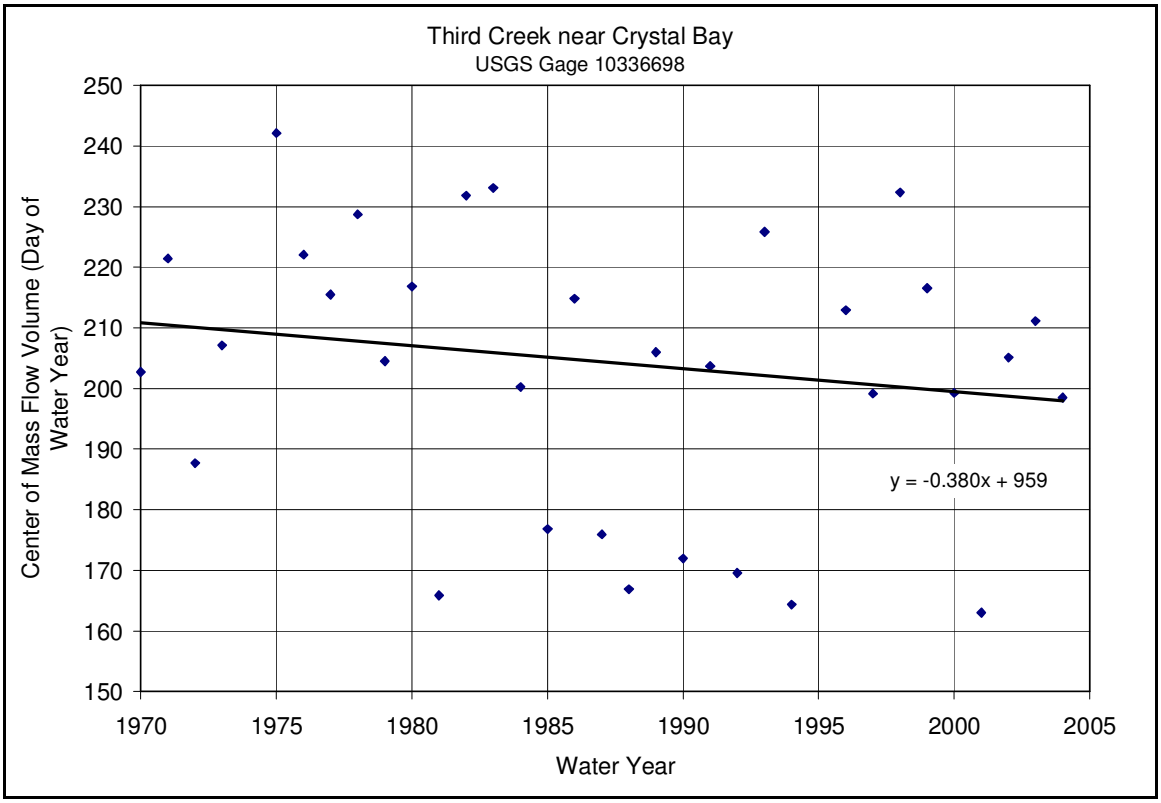

Figure D12. Third Creek near Crystal Bay streamflow center of mass.

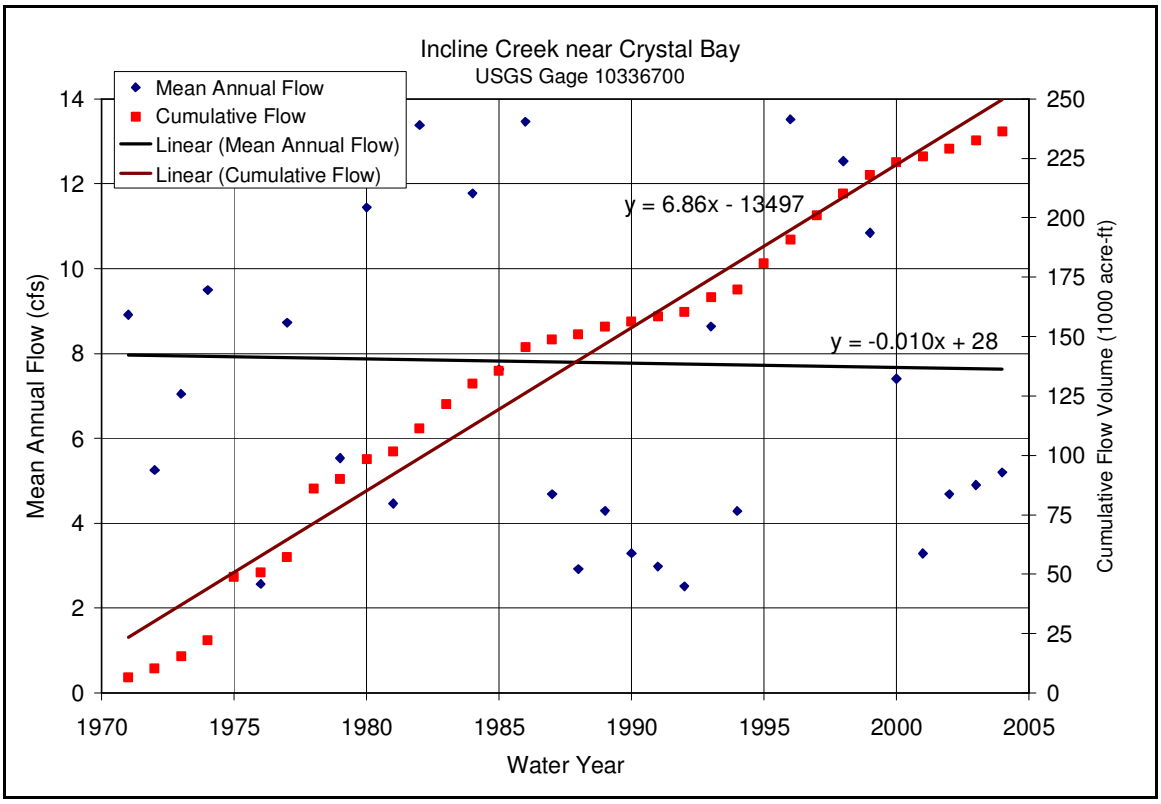

Figure D13. Incline Creek near Crystal Bay annual streamflow.

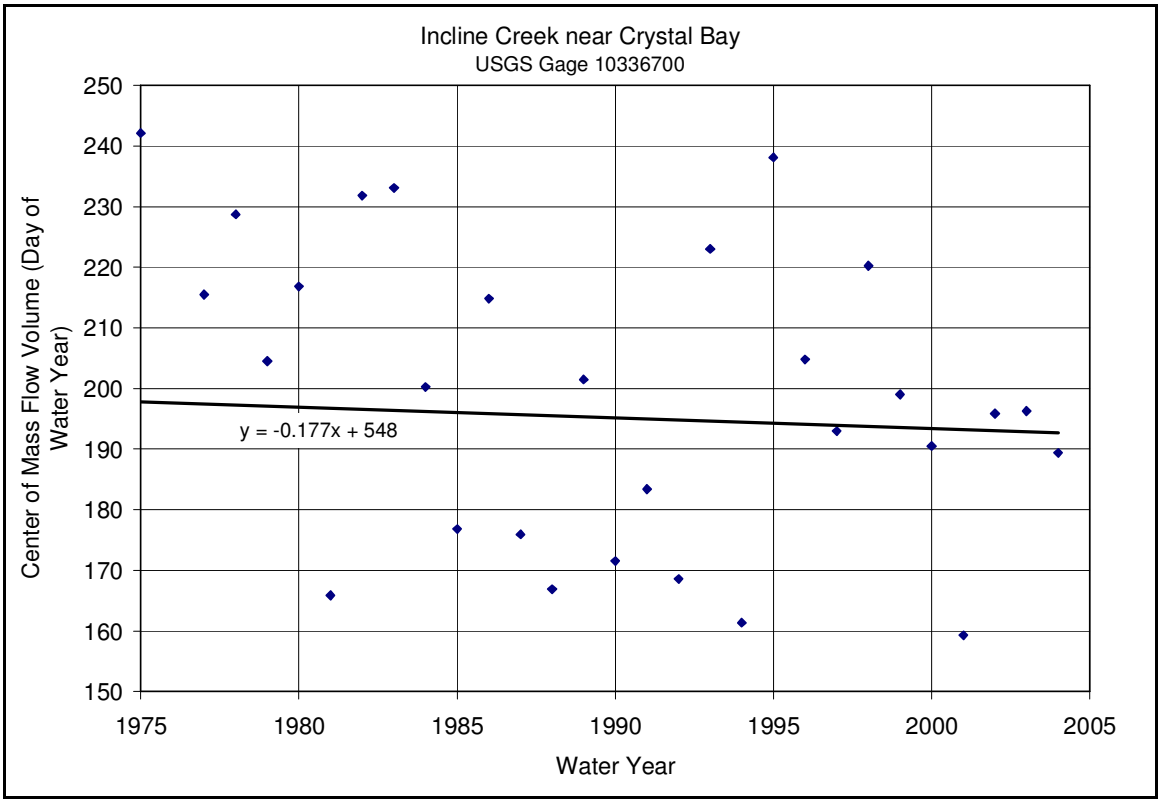

Figure D14. Incline Creek near Crystal Bay streamflow center of mass.

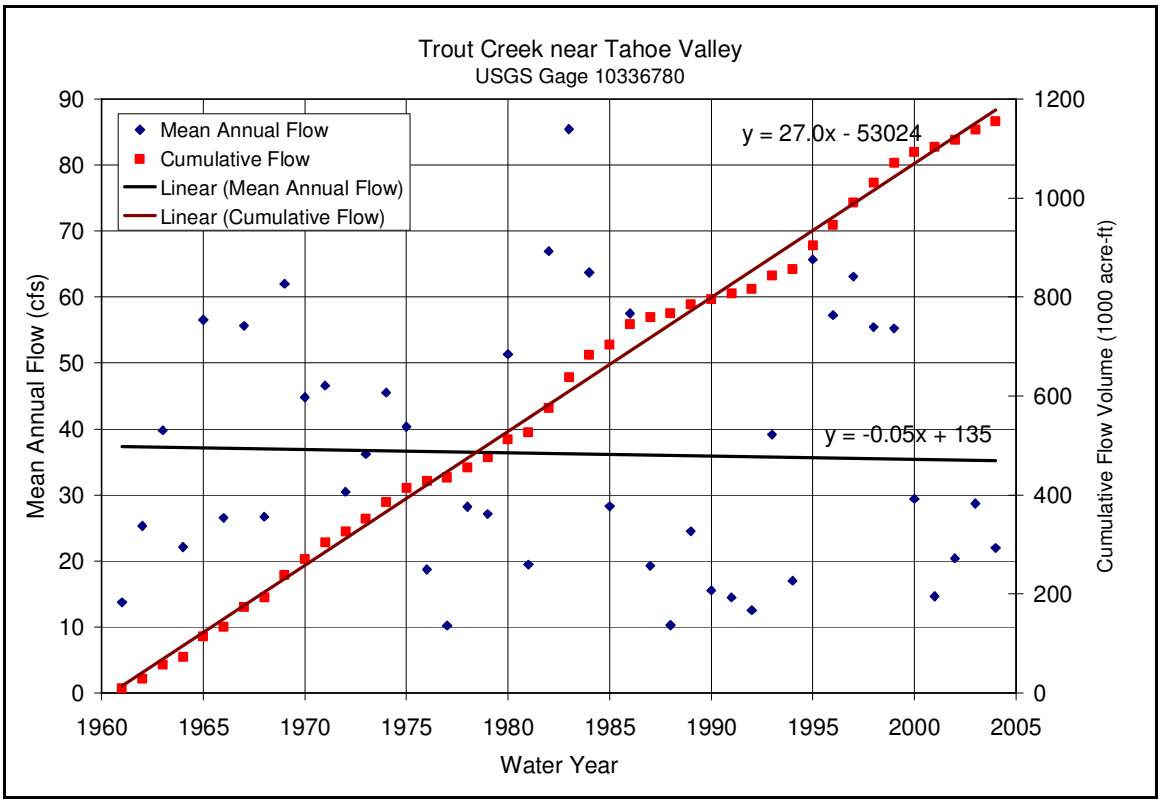

Figure D15. Trout Creek near Tahoe Valley annual streamflow.

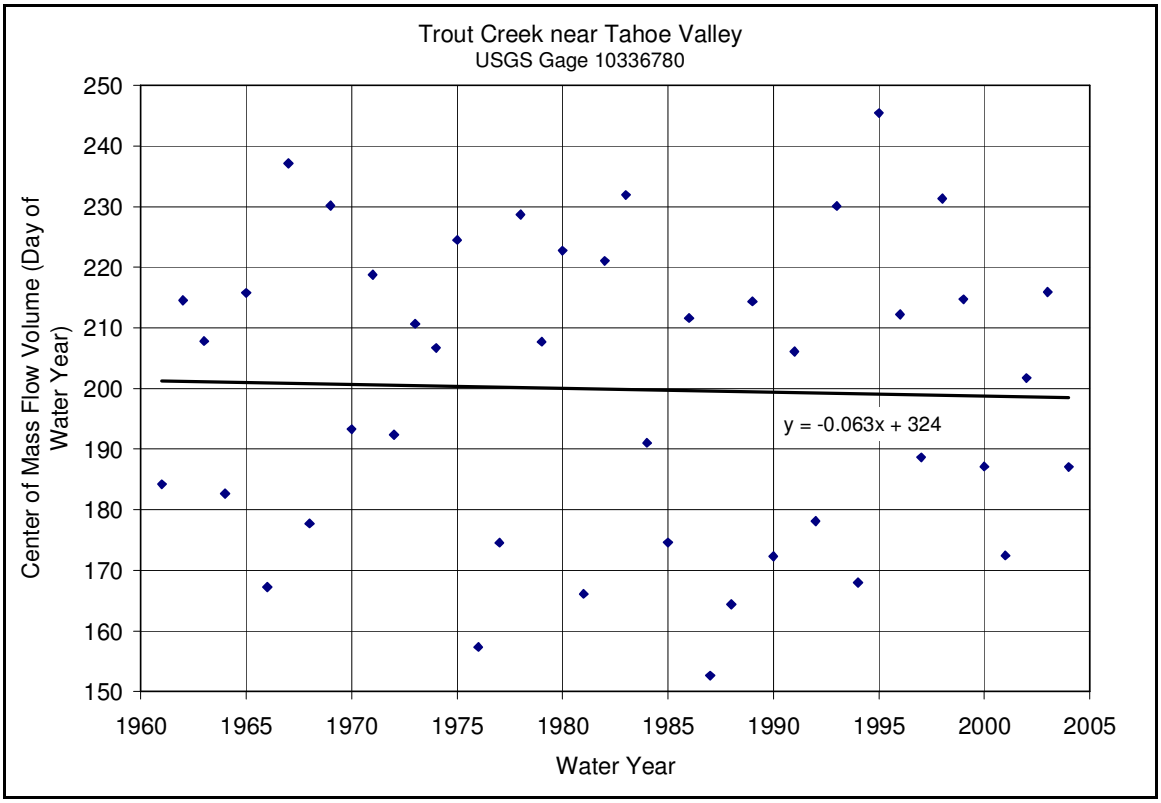

Figure D16. Trout Creek near Tahoe Valley streamflow center of mass.

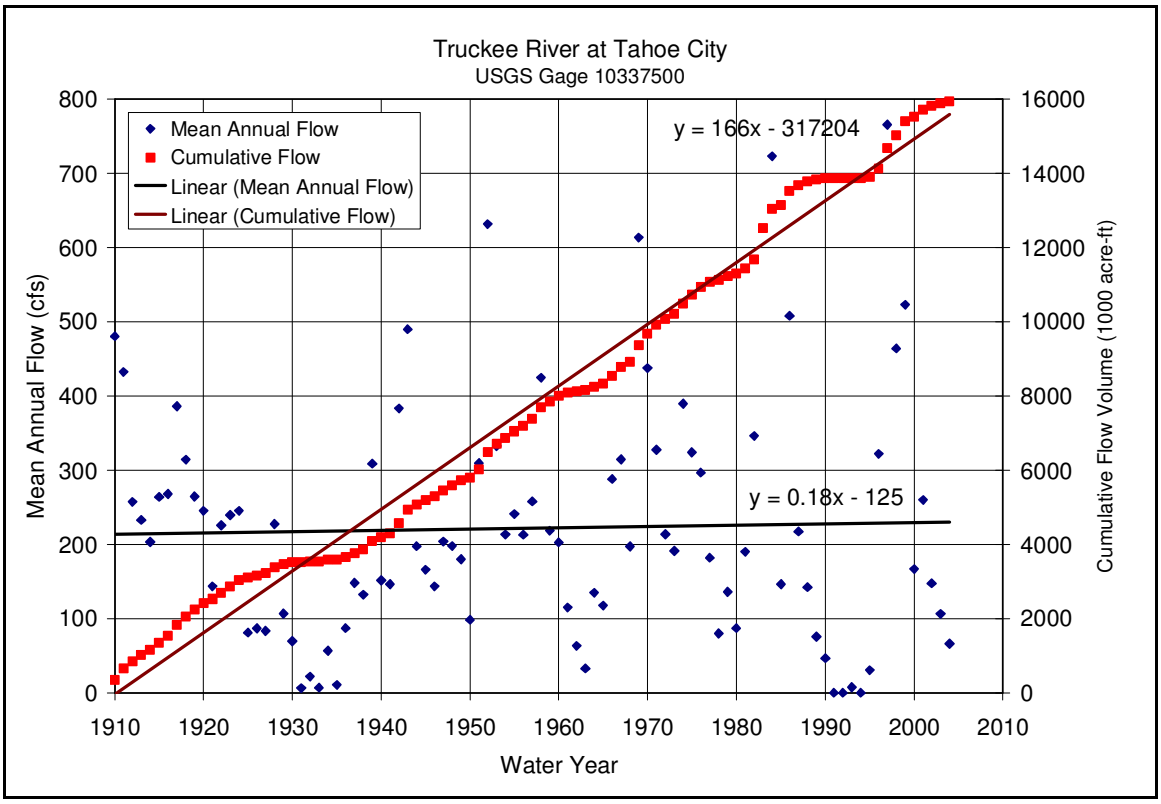

Figure D17. Truckee River at Tahoe City annual streamflow.

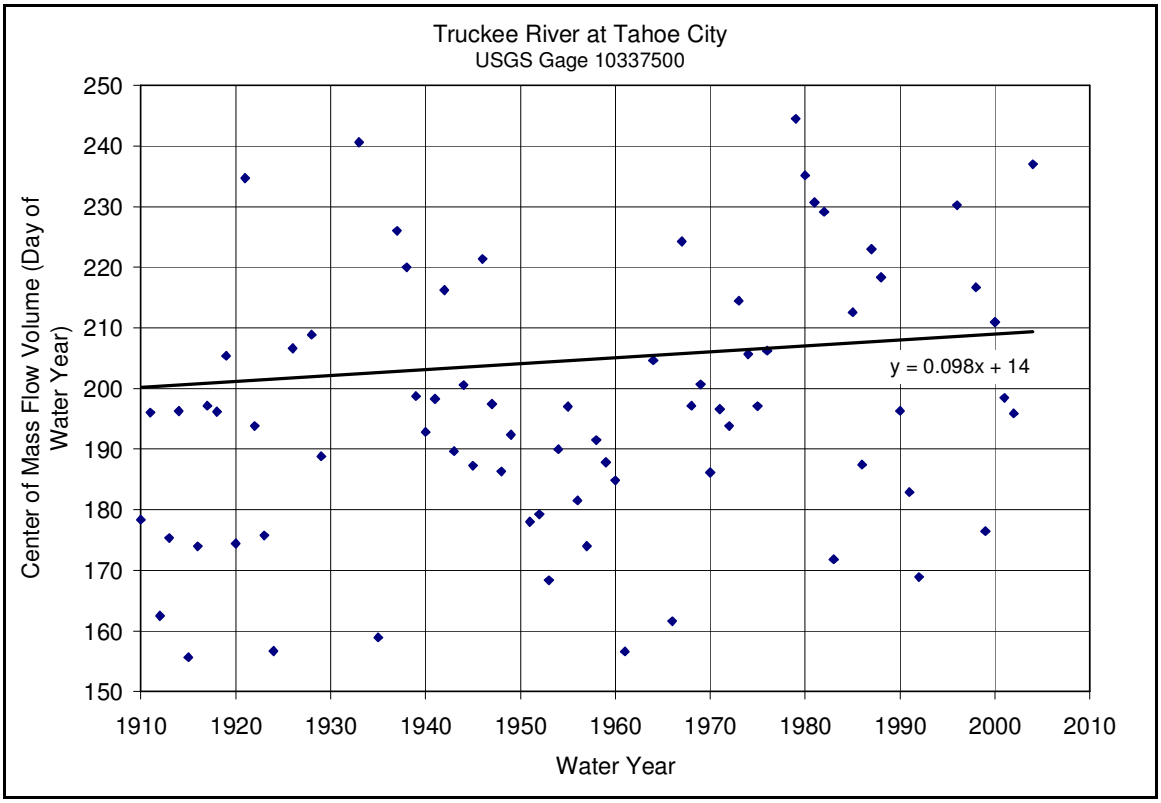

Figure D18. Truckee River at Tahoe City streamflow center of mass.

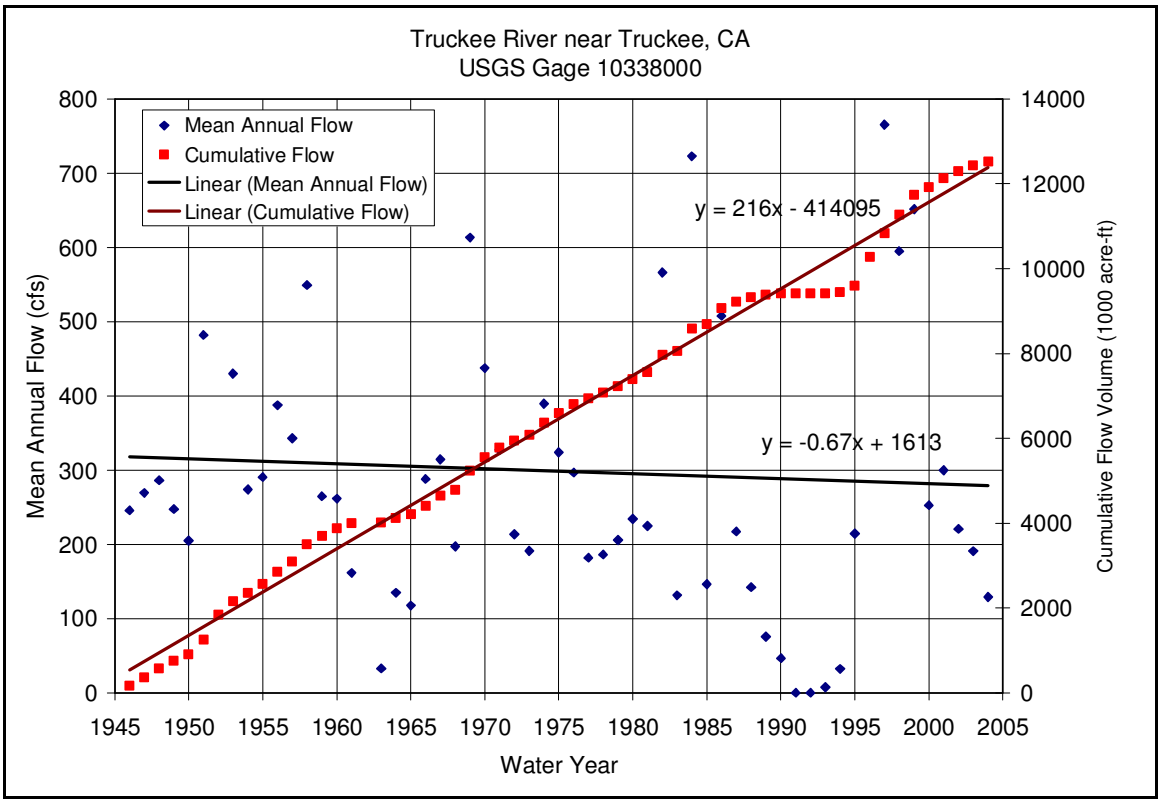

Figure D19. Truckee River near Truckee, CA annual streamflow.

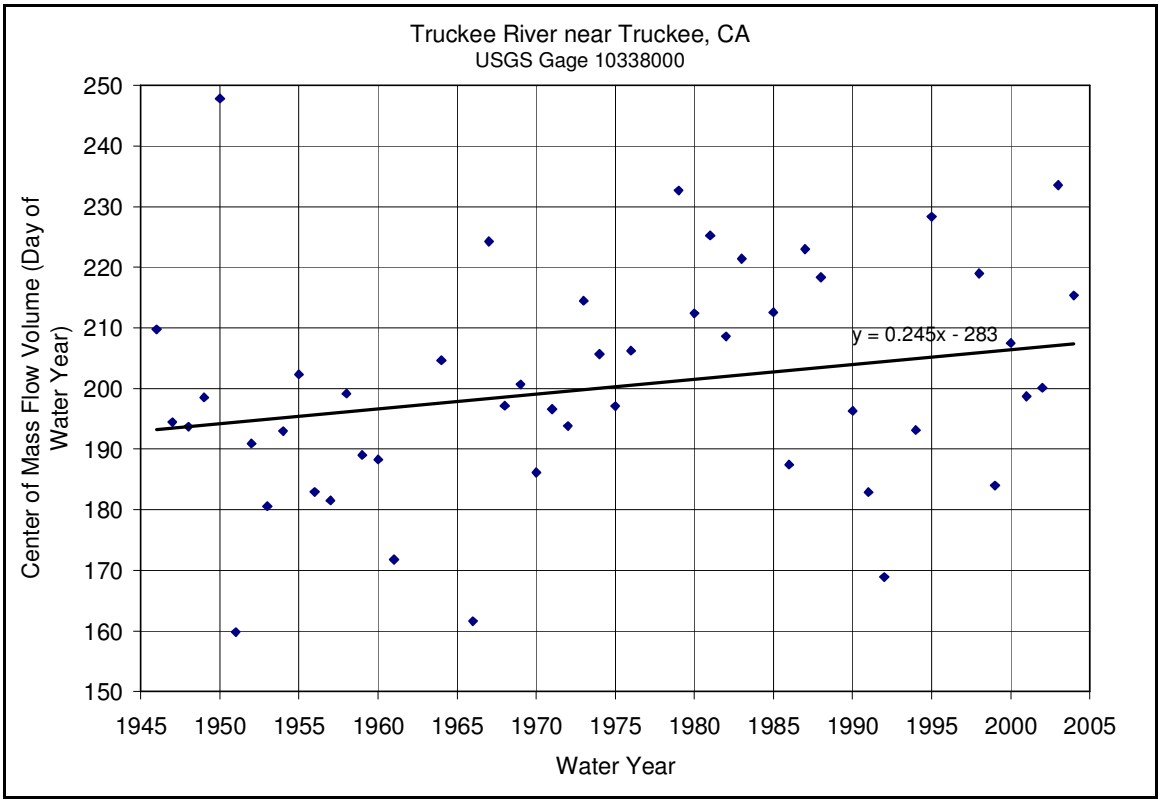

Figure D20. Truckee River near Truckee, CA streamflow center of mass.

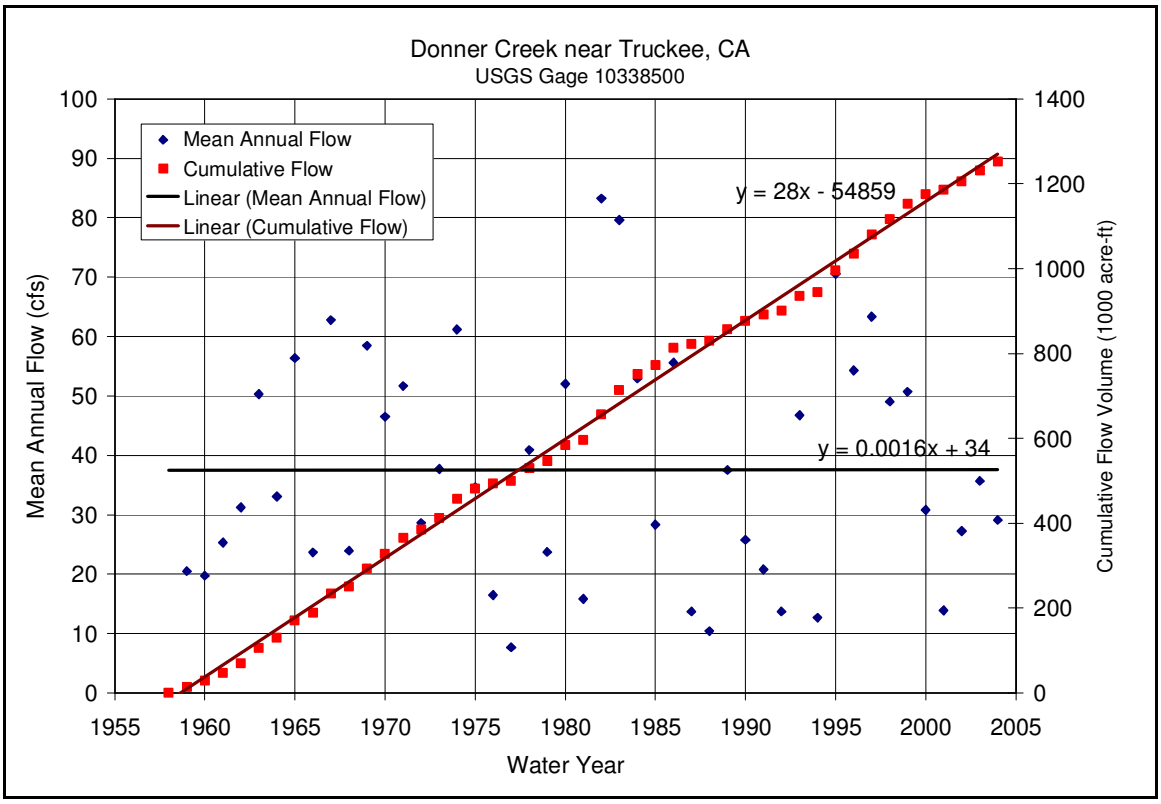

Figure D21. Donner Creek near Truckee, CA annual streamflow.

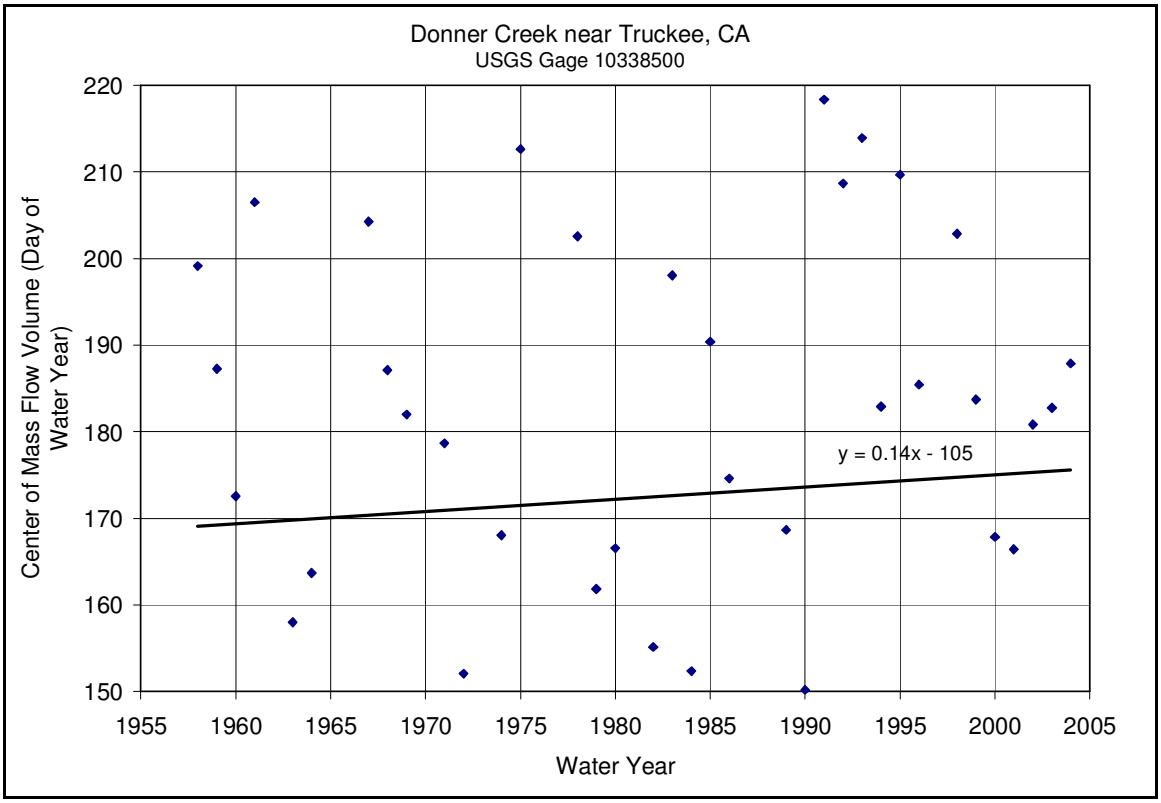

Figure D22. Donner Creek near Truckee, CA streamflow center of mass.

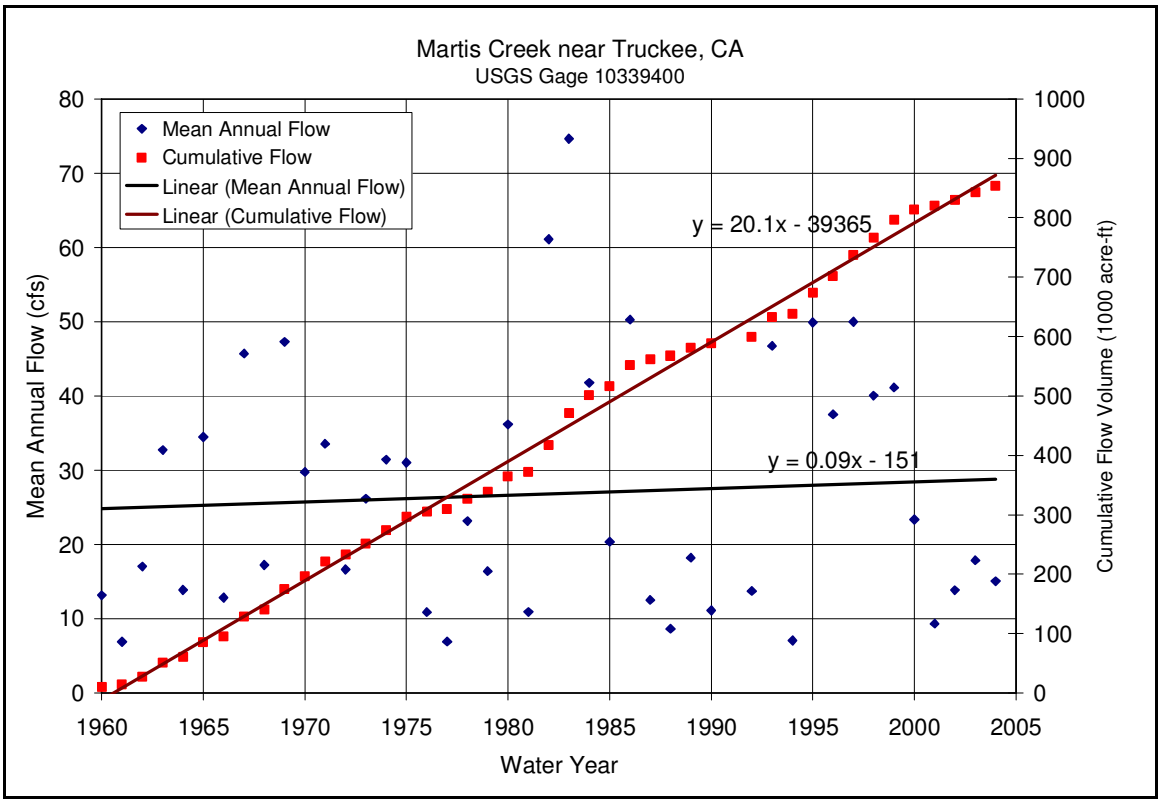

Figure D23. Martis Creek near Truckee, CA annual streamflow.

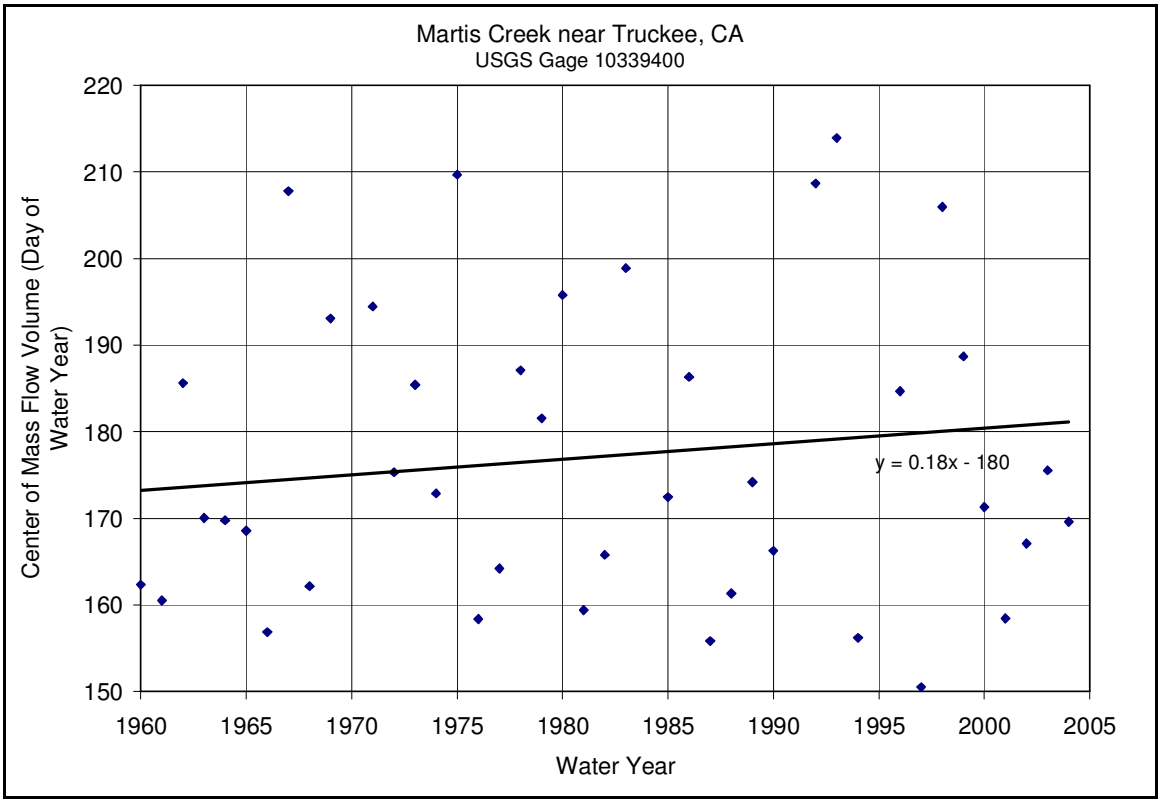

Figure D24. Martis Creek near Truckee, CA streamflow center of mass.

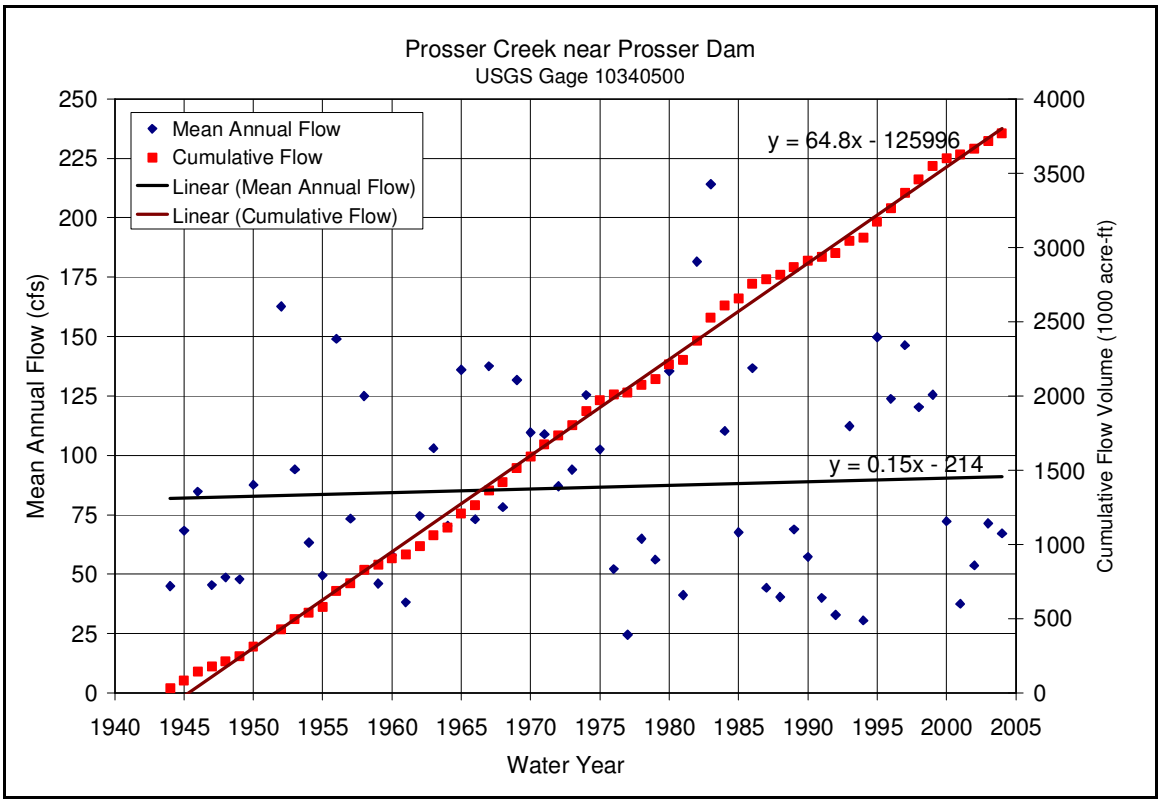

Figure D25. Prosser Creek near Prosser Dam annual streamflow.

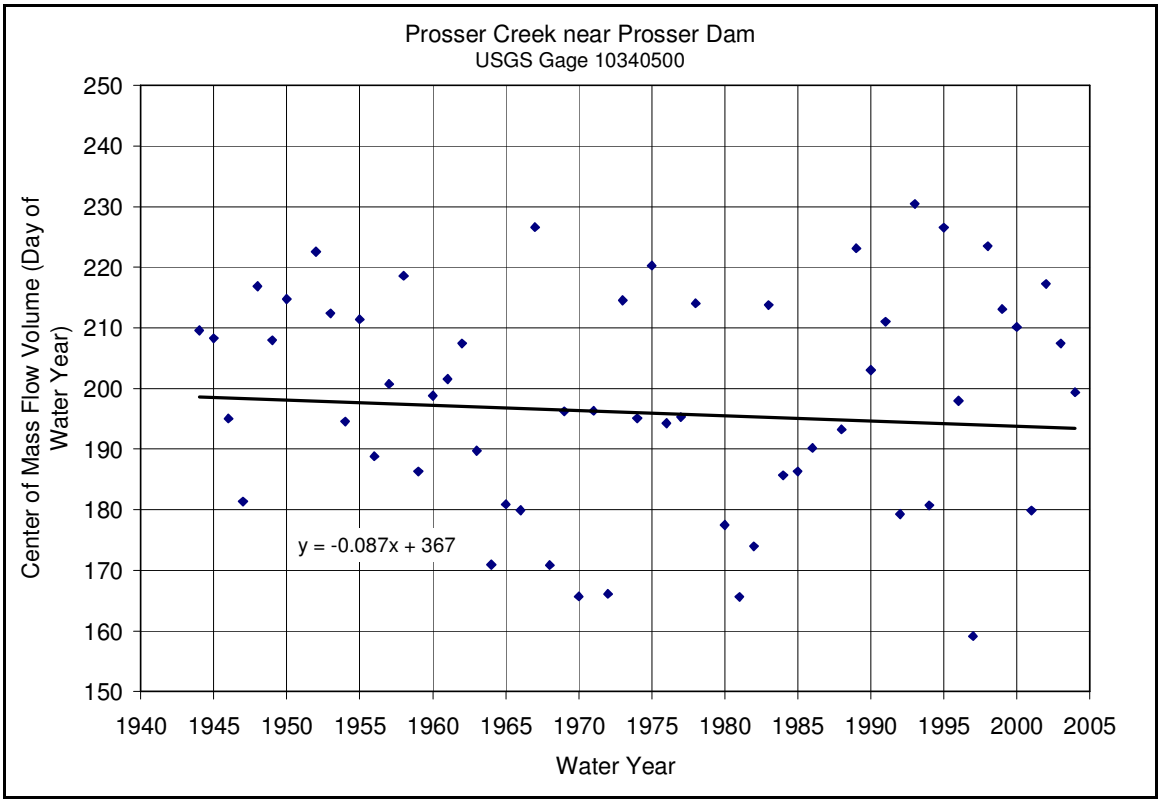

Figure D26. Prosser Creek near Prosser Dam streamflow center of mass.

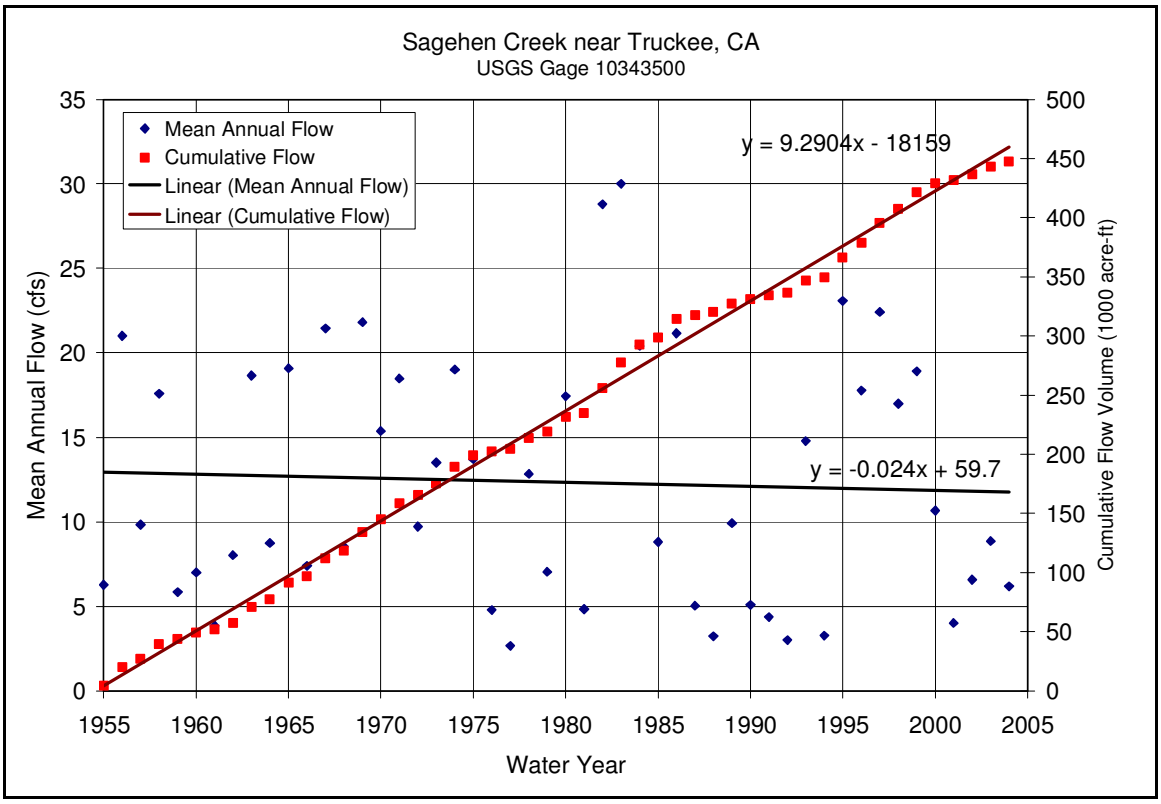

Figure D27. Sagehen Creek near Truckee, CA annual streamflow.

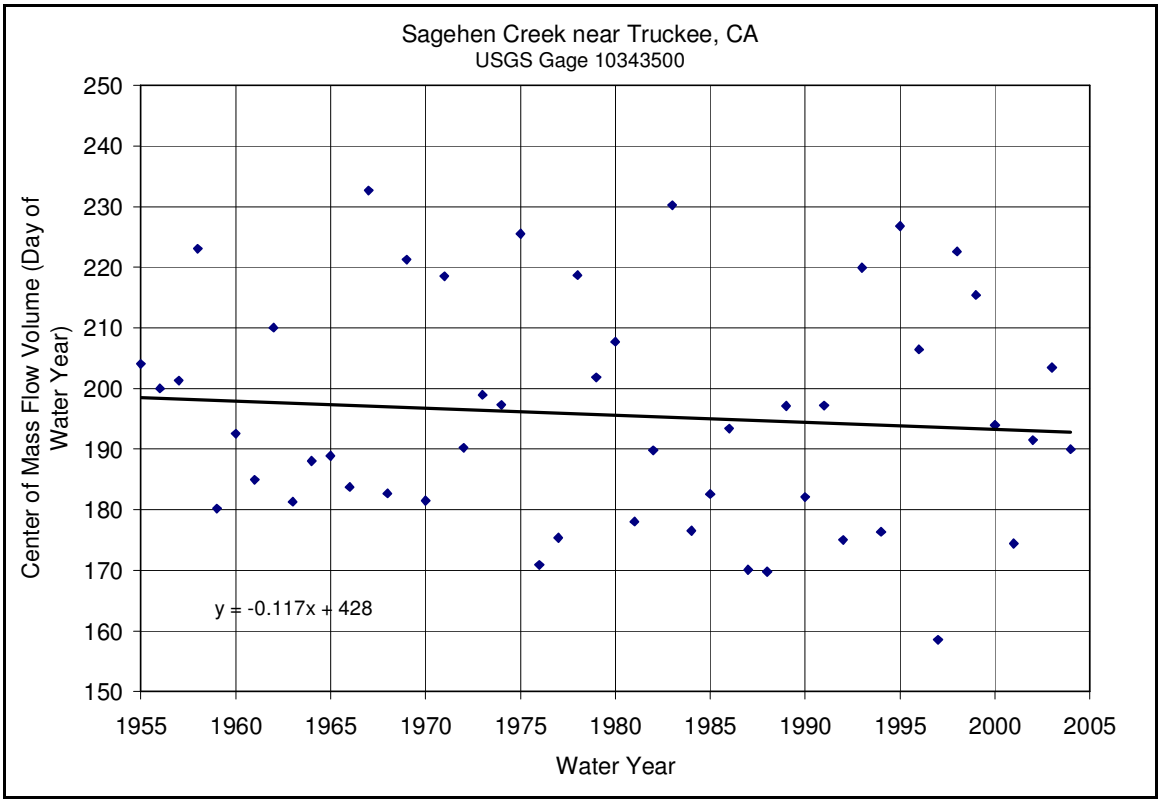

Figure D28. Sagehen Creek near Truckee, CA streamflow center of mass.

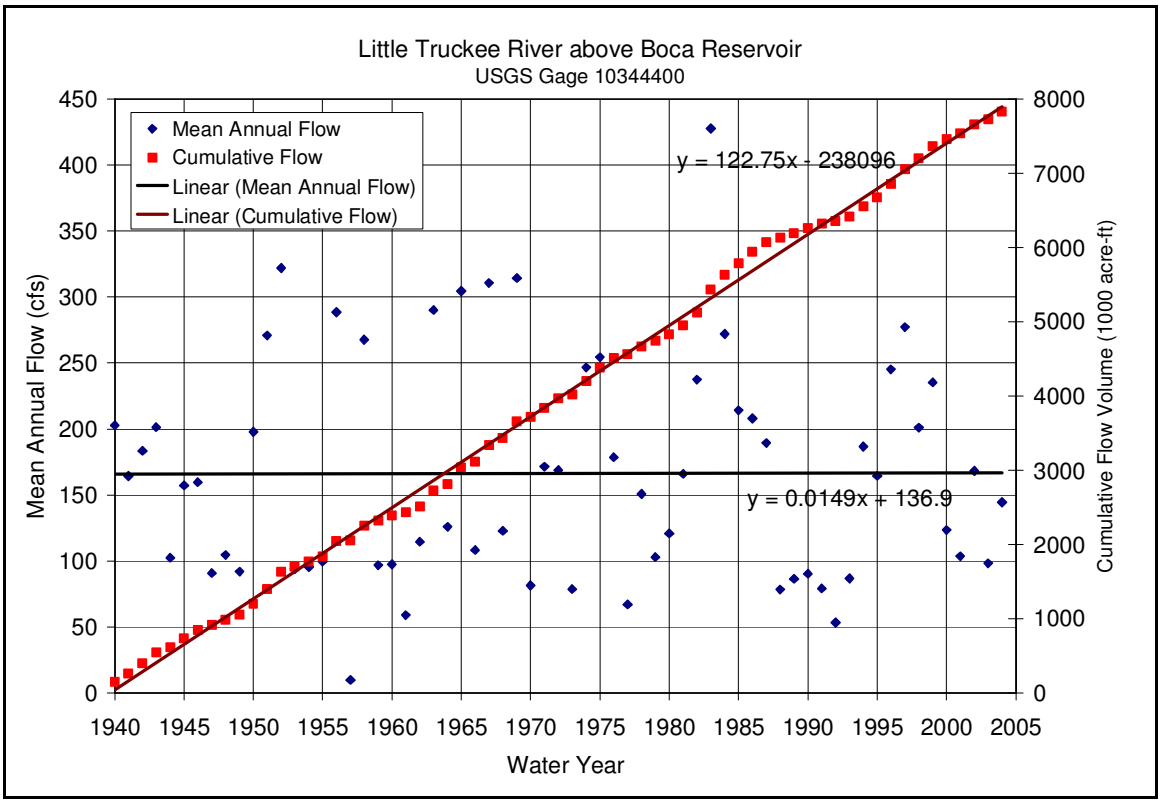

Figure D29. Little Truckee River above Boca Reservoir annual streamflow.

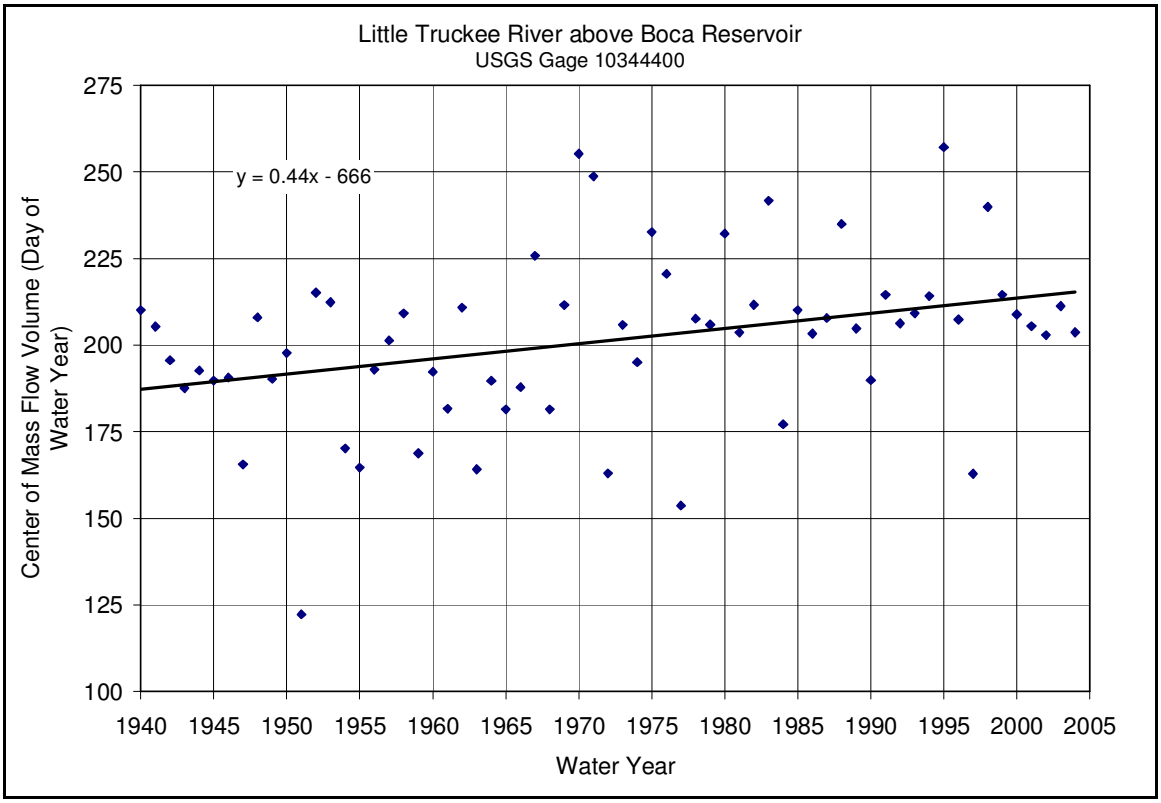

Figure D30. Little Truckee River above Boca Reservoir streamflow center of mass.

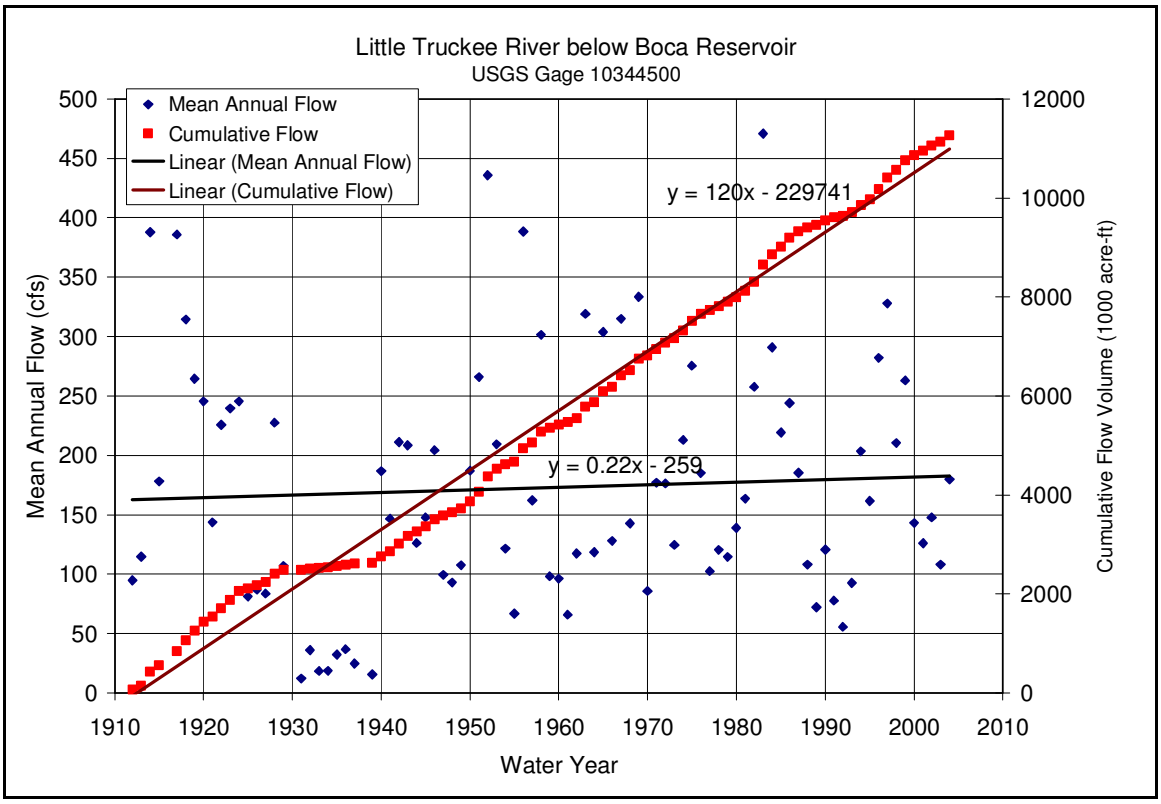

Figure D31. Little Truckee River below Boca Reservoir annual streamflow.

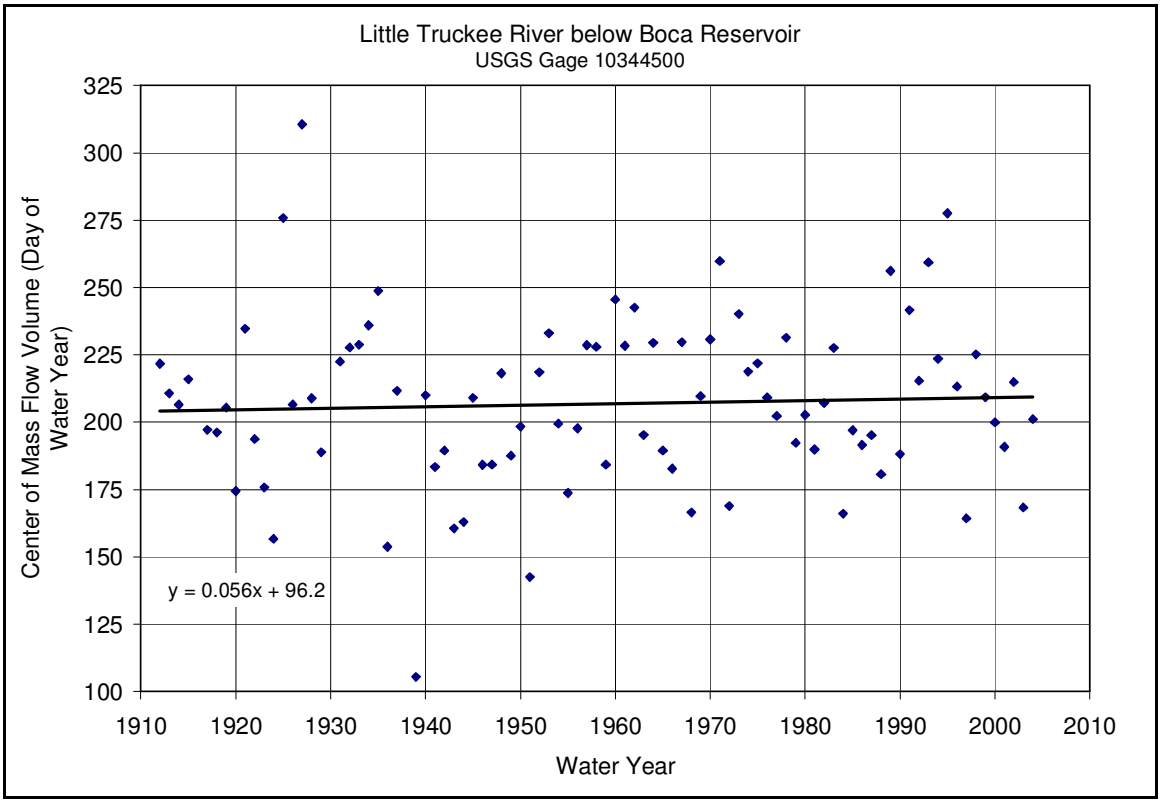

Figure D32. Little Truckee River below Boca Reservoir streamflow center of mass.

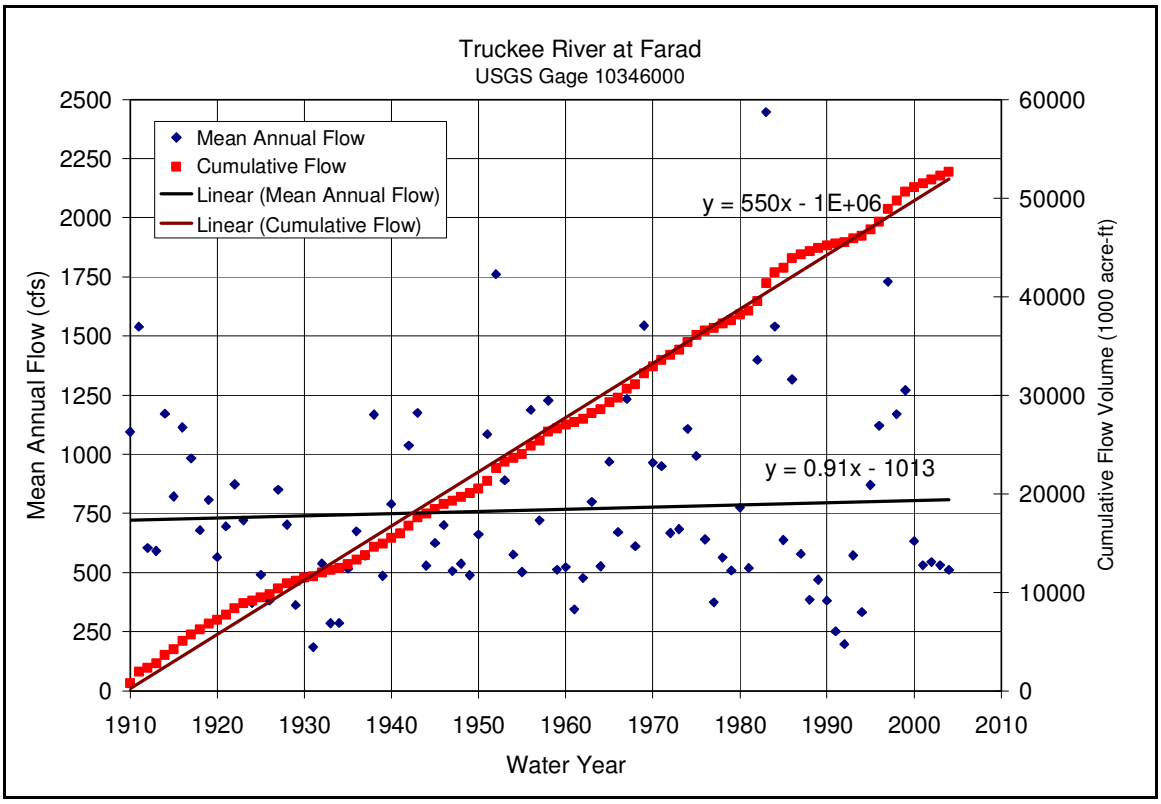

Figure D33. Truckee River at Farad annual streamflow.

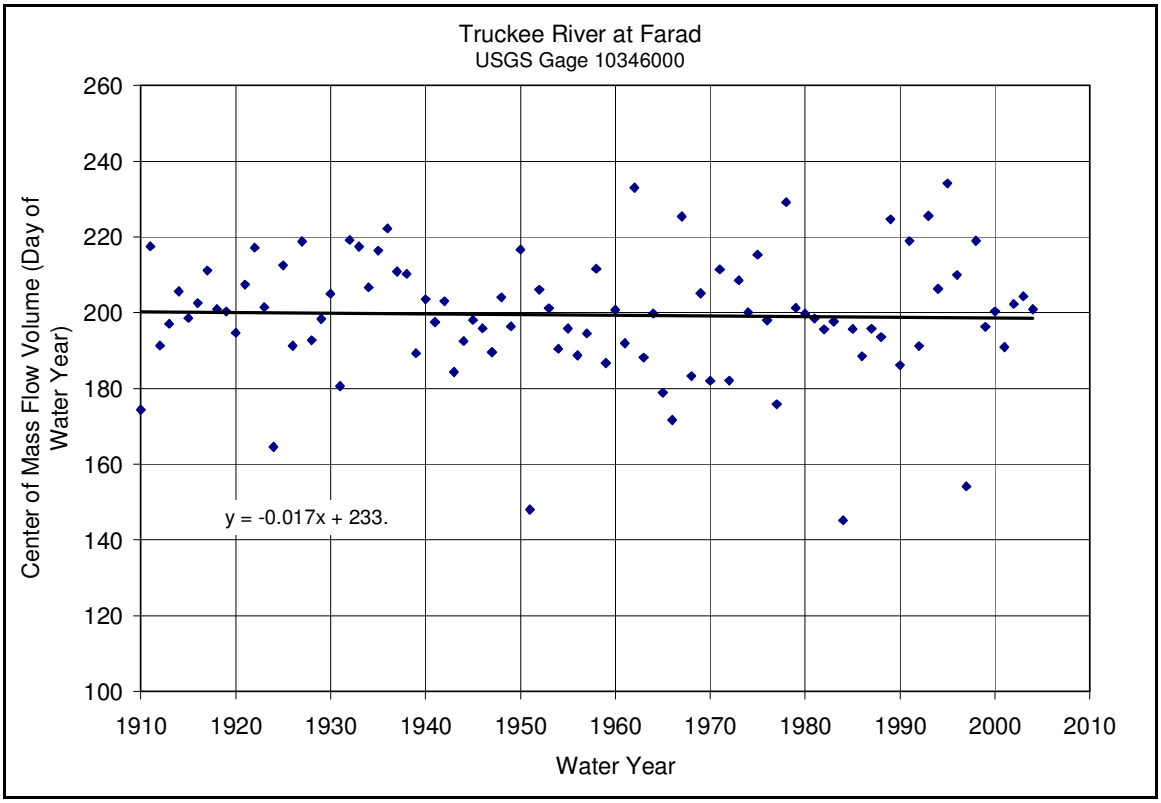

Figure D34. Truckee River at Farad streamflow center of mass.

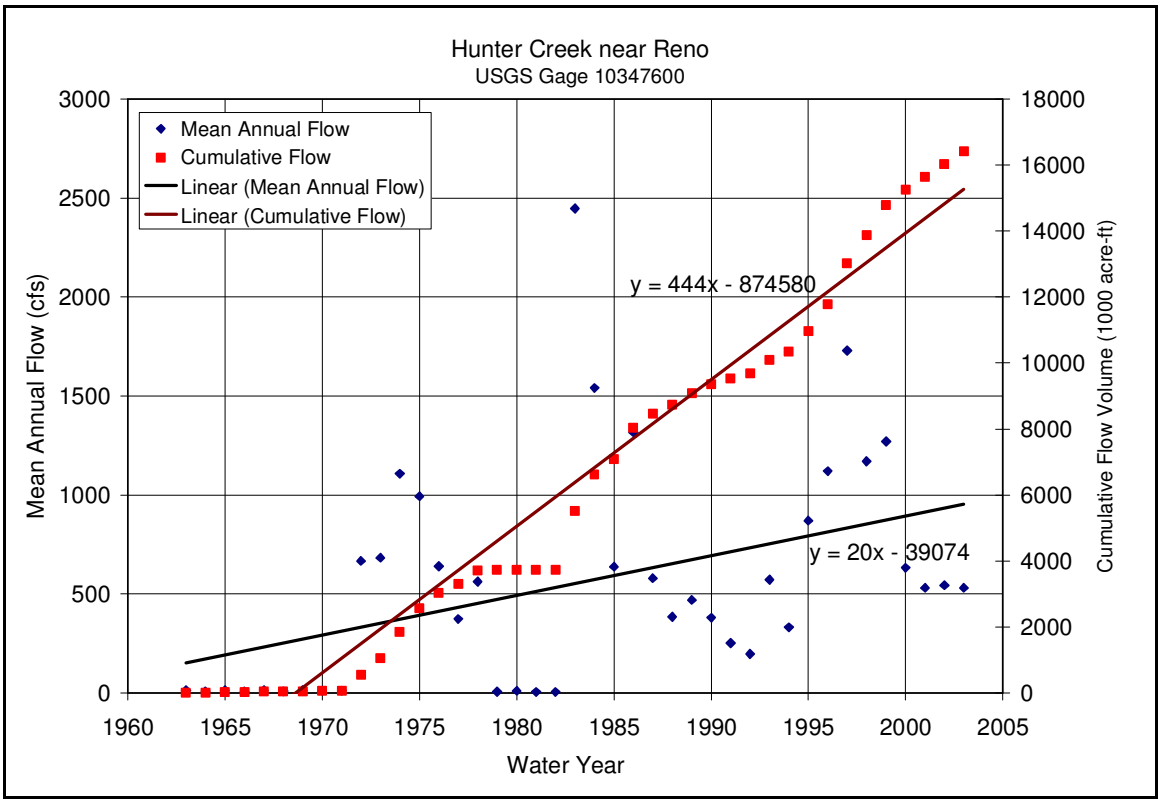

Figure D35. Hunter Creek near Reno annual streamflow.

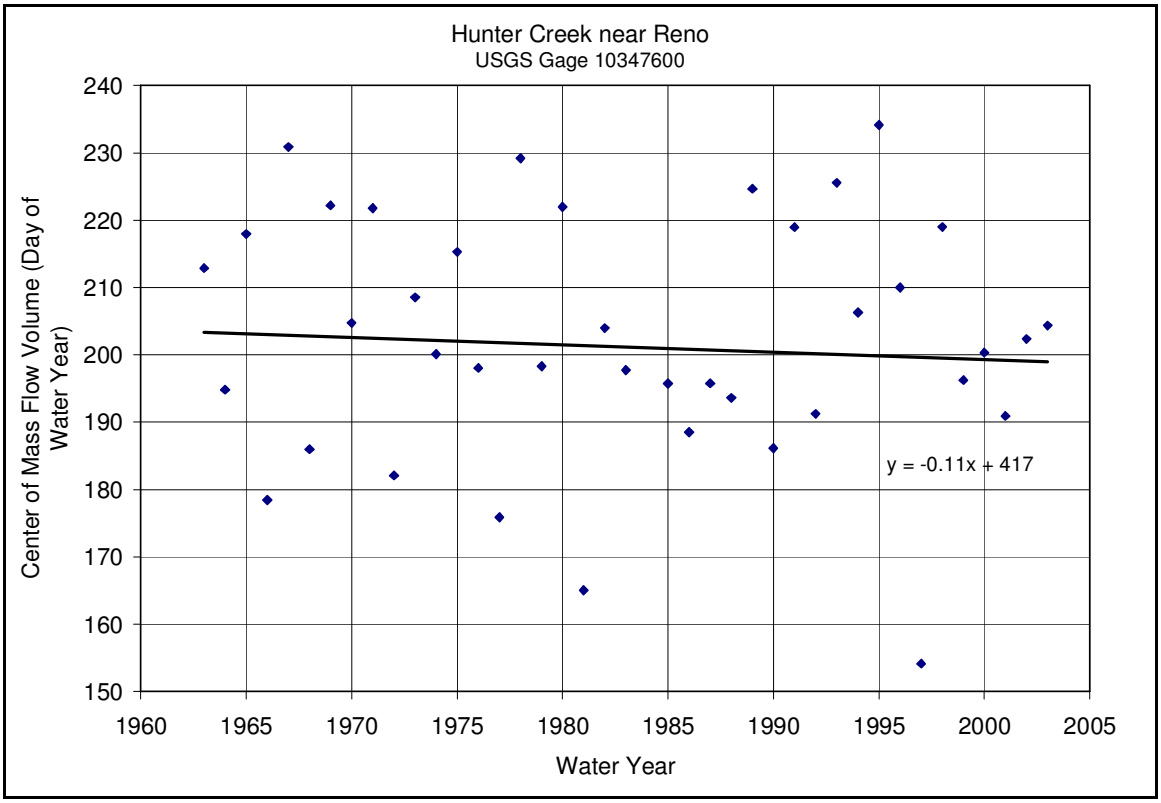

Figure D36. Hunter Creek near Reno streamflow center of mass.

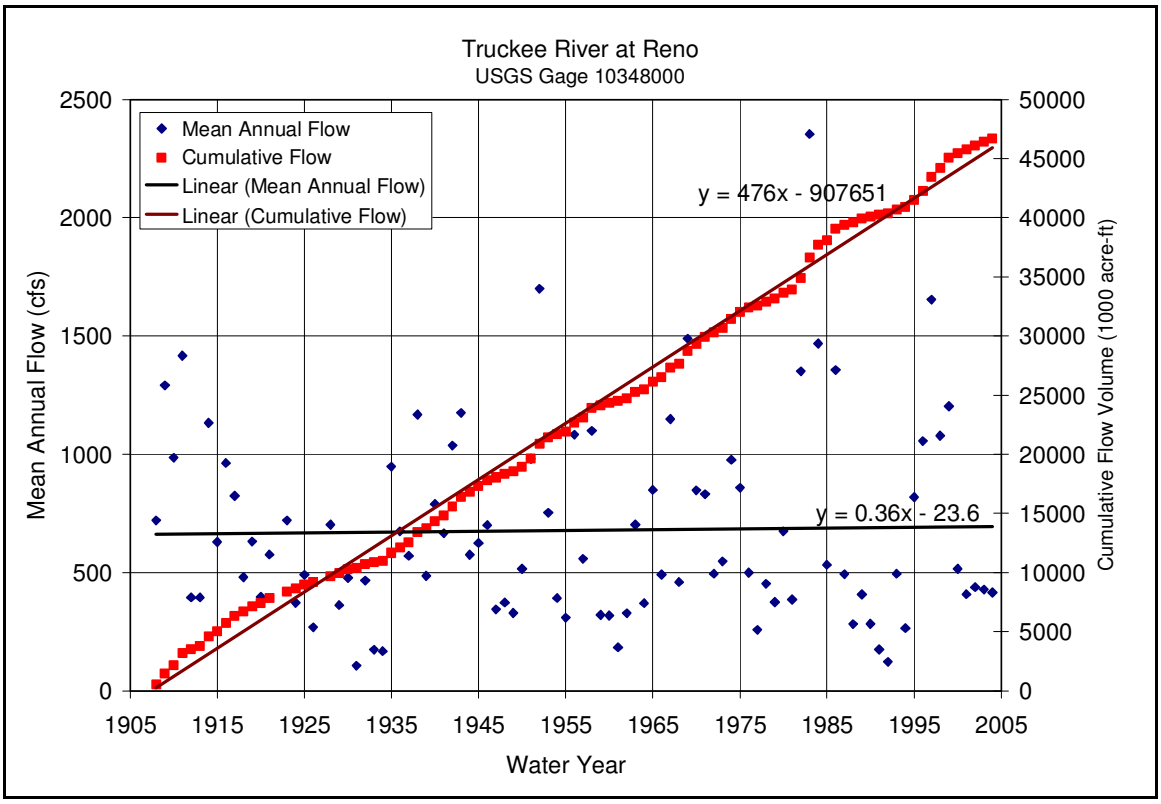

Figure D37. Truckee River at Reno annual streamflow.

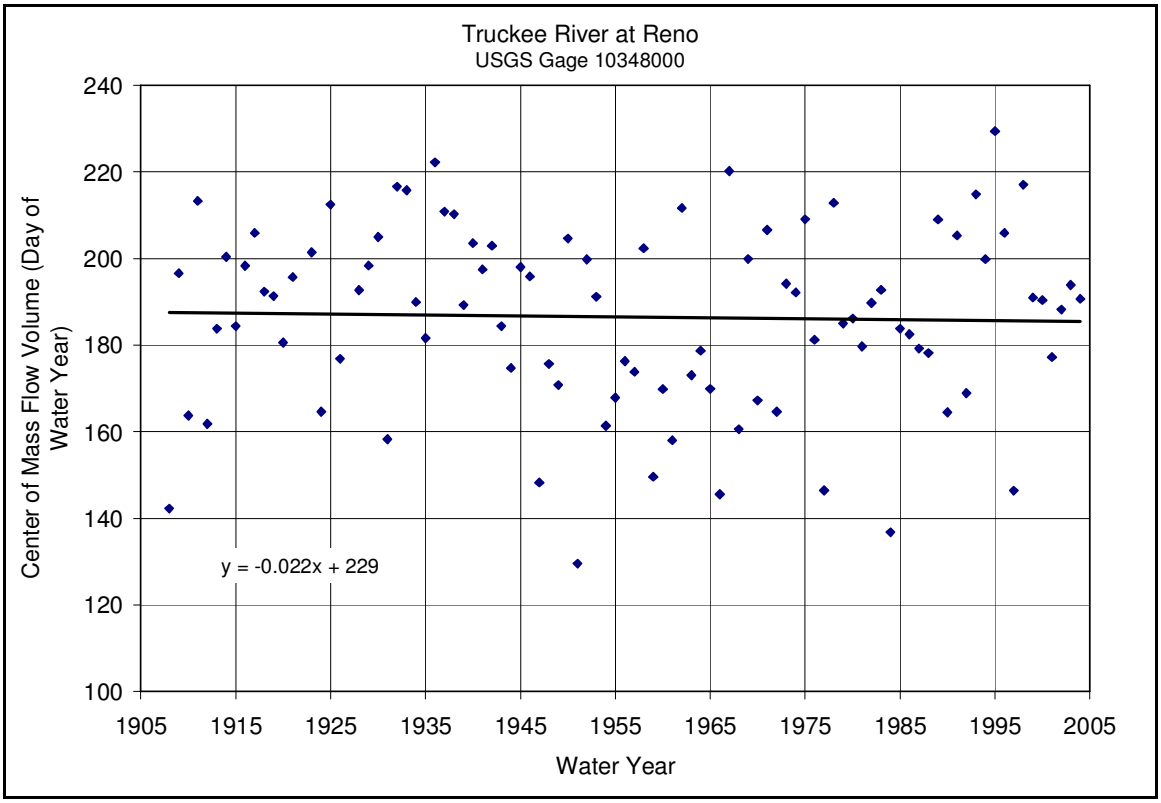

Figure D38. Truckee River at Reno streamflow center of mass.

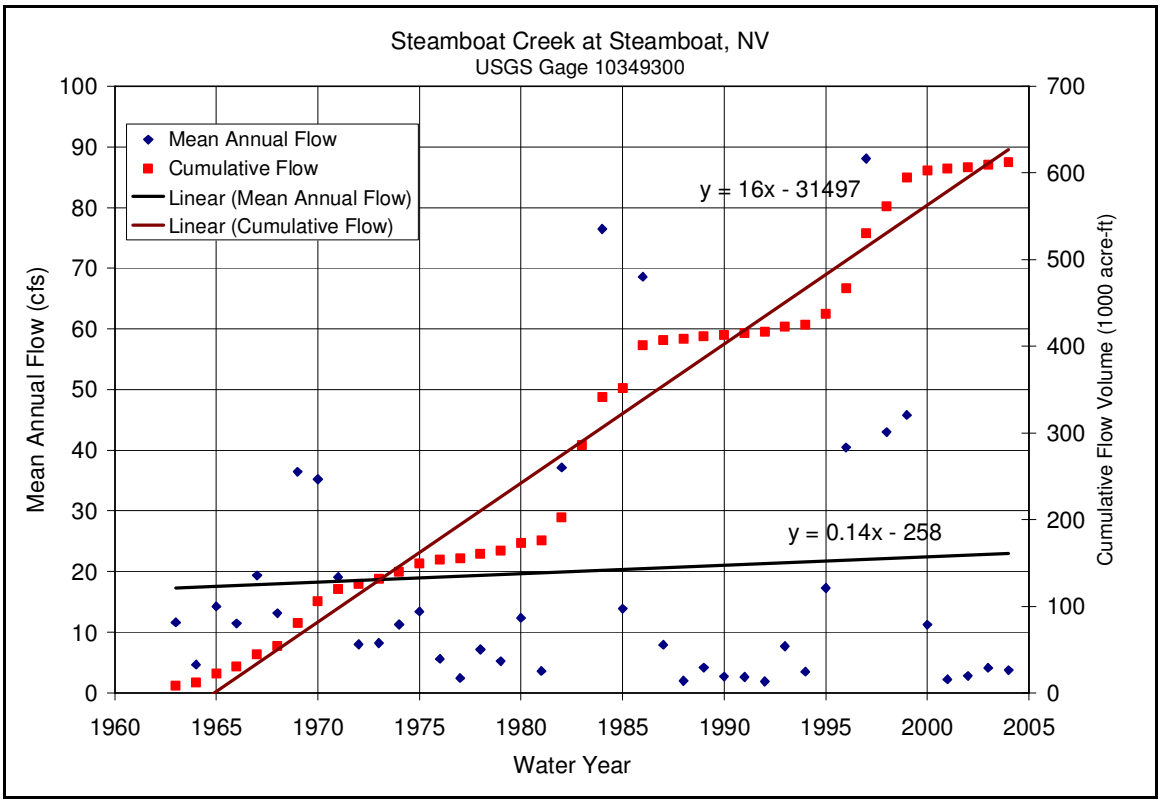

Figure D39. Steamboat Creek at Steamboat, NV annual streamflow.

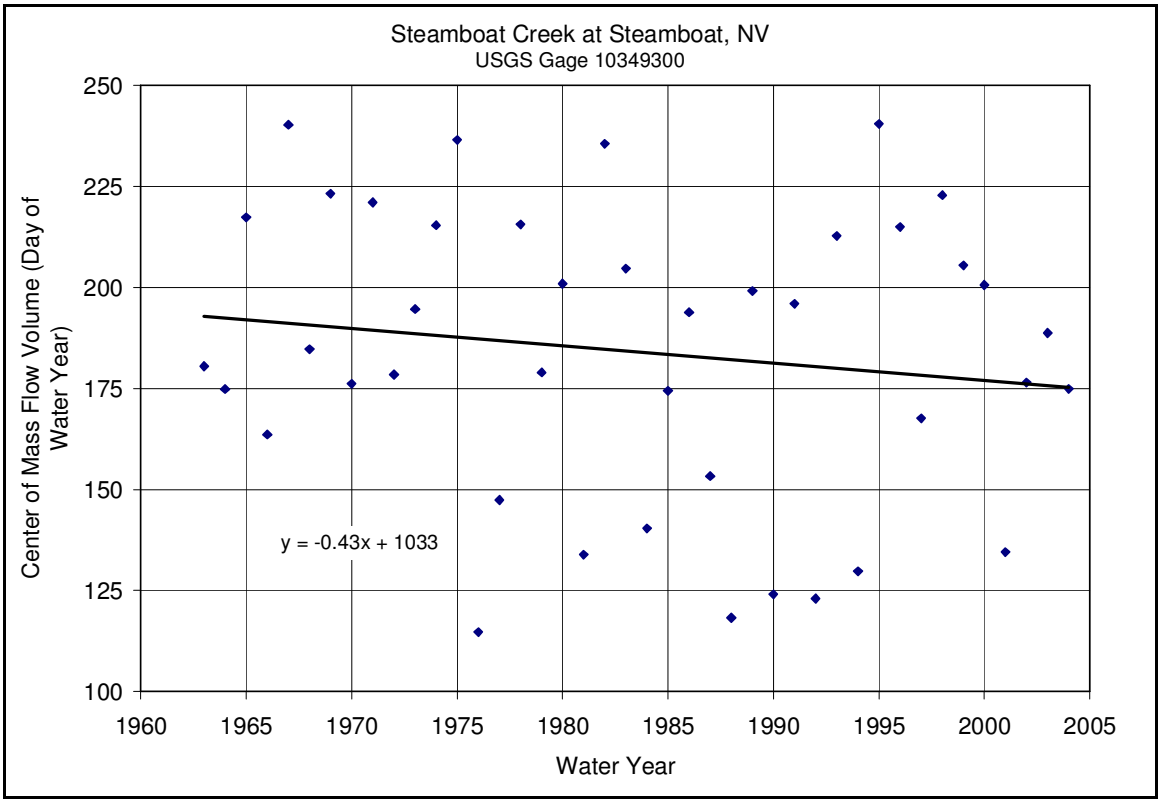

Figure D40. Steamboat Creek at Steamboat, NV streamflow center of mass.

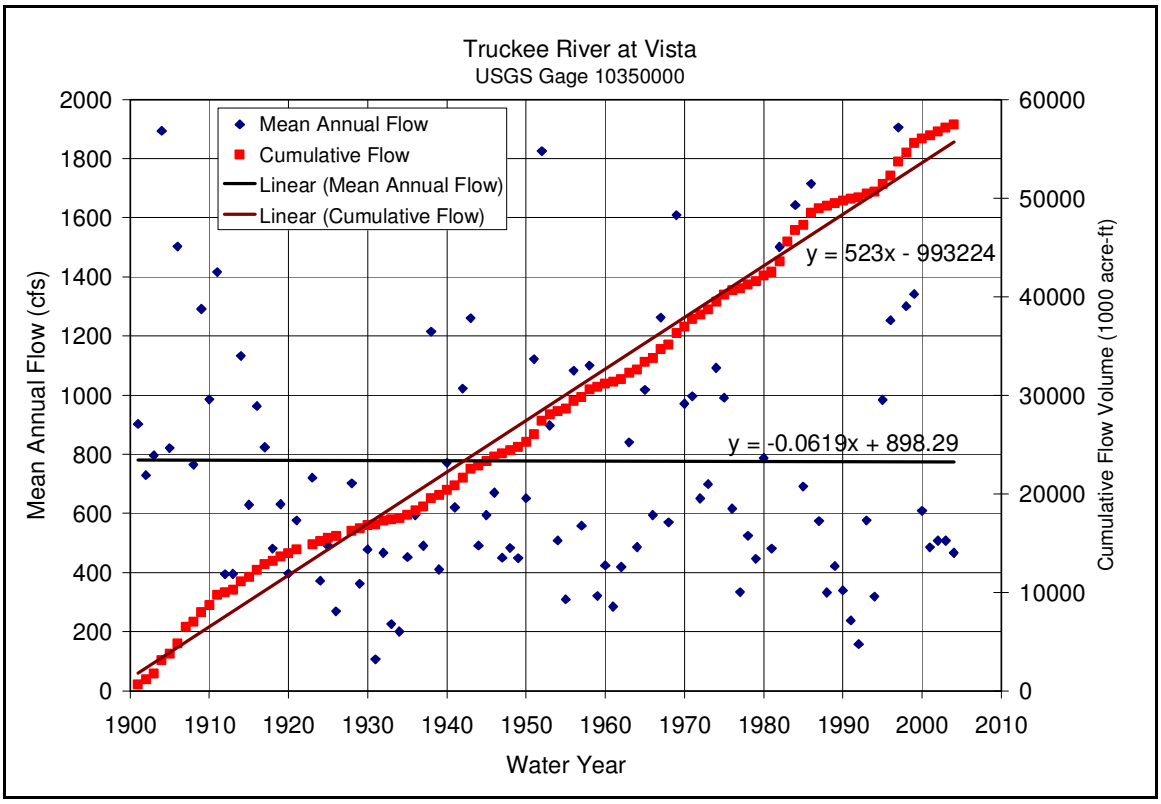

Figure D41. Truckee River at Vista annual streamflow.

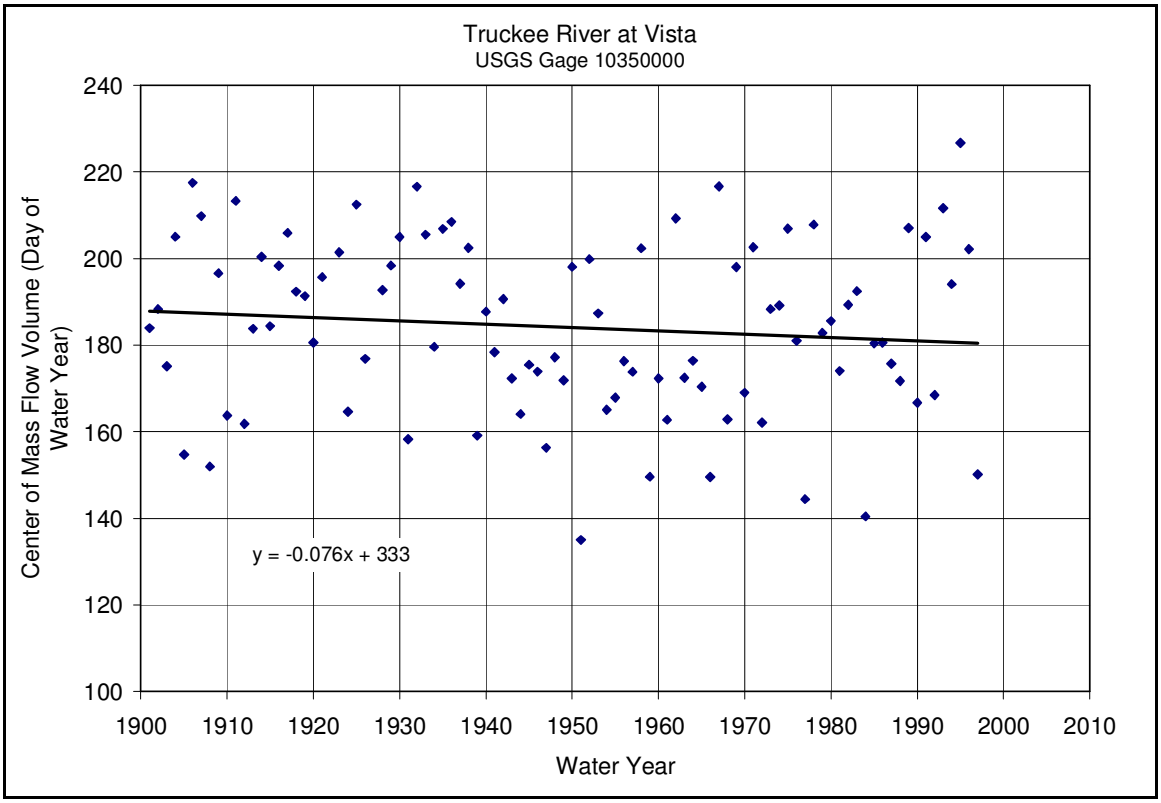

Figure D42. Truckee River at Vista streamflow center of mass.

Appendix E

Reservoir Volumes

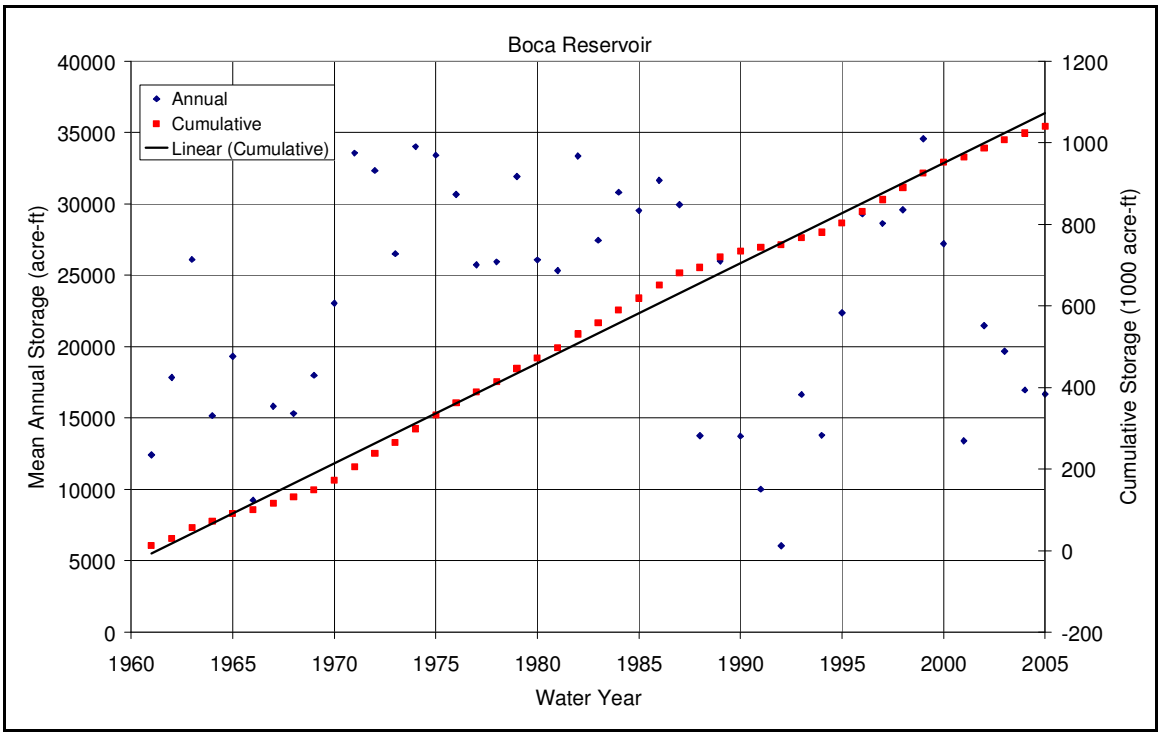

Figure E1. Mean annual storage and cumulative storage for Boca Reservoir.

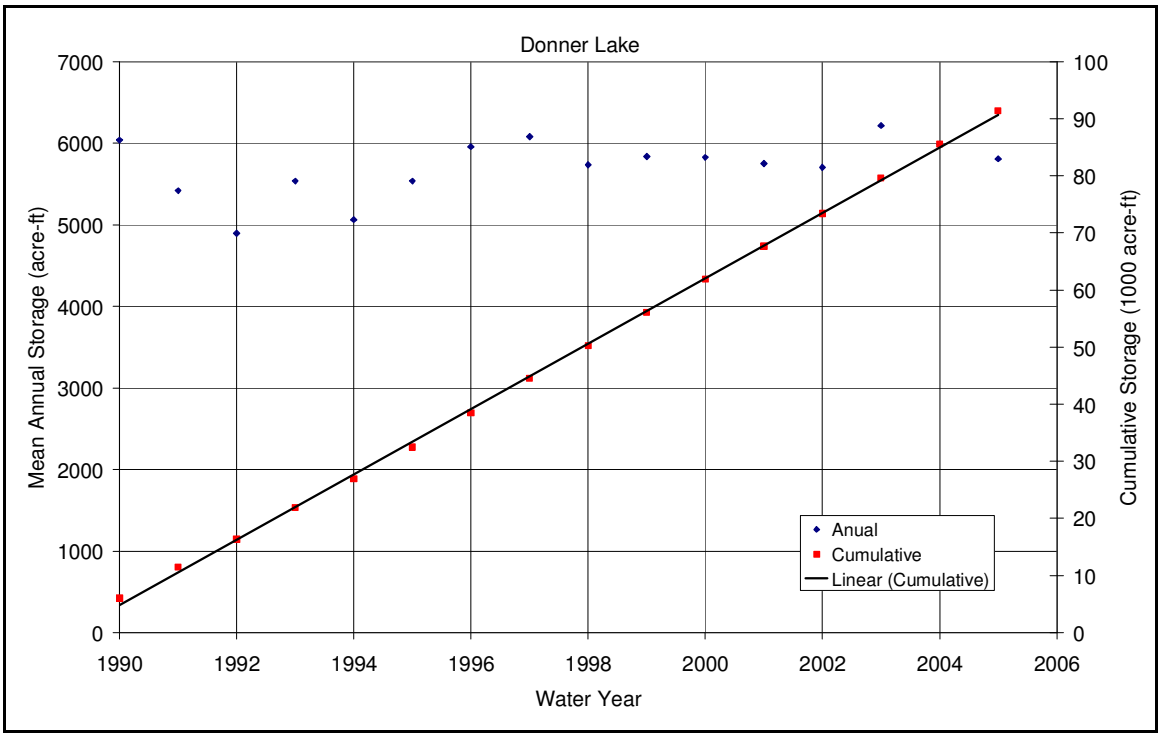

Figure E2. Mean annual storage and cumulative storage for Donner Lake.

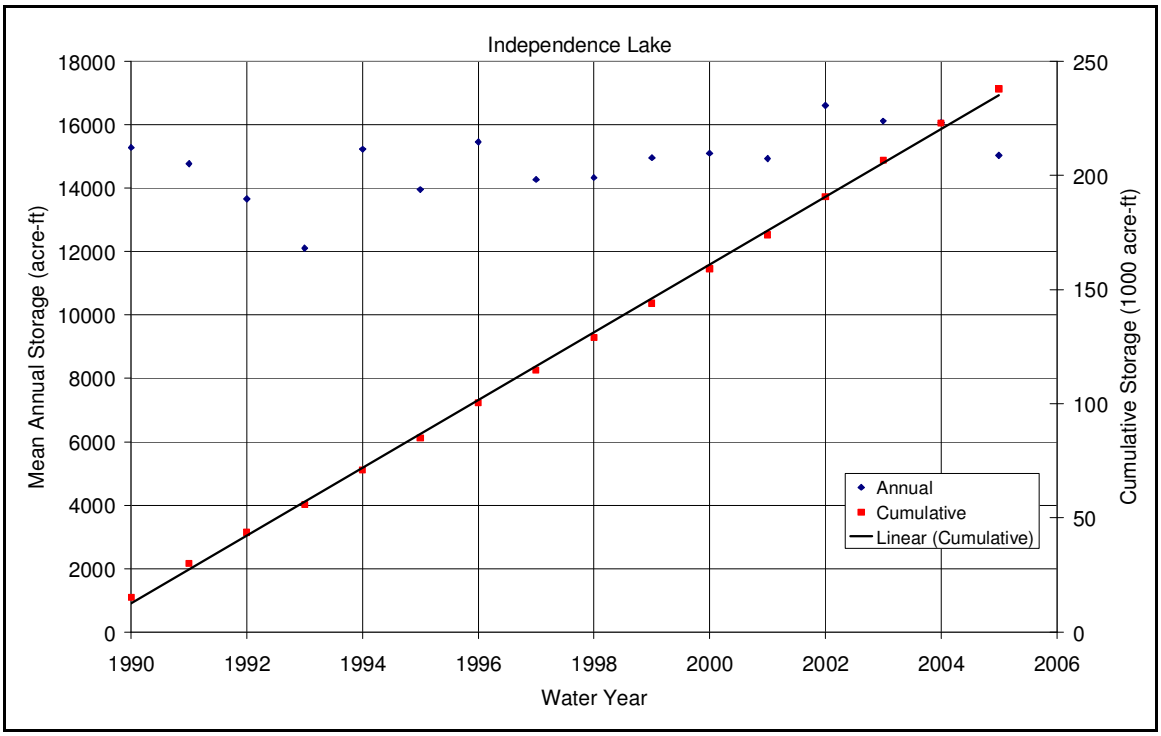

Figure E3. Mean annual storage and cumulative storage for Independence Lake.

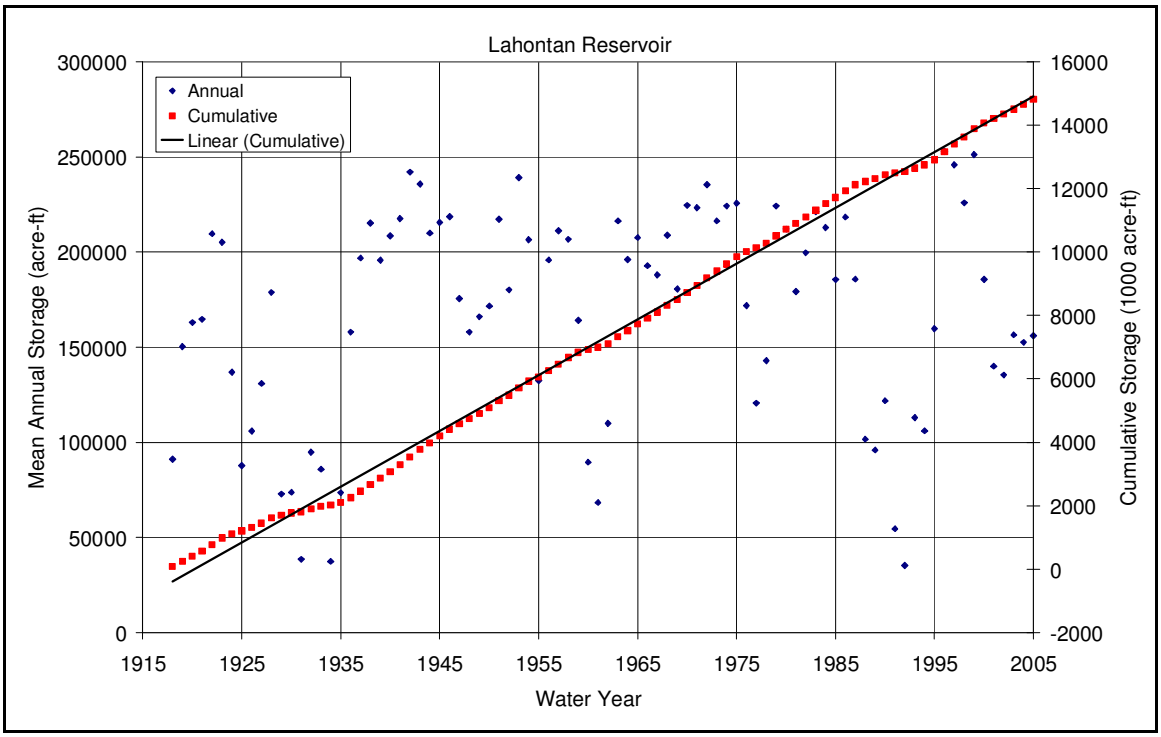

Figure E4. Mean annual storage and cumulative storage for Lahontan Reservoir.

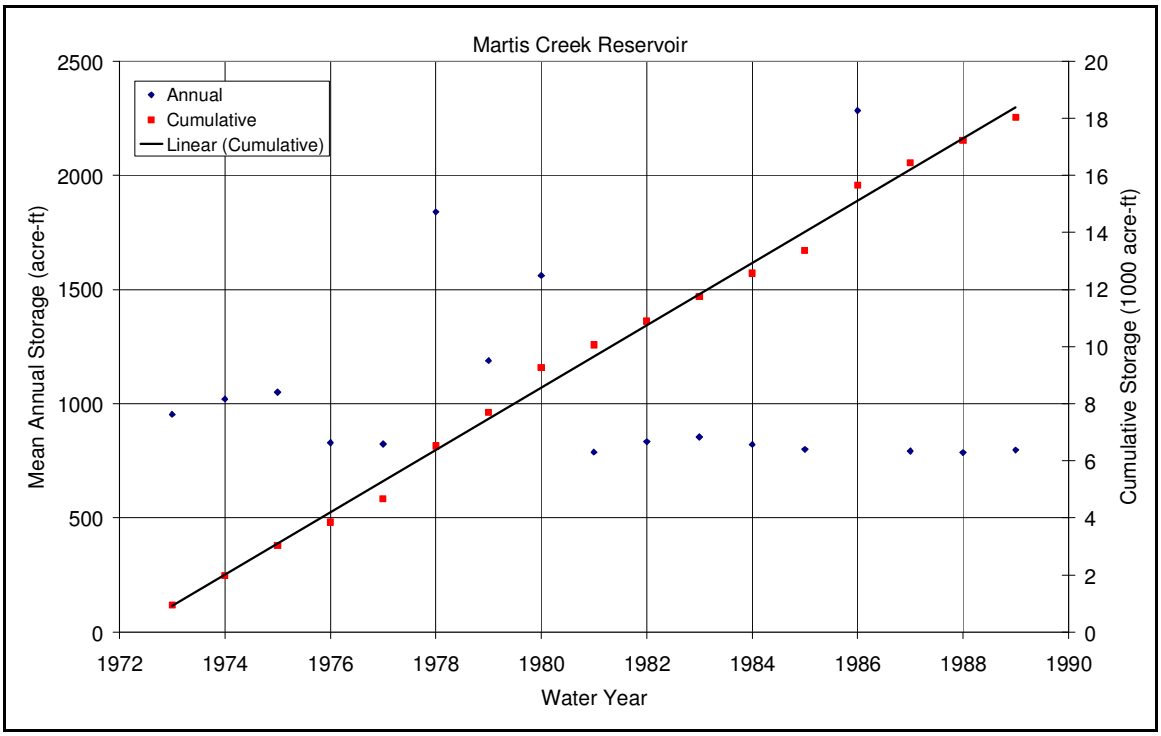

Figure E5. Mean annual storage and cumulative storage for Martis Creek Reservoir.

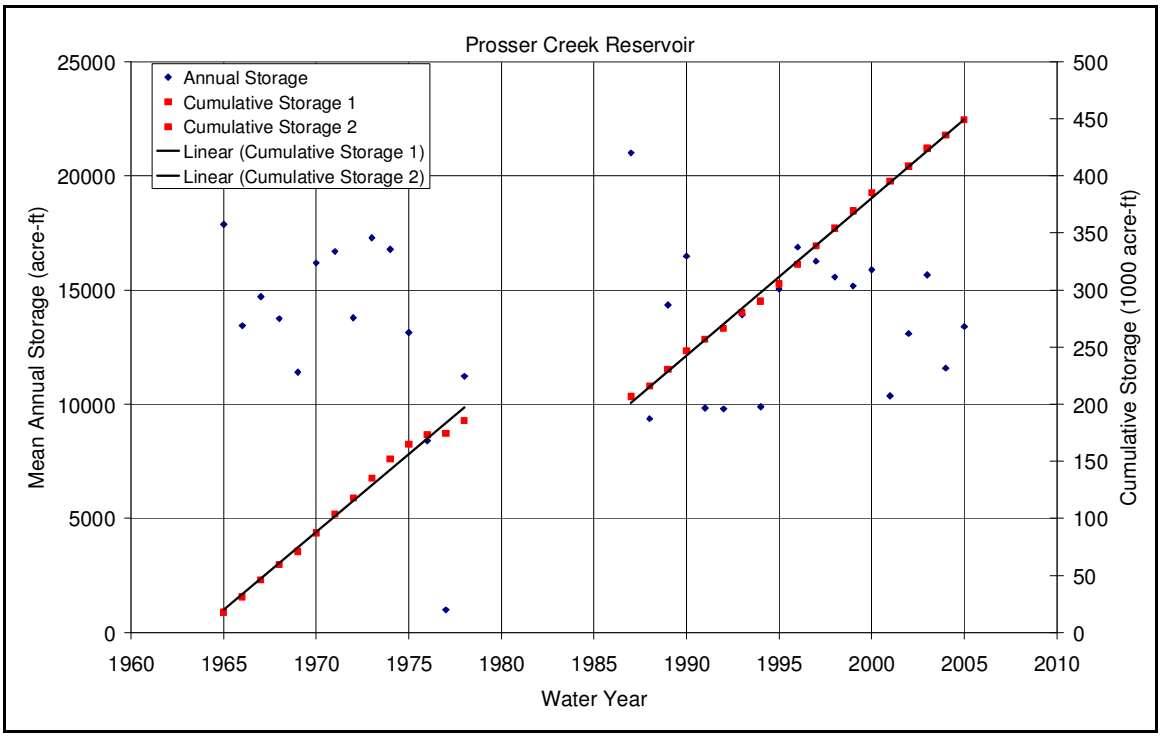

Figure E6. Mean annual storage and cumulative storage for Prosser Creek Reservoir.

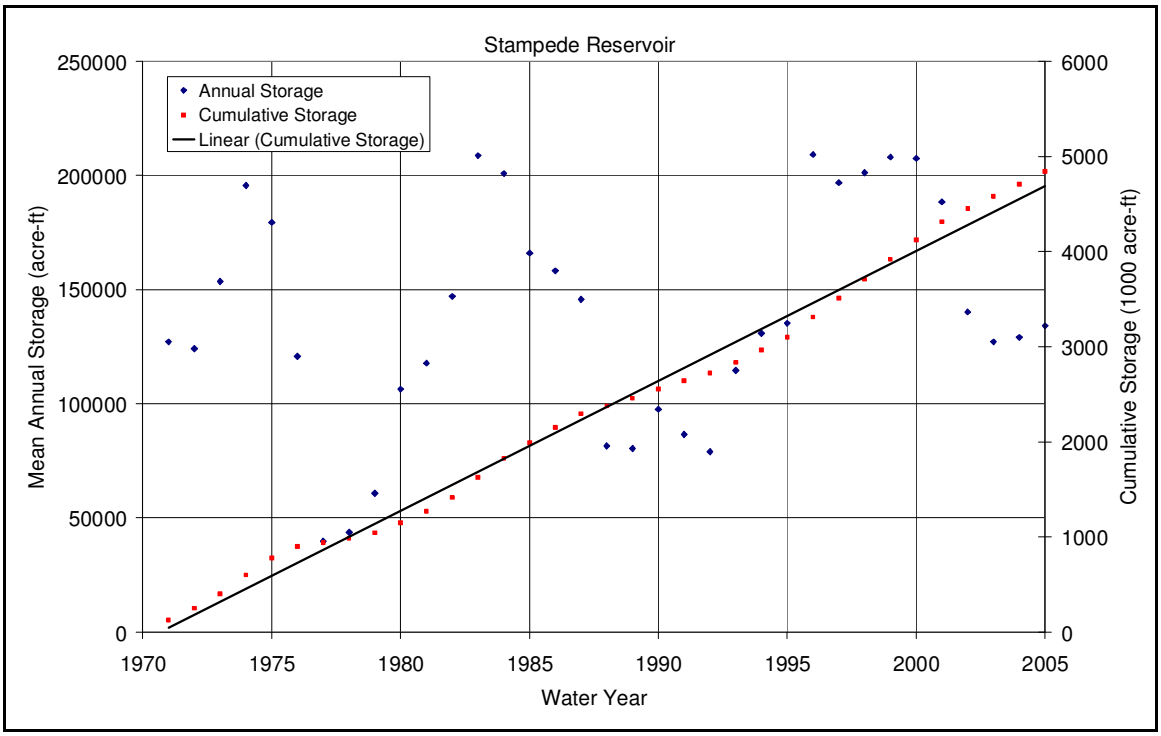

Figure E7. Mean annual storage and cumulative storage for Stampede Reservoir.

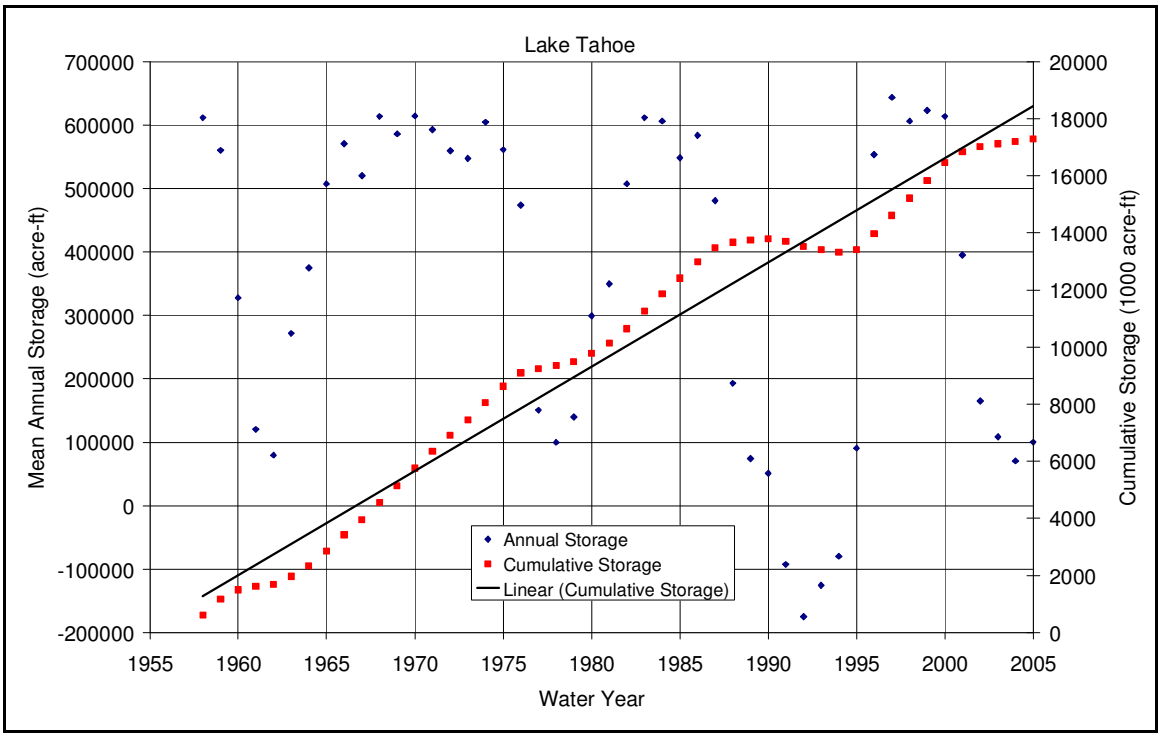

Figure E8. Mean annual storage and cumulative storage for Lake Tahoe.

Appendix F

Double Mass Curve Analysis
Precipitation and Snowpack

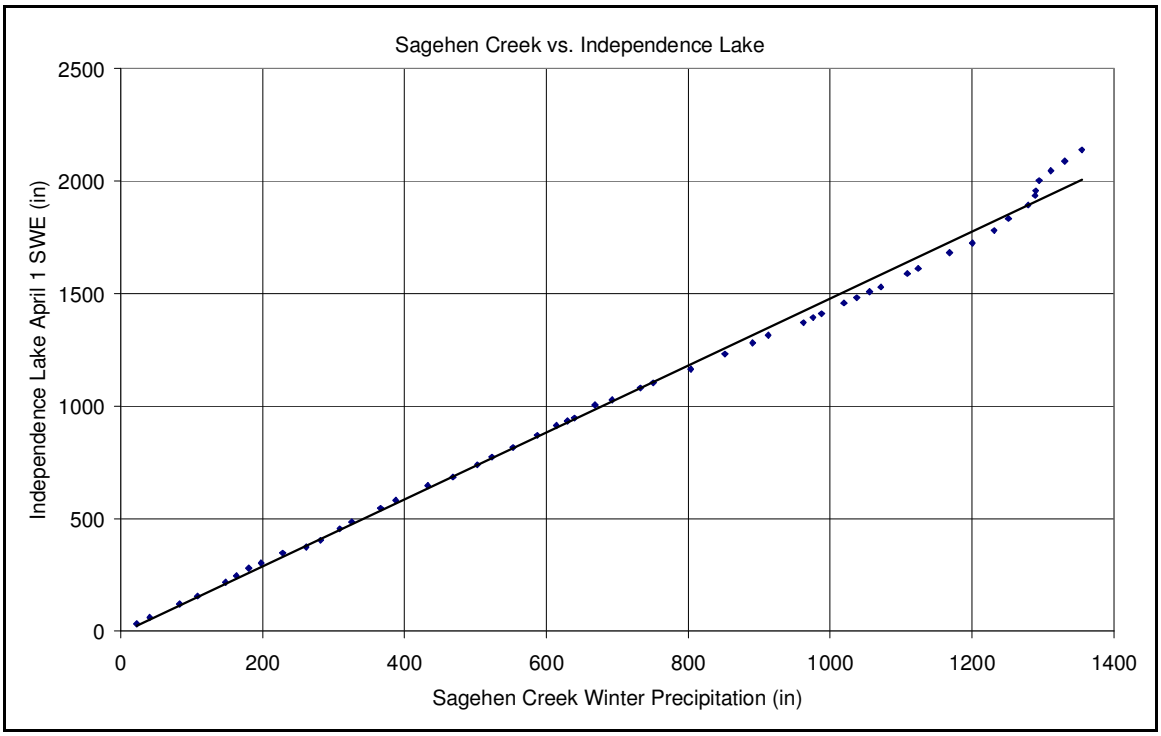

Figure F1. Double mass curve for Independence Lake snowcourse station April 1 SWE and Sagehen Creek winter precipitation.

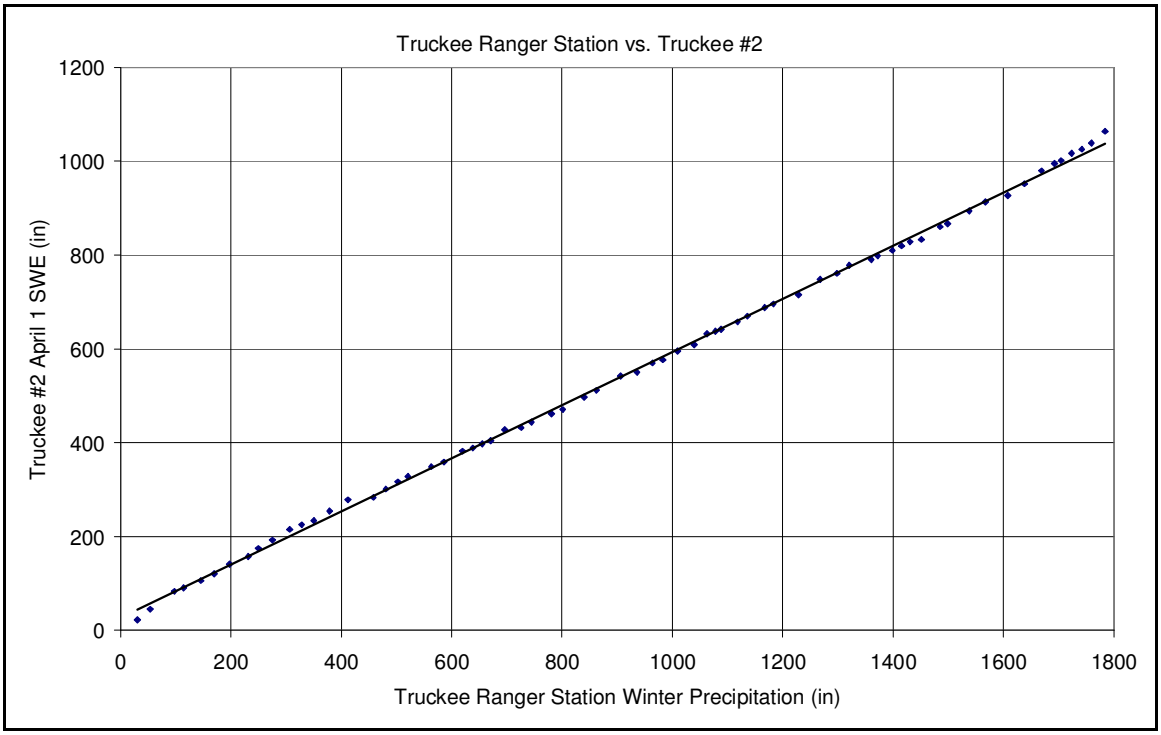

Figure F2. Double mass curve for Truckee #2 snowcourse station April 1 SWE and Truckee Ranger Station winter precipitation.

Appendix G

Double Mass Curve Analysis
Precipitation vs. Streamflow

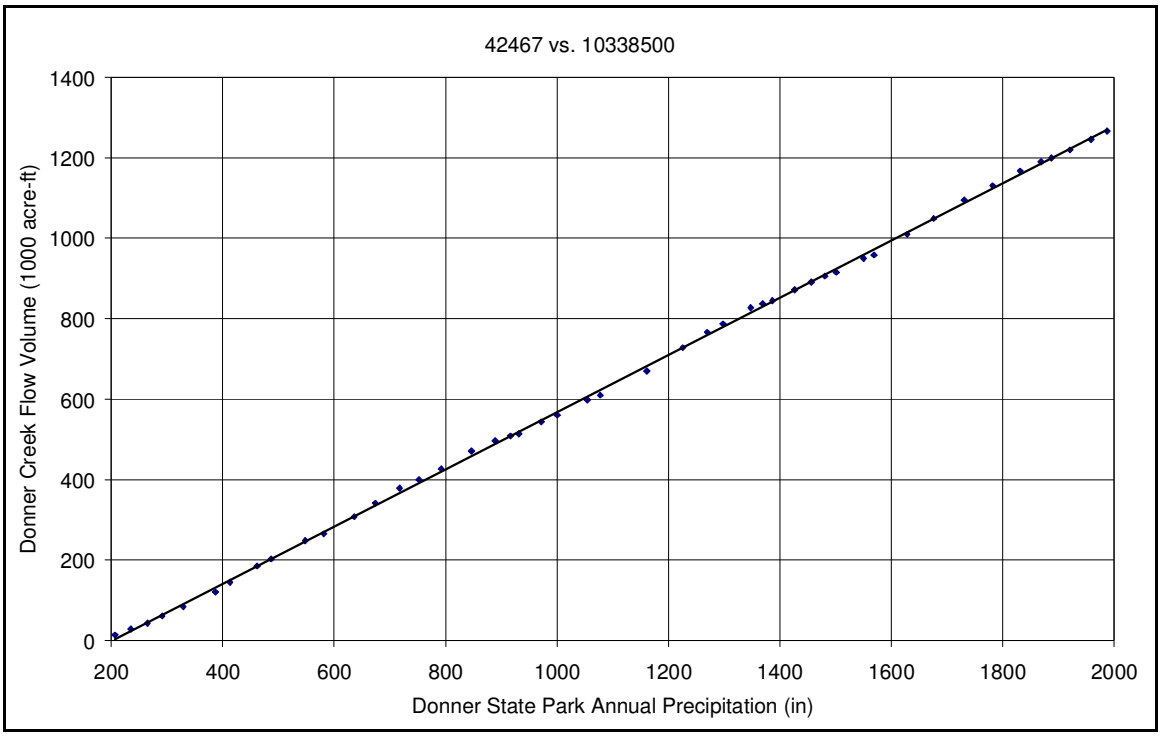

Figure G1. Double mass curve for streamflow volume for Donner Creek and annual precipitation at Donner State Park.

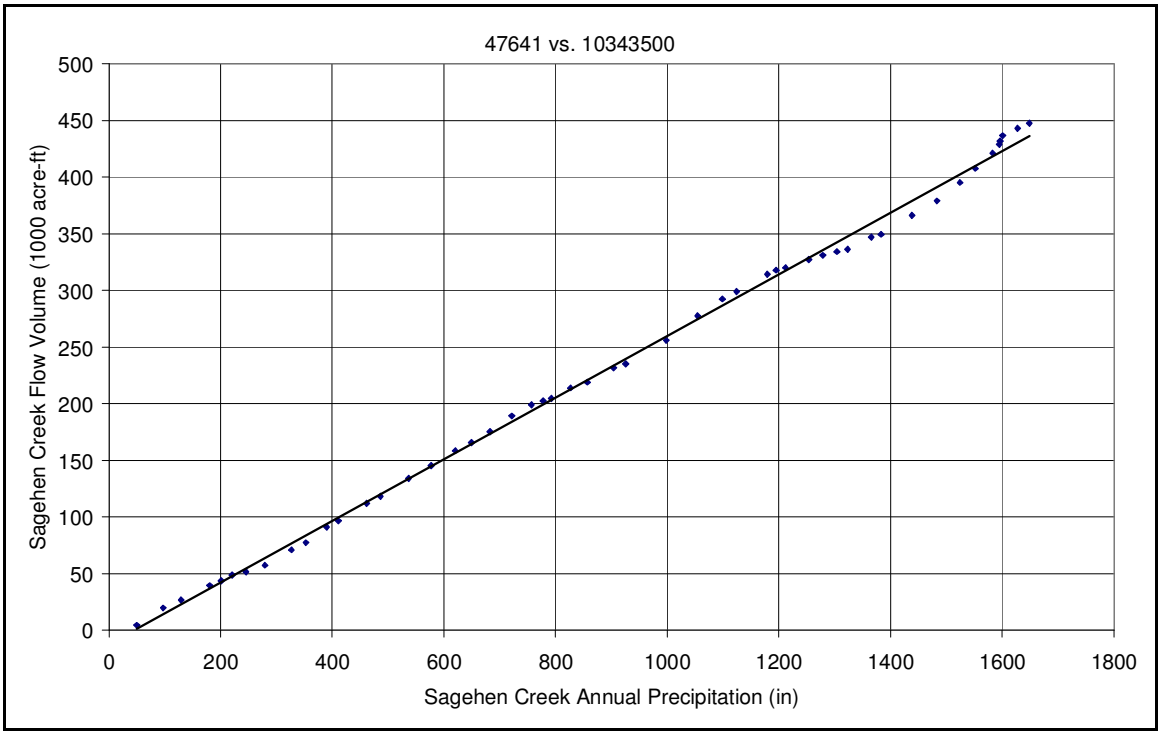

Figure G2. Double mass curve for Sagehen Creek streamflow volume and annual precipitation at the Sagehen weather station.

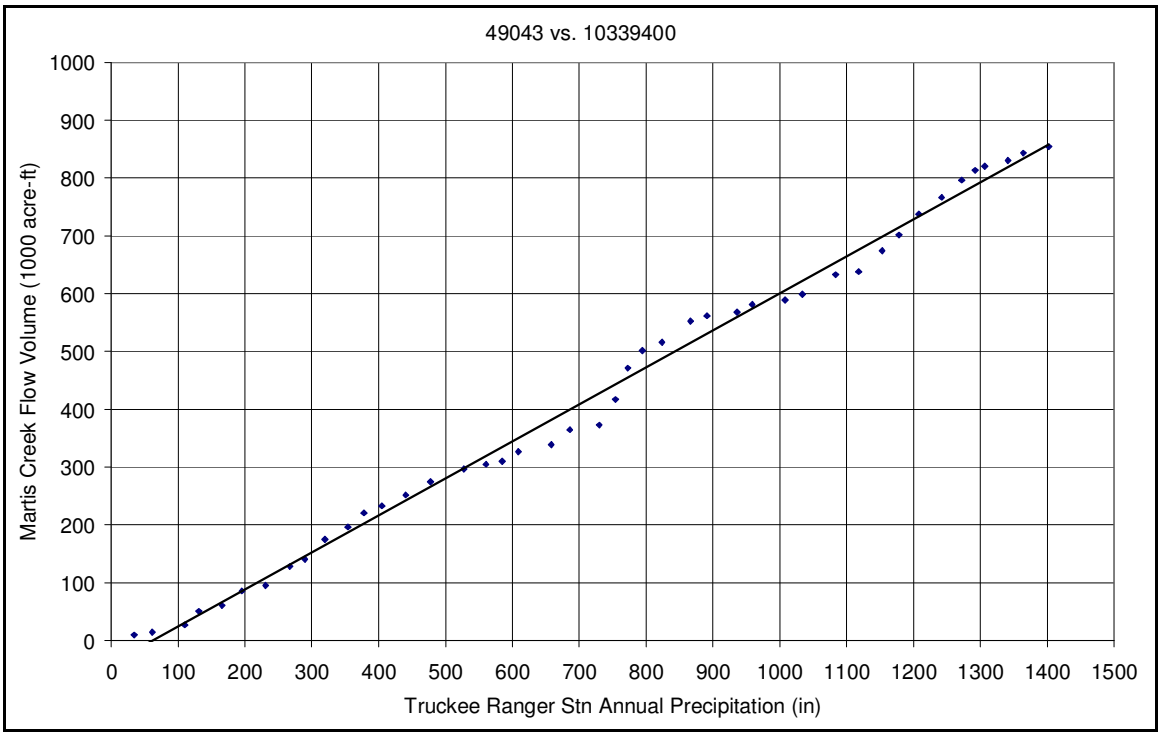

Figure G3. Double mass curve for Martis Creek streamflow volume and annual precipitation at the Truckee Ranger Station.

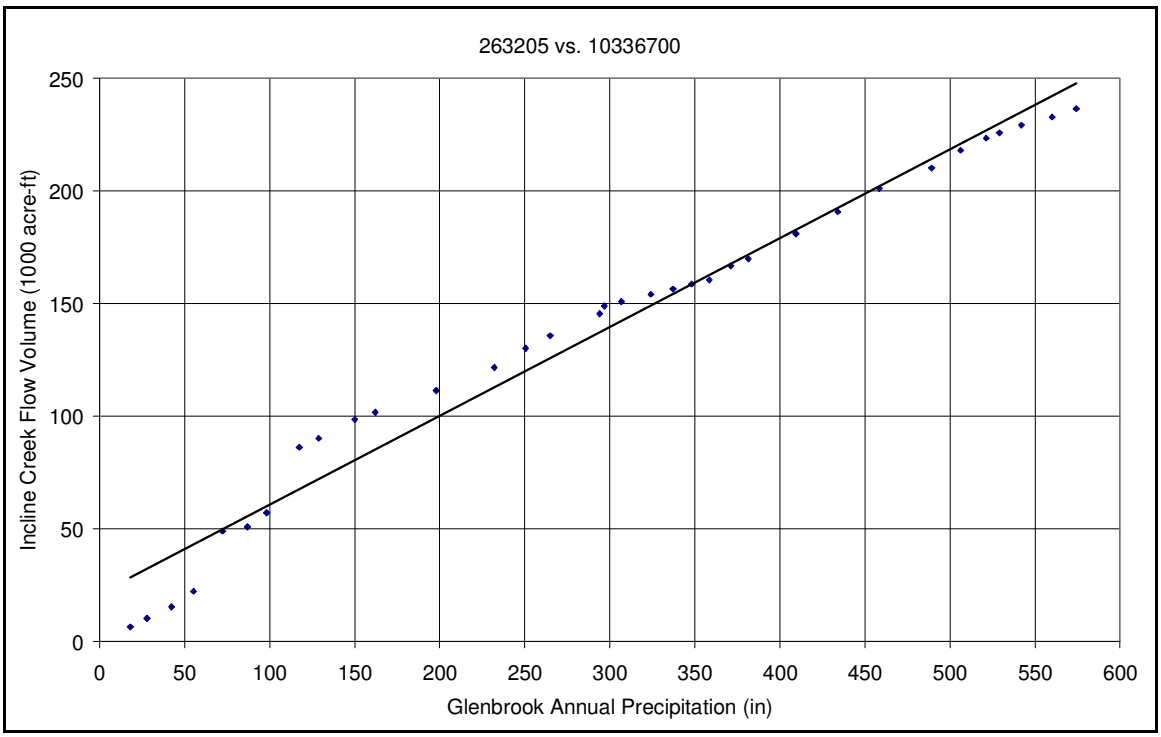

Figure G4. Double mass curve for Incline Creek streamflow volume and annual precipitation at the Glenbrook weather station.

Appendix H

Double Mass Curve Analysis
Precipitation vs. Reservoir Volumes

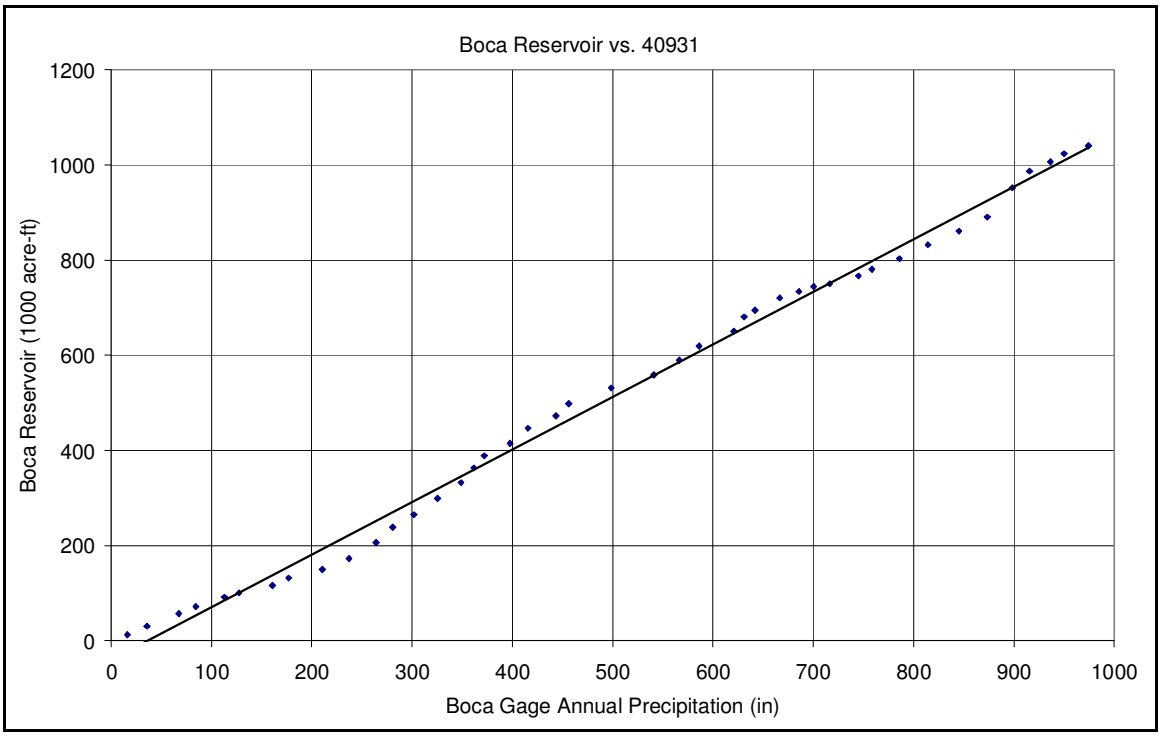

Figure H1. Double mass curve of Boca Reservoir storage and Boca annual precipitation.

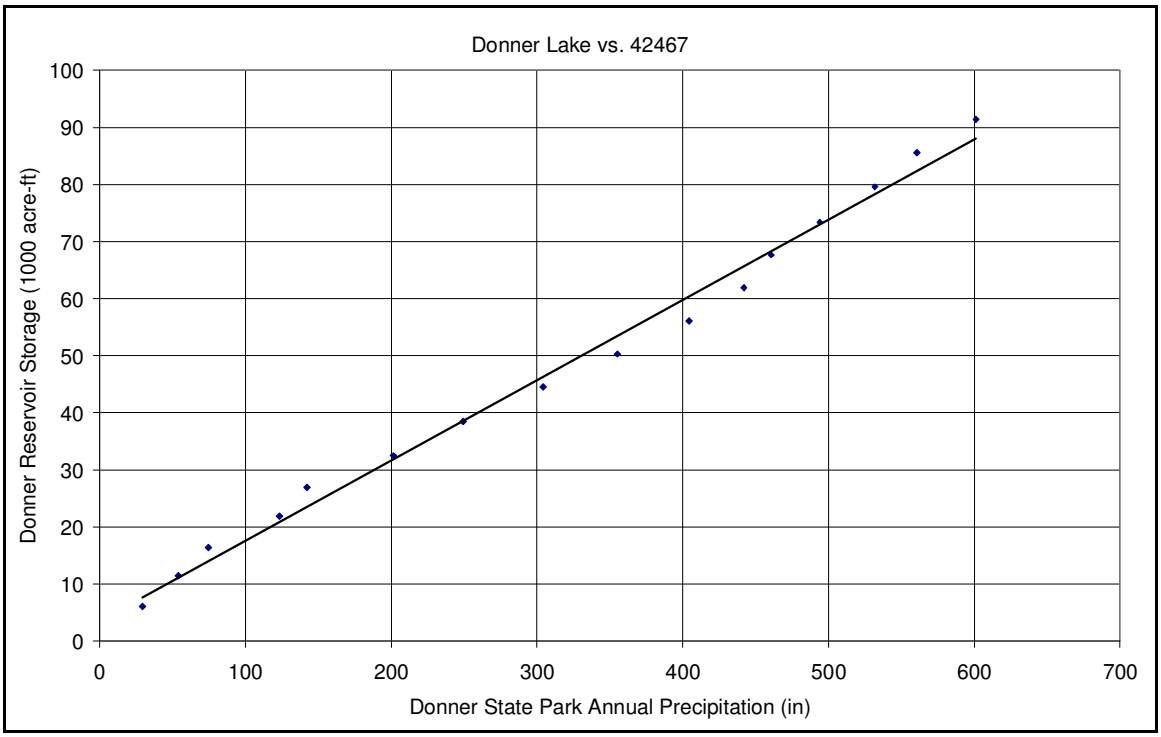

Figure H2. Double mass curve of Donner Lake storage and Donner State Park annual precipitation.

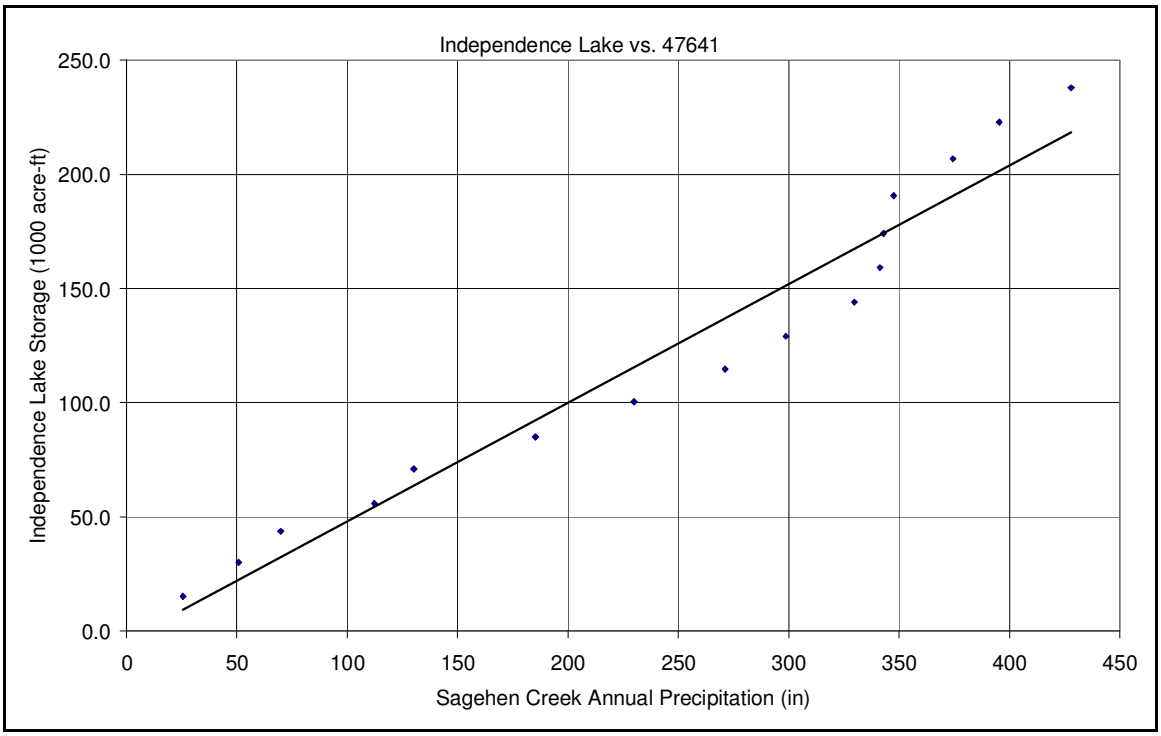

Figure H3. Double mass curve of Independence storage and Sagehen Creek annual precipitation.

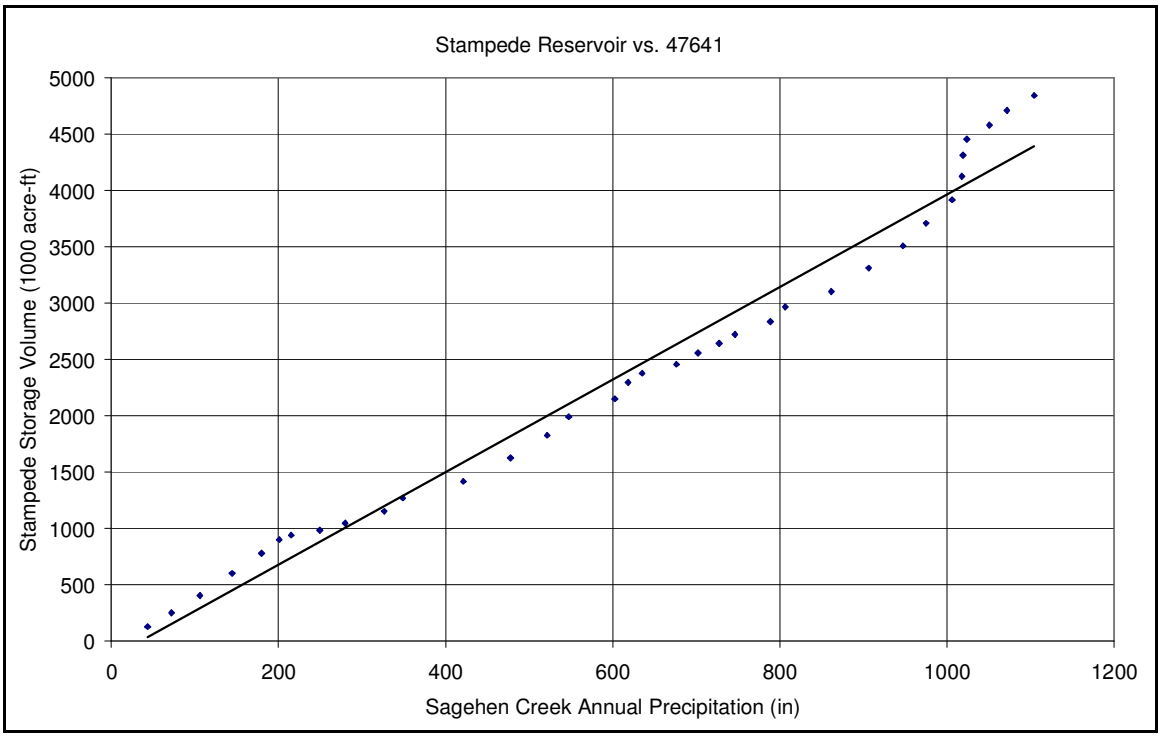

Figure H4. Double mass curve of Stampede Reservoir storage and Sagehen Creek annual precipitation.

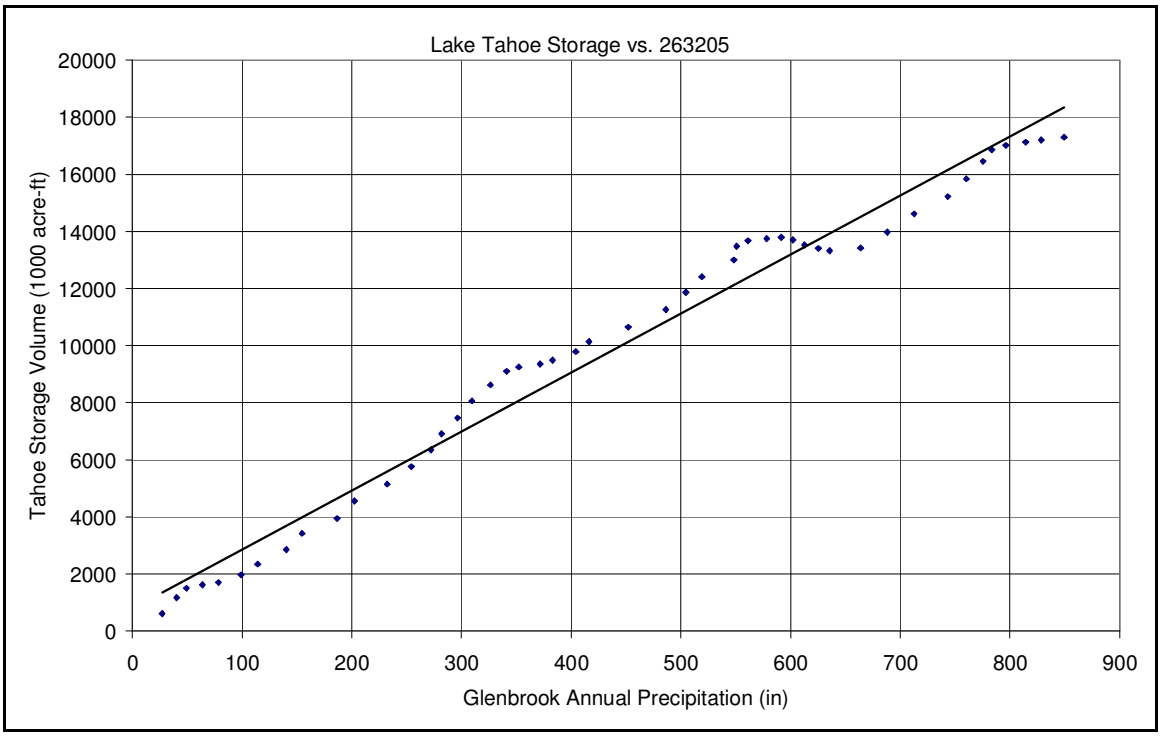

Figure H5. Double mass curve of Lake Tahoe storage and Glenbrook gage annual precipitation.

Appendix I

Double Mass Curve Analysis
Streamflow vs. Snowpack

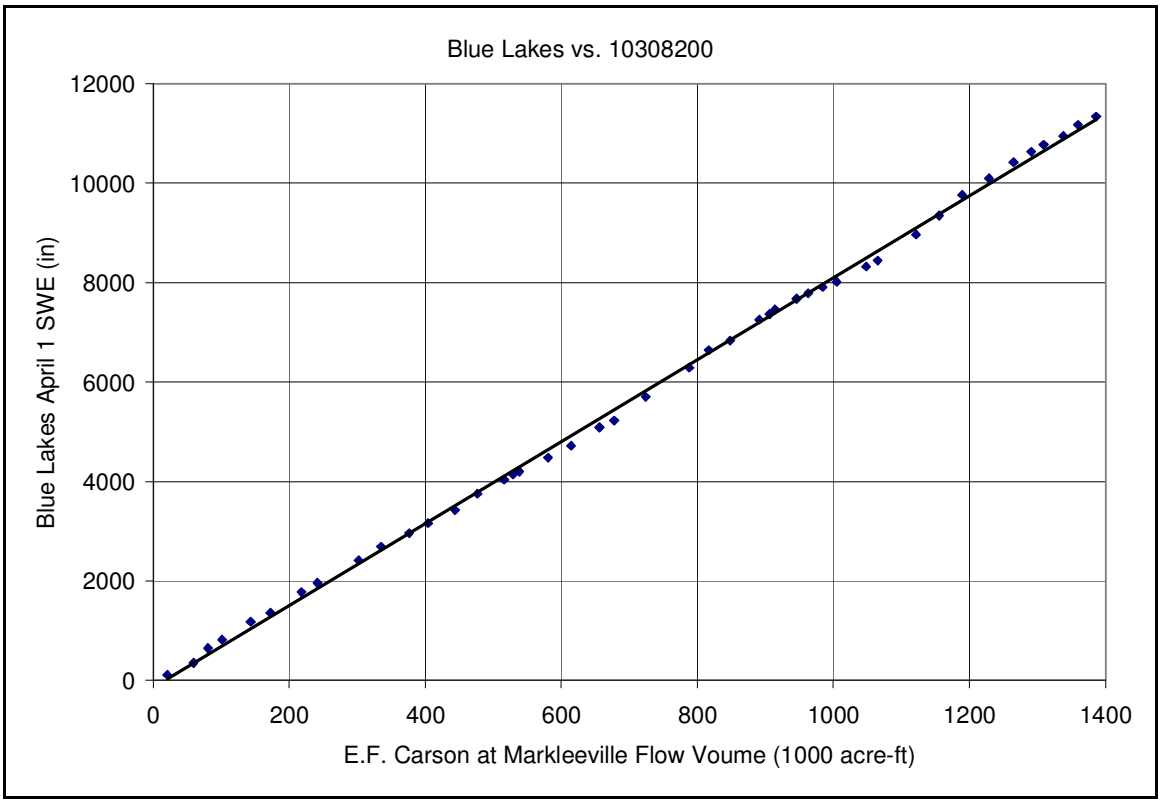

Figure I1. Blue Lakes SWE and streamflow in the E. Fork of the Carson at Markleevilles.

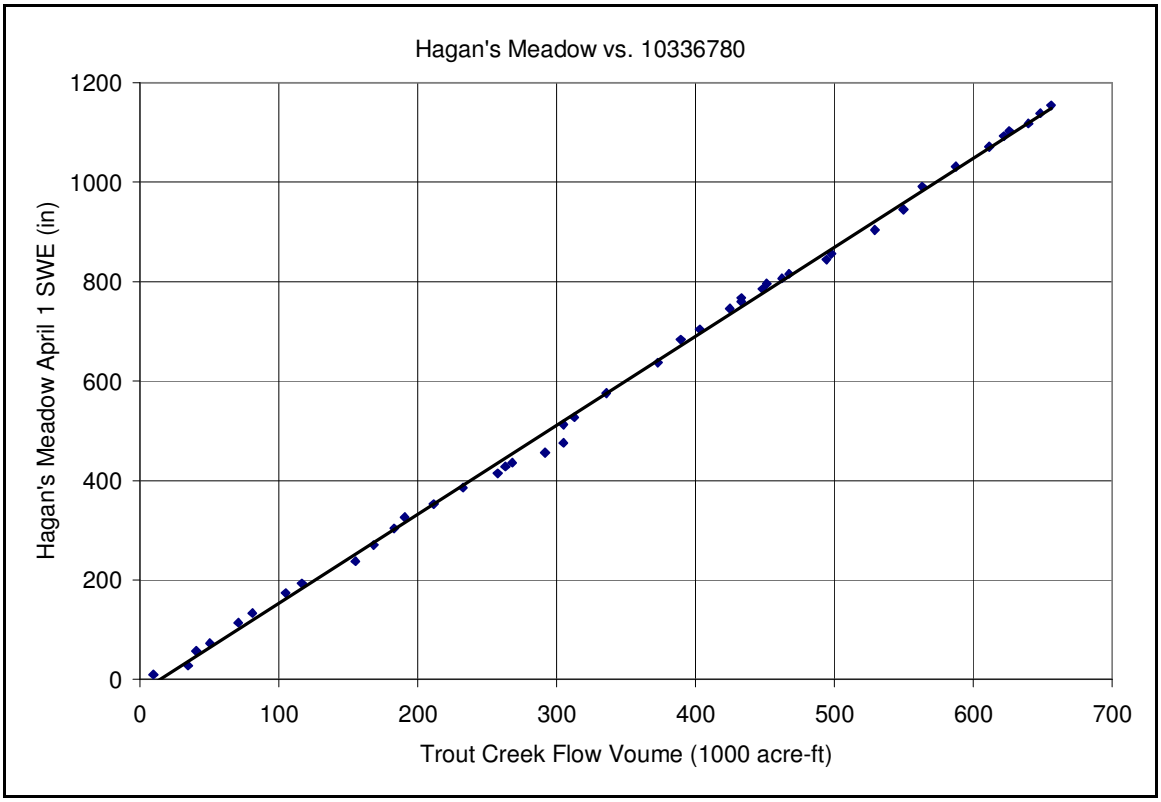

Figure I2. Hagan's Meadow SWE and Trout Creek streamflow volumes.

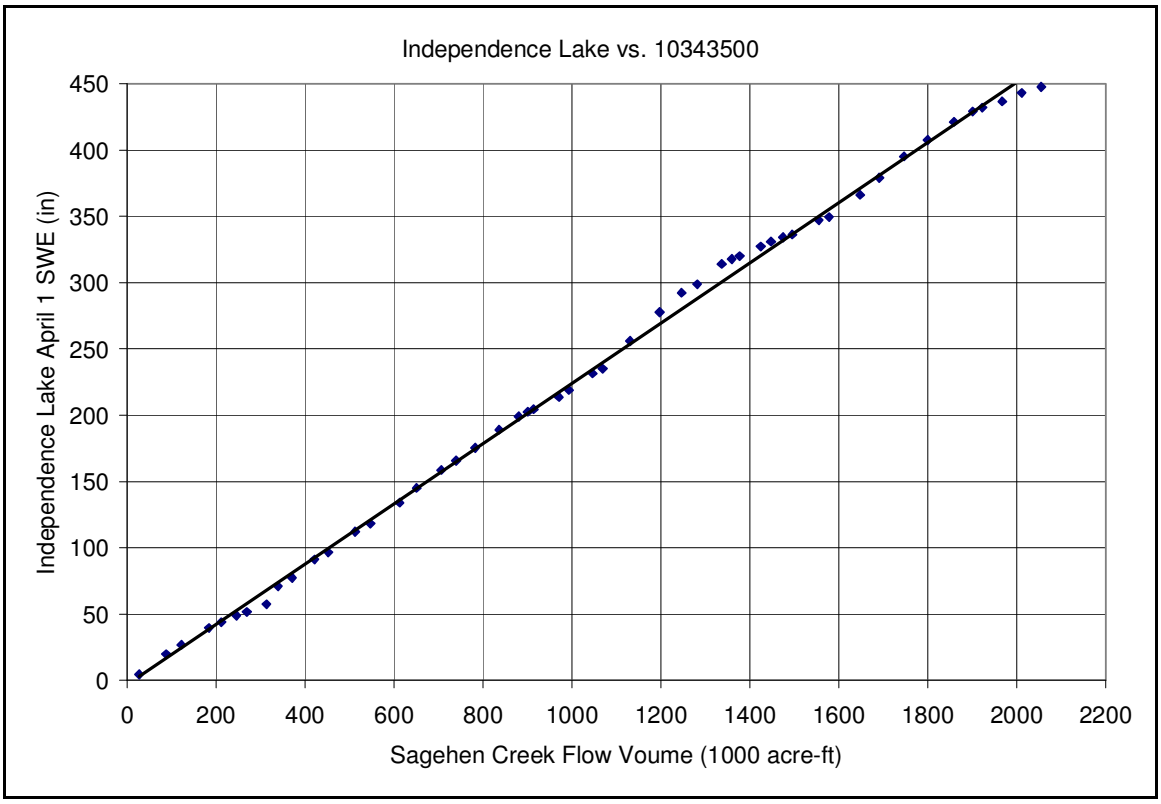

Figure I3. Independence Lake SWE and Sagehen Creek streamflow volumes.

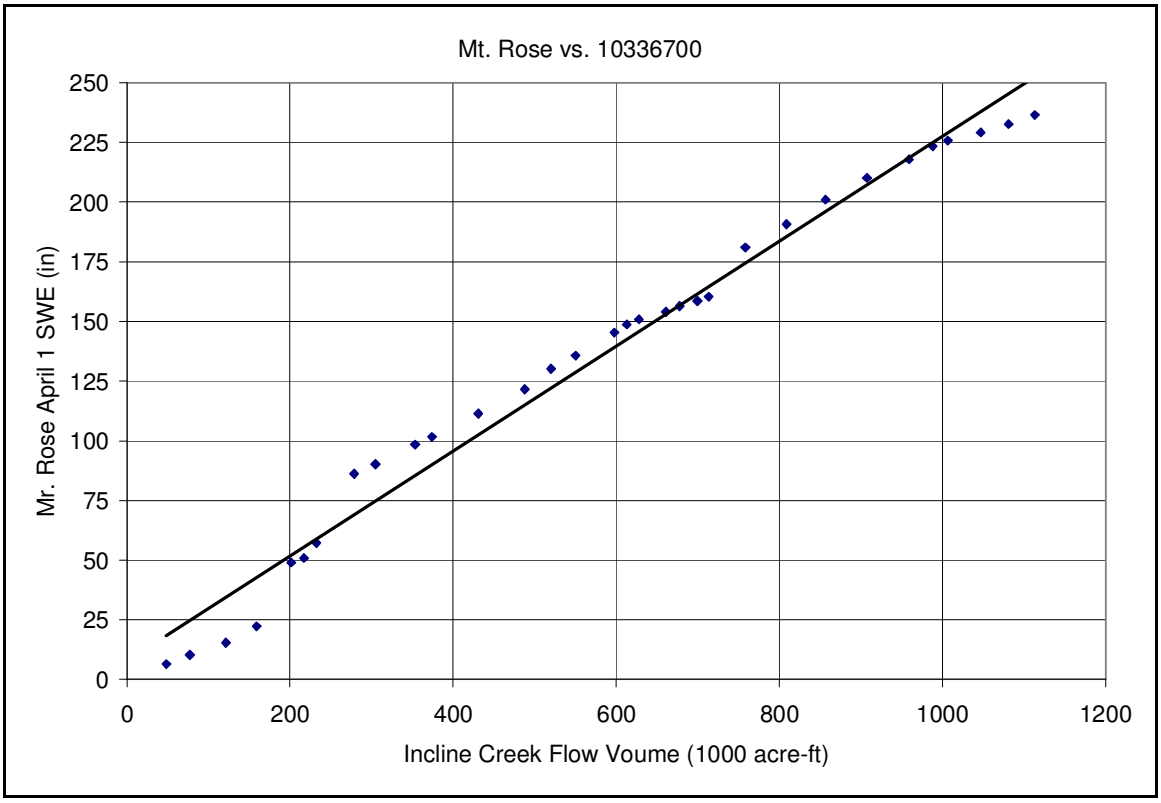

Figure I4. Mt. Rose SWE and Incline Creek streamflow volumes.

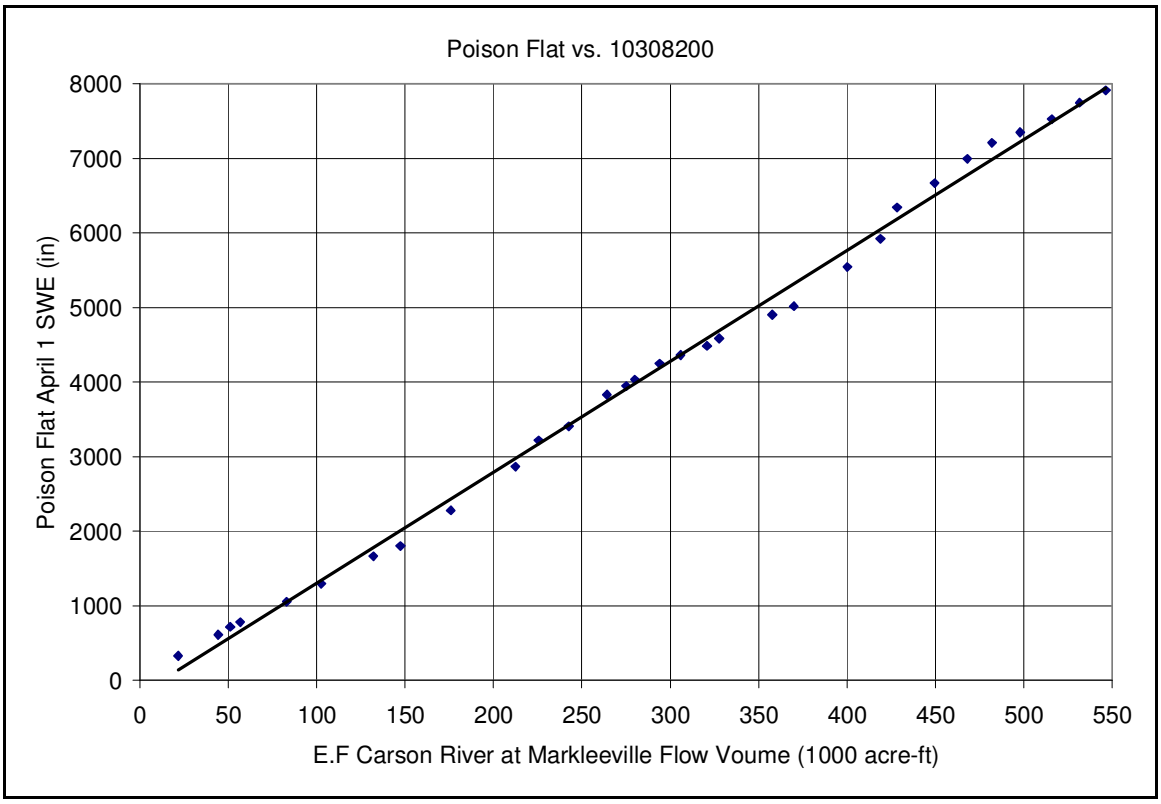

Figure I5. Poison Flat SWE and E.F Carson River at Markleeville streamflow volumes.

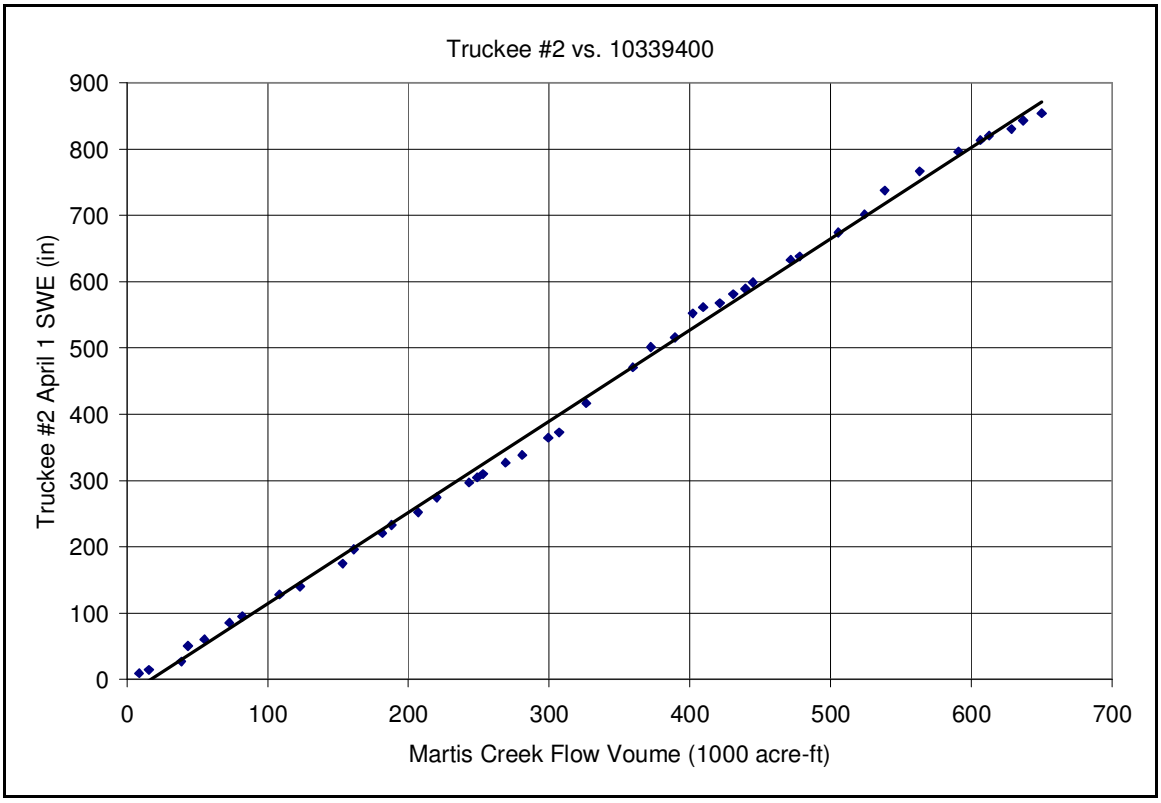

Figure I6. Truckee #2 SWE and Martis Creek streamflow volumes.

Appendix J

Double Mass Curve Analysis
Streamflow vs. Reservoir Volumes

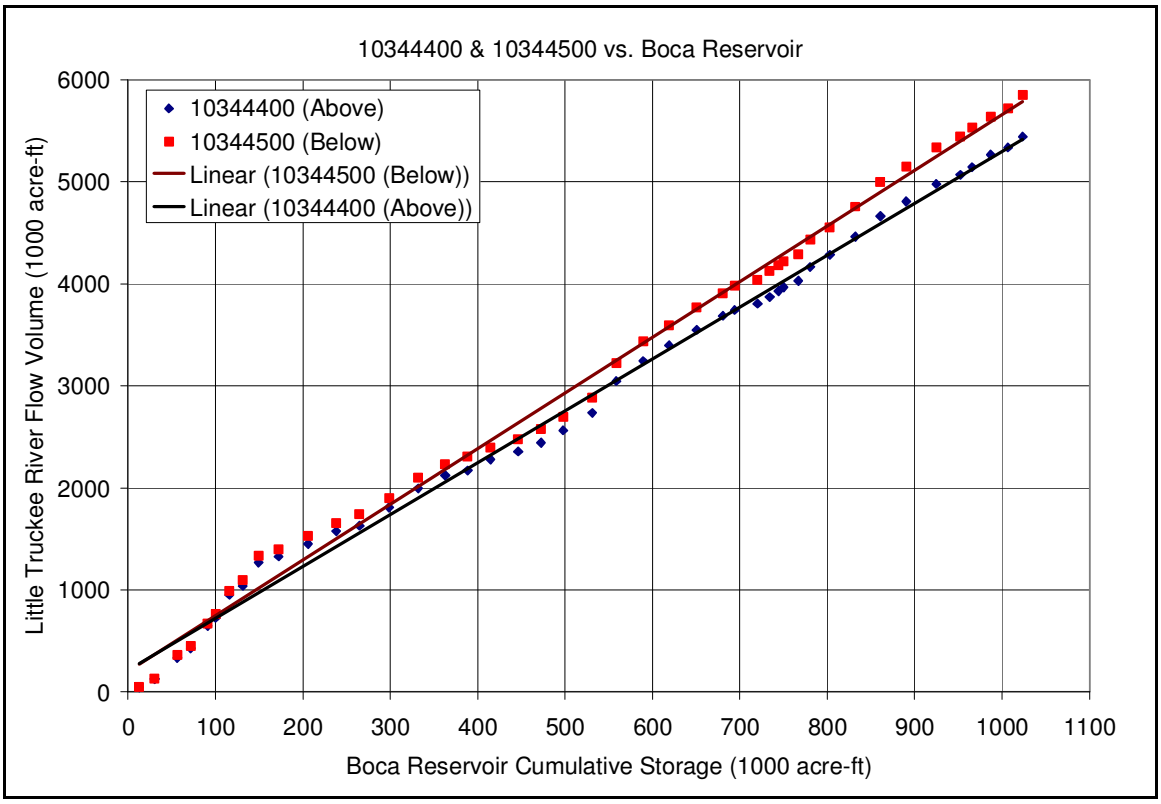

Figure J1. Little Truckee River streamflow volume and Boca Reservoir storage.

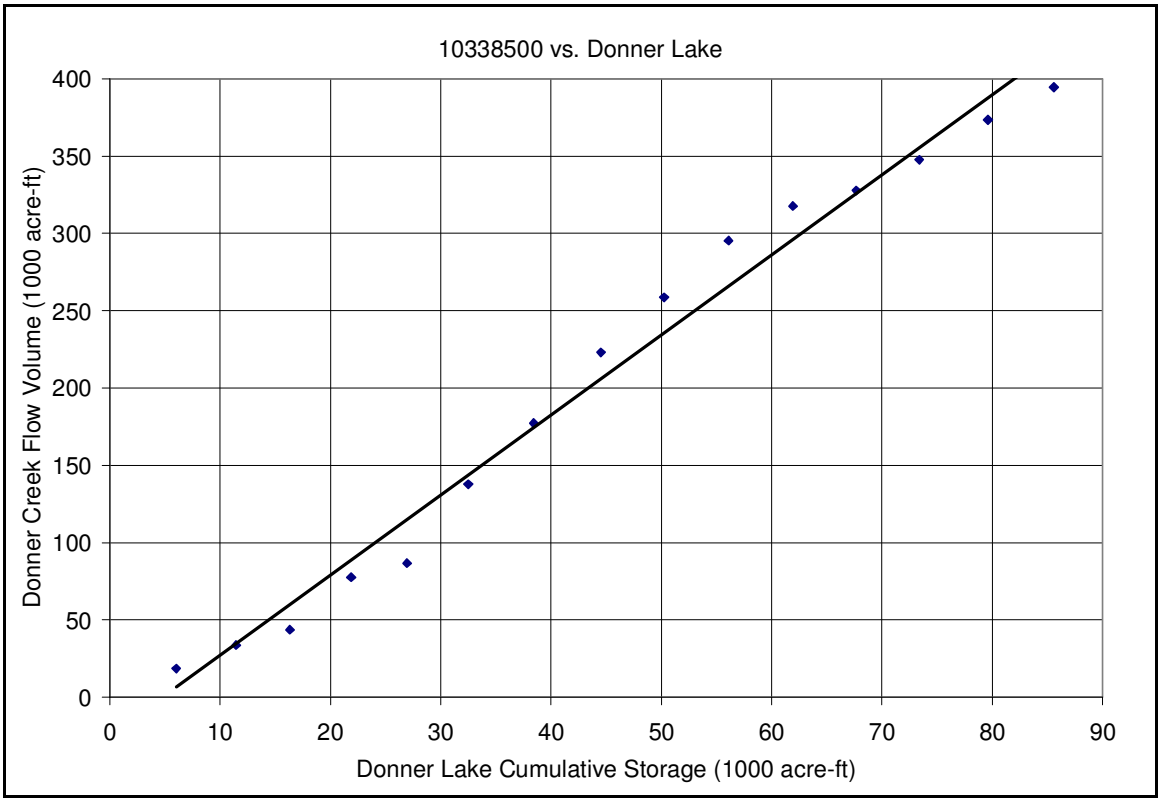

Figure J2. Donner Creek streamflow volume and Donner Lake storage.

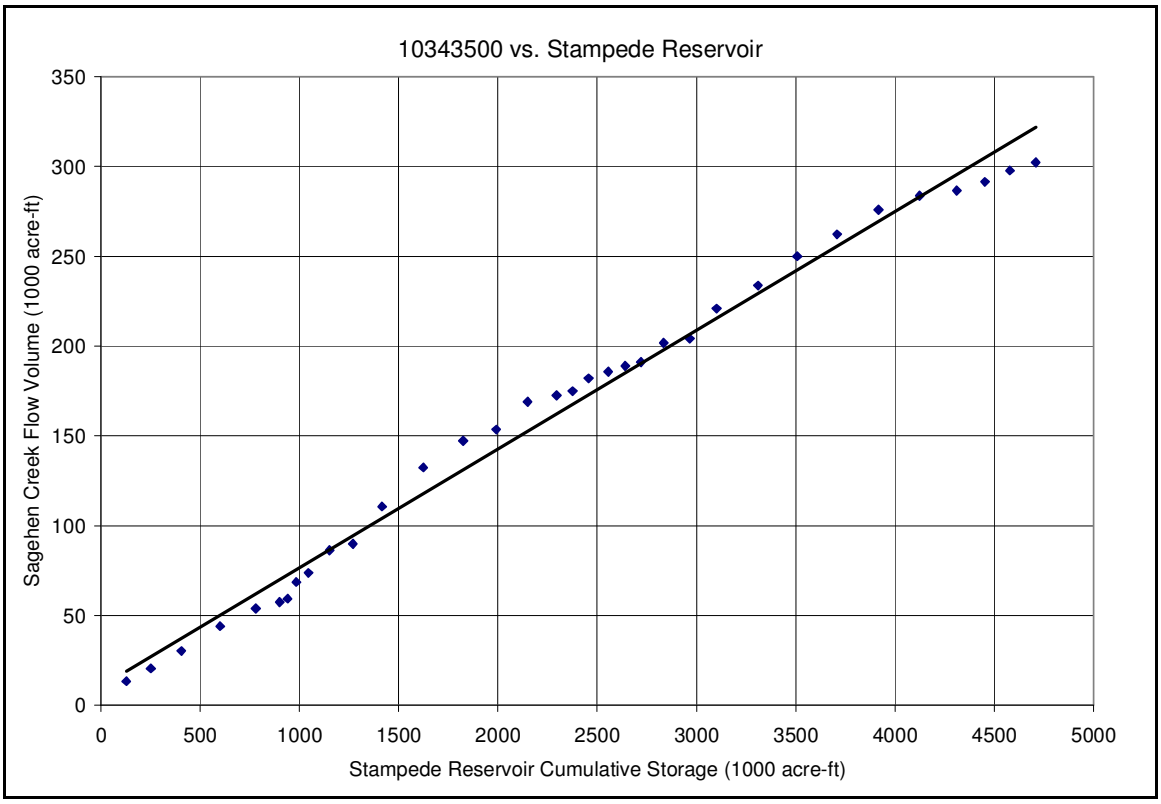

Figure J3. Sagehen Creek streamflow volume and Stampede Reservoir storage.

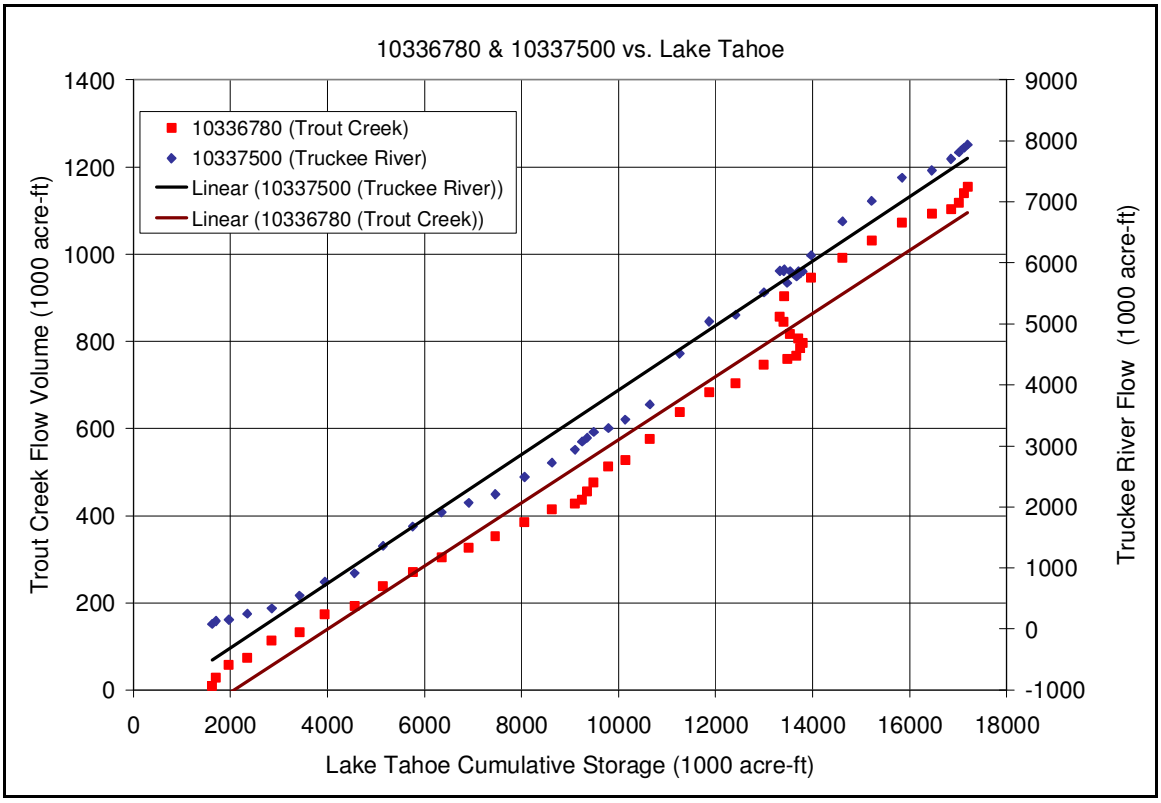

Figure J4. Trout Creek streamflow volume and Lake Tahoe storage.

Appendix K

Double Mass Analysis
Reservoir Volume vs. Snowpack

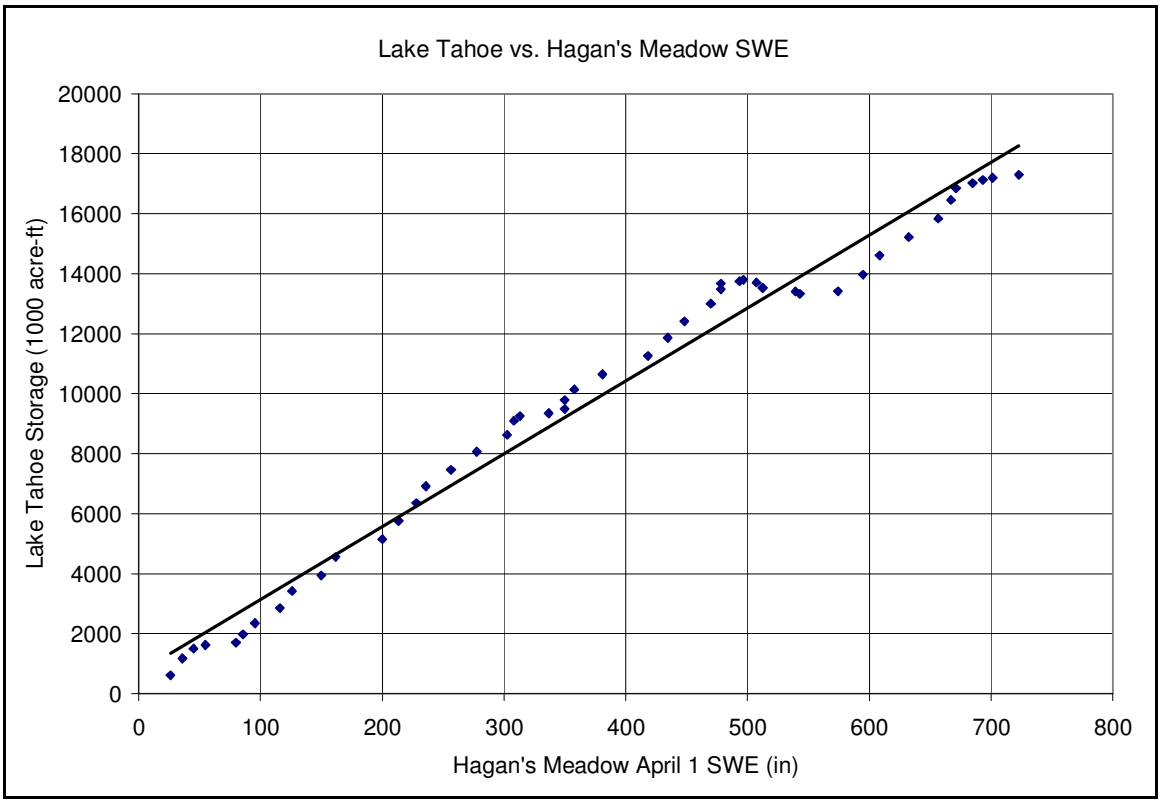

Figure K1. Lake Tahoe storage and April 1 SWE at Hagen's Meadow snowcourse station.

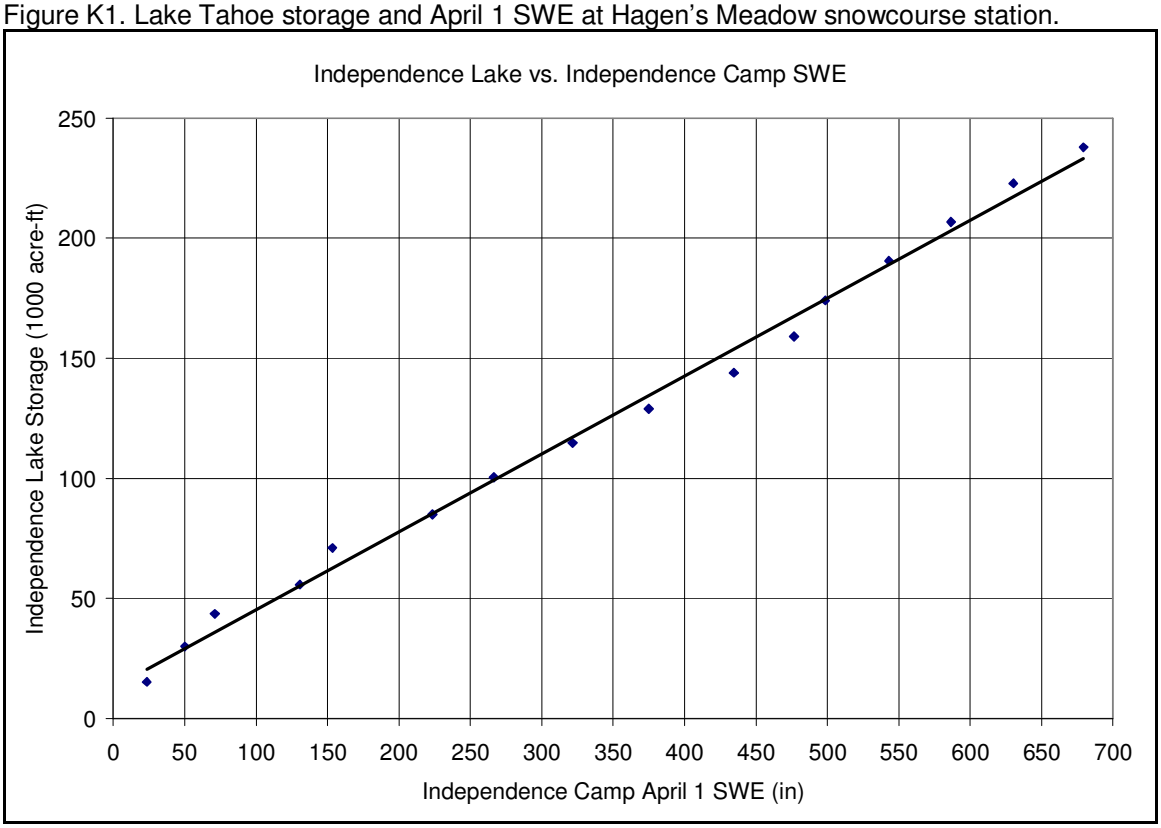

Figure K2. Independence Lake storage and April 1 SWE at Independence camp.

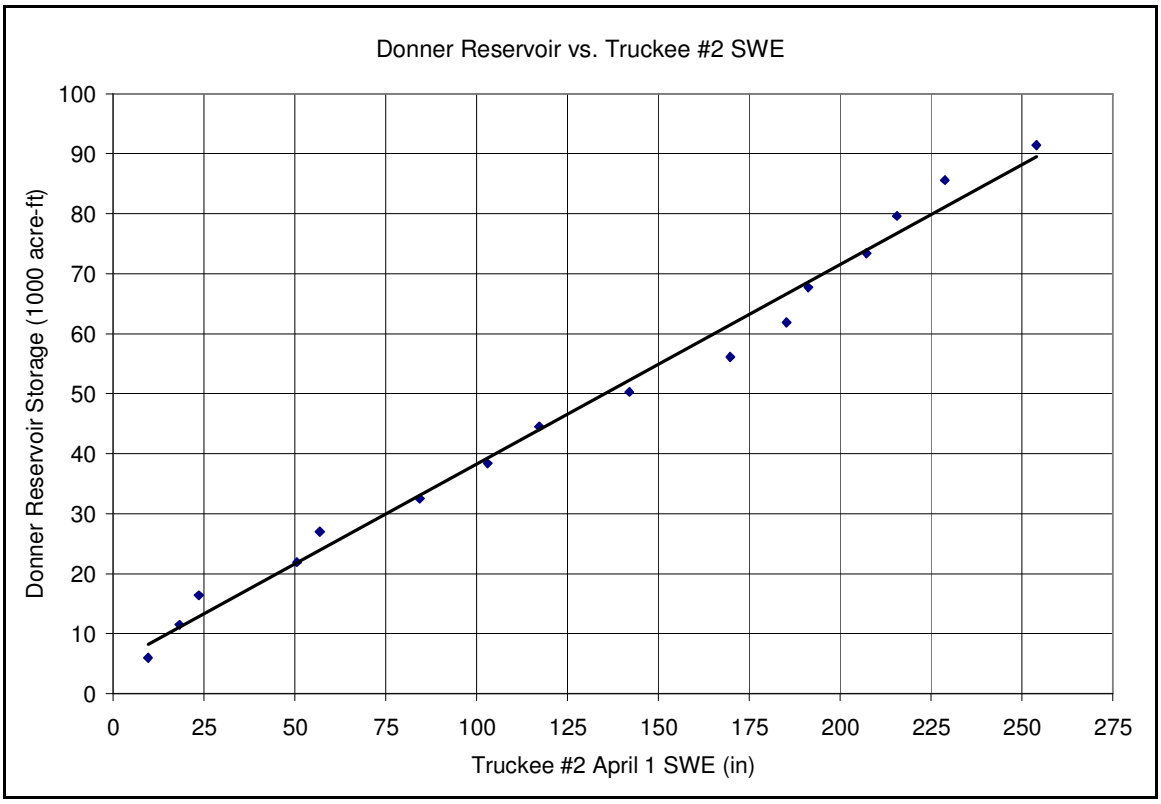

Figure K3. Donner Reservoir storage and April 1 SWE at Truckee #2 snowcourse station.

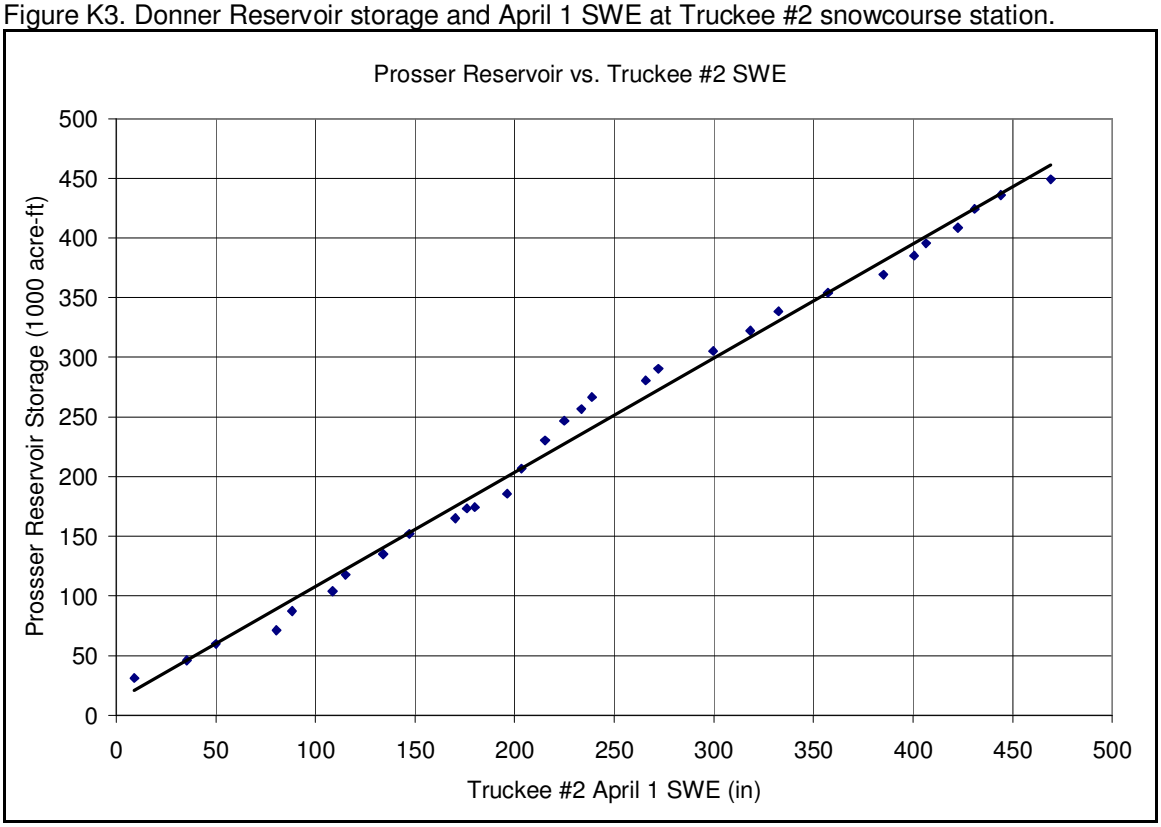

Figure K4. Prosser Reservoir storage and April 1 SWE at Truckee #2 snowcourse station.

Appendix L

Database Descriptions

Table L1. Snowcourse database information.

Name	*ID*	*Latitude*	*Longitude*	*Start*	*End*
Poison Flat	19|06s	38.5055	-119.6261	1942	2005
Blue Lakes	19|05s	38.6078	-119.9244	1918	2005
Hagen's Meadow	19|03s	38.8519	-119.9374	1916	2005
Independence Creek	20k03s	39.4902	-120.2813	1930	2005
Independence Camp	20k04s	39.4528	-120.2927	1941	2005
Independence Lake	20k05s	39.4275	-120.3134	1937	2005
Rubicon	20|02s	38.9992	-120.1303	1912	2005
Truckee	20k13s	39.3009	-120.1841	1931	2005
Marlette Lake	19k04s	39.1640	-119.8967	1915	2005
Mt. Rose Ski Area	19k07s	39.3157	-119.8947	1910	2005

Source: Natural Resources Conservation Service, National Water and Climate Center
http://www3.wcc.nrcs.usda.gov/snow/snowhist.html

Table L2. Streamgage database information.

Name	**ID**	**Latitude**	**Longitude**	**Start**	**End**
E.F. Carson R @ Markleeville	10308200	38.7146	-119.7649	1960	2005
E.F. Carson R @Gardnerville	10309000	38.8449	-119.7046	1900	2005
W.F. Carson R @Woodfords	10310000	38.7696	-119.8338	1900	2005
Clear Creek @ Carson City	10310500	39.1132	-119.7982	1948	2005
Carson R @ Cason City	10311000	39.1077	-119.7132	1939	2005
Carson R @ Fort Churchill	10312000	39.2917	-119.3111	1911	2005
Blackwood Cr. @ Tahoe City	10336660	39.1074	-120.1621	1960	2005
Third Cr. @ Crystal Bay	10336698	39.2405	-119.9466	1969	2005
Incline Cr. @ Crystal Bay	10336700	39.2402	-119.9449	1969	2005
Trout Cr. @ Tahoe Valley	10336780	38.9199	-119.9724	1960	2005
Truckee R @ Tahoe City	10337500	39.1663	-120.1444	1900	2005
Truckee R @ Truckee	10338000	39.2963	-120.2055	1944	2005
Donner Cr. @ Donner Lake	10338500	39.3235	-120.2344	1929	2005
Martis Cr. @ Truckee	10339400	39.3288	-120.1177	1958	2005
Prosser Cr. Bl. Prosser Dam	10340500	39.3732	-120.1316	1942	2005
Sagehen Cr. @ Truckee	10343500	39.4316	-120.2380	1953	2005
Little Truckee R. above Boca	10344400	39.4357	-120.0844	1939	2005
Little Truckee R. below Boca	10344500	39.3869	-120.0955	1911	2005
Truckee R. @ Farad	10346000	39.4280	-120.0341	1909	2005
Hunter Cr. @ Reno	10347600	39.4909	-119.8997	1961	2005
Truckee R. @ Reno	10348000	39.5302	-119.7955	1906	2005
Galena Cr. @ Streamboat	10348900	39.3619	-119.8267	1961	1994
Streamboat Cr. @ Steamboat	10349300	39.3771	-119.7437	1961	2005
Truckee R. @ Vista	10350000	39.5205	-119.7010	1900	2005

Source: U.S. Geological Survey, National Water Information System: Web Interface
http://water.usgs.gov

Table L3. COOP weather station database information.

Name	ID	Latitude	Longitude	Start	End
Boca	40931	39.3833	-120.1000	1936	2005
Donner Memorial St. Park	42467	39.3167	-120.2333	1953	2005
Markleeville	45356	38.7000	-119.7833	1931	2004
Sagehen Creek	47641	39.4333	-120.2333	1953	2005
Truckee Ranger Station	49043	39.3333	-120.1833	1935	2005
Carson City	261485	39.1500	-119.7667	1931	2005
Glenbrook	263205	39.0833	-119.9500	1945	2005
Lahontan Dam	264349	39.4667	-119.0667	1931	2005
Minden	265191	39.0000	-119.7500	1931	2005
Reno Airport	266779	39.5000	-119.7833	1937	2005
Virginia City	268761	39.3000	-119.6333	1951	2005

Source: National Weather Service, Cooperative Observer Program, via the Western Regional Climate Center
http://www.nws.noaa.gov/om/coop/
http://www.wrcc.dri.edu/

Table L4. Reservoir and Lake storage database information.

Name	ID	Latitude	Longitude	Start	End
Boca Reservoir	BOC	39.3830	-120.1000	1960	2005
Donner Lake	DNL	39.3240	-120.2330	1989	2005
Independence Lake	INL	39.4500	-120.2830	1988	2005
Lahontan Reservoir	10312100	39.2750	-119.0400	1917	2005
Martis Creek Reservoir	MRT	39.3270	-120.1130	1972	2005
Prosser Reservoir	PRS	39.3794	-120.1367	1964	2005
Stampede Lake	STP	39.4710	-120.1030	1970	2005
Lake Tahoe	TAH	39.1810	-120.1180	1957	2005

Source: California Department of Water Resources, Division of Flood Management, by request
http://cdec.water.ca.gov/misc/resinfo.html
Except for Lahontan Reservoir, which was from the USGS National Water Information System: Web Interface
http://waterdata.usgs.gov/nv/nwis/

PRELIMINARY EVALUATION OF CLIMATIC DATA IN TRUCKEE MEADOWS REGION

TABLE OF CONTENTS

LIST OF FIGURES

LIST OF TABLES

1 INTRODUCTION

Our climate has always been in a state of change. Within the last 1000 years, the Sierra Nevada Mountains have undergone two warm, dry periods of 150 and 200 year duration during AD 900–1350, and a Little Ice Age, from AD 1400 to 1900 (Millar and Wolfenden, 1999). Any changes to the climate in the present times have the potential to severely disrupt the growth and survival of our civilization. Of all avenues which are affected by climate change, water availability is one of the most significant. The survival and growth of a number of our cities, agricultural areas, environmental reserves, natural resources, etc. will depend upon our preparedness for reacting towards changing climate and water availability.

Annual precipitation has increased for most of North America with large increases in northern Canada, but with decreases in the southwest U.S., the Canadian Prairies and the eastern Arctic (Trenberth et al., 2007; Shein, 2006). Heavy precipitation frequencies in the U.S. were at a minimum in the 1920s and 1930s, and increased to the 1990s (1895 to 2000) (Kunkel, 2003; Groisman et al., 2004). Streamflow in the eastern U.S. has increased 25% in the last 60 years (Groisman et al., 2004), but over the last century has decreased by about 2%/decade in the central Rocky Mountain region (Rood et al., 2005). Since 1950, stream discharge in both the Colorado and Columbia River basins has decreased, at the same time annual evapotranspiration (ET) from the conterminous U.S. increased by 55 mm (Walter et al., 2004). The fraction of annual precipitation falling as rain (rather than snow) increased at 74% of the weather stations studied in the western mountains of the U.S. from 1949 to 2004 (Knowles et al., 2006).

As is clear from the studies cited above, climate change has a multi-pronged effect on water resources. It not only changes the inflow of water into the water bodies, but also the outflow by changing withdrawals, evaporation from the water surface, and transpiration by plants. Several regions in the world are expected to face water shortages due to climatic changes but the situation is expected to be more severe in regions which are already arid or semi-arid. The US South West is one such region where water might be a limiting factor to further development. Several studies have been conducted to evaluate the impacts of climate change and their mitigation in river basins in the Western US (Payne et al, 2004; Hamlet and Lettenmaier, 1999; VanRheenen et al, 2004; Christensen et al, 2004).

Climate change projections for Southwestern United States remain uncertain about the magnitude of temperature and precipitation changes. Nonetheless, most climate change projections agree upon an increase in temperature and a reduction in precipitation in this region (IPCC, 2007; Seager et al., 2007). This will result in a greater portion of precipitation occurring as rainfall and an increased rate of snowmelt in the Sierra Nevada Mountains (Pupacko, 1993; Dettinger, 2005). Additionally this would cause an increase in streamflow during the spring season and drier conditions during summers, thus changing the entire hydrological cycle of the watershed by altering the flow hydrograph of streams and rivers (Knowles et al., 2006; Stewart et al., 2004; Stewart et al, 2005).

Historical records show that global runoff increases by 4% for every 1°C rise in temperature (Labat et al., 2004) but the changes may vary regionally and must be studied in greater detail for effective policy making.

Climate of the Western US has experienced large changes. It is estimated that since the 1940s the temperature in the western US has risen by 1-2°C with a more pronounced increase in winter and spring temperatures (Karl et al, 1993; Dettinger et al, 1995; Lettenmaier et al, 1994; Vincent et al, 1999). Spring in this region onsets earlier these days and spring snowmelt pulses in streams have shifted back (Cayan et al, 2001, Regonda et al, 2005). An analysis of certain climate change scenarios for California revealed a significant warming of the region and significant losses in snow cover in Northern and Central Sierra Nevada Mountains (Cayan et al, 2008; Pierce et al, 2008). April 1 snow water equivalent (SWE) has declined 15 to 30% since 1950 in the western mountains of North America, particularly at lower elevations and primarily due to warming rather than changes in precipitation (Mote, 2003; Mote et al., 2005; Lemke et al., 2007).

The changes in climate are expected to increase the intensity and frequency of major flood events in the river basins of Sierra Nevada Mountains (Kim 2005). Most existing modeling studies of increased atmospheric CO_2 point to increased precipitation variability (Giorgi et al., 1994; Maurer et al, 2006; Mearns et al., 1995a, b; Trenberth et al, 2003). Significant changes in patterns in streamflow through the year can be expected in the future due to climate change (Maurer 2007) with increases in winter streamflow and decreases in summer stream flows and a shift of flow towards the earlier part of the year (Maurer and Duffy, 2005). Climate change is also estimated to have major negative impacts on the reservoirs relying on the runoff from Sierra Nevada Mountains. This will severely limit the potential of such reservoirs in fulfilling their designated purposes of water supply, hydropower generation, environmental, and ecological functions (Vicuna et al, 2007).

The Truckee Meadows Water Authority (TMWA), which is the largest water purveyor in the Reno-Sparks region, in the western US, relies primarily on the snowmelt and runoff from the Sierra Nevada Mountains to provide 85% of the water it delivers to its customers via Truckee River diversions. The Truckee River which is a 140 miles long river originating at Lake Tahoe and draining into Lake Pyramid. Primary source of water for Lake Tahoe and consequently Truckee River is the snowpack on the Sierra Nevada Mountains. Therefore, it is one of those regions which can experience a significant change in the water availability in the future because of the changing climate.

One of the principal responsibilities of the Truckee Meadows Water Authority (TMWA) is to assure that the water resources are developed and managed to fulfill the present and future water needs of the greater Truckee Meadows community (Chapter 277, NRS). In order to achieve this objective, TMWA has a 20 year water resource plan that is updated every 3 to 5 years. Climate change, because of its uncertainty of magnitude, and implications on hydrology, poses a major challenge in the course of efficient planning.

Therefore, planners and decision makers must have access to the latest developments in the field of climate change science and the study of its impacts on water availability.

Another difficulty in planning for climate change arises due to a lack of spatial resolution suitable enough to be adopted for most watersheds (Giorgi and Mearns, 1991; Leung et al., 2003). Forecasts that may be applicable to a large region in general may not be applicable to smaller watersheds on a finer temporal resolution. Therefore, it is necessary to combine information from various sources to make the projections more adaptable to the Truckee Meadows region. This report compiles the knowledge from the latest studies, field data, experiments, and computer simulations and brings an integrated assessment of the climatic changes experienced by the Truckee Meadows and changes that it should prepare to expect in the future. It will be helpful to the decision makers while framing water management policies by providing them with an insight into the changes anticipated in the hydrological processes in the Truckee Meadows region due to climate change and to examine their policies so as to mitigate its potential effects.

Future climate changes have the potential to threaten the sustainability of water resources of Truckee Meadows by disturbing the hydrological processes and changing the water availability patterns. Scientific knowledge and the latest information on the developments in the field of climate change and hydrology is a very powerful tool in the hands of planners to develop well directed policies. In view of this, in 2006, Dr. Mark Stone of the Desert Research Institute prepared two reports for TMWA on climate change and its impacts on the hydrology of the region. The first document summarized the state of the science in climate change research with an emphasis on potential impacts on water resources. The second report contained an extensive analysis of the gauged weather, streamflow, and reservoir data in the Truckee River and Lake Tahoe basins to attempt to identify early signs of climate change impacts in the region. The purpose of these reports was to inform the TMWA management of how climate change could impact their ability to carry out their mission of water delivery to their customers. The present report updates those reports with current information and additional data sources which have become available over the past 3 years. This additional information is important to consider due to the recent proliferation of climate change research. Further, this report also includes the analysis of spatially explicit gridded datasets available from various sources to expand the analysis of station data carried out in previous reports.

This study will improve the understanding of the impact of potential climatic changes on the water resources of the Truckee Meadows region. The primary deliverables of the proposed research is this updated report on the state of the science of climate change impacts research and on the trends analysis which incorporates the gridded data described above.

1.1 Study Area

The study area is located in the north western part of Nevada on the Border with California. It contains the urban areas of Reno with a population of 214,853, Sparks with a population of 87,139, and Carson City with population of 54,939 (US Census Bureau). Figure 1 shows the relief of the study area. The western edge of the study area lies on the

Sierra Nevada Mountains and has an elevation of up to 3200 m above sea level. Carson Desert and Pyramid Winnemucca Lakes which are the lowest points in the study area lie on the floor of the Great Basin and have elevation of 1100 m. A significant portion of the snowcaps on the Sierra Nevada Mountains, which are the primary source of water to Lake Tahoe, Truckee River and Carson River, lie in California. However, a greater portion of the study area lies in the Great Basin in Nevada.

.

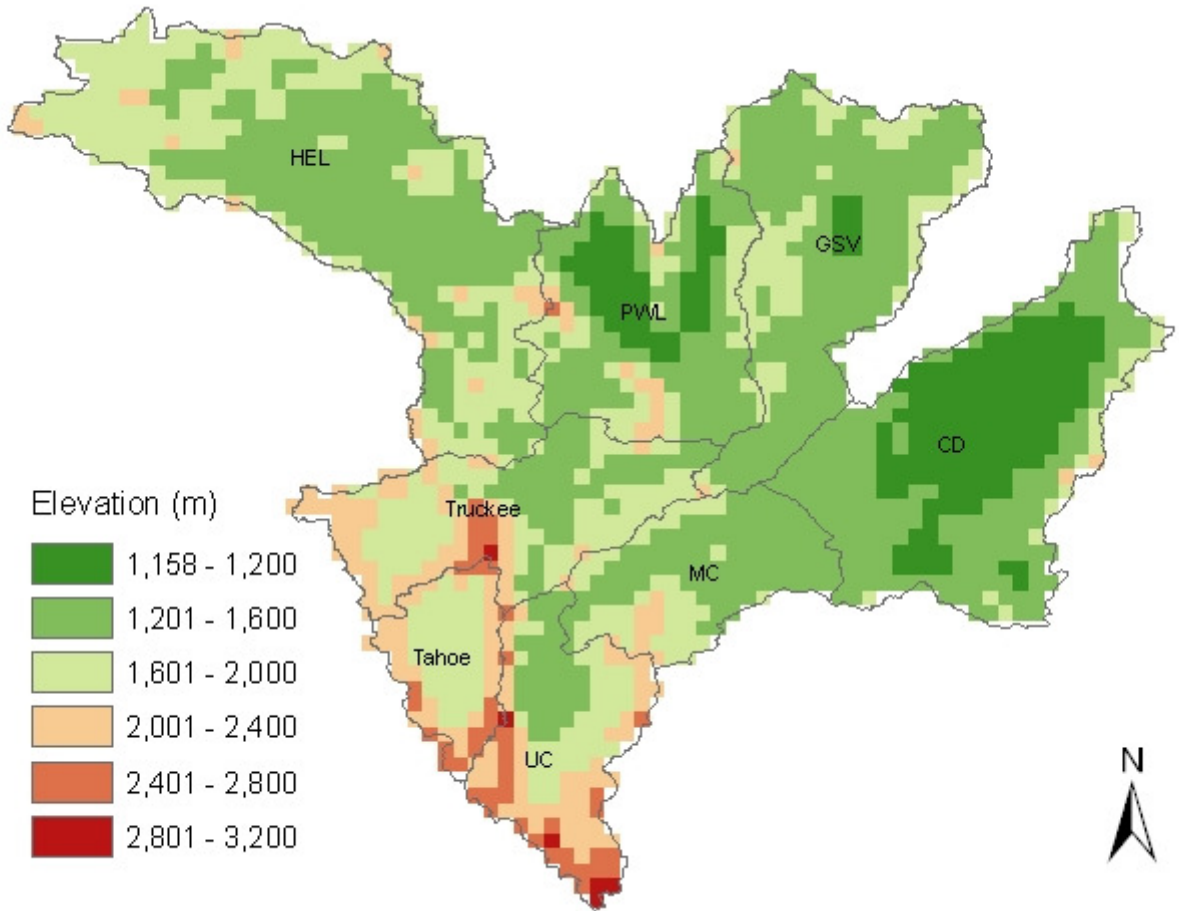

Figure 1 Elevation of the study area above MSL.

1.2 Objectives

Weather stations, stream gauges, and reservoir levels can all provide insights into long term trends in climate and hydrology. These sources include data from Natural Resources Conservation Service Snowpack Telemetry (SNOTEL), NWS Cooperative Network, Remote Automated Weather Stations, USGS High Altitude Precipitation, USGS streamflow gages, USGS groundwater monitoring wells, and Snow Course Stations. These stations were used in the 2006 report to study potential trends in the region. However, there are several limitations to gauged data which have led researchers to enhance the usefulness of the measured records by interpolating them over an extended area. Gauged data is collected at a single point and therefore has serious limitations in terms of studying spatial patterns in data. Further, inconsistencies in measuring techniques in both time and space often makes comparison studies quite complicated.

This limitation can be overcome through the use of gridded datasets which are based on a re-analysis of historical data using process based simulation models that ingest historic data. Precipitation-elevation Regressions on Independent Slopes Model (PRISM) and The Variable Infiltration Capacity (VIC) are examples of spatially gridded data that are used in this study to add to the data analysis task performed in the previous reports. Each of these is explained in brief in the following paragraphs.

PRISM, developed by the Spatial Climate Analysis Service and Oregon Climate Service, is an analytical model that uses station point data, a digital elevation model and additional spatial datasets to produce 4 km resolution grids of monthly temperature and precipitation across the continental US (Daly et al., 2002; Daly et al., 1994). As the model is also designed to incorporate high elevation data from mountainous regions and to accommodate difficult climate mapping situations in innovative ways, PRISM is well suited to capture the complex climatological conditions present in the western US (Nanus et al., 2003). PRISM is currently the primary dataset being used in WestMap, and is also implemented in the California Climate Tracker (CCT) to bolster climate information across sparsely monitored locations in the state of California. PRISM has also been adopted by NOAA's NWS for a number of products and projects. Monthly accumulated precipitation along with monthly averaged maximum and minimum temperatures will be used as inputs to derive a number of the drought indices of interest.

The VIC model (Liang et al., 1996) is a macroscale hydrologic model that is capable of distinguishing characteristics of subgrid heterogeneity in soils, vegetation, topography and precipitation. The VIC dataset is advantageous for examining hydrologic changes over the study area given its 1/8 degree or 10x12 km horizontal spatial and daily temporal resolution. VIC provides information of temperature, precipitation, snow water equivalent, soil moisture, runoff, and evapotranspiration for every pixel. One of the premier advantages of VIC is its simulation of the snow water and energy balance which is a key component of the hydrologic setting of the study area. VIC has been implemented in numerous research studies and operational products, and is well established for usage across the western US (Lettenmaier et al., 1999; VanRheenen et al., 2004; Christensen et al., 2004).

The broad objectives of this study can be summarized as follows.
Objective 1: Update the state of the science literature review, which was completed in 2006, with relevant publications and products released over the past 3 years.
Objective 2: Expand the data analysis task by evaluating spatial patterns and extended records available from the gridded datasets.
Objective 3: Perform a cursory analysis of existing climate change scenarios that have been downscaled for the Truckee basin to provide an overview of expected trends and related uncertainty.

2 PAST CLIMATE TRENDS

2.1 PRISM

It has been shown in a number of studies that topography plays a major role in the distribution of precipitation and temperature over an area especially in mountainous regions. The rate of precipitation as well as temperature varies considerably at different elevations and on the different faces of a relief. This feature, however, is not adequately represented by statistical or graphical methods of precipitation interpolation. Parameter-elevation Regressions on Independent Slopes Model (PRISM) is an analytical model that can be used to distribute point measurements of monthly, seasonal, and annual precipitation to a geographic grid. PRISM uses data from weather stations and digital elevation models to model annual, monthly and event based climate events that are gridded and GIS compatible.

The Lake Tahoe watershed primarily comprises of mountainous regions of the Sierra Nevada Mountains. In such topography, conventional interpolation methods are not sufficient to model climate parameters such as precipitation, temperature, etc. Therefore, this study utilizes the outputs from PRISM to evaluate the changes that have occurred to the climate of the region in the past decades. A collaborative effort between the Spatial Climate Analysis Service and the Oregon Climate Service has resulted in detailed, high-quality spatial climate datasets, referred to as PRISM maps (Daly et al., 2001). PRISM is an analytical model that distributes point measurements of monthly, seasonal, and annual precipitation to a geographic grid of four kilometers by four kilometers. By use of a resampling algorithm, two-kilometer by two-kilometer resolution grids can be estimated. These grids are produced in a GIS compatible latitude-longitude grid or a gridded map projection.

Digital elevation models (DEMs) are used in conjunction with observed precipitation values in the PRISM model to determine variation in precipitation as a function of elevation. DEMs contain information that describes the earth's topography, including slope, aspect, and elevation. Because the PRISM precipitation dataset is a function of the observed data and topography, orographic precipitation and rain shadows are uniquely and accurately modeled in PRISM (Daly et al., 2001).

Three existing climate datasets are used by PRISM to create maps: the National Climatic Data Center 1961-1990 normals dataset (CLIM-81) observed by the National Weather Service Cooperative Climate Network; the NRCS SNOTEL (SNOwpack TELemetry) network dataset, and supplemental datasets submitted by the individual State Climatologists or regional climate centers (Daly et al., 2001). The PRISM Evaluation Group (PEG), composed of State and Regional Climatologists, representatives of national agencies, NRCS representatives and other state and local government users, evaluated and endorsed the PRISM model for Idaho, Nevada, Oregon, and Utah data (Daly et al., 2001). An examination of average annual PRISM precipitation values in the Willamette River basin, northern Oregon, resulted in 0.1 cm (1.0 percent of observation) cross

validation bias and 17 cm (10 percent of observation) mean absolute error (Daly et al., 1994).

PRISM is designed and updated to map climate parameters in varying terrains, including high mountains, rain shadows, coastal regions, and other complex climatic regimes. PRISM accounts for topographic facet (hill slope orientation) to handle rain shadows, and for elevation, a primary driver of climate patterns (Daly et al., 2001). Two main advantages of using PRISM data are that precipitation values are available on a regular grid size of four kilometers by four kilometers, and the data are available in digital form. These two factors allow PRISM data to be easily integrated with other water budget components and calculations within a Geographic Information System (GIS) environment.

To analyze the PRISM data, the study area was segmented into eight smaller sub basins. The sub basins used for this purpose were derived from the hydrologic units shapefile obtained from the National Atlas website last downloaded on August 7, 2009 (http://www.nationalatlas.gov/atlasftp.html#hucs00m). Table 1 shows the details of the watersheds studied using PRISM data.

Table 1 Division of the study area.

Sub-watershed	Denomination	Pixels	Area (Km^2)
Carson Desert	CD	335	5360
Granite Springs Valley	GSV	263	4208
Honey Eagle Lakes	HEL	437	6992
Middle Carson	MC	139	2224
Pyramid Winnemucca Lakes	PWL	215	3440
Lake Tahoe	Tahoe	79	1264
Truckee River	Truckee	191	3056
Upper Carson	UC	147	2352
Entire Watershed	Entire	1806	28896

Monthly precipitation, average monthly minimum and maximum temperature data were downloaded from the PRISM Group's ftp site for the years 1895 to 2008. These files stretch on a four kilometer by four kilometer grid scale covering the entire continental United States. Because a very small window of the entire United States dataset was needed, clipping of the data to the study area was completed as an initial step using the eight smaller subdivisions of the region. These clipped data were then used for determining the temperature and precipitation values over the watershed for the above mentioned time period on a monthly time scale. The end product of data processing resulted in precipitation data in millimeters, and monthly average maximum and minimum temperatures in ^{o}C. The monthly temperature and precipitation values were then tabulated and trends were generated. A detail of the data processing procedure is provided in the Appendix 6.1.

Figure 2 and Figure 3 show the average maximum and minimum monthly temperatures for the study area in 2007. Temperature variation within the study area shows an expected increase from west to east because of lowering of elevation. Similarly, Figure 4

shows the precipitation distribution over the study area. The south western edge of the study area, which has the maximum elevation, also receives the highest amount of precipitation. It decreases from west to east because of the rain shadow effect produced by the Sierra Nevada Mountains on the west portion of the study area.

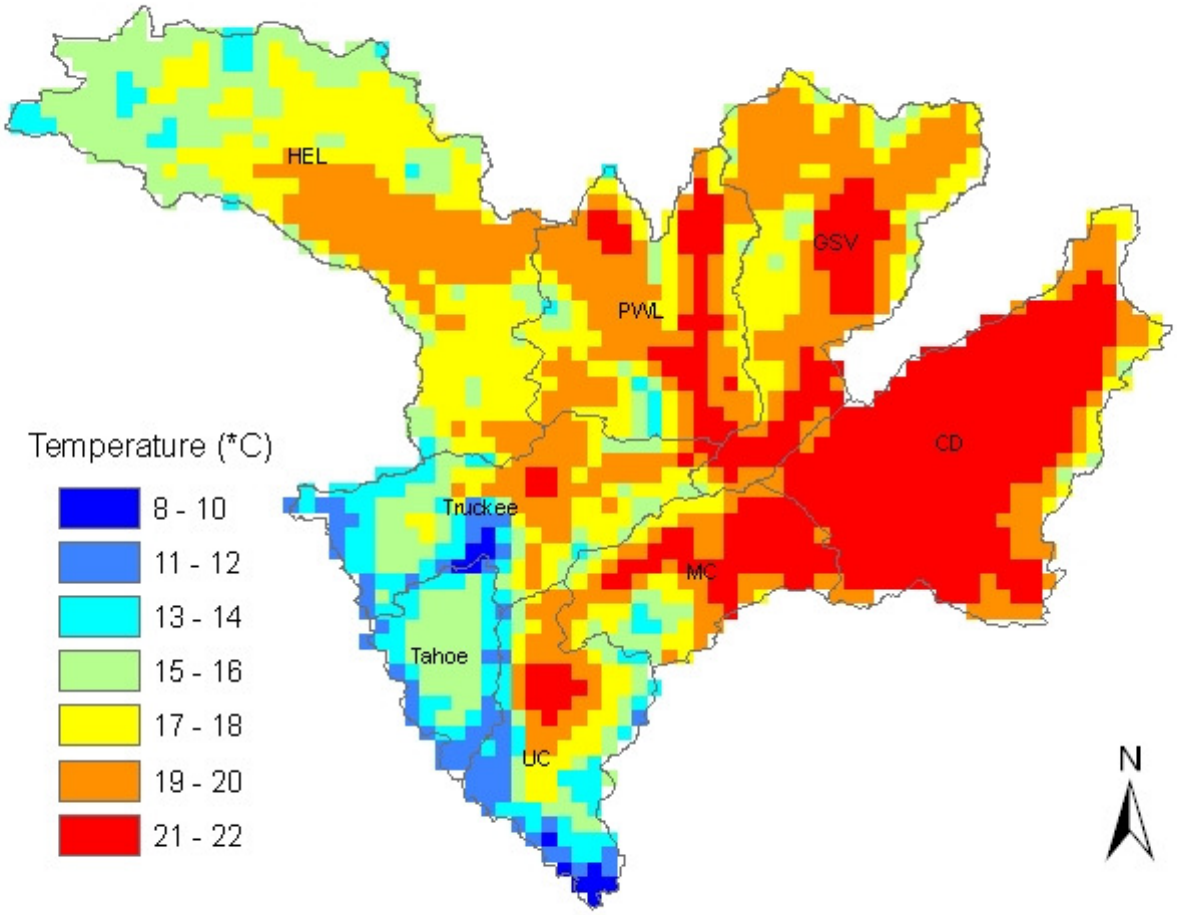

Figure 2 Average maximum monthly temperature for 2007.

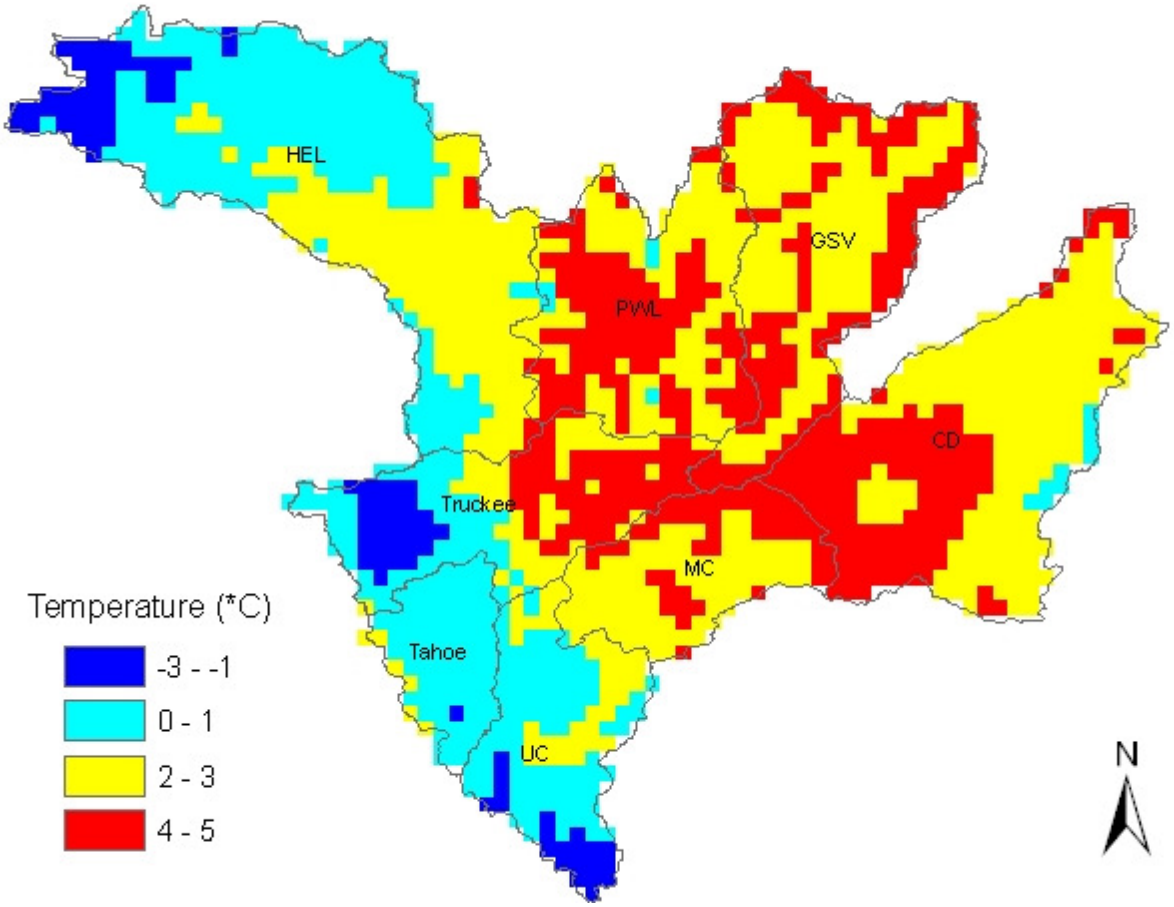

Figure 3 Average minimum monthly temperature for 2007.

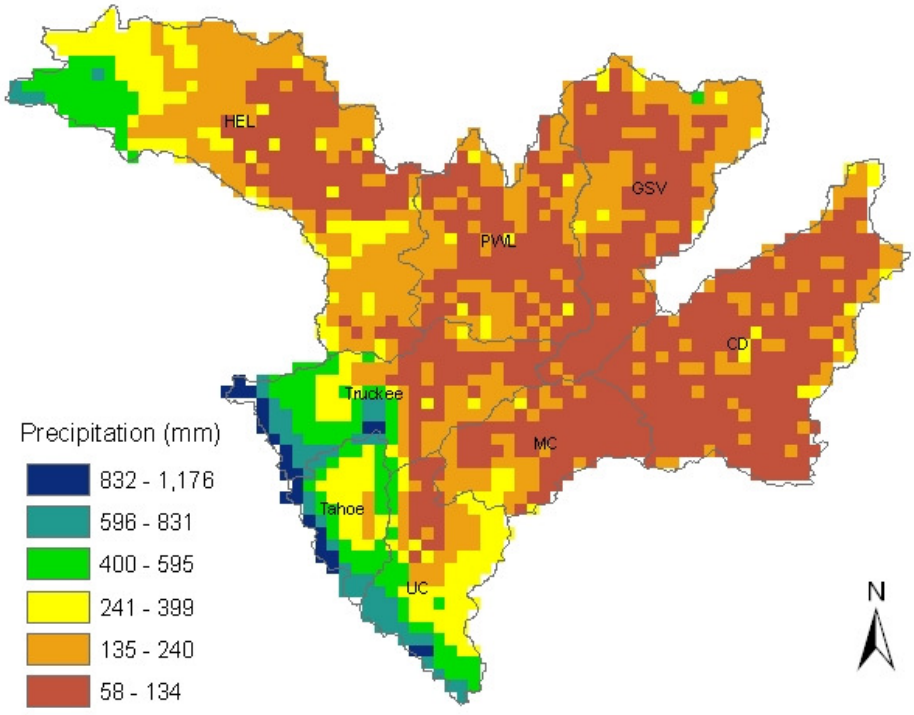

Figure 4 Total precipitation for 2007.

Analysis of precipitation data for the eight sub regions shows that annual precipitation has experienced an increasing trend in six of the sub regions excluding Honey Eagle Lakes and Upper Carson (Table 2). Figure 5 shows the variation in annual precipitation in the Lake Tahoe Basin. Breaking down the annual precipitation trends into the four seasons reveal that the increase is not uniform throughout the year. All but GSV show a decrease in winter precipitation with UC experiencing the largest rate of decrease. In case of spring season, all regions at lower altitudes experienced an increasing trend in precipitation during the study period and all the high altitude regions show a decline in spring precipitation. However, for the summer months, all regions show similar increasing trends. The high altitude regions which show a decreasing trend for spring precipitation show the greatest rates of increase in fall precipitation thus more than compensating for the decline experienced in winter and spring seasons. The lower regions also experience an increase in fall precipitation but at a smaller rate.

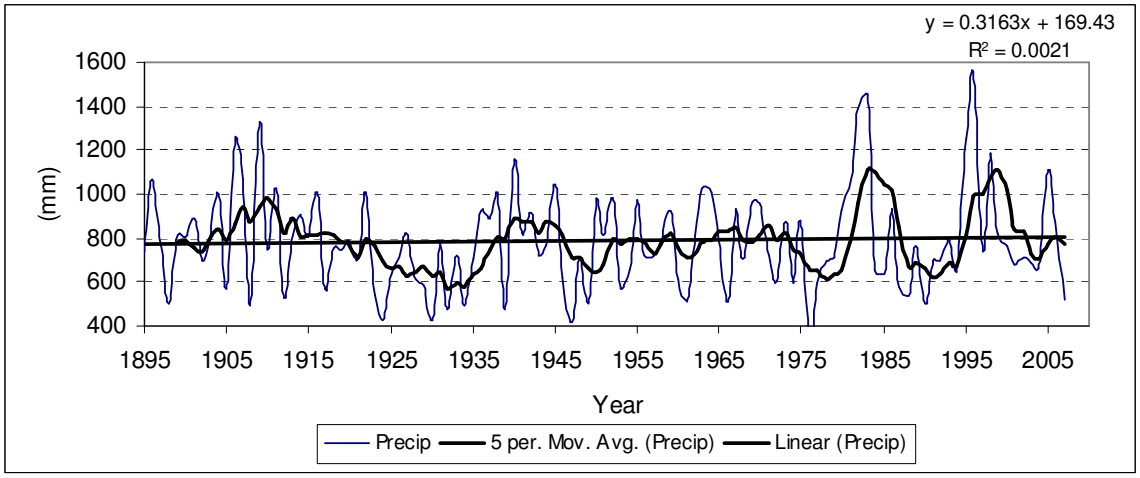

Figure 5 Annual precipitation for Lake Tahoe Basin.

Table 2 Annual average rate of change in precipitation.

Precipitation Trends		Winter	Spring	Summer	Fall	Annual
Carson Desert	CD	-0.0068	0.1335	0.1216	0.1006	0.3423
Granite Springs Valley	GSV	0.0007	0.1594	0.1471	0.1192	0.4283
Honey Eagle Lakes	HEL	-0.0432	-0.0679	0.114	-0.0022	-0.0198
Middle Carson	MC	-0.1408	0.0157	0.114	0.1052	0.0756
Pyramid Winnemucca Lakes	PWL	-0.1414	0.0165	0.1051	0.0579	0.0343
Lake Tahoe	Tahoe	-0.0797	-0.2516	0.1663	0.5514	0.3163
Truckee River	Truckee	-0.0086	-0.2608	0.1221	0.4065	0.214
Upper Carson	UC	-0.3452	-0.2393	0.1526	0.3977	-0.0823
Entire Study Area	Entire	-0.0718	-0.0233	0.1255	0.1500	0.1607

The monthly maximum and minimum temperatures for the Lake Tahoe basin have been rising as seen in Figure 6 and Figure 7. Temperature trends for all sub regions in the study area show consistent rising trends over the period of study (Table 3 & Table 4).

The analyses of average monthly minimum and maximum temperatures show that the rate of change was not uniform for the four seasons.
Maximum temperatures increased all over the study area for all seasons but average maximum temperature for winters displayed the highest rate of increase. Minimum temperatures on the other hand show a reversed trend for the winter season with the lowest rate of increase of all seasons.

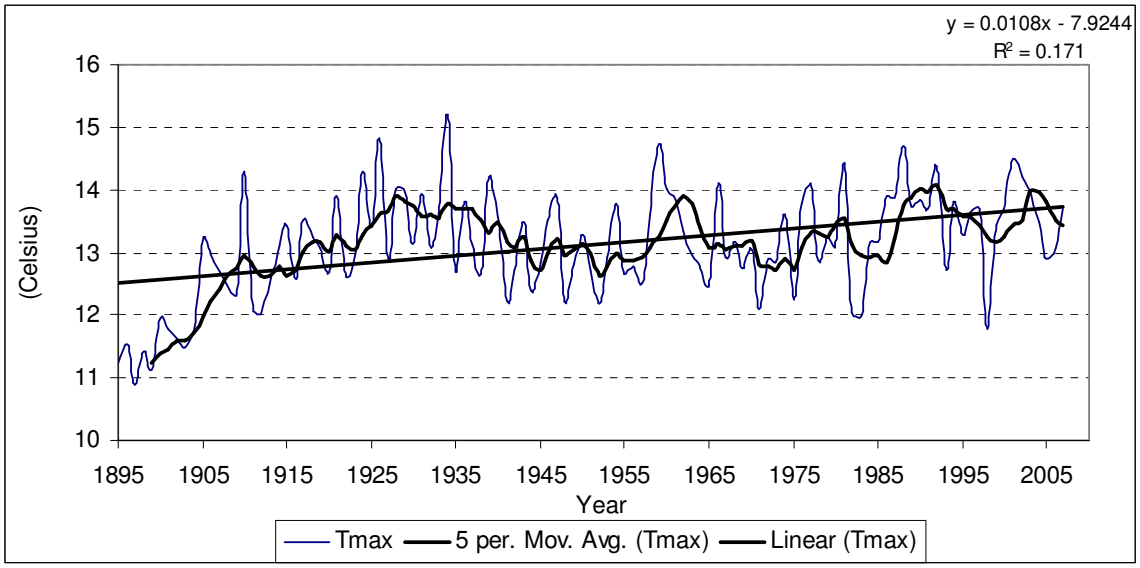

Figure 6 Annual average monthly maximum temperatures for Lake Tahoe Basin.

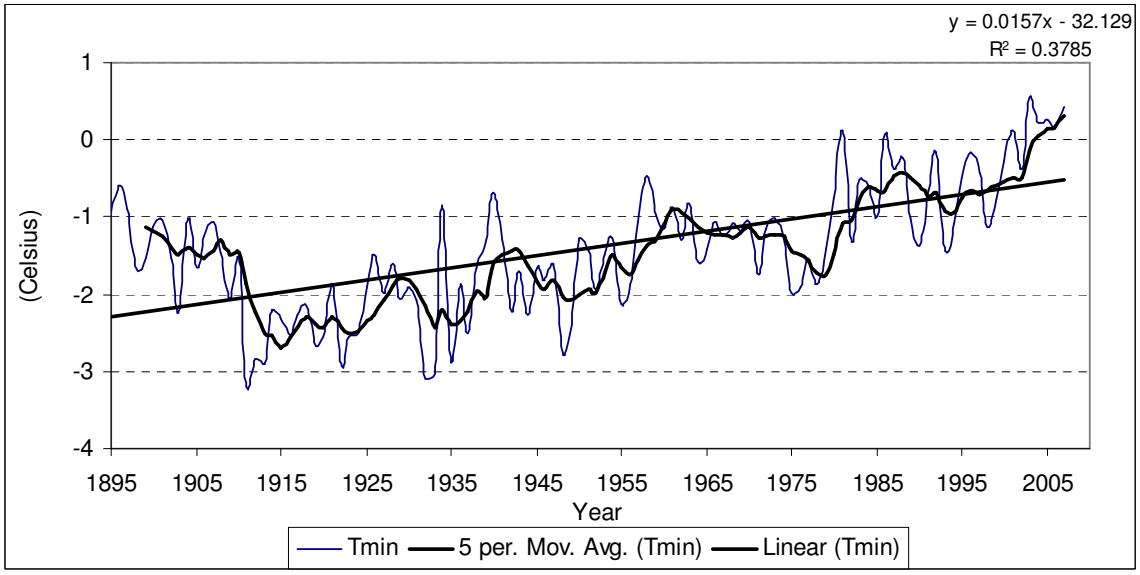

Figure 7 Annual average monthly minimum temperatures for Lake Tahoe Basin.

Table 3 Annual average rate of change in maximum temperatures.

Maximum Temperature		**Winter**	**Spring**	**Summer**	**Fall**	**Annual**
Carson Desert	CD	0.0234	0.0121	0.0109	0.0107	0.0143
Granite Springs Valley	GSV	0.017	0.0101	0.0102	0.0006	0.0095

Honey Eagle Lakes	HEL	0.0202	0.0103	0.0091	0.0004	0.01
Middle Carson	MC	0.015	0.0093	0.0108	0.0064	0.0104
Pyramid Winnemucca Lakes	PWL	0.0214	0.0123	0.0139	0.0032	0.0127
Lake Tahoe	Tahoe	0.0144	0.011	0.0101	0.0077	0.0108
Truckee River	Truckee	0.0172	0.0122	0.0201	0.0088	0.0146
Upper Carson	UC	0.0131	0.011	0.0088	0.009	0.0105
Entire Watershed	Entire	0.0189	0.011	0.0115	0.005	0.0116

Table 4 Annual average rate of change in minimum temperatures.

Minimum Temperature		**Winter**	**Spring**	**Summer**	**Fall**	**Annual**
Carson Desert	CD	0.0122	0.0142	0.0101	0.0093	0.0153
Granite Springs Valley	GSV	0.0095	0.0072	0.0133	0.0098	0.001
Honey Eagle Lakes	HEL	0.0064	0.0095	0.0164	0.0143	0.0117
Middle Carson	MC	0.012	0.0155	0.0171	0.0179	0.0155
Pyramid Winnemucca Lakes	PWL	0.0101	0.0119	0.0198	0.0166	0.0147
Lake Tahoe	Tahoe	0.0145	0.0144	0.017	0.0169	0.0157
Truckee River	Truckee	0.0067	0.01	0.0122	0.0136	0.011
Upper Carson	UC	0.0118	0.0116	0.0214	0.0167	0.0154
Entire Watershed	Entire	0.0096	0.0104	0.0153	0.0146	0.0125

2.2 VIC Hydrological Model

This study also uses the outputs of the Variable Infiltration Capacity (VIC) hydrological model to analyze the changes occurring to the snow water equivalent (SWE) in the region between 1915 and 2005. Daily gridded meteorological data obtained from the Surface Water Modeling group at the University of Washington from their web site at http://www.hydro.washington.edu/Lettenmaier/Data/gridded/, the development of which is described by Hamlet and Lettenmaier (2005) and Maurer et al., (2002). VIC is a macroscale hydrologic model that balances both surface energy and water over a grid mesh, typically at resolutions ranging from a fraction of a degree to several degrees latitude by longitude. The primary sources of meteorological data used in the data-processing sequence include NCDC Co-op data, monthly time step HCN and HCCD data, and PRISM data (Hamlet and Lettenmaier, 2005).

Most of the grid cells selected for the analysis lie along the periphery of Lake Tahoe. Figure 8 displays the grid cells from VIC model outputs which are used for the analysis of SWE changes. Each grid cell covers 1/8th of a degree grid cell (i.e. 13.8 km along the longitudes and approximately 10.1 km along the latitudes). To determine the changes in SWE over the time horizon afforded by VIC data, average SWE for January was calculated for each year. Figure 9 shows that the mean SWE for January has increased by almost 1mm per year. SWE calculations for April 1 were also carried out which showed a decline for all the grid cells. Therefore, to understand this inconsistency, March 1 and February 1 SWE were calculated for all the cells. The results show a rise in the SWE for January 1 and February 1 for all the grid cells whereas all the grid cells evaluated display a decline in April 1 SWE (Table 5). The average change in SWE per year ranges from 0.22 mm/yr to 1.07 mm/yr.

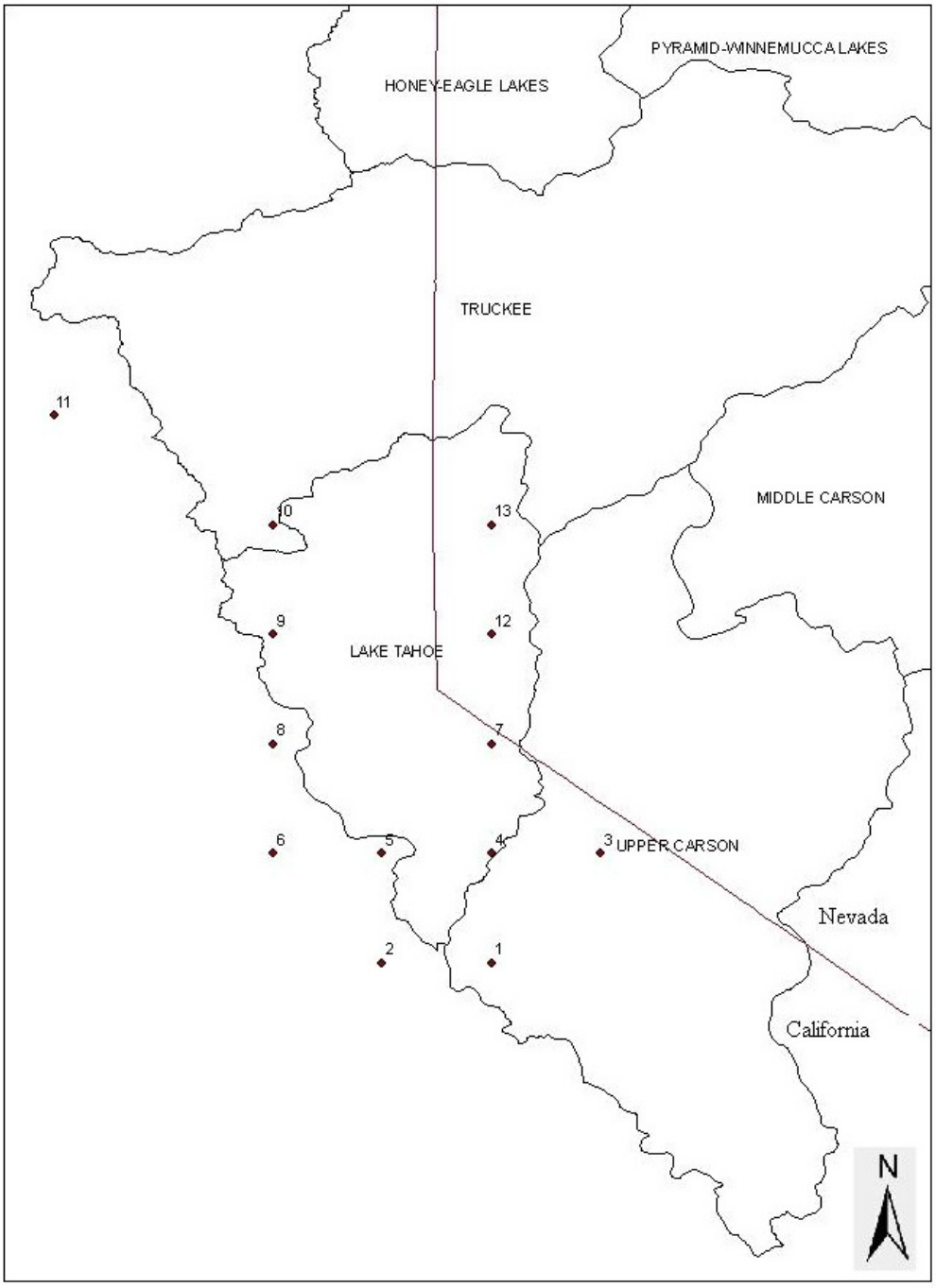

Figure 8 Location of VIC grid cells used for estimating SWE variations.

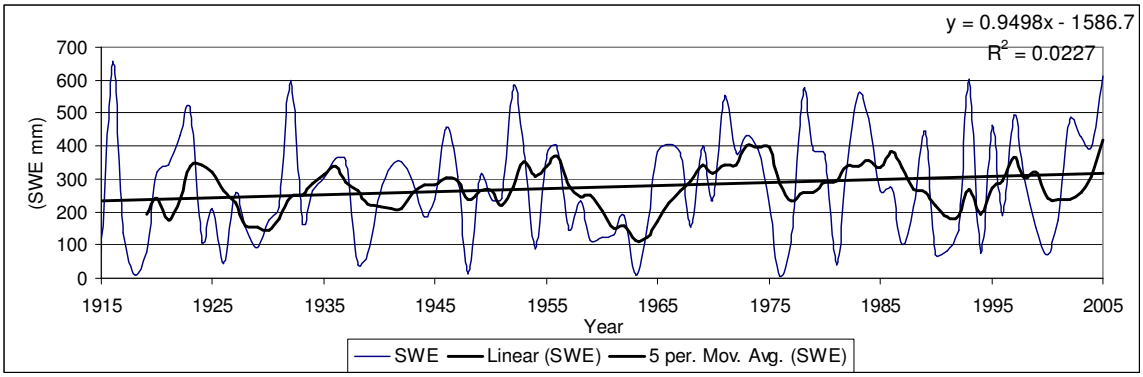

Figure 9 Mean January SWE variation for grid cell #1.

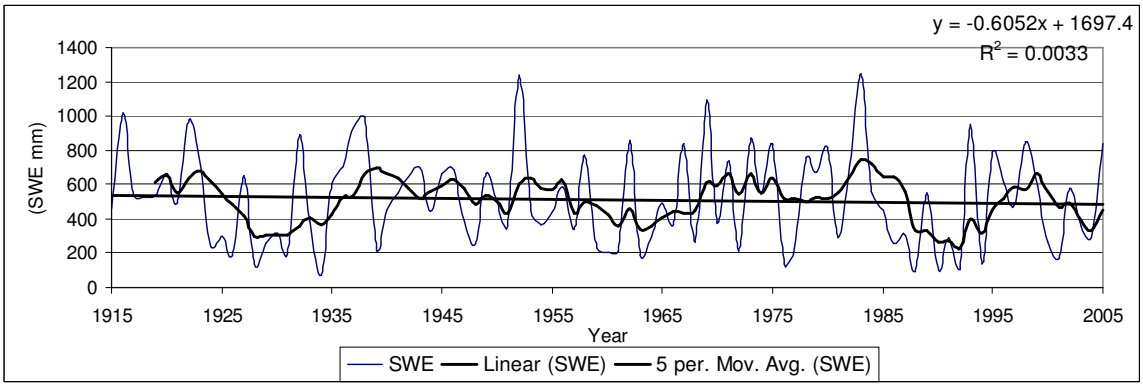

Figure 10 April 1 SWE for grid cell #2.

Table 5 VIC results for SWE variations.

Grid Cell	Latitude	Longitude	Average Change/Year (mm)				
			Mean Jan	1-Apr	1-Mar	1-Feb	1-Jan
1	38.6875	-119.938	1.079	-0.0413	0.3831	0.9179	1.1618
2	38.6875	-120.063	0.9498	-0.6052	0.0154	0.7107	1.1386
3	38.8125	-119.813	0.2191	-0.1405	-0.1725	0.0609	0.3279
4	38.8125	-119.938	1.0508	-0.0709	0.2505	0.8597	1.1997
5	38.8125	-120.063	1.0261	-0.3269	0.2751	0.8396	1.1811
6	38.8125	-120.188	0.4951	-0.5896	-0.2314	0.2683	0.7333
7	38.9375	-119.938	0.5468	-0.3521	-0.1536	0.363	0.7069
8	38.9375	-120.188	1.0262	-0.5268	0.1914	0.8565	1.1877
9	39.0625	-120.188	0.4471	-1.072	-0.4237	0.22	0.6665
10	39.1875	-120.188	0.7225	-0.101	0.1599	0.5842	0.8456
11	39.3125	-120.438	0.9876	-0.4272	0.1807	0.6736	1.1597
12	39.0625	-119.938	0.2212	-0.4176	-0.1687	0.0821	0.4019
13	39.1875	-119.938	0.3266	-0.5255	-0.2924	0.1996	0.5101

3 FUTURE CLIMATE CHANGE

3.1 Emission Scenarios

Green House Gas (GHG) emissions are dependent on a large number of factors which are interrelated in very complex and dynamic system. The emissions are driven by factors such as demographic development, socio-economic development, and technological change. Predicting the evolution of these factors is extremely difficult but a number of possible alternative paths, along which the future might unfold, can be postulated. These scenarios assist in analyzing the effects of changing climate on available resources and comparing available measures to mitigate its effects. Emission scenarios provide us with several alternative paths along which the world may progress and thus how GHG emissions might change over time. A number of such scenarios based on a wide array of driving forces have been developed by researchers all around the world.

Four different narrative storylines describing a range of possible alternative paths, excluding "surprise" or "disaster" scenarios have been generated by the IPCC based on literature. These were developed to describe consistently the relationships between emission driving forces and their evolution and add context for the scenario quantification. Each storyline represents different combination of demographic, social, economic, technological, and environmental developments. All scenarios based on the same storyline constitute a scenario "family". Each scenario represents a specific quantitative interpretation of one of four storylines described below.

Four qualitative storylines yield four sets of scenarios called "families": A1, A2, B1, and B2. All are equally valid with no assigned probabilities of occurrence. The set of scenarios consists of six scenario groups drawn from the four families described in Table 6: one group each in A2, B1, B2, and three groups within the A1 family, characterizing alternative developments of energy technologies: A1FI (fossil fuel intensive), A1B (balanced), and A1T (predominantly non-fossil fuel). Within each family and group of scenarios, some share "harmonized" assumptions on global population, gross world product, and final energy. These are marked as "HS" for harmonized scenarios. "OS" denotes scenarios that explore uncertainties in driving forces beyond those of the harmonized scenarios.

The A1 storyline and scenario family describes a future world of very rapid economic growth, global population that peaks in mid-century and declines thereafter, and the rapid introduction of new and more efficient technologies. Major underlying themes are convergence among regions, capacity building, and increased cultural and social interactions, with a substantial reduction in regional differences in per capita income. The A1 scenario family develops into three groups that describe alternative directions of technological change in the energy system. The three A1 groups are distinguished by their technological emphasis: fossil intensive (A1FI), non-fossil energy sources (A1T), or a balance across all sources (A1B).

The A2 storyline and scenario family describes a very heterogeneous world. The underlying theme is self-reliance and preservation of local identities. Fertility patterns

across regions converge very slowly, which results in continuously increasing global population. Economic development is primarily regionally oriented and per capita economic growth and technological changes are more fragmented and slower than in other storylines.

The B1 storyline and scenario family describes a convergent world with the same global population that peaks in mid-century and declines thereafter, as in the A1 storyline, but with rapid changes in economic structures toward a service and information economy, with reductions in material intensity, and the introduction of clean and resource-efficient technologies. The emphasis is on global solutions to economic, social, and environmental sustainability, including improved equity, but without additional climate initiatives.

The B2 storyline and scenario family describes a world in which the emphasis is on local solutions to economic, social, and environmental sustainability. It is a world with continuously increasing global population at a rate lower than A2, intermediate levels of economic development, and less rapid and more diverse technological change than in the B1 and A1 storylines. While the scenario is also oriented toward environmental protection and social equity, it focuses on local and regional levels.

Table 6 Summary of four SRES storylines

	A1	**A2**
World	Market Oriented	Differentiated
Economy	Fastest Per Capita	Regionally oriented, lowest per capita growth
Population	2050 peak, then decline	Continuously increasing
Governance	Strong regional	Self reliance with preservation of local identities
Technology	Three groups: A1F1 (Fossil fuel), A1T (Non-fossil), & A1B Balanced)	Slowest and the most fragmented growth
	B1	**B2**
World	Convergent	Local solutions
Economy	Service and information based, lower growth than A1	Intermediate growth
Population	Same as A1	Continuously increasing at a rate lower than A2
Governance	Global solutions to economic, social and environmental sustainability	Regional solutions to environmental protection and social equity
Technology	Clean and resource efficient	More rapid than A2; less rapid and more diverse than A1/B1

The shortwave impact of changes in boundary-layer clouds, and to a lesser extent midlevel clouds, constitutes the largest contributor to inter-model differences in global cloud feedbacks.

3.2 Climate Models

Eighteen modeling groups performed a set of coordinated, standard experiments, and the resulting model output, analyzed by hundreds of researchers worldwide, forms the basis for much of the current IPCC assessment of model results. A total of 23 models by 18 groups are currently used by IPCC to generate the future climate change scenarios. (Randall et al., 2007). The modeling groups and models used for this purpose are mentioned in Table 7.

Table 7 AOGCMs featured in IPCC Reports.

Model	Sponsors/Country	References
CSIRO-MK3	Commonwealth Scientific and Industrial Research Organisation (CSIRO) Atmospheric Research, Australia	Gordon et al., 2002; O'Farrell, 1998.
MIROC3.2 (medres)	Center for Climate System Research (University of Tokyo), National Institute for Environmental Studies , and Frontier Research Center for Global Change (JAMSTEC), Japan	K-1 Developers, 2004; Oki and Sud, 1998.
UKMO-HadCM3	Hadley Centre for Climate Prediction and Research/Met Office, UK	Pope et al., 2000; Gordon et al., 2000; Cattle and Crossley,1995; Cox et al., 1999.

Figure 11 shows the continuation of the 20th-century simulations for warming trends. Lines show the multi-model means, shading denotes the ±1 standard deviation range of individual model annual means. Discontinuities between different periods have no physical meaning and are caused by the fact that the number of models that have run a given scenario is different for each period and scenario, as indicated by the coloured numbers given for each period and scenario at the bottom of the panel. For the same reason, uncertainty across scenarios should not be interpreted from this figure (see Section 10.5.4.6 for uncertainty estimates).

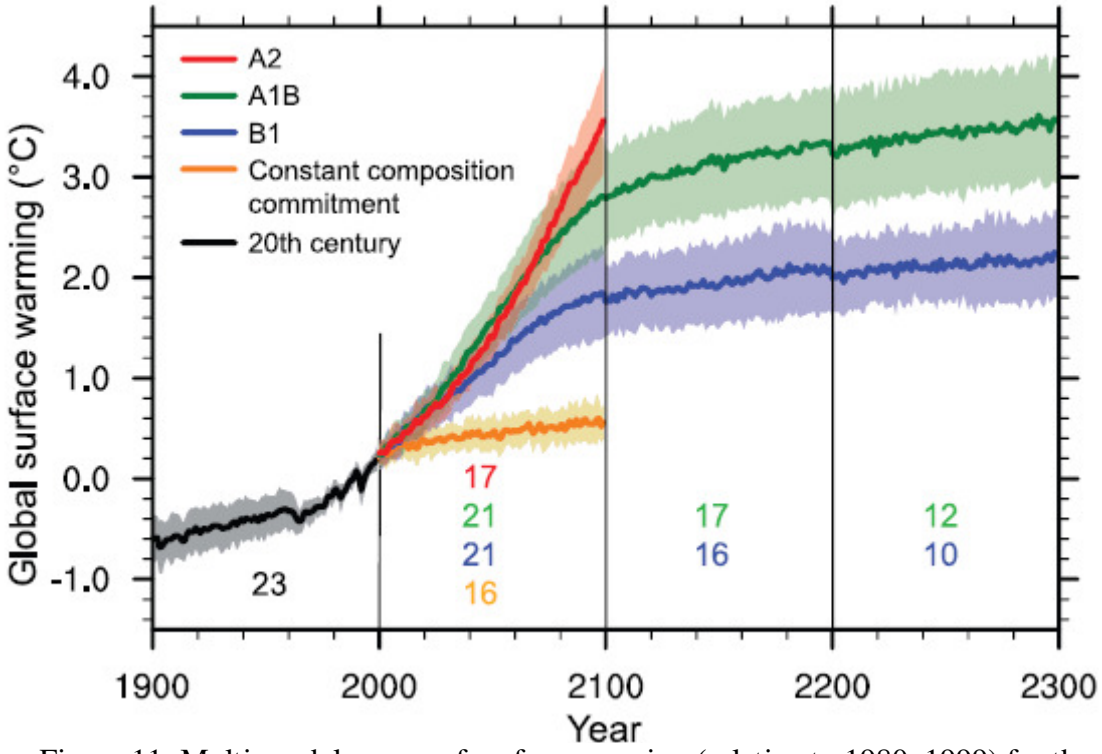

Figure 11: Multi-model means of surface warming (relative to 1980–1999) for the scenarios A2, A1B and B1. (Source: IPCC FAR)

3.3 Climate Change Projections

Accurate climate projections play a crucial role in determining the success of water management plans by providing an estimate of changes occurring to temperature and precipitation patterns which govern water availability. This section of the report compiles the climate change projections up to the end century obtained from three major coupled atmosphere-ocean general circulation models MIROC-M3, UKMO-HadCM3, and CSIRO-Mk3.0 for three emission scenarios namely A2, A1B, and B1.

Figure 12 shows the time series of globally averaged (left) surface warming (surface air temperature change, °C) and (right) precipitation change (%) from the various global coupled models for the scenarios A2 (top), A1B (middle) and B1 (bottom). Numbers in parentheses following the scenario name represent the number of simulations shown. Values are annual means, relative to the 1980 to 1999 average from the corresponding 20th-century simulations, with any linear trends in the corresponding control run simulations removed. A three-point smoothing was applied. Multi-model (ensemble) mean series are marked with black dots.

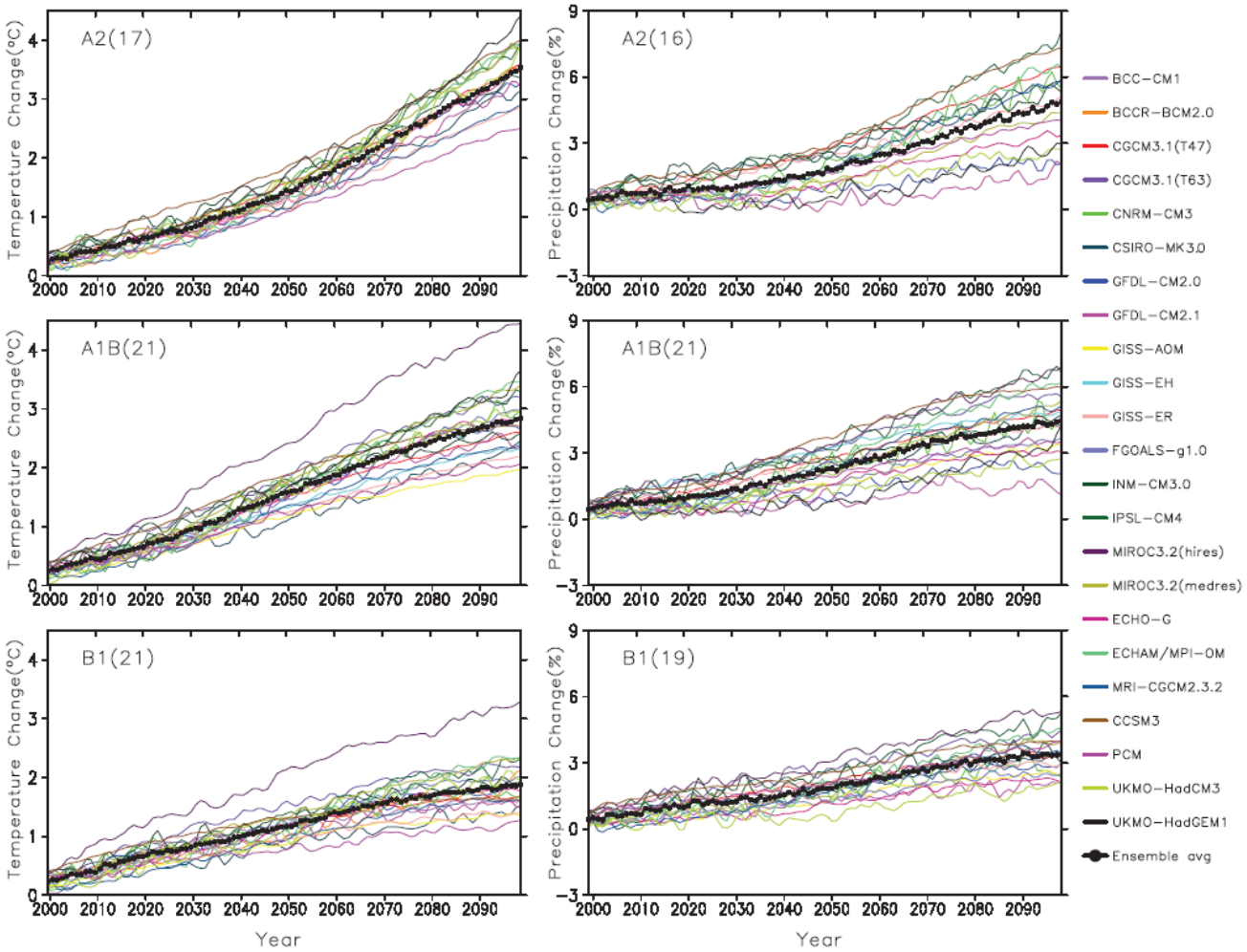

Figure 12: Time series of globally averaged surface air temperature and precipitation changes. (Source: IPCC FAR)

Confidence in climate models comes from the physical science behind their creation, and their skill at reproducing observed climate and past climate changes. Models have proven to be extremely important tools for simulating and understanding climate, and there is considerable confidence that they are able to provide credible quantitative estimates of future climate change, particularly at larger scales. Nonetheless, most models still suffer from a number of drawbacks which impose significant limitations on their results. Some of these drawbacks include their ability in representing clouds and man made aerosols etc which lead to uncertainties in the magnitude, timing, and spatial detail of predicted climate change. Nevertheless, over several decades of model development, they have consistently provided a robust and unambiguous picture of significant climate warming in response to increasing greenhouse gases at a global scale. However, since confidence in the changes projected by global models decreases at smaller scales, other techniques, such as the use of regional climate models, or downscaling methods, should be preferred for the study of regional and local scale climate change.

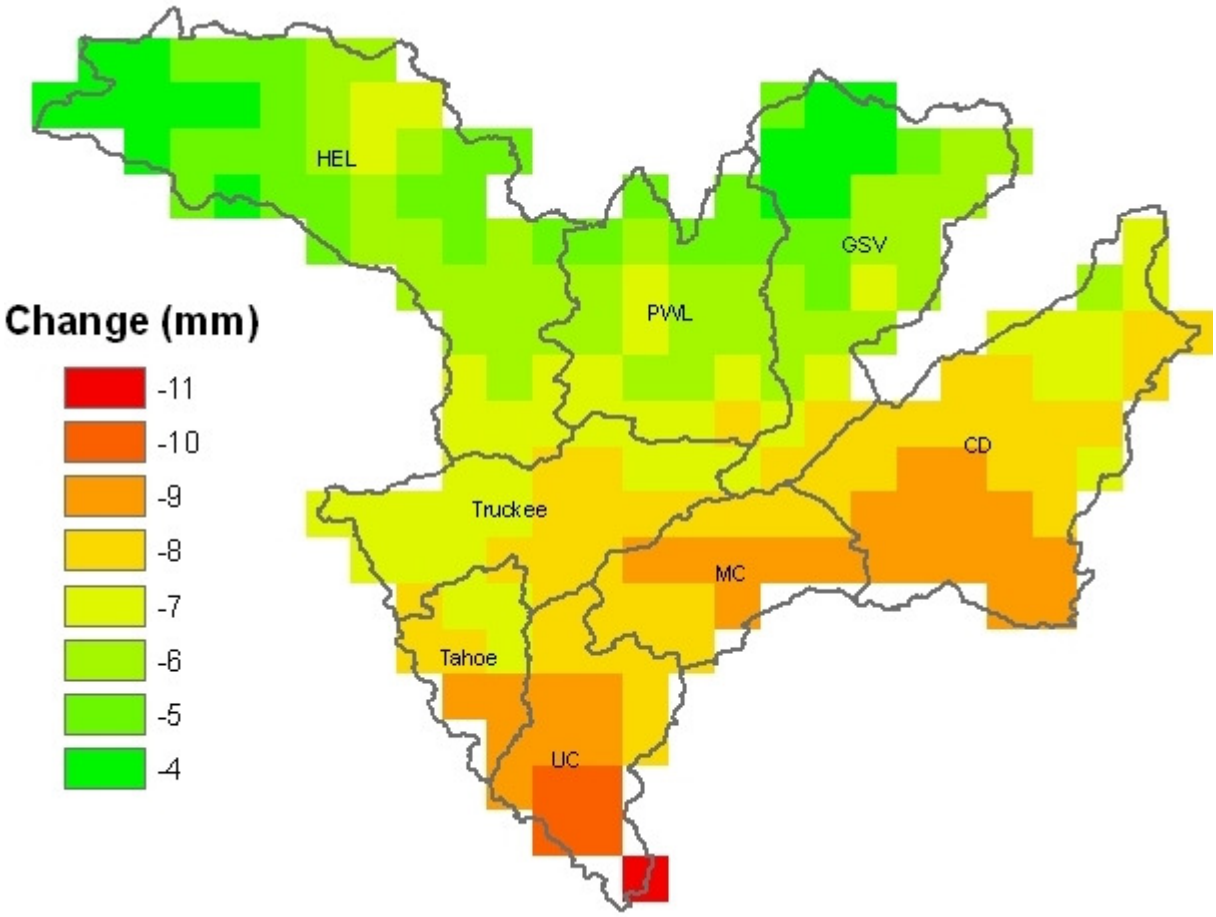

Figure 13 Precipitation change by mid 21st century as suggested by ensemble results from the three model outputs used in this study.

Figure 13 shows the anticipated mean precipitation departure by mid 21st century. The figure shows the estimated change in annual precipitation averaged over a period between 2040 and 2060. The change is compared to the mean historic data from 1961 to 1990. Figure 14 shows the reduction in precipitation by the end of 21st century. Both figures show significant decreases in annual precipitation in the high altitude regions of the study area. This region corresponds to the watershed of Lake Tahoe, Truckee River, and the Carson River and hence a decrease in precipitation in this area can significantly reduce the flow into these water bodies.

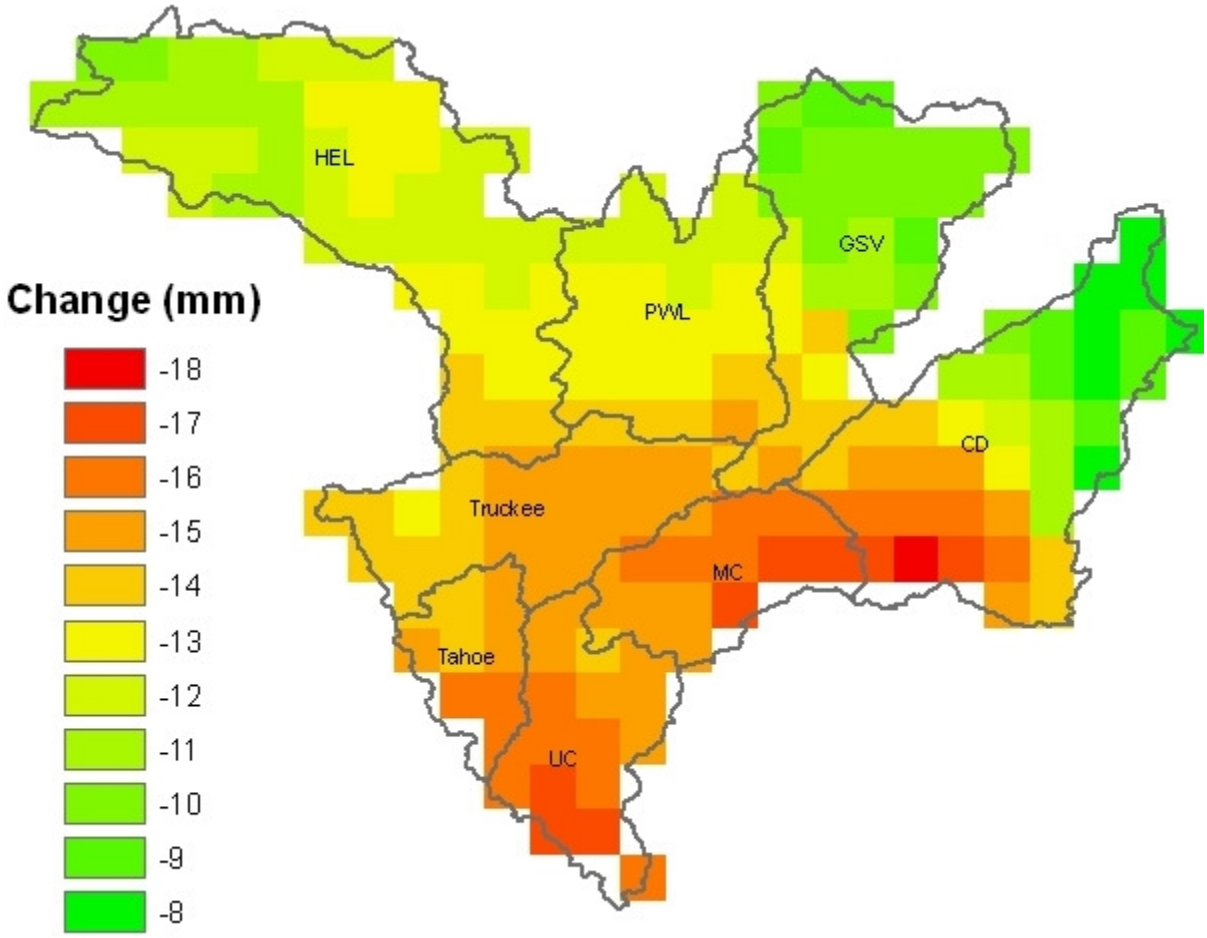

Figure 14 Precipitation change by the end of 21st century.

Table 8 and Table 9 provide a summary of the changes in precipitation and temperatures anticipated over the study area during the span of the 21st century. For all scenarios, an increase in average temperature and a decrease in annual precipitation are observed. The models predict an increase of 2.5 to 5.5 ^{o}F by 2050 and 4 to 11^{o}F by 2100. The increase is expected to be more pronounced in the summer and fall as compared to winters and spring.

Table 8 (a-c) Ensemble average from MIROC-M3, UKMO-HadCM3, and CSIRO-Mk3.0 models Summary of anticipated changes in precipitation and temperature by mid 21st century under emission scenarios (a) A2, (b) A1B, and (c) B1.

Table 8(a)

Period	Variable	Change	Units
Dec-Feb	Temp	4.00	F
Mar-May		4.50	F
Jun-Aug		5.00	F
Sep-Nov		5.00	F
Annual		5.50	F
Dec-Feb	Precip	7.50	%
Mar-May		-18.50	%
Jun-Aug		-15.91	%
Sep-Nov		-7.00	%
Annual		-11.00	%

Table 8(b)

Period	Variable	Change	Units
Dec-Feb	Temp	4.50	F
Mar-May		3.50	F
Jun-Aug		5.50	F
Sep-Nov		5.50	F
Annual		5.50	F
Dec-Feb	Precip	-6.00	%
Mar-May		-15.00	%
Jun-Aug		-21.84	%
Sep-Nov		-14.92	%
Annual		-7.50	%

Table 8(c)

Period	Variable	Change	Units
Dec-Feb	Temp	3.50	F
Mar-May		2.50	F
Jun-Aug		4.50	F
Sep-Nov		4.00	F
Annual		4.00	F
Dec-Feb	Precip	-3.00	%
Mar-May		-7.00	%
Jun-Aug		-6.00	%
Sep-Nov		1.50	%
Annual		-4.50	%

Table 9 (a-c) Ensemble average from MIROC-M3, UKMO-HadCM3, and CSIRO-Mk3.0 models Summary of anticipated changes in precipitation and temperature by the end of 21st century under emission scenarios (a) A2, (b) A1B, and (c) B1.

Table 9(b)

Period	Variable	Change	Units
Dec-Feb	Temp	6.50	F
Mar-May		5.50	F
Jun-Aug		9.50	F
Sep-Nov		7.50	F
Annual		7.50	F
Dec-Feb	Precip	-11.00	%
Mar-May		-17.00	%
Jun-Aug		-16.50	%
Sep-Nov		-8.18	%
Annual		-13.00	%

Table 9 (a)

Period	Variable	Change	Units
Dec-Feb	Temp	6.50	F
Mar-May		6.50	F
Jun-Aug		11.00	F
Sep-Nov		8.50	F
Annual		8.50	F
Dec-Feb	Precip	-4.50	%
Mar-May		-29.33	%
Jun-Aug		-9.44	%
Sep-Nov		9.50	%
Annual		-7.00	%

Table 9(c)

Period	Variable	Change	Units
Dec-Feb	Temp	4.50	F
Mar-May		4.00	F
Jun-Aug		6.50	F
Sep-Nov		5.50	F
Annual		6.00	F
Dec-Feb	Precip	-12.50	%
Mar-May		-17.00	%
Jun-Aug		-17.00	%
Sep-Nov		-1.17	%
Annual		-10.50	%

4 CONCLUSIONS

Analysis of precipitation data shows that annual precipitation has increased during the last century. On dividing the trends into the four seasons, it was observed that the increase was not consistent for all the seasons. Winter precipitation has decreased over the last century whereas summer and fall precipitation has increased. Furthermore, the largest decrease in winter precipitation was experienced by the regions located at a high altitude in the Sierra Nevada Mountains. These regions are responsible for feeding Lake Tahoe, the Truckee River and the Carson River. Therefore, a decrease in winter precipitation in these regions means lesser snowpack and consequently lower inflows into the water bodies.

The results from VIC outputs show a rise in the SWE for January 1 and February 1 for all the grid cells whereas all the grid cells evaluated display a decline in April 1 SWE. These results obtained from VIC outputs are in agreement with the findings from PRISM data which suggest that precipitation during the fall season (Oct to Dec) has increased during the same period. The lowered SWE in the later half of winter months also corroborates the finding from PRISM data which shows that precipitation during the winter months has decreased.

Temperature trends for all sub regions in the study area show consistent rising trends over the last century. Increased temperatures in combination with changing precipitation patterns can change the hydrology of the study area. The results from this study cannot conclusively estimate the individual effects of temperature and precipitation changes on SWE but this combination is likely to be a major factor causing the shifting of SWE bulk towards the first half of the winters.

Future estimates from the climate models used in this study show decreases in annual precipitation throughout the study area. In addition the projections suggest a decrease in precipitation for all seasons throughout the watershed for all emission scenarios. The decreases are greater in magnitude in the high altitude regions of the study area. This region corresponds to the watershed of Lake Tahoe, the Truckee River, and the Carson River and hence a decrease in precipitation in this area can significantly reduce the flow into these water bodies. This finding however is inconsistent with the results obtained from PRISM and VIC outputs which show an increase in summer and fall precipitation in the study area over the last century. This inconsistency could be a result of the topography of the study area and the inability of climate models to generate accurate future trends for relatively small regions with abrupt changes in topography.

(notes: I have a general concern about the significance of the trend lines created in the Excel charts. The very low R^2 points one to conclude that the trend might not be statistically significant. If possible have Dinesh add 95% confidence interval to some of key statistics. I am going to try to do some time series test on some of the data to see if the trend lines are significant.

5 REFERENCES

Cattle, H., and J. Crossley (1995) *Modelling Arctic climate change*. Philos. Trans. R. Soc. London Ser. A, 352, 201–213.

Cayan, D. R., S. A. Kammerdiener, M. D. Dettinger, J. M. Caprio, and D. H. Peterson, (2001) *Changes in the onset of spring in the western United States*. Bull. Am. Meteor. Soc., 82, 399–415.

Cayan, D. R., E. P. Maurer, M. D. Dettinger, M. Tyree and K. Hayhoe (2008) *Climate Change Scenarios for the California Region*. Clim. Change 87, 21-42.

Christensen, N. S., A. W. Wood, D. P. Lettenmaier, and R. N. Palmer (2004) *Effects of Climate Change on the Hydrology and Water Resources of the Colorado River Basin*. Clim. Change 62, 337–363.

Cox, P.M., et al., (1999) *The impact of new land surface physics on the GCM simulation of climate and climate sensitivity*. Clim. Dyn., 15, 183–203.

Daly, C., R.P. Neilson, and D.L. Phillips (1994) *A Statistical-Topographic Model for Mapping Climatological Precipitation over Mountanious Terrain*. J. Appl. Meteor., 33, 140-158.

Daly C, G. H. Taylor, W. P. Gibson, T. W. Parzybok, G. L. Johnson, P. Pasteris (2001) *High-quality spatial climate data sets for the United States and beyond*. Trans. Am. Soc. Agric. Eng. 43:1957–1962

Daly, C., W. P. Gibson, G. H. Taylor, G. L. Johnson, P. Pasteris.(2002) *A knowledge-based approach to the statistical mapping of climate*. Clim. Res., 22, 99-113.

Dettinger, M. D. (2005) *From Climate Change Spaghetti to climate change distributions for 21st Century*, San Francisco Estuary and Watershed Science, 3(1).

Dettinger, M. D., and D. R. Cayan (1995) *Large-scale atmospheric forcing of recent trends toward early snowmelt runoff in California*. J. Clim., 8, 606–623.

Giorgi, F. and L. O. Mearns (1991) *Approaches to the simulation of regional climate change: A review*. Reviews in Geophysics, 29, 191-216.

Giorgi, F., C. S. Brodeur, and G. T. Bates (1994) *Regional climate change scenarios over the United States produced with a nested regional climate model: Spatial and seasonal characteristics.* J. Clim. 7, 375–399.

Gordon, C., et al., (2000): *The simulation of SST, sea ice extents and ocean heat transports in a version of the Hadley Centre coupled model without flux adjustments*. Clim. Dyn. 16, 147–168.

Gordon, H.B., et al., (2002) *The CSIRO Mk3 Climate System Model*. CSIRO Atmospheric Research Technical Paper No. 60, Commonwealth Scientific and Industrial Research Organisation Atmospheric Research, Aspendale, Victoria, Australia, 130 pp, http://www.cmar.csiro.au/e-print/open/gordon_2002a.pdf.

Groisman, P. Y., R. W. Knight, T. R. Karl, D. R. Easterling, B. Sun and J. H. Lawrimore (2004) *Contemporary changes of the hydrological cycle over the contiguous United States: trends derived from in situ observations*. J. Hydrometeorol., 5, 64-85.

Hamlet A. F., D. P. Lettenmaier (2005) *Production of Temporally Consistent Gridded Precipitation and Temperature Fields for the Continental U.S.* J of Hydrometeorol. 6 (3), 330-336.

Hamlet, A. F. and D. P. Lettenmaier (1999) *Effects of Climate Change on Hydrology and Water Resources in the Columbia River Basin*. J. of Am. Water Res Assn 35(6), 1597–1623.

Hengeveld, H., B. Whitewood and A. Fergusson (2005) *An Introduction to Climate Change: A Canadian Perspective*. Environment Canada, Downsview, Ontario, 55 pp.

IPCC, 2007: *Climate Change 2007: The Physical Science Basis. Contribution of Working Group I to the Fourth Assessment Report of the Intergovernmental Panel on Climate Change*. Cambridge University Press, Cambridge, United Kingdom and New York, NY, USA.

Karl, T. R., P. Y. Groisman, R. W. Knight, and R. R. Heim (1993) *Recent variations of snow cover and snowfall in North America and their relations to precipitation and temperature variations*. J. of Clim. 6, 1327–1344.

Kim, J. (2005) *A projection of the effects of the climate change induced by increased CO2 on extreme hydrologic events in the western U.S.,* Clim. Change.

Knowles, N., M. D. Dettinger, and D. R. Cayan (2006) *Trends in snowfall versus rainfall in the Western United States*, J. Clim. 19, 4545– 4559.

Labat, D., Y. Godderis, J.L. Probst, J.L. Guyot, (2004) *Evidence for global runoff increase related to climate warming*. Adv. in Water Res. 27, 631–642.

K-1 Model Developers, (2004): *K-1 Coupled Model (MIROC) Description*. K-1 Technical Report 1 [Hasumi, H., and S. Emori (eds.)]. Center for Climate System Research, University of Tokyo, Tokyo, Japan, 34 pp. http://www.ccsr.u-tokyo.ac.jp/kyosei/hasumi/MIROC/tech-repo.pdf.

Kunkel, K. E. (2003)*Temporal variations of extreme precipitation events in the United States: 1895-2000*. Geophys. Res. Lett., 30.

Lemke, P., et al. (2007*) Observations: Changes in snow, ice and frozen ground, in Climate Change 2007: The Physical Science Basis*. edited by S. Solomon et al., pp. 337–383, Cambridge Univ. Press, New York.

Lettenmaier, D. P., E. F. Wood, and J. R. Wallis (1994) *Hydroclimatological trends in the continental United States, 1948–88*. J. Clim, 7, 586–607.

Leung, L. R., Y. Qian, and X. Bian (2003) *Hydroclimate of the western United States based on observations and regional climate simulation of 1981– 2000, part I: Seasonal statistics*, J. Clim., 16(12), 1892– 1911.

Maurer, E. P., A. W. Wood, J. C. Adam, D. P. Lettenmaier, and B. Nijssen (2002) *A Long-Term Hydrologically Based Dataset of Land Surface Fluxes and States for the Conterminous United States*. J. of Clim. 15, 3237-3251.

Maurer, E. P. (2007) *Uncertainty in hydrologic impacts of climate change in the Sierra Nevada, California under two emissions scenarios*. Clim. Change, 82, 309–325.

Maurer, E. P. and P. B. Duffy (2005) *Uncertainty in projections of streamflow changes due to climate change in California*. Geophys. Res. Lett., 32.

Mearns, L., F. Giorgi, L. McDaniel, and C. Shields (1995a) *Analysis of daily variability of precipitation in a nested regional climate model: Comparison with observation and doubled CO2 results.* Global Planet. Change 10, 55–78.

Mearns, L., F. Giorgi, L. McDaniel, and C. Shields (1995b) *Analysis of variability and diurnal range of daily temperature in nested regional climate model: Comparison with observation and doubled CO2 results*. Clim. Dyn. 10, 55–78.

Millar, C. I., W. B. Woolfenden (1999) *The Role of Climate Change in Interpreting Historical Variability*. Ecological Applications 9(4), 1207-1216.

Mote, P. W. (2003) *Trends in snow water equivalent in the Pacific Northwest and their climatic cause*s. Geophys. Res. Lett., 30, 1601, doi: 10.1029/2003GL017258.

Mote, P. W., A. F. Hamlet, M. P. Clark, and D. P. Lettenmaier (2005) *Declining mountain snowpack in western North America*. Bull. Amer. Meteor. Soc., 86, 39–49.

Nanus, L., D. H. Campbell, G. P. Ingersoll, D. W. Clow, and M. A. Mast, (2003) *Atmospheric deposition maps for the Rocky Mountains.* Atm. Env. 37, 4881–4892.

O'Farrell, S.P. (1998) *Investigation of the dynamic sea ice component of a coupled atmosphere sea-ice general circulation model*. J. Geophys. Res.,103, 15751–15782.

Oki, T., and Y. C. Sud (1998): *Design of total runoff integrating pathways (TRIP)—A global river channel network*. Earth Interactions 2, 1–37.

Payne, J. T., A. W. Wood, A. F. Hamlet, R. N. Palmer and D. P. Lettenmaier (2004). *Mitigating the effects of climate change on the water resources of the Columbia River basin*. Clim. Change 62, 233-256.

Pierce, D. W., T. P. Barnett, H. G. Hidalgo, T. Das, C. Bonfils, B. D. Santer, G. Bala, M. D. Dettinger, D. R. Cayan, A. Mirin, A. W. Wood and T. Nozawa (2008) *Attribution of Declining Western U.S. Snowpack to Human Effects*. J. Climate, 21, 6425-6444.

Pope, V.D., M.L. Gallani, P.R. Rowntree, and R.A. Stratton (2000) *The impact of new physical parametrizations in the Hadley Centre climate model: HadAM3*. Clim. Dyn., 16, 123–146.

Pupacko, A. (1993) *Variations in northern Sierra Nevada streamflow: Implications of climate change.* Water Resour. Bull. 29(2), 283-290.

Randall, D. A., R. A. Wood, S. Bony, R. Colman, T. Fichefet, J. Fyfe, V. Kattsov, A. Pitman, J. Shukla, J. Srinivasan, R. J. Stouffer, A. Sumi and K. E. Taylor (2007) *Cilmate Models and Their Evaluation. In: Climate Change 2007: The Physical Science Basis. Contribution of Working Group I to the Fourth Assessment Report of the Intergovernmental Panel on Climate Change* [Solomon, S., D. Qin, M. Manning, Z. Chen, M. Marquis, K.B. Averyt, M.Tignor and H.L. Miller (eds.)]. Cambridge University Press, Cambridge, United Kingdom and New York, NY, USA.

Regonda, S. K., B. Rajagopalan, M. Clark, and J. Pitlick (2005) *Seasonal cycle shifts in hydroclimatology over the western United States*. J. Climate 18, 372–384.

Rood, S. B., G. M. Samuelson, J. K.Weber and K. A.Wywrot (2005) *Twentieth-century decline in streamflows fromthe hydrographic apex of NorthAmerica*. J. Hydrol. 306, 215-233

Shein, K. A. (2006) *State of the climate in 2005, including executive summary*. Bull. Amer. Meteorol. Soc., 87, 801-805,

Stewart, I. T., Cayan, D. R., Dettinger, M. D. (2004) *Changes in snowmelt runoff timing in western North America under a 'business as usual' climate change scenario.* Clim. Change, 62, 217-232.

Stewart, I.T., Cayan D. R., Dettinger, M. D. (2005) *Changes toward Earlier Streamflow Timing across Western North America*. J. Clim., 18(8), 1136–1155.

Seager R., Ting M., Held I., Kushnir Y., Lu J., Vecchi G., Huang H. P., Harnik N., Lau N. C., Li C. et al. (2007) *Model projections on an inminent transition to a more arid climate in southwestern North America*. Science 316: 1181– 1184.

Trenberth, K. E., A. Dai, R. M. Rasmussen, and D. B. Parsons (2003) *The changing character of precipitation*. Bull. Amer. Meteor. Soc., 84, 1205–1217.

Trenberth, K. E., L. Smith, T. Qian, A. Dai, and J. Fasullo (2007), *Estimates of the global water budget and its annual cycle using observational and model data*, J. Hydrometeorol. 8, 758-769.

US Census Bureau, Population Division. http://www.census.gov/popest/cities/SUB-EST2008-states.html Retrieved on July 18, 2009.

VanRheenen, N. T., A. W. Wood, R. N. Palmer and D. P. Lettenmaier (2004) *Potential Implications of PCM Climate Change Scenarios for California Hydrology and Water Resources*. Clim. Change 62, 257–281.

Vicuna S., E. P. Maurer, B. Joyce, J. A. Dracup, D. Purkey (2007) *The sensitivity of California water resources to climate change scenarios*. J Am Water Res Assoc 43(2): 482 –498

Vincent, L. A., X. Zhang, and W. D. Hogg (1999) *Maximum and minimum temperature trends in Canada for 1895–1995 and 1945–1995*. 10th Symp. on Global Change Studies, Dallas, TX, Amer. Meteor. Soc., 95–98.

Walter, M. T., D. S. Wilks, J.-Y. Parlange, and R. L. Schneider (2004*) Increasing evapotranspiration from the conterminous United States*, J. Hydrometeorol., 5, 405– 408.

6 APPENDICES

6.1 Processing steps for PRISM Dataset

Step 1.Downloading Data: PRISM data can either be downloaded interactively from (http://mole.nacse.org/prism/nn/index.phtml?vartype=ppt&year0=2003&year1=2003) or from the PRISM Group's ftp site (ftp://prism.oregonstate.edu/pub/prism/us/grids/)

Step 2.Unzipping: The files downloaded from the sources mentioned in Step 1 were unzipped and converted to ascii files by changing the extension to <*.asc>. Due to a large number of files, individual unzipping would have been impractical. Therefore, "7-zip" freeware was used for this process.

Step 3.Processing in ArcGIS: Resulting files from Step 2 were imported into ArcGIS and converted into raster format. "Modelbuilder" feature in ArcMap was used to automate the processing of files for this step and all other subsequent steps due to the large number of files.

Step 4.Raster files obtained from Step 3 were then clipped using the watershed shapefiles.

Step 5.Attributes tables were created for all the clipped raster files.

Step 6.Additional field ("precip" for precipitation files and "temp" for temperature files) was created in the attributes tables for the clipped raster files to hold the product of the fields "Value" and "Count".

Step 7."Summary Statistics" tool in ArcMap was used to obtain the mean of the field "precip/temp" and sum of the field "count". In addition,

Step 8.Summary statistics obtained as *.dbf files, for each corresponding raster file, were converted into *.xls files for processing in Matlab.

Step 9.A Matlab program was used to read the statistics of "precip/temp" and "Count" from the .xls files created in Step 8.

Step 10.The average temperature or depth of precipitation over the watershed were calculated using

$$X = Y \times C / P$$

Where
X =
Y = precip or temp read in Step 9
C = Count read in Step 9
P = Number of pixels the raster file for the corresponding watershed.

6.2 Notes:

ArcMap was unable to process all the files simultaneously using Modelbuilder. Therefore, files were processed one watershed at a time.

Due to naming protocols in ArcMap, files obtained after processing had complicated names. Renaming was found to be useful to prevent mixing up of files.

Theoretically it is possible to combine Steps 3 to 8 in one model but difficulties were encountered while running these processes in a single model. Modelbuilder failed to execute certain steps when multiple processes were combined in a single model.

The following Matlab code was used to execute the process described in Step 9.

```
xlsFiles = dir('Path\*.xls')
Matrix = zeros (length(xlsFiles),1)
for k = 1:length(xlsFiles);
  filename = xlsFiles(k).name
  data = xlsread(filename, 'a2:a2')
  Matrix(k) = data
end
xlswrite ('Path'\output_filename.xls', Matrix, 'Sheet1')
```